

# **RADIO RESOURCE MANAGEMENT AND SMALL CELL DEPLOYMENT STRATEGIES FOR HETEROGENEOUS BWA NETWORKS: A GREEN COMMUNICATION PERSPECTIVE**

THESIS SUBMITTED BY  
**ARIJEET GHOSH**

**DOCTOR OF PHILOSOPHY (ENGINEERING)**

DEPARTMENT OF ELECTRONICS AND TELECOMMUNICATION  
ENGINEERING

FACULTY COUNCIL OF ENGINEERING & TECHNOLOGY

JADAVPUR UNIVERSITY

KOLKATA-700032, INDIA

2023

---



JADAVPUR UNIVERSITY  
KOLKATA-700032, INDIA

INDEX NO-98/16/17/E

**1. Title of the Thesis:**

Radio Resource Management and Small Cell  
Deployment Strategies for Heterogeneous BWA  
Networks: A Green Communication Perspective

**2. Name, Designation & Institution of the  
Supervisor:**

**PROF. ITI SAHA MISRA**

Professor

Department of Electronics & Telecommunication  
Engineering

Jadavpur University

Kolkata-700032, India

Email: [itisahamisra@yahoo.co.in](mailto:itisahamisra@yahoo.co.in)

---

### 3. List of Publications

*(From the Contents of the Dissertation)*

#### SCI-Indexed Journal Publications

- I. **Arijeet Ghosh**, Iti Saha Misra, and Anindita Kundu, “Coverage and rate analysis in two-tier heterogeneous networks under suburban and urban scenarios.” Transactions on Emerging Telecommunications Technologies, 30(12), p.e3648. Impact Factor: 3.310. DOI:<https://doi.org/10.1002/ett.3648>
- II. **Arijeet Ghosh**, and Iti Saha Misra, “A joint CAC and dynamic bandwidth allocation technique for capacity and QoS analysis in heterogeneous LTE based BWA network: few case studies.” Wireless Personal Communications, Springer, 97(2), pp.2833-2857. Impact factor: 2.017. DOI: <https://doi.org/10.1007/s11277-017-4637-x>



## International Conferences

- I. **Arijeet Ghosh** and Iti Saha Misra., Ultra Dense Three-Tier 5G Heterogeneous Network Model for Improved Coverage and Rate. In *2022 IEEE Calcutta Conference (CALCON)* (pp. 60-64). IEEE. 2022. DOI: [10.1109/CALCON56258.2022.10060694](https://doi.org/10.1109/CALCON56258.2022.10060694)
- II. **Arijeet Ghosh**, Iti Saha Misra, “Role of different spatial point processes on network densification towards 5G development: Coverage and Rate analysis”, In *2020 IEEE Calcutta Conference (CALCON)*, pp. 15-19. IEEE, 2020. DOI: [10.1109/CALCON49167.2020.9106542](https://doi.org/10.1109/CALCON49167.2020.9106542)
- III. **Arijeet Ghosh**, Iti Saha Misra, “Effect of propagation path loss in designing two-tier 5G Het-Nets for coverage and rate”, In *2019 URSI Asia-Pacific Radio Science Conference (AP-RASC 2019)*, pp. 1-2, IEEE, 2019. DOI: [10.23919/URSIAP-RASC.2019.8738431](https://doi.org/10.23919/URSIAP-RASC.2019.8738431)
- IV. **Arijeet Ghosh**, Iti Saha Misra, “An analytical model for a resource constrained QoS guaranteed SINR based CAC scheme for LTE BWA Het-Nets”, In *International Conference on Advances in Computing, Communications and Informatics (ICACCI 2016)*, pp. 2186-2192, IEEE, 2016. DOI: [10.1109/ICACCI.2016.7732376](https://doi.org/10.1109/ICACCI.2016.7732376)
- V. **Arijeet Ghosh**, Iti Saha Misra, “A QoS based comparative analysis between relay assisted and small eNodeB based two-tier LTE network”, In *International Conference on Computers and Devices for Communication, (CODEC 2015)*, pp. 1-5, IEEE, 2015. DOI: [10.1109/CODEC.2015.7893051](https://doi.org/10.1109/CODEC.2015.7893051)

#### **4. List of patents: NIL**

## 5. List of Presentation in International Conferences

*(Related to thesis)*

- I. **Arijeet Ghosh** and Iti Saha Misra., Ultra Dense Three-Tier 5G Heterogeneous Network Model for Improved Coverage and Rate. In 2022 *IEEE Calcutta Conference (CALCON)* (pp. 60-64). IEEE. 2022. DOI: [10.1109/CALCON56258.2022.10060694](https://doi.org/10.1109/CALCON56258.2022.10060694)
- II. **Arijeet Ghosh**, Iti Saha Misra, “Role of different spatial point processes on network densification towards 5G development: Coverage and Rate analysis”, In 2020 IEEE Calcutta Conference (CALCON), pp. 15-19. IEEE, 2020. DOI: [10.1109/CALCON49167.2020.9106542](https://doi.org/10.1109/CALCON49167.2020.9106542)
- III. **Arijeet Ghosh**, Iti Saha Misra, “Effect of propagation path loss in designing two-tier 5G Het-Nets for coverage and rate”, In 2019 URSI Asia-Pacific Radio Science Conference (AP-RASC 2019), pp. 1-2, IEEE, 2019. DOI: [10.23919/URSIAP-RASC.2019.8738431](https://doi.org/10.23919/URSIAP-RASC.2019.8738431)
- IV. **Arijeet Ghosh**, Iti Saha Misra, “An analytical model for a resource constrained QoS guaranteed SINR based CAC scheme for LTE BWA Het-Nets”, In International Conference on Advances in Computing, Communications and Informatics (ICACCI 2016), pp. 2186-2192, IEEE, 2016. DOI: [10.1109/ICACCI.2016.7732376](https://doi.org/10.1109/ICACCI.2016.7732376)
- V. **Arijeet Ghosh**, Iti Saha Misra, “A QoS based comparative analysis between relay assisted and small eNodeB based two-tier LTE network”, In International Conference on Computers and

Devices for Communication, (CODEC 2015), pp. 1-5, IEEE,  
2015. **DOI:** [10.1109/CODEC.2015.7893051](https://doi.org/10.1109/CODEC.2015.7893051)

## **“STATEMENT OF ORIGINALITY”**

I, Arijeet Ghosh, registered on **25th October, 2016** do hereby declare that this thesis entitled **“Radio Resource Management and Small Cell Deployment Strategies for Heterogeneous BWA networks: A Green Communication Perspective”** contains literature survey and original research work done by the undersigned candidate as part of Doctoral studies.

All information in this thesis have been obtained and presented in accordance with existing academic rules and ethical conduct. I declare that, as required by these rules and conduct, I have fully cited and referred all material and results that are not original to this work.

I also declare that I have checked this thesis as per the “Policy on Anti Plagiarism, Jadavpur University, 2019”, and the level of similarity as checked by iThenticate software is 3 %.

Signature of the Candidate: *Arijeet Ghosh*

Date: *11/07/2023*

Certified by Supervisor: *Iti Saha Misra*  
*11/07/2023*

**DR. ITI SAHA MISRA**  
PROFESSOR  
Dept. of ETCE  
JADAVPUR UNIVERSITY  
Kolkata - 700 032



## CERTIFICATE FROM THE SUPERVISOR

This is to certify that the thesis entitled “ **Radio Resource Management and Small Cell Deployment Strategies for Heterogeneous BWA networks: A Green Communication Perspective**” submitted by **Shri Arijeet Ghosh**, who got his name registered on **25<sup>th</sup> October, 2016** for the award of Ph. D. (Engg.) degree of Jadavpur University is absolutely based upon his own work under the supervision of Prof. (Dr.) Iti Saha Misra and that neither his thesis nor any part of the thesis has been submitted for any degree/diploma or any other academic award anywhere before.

*Iti Saha Misra*

*Signature of the Supervisor* 11/07/2023

Prof. Iti Saha Misra  
Department of Electronics and  
Telecommunication Engineering  
Jadavpur University  
Kolkata-700032, India

**DR. ITI SAHA MISRA**  
PROFESSOR  
Dept. of ETCE  
JADAVPUR UNIVERSITY  
Kolkata - 700 032

Email: iti@etce.jdvu.ac.in  
itisahamisra@yahoo.co.in







*Dedicated to my parents my family, my teachers my  
friends esteemed reviewers of my papers and all my well  
wishers*





# Acknowledgement

Evolution is central to the existence and this thesis along with representing my work at the keyboard, inherently reflects on the idea of the evolution of a learner to manifest a latent research idea into reality following the stepping-stones of the invaluable guidance, the progressive learning and the required action. First and foremost, the esteemed institution, Jadavpur University, especially the Department of ETCE has played a key role by providing me with the necessary financial support through State Govt. Fellowship Scheme, which helped me in pursuing my doctoral research. This thesis is an upshot of multifarious experiences I have encountered at JU from a myriad of gracious individuals who I also wish to acknowledge wholeheartedly.

At the outset, I would like to express my sincere gratitude to Prof. Iti Saha Misra, the founder of JU Qualnet Laboratory for facilitating the process of learning to become enriched more holistically. She has been a constant source of inspiration from when I started working on the topic as a PhD student. I also extend my gratitude to ISM Madam for the thorough discussions on the intricacies of the subject during the research work, for providing me with her multidimensional perspectives and innumerable significant opportunities. She has taught me, both consciously and unconsciously, how good engineering is done using both mathematics and hands-on exploration. During the most difficult times when writing this thesis, she gave me the moral support and the freedom I needed to move on. Without her guidance and constant feedback, this Ph.D. would not have been achievable.

I am also heartily grateful to Prof. Salil Kumar Sanyal, for his insightful advice. His incredible experience in the wireless communication domain, scientific inputs, and necessary guidance during multiple events has always helped me to surpass many hurdles.

My life at JU was memorable due to the some close people who have gradually become a very important part of my day-to-day life. I am grateful to my seniors Dr. Prasun Choudhury, Dr. Anindita Kundu, Dr. Tamal Chakraborty, and Dr. Tanumay Manna, Mr. Sudipta dey, and fellow lab mates, Sreya, Gaurav, Aritra, Arnab, Subhajit and many more for all the memorable moments.

Lastly, I would like to thank my family for all their love, support, and encouragement through every up and down in this journey. I bow down to all of you with immense gratitude from the bottom of my heart for being an inseparable part of my life.

# Abstract

*During the past three decades, the world has witnessed rapid growth in wireless technologies from 2G to 5G and beyond. Throughout this period, the main objective behind this evolution has been to increase the capacity (to accommodate more users), extend the coverage (to deliver service to the last mile), improve the Quality of Service (QoS) (for every individual service), and last but not least, utilize the most essential intangible resource i.e. bandwidth. 2G digital cellular systems significantly increased voice capacity, improved voice quality, and began support for data applications such as Internet access. The circuit-switched paradigm based on which these systems were built made 2G systems very inefficient for data, and hence supported low-data rate with limited capacity. Third-generation (3G) systems were a significant leap over 2G, providing much higher data rates, a significant increase in voice capacity, and supporting advanced services and applications, including multimedia. Further advancements in mobile wireless technology led to the evolution of 3GPP LTE or Long Term Evolution – a technology referred to as 4G.*

*LTE has brought heterogeneity in terms of different radio access technologies, multi-tier architectures, and co-implementation of various protocols to support various types of services with desired Quality of Service (QoS) for the subscribers. However, due to limited bandwidth and the high demand for LTE networks, effective network planning is required to utilize the available radio resources in an efficient way. The inevitable expansion of the modern telecommunication sector has sought the attention of researchers to develop scalable architectures as well as planned management of available resources to meet the preferred QoS demand. Without using a single base station (abbreviated as eNodeB in 3GPPLTE), Internet Service Providers (ISPs) are eager to implement flexible heterogeneous network (Het-Net) architectures with the aim of providing a cost-effective improvement in terms of both coverage and capacity. As HetNets emerge as one of the most promising developments toward realizing the target specifications of Long Term Evolution (LTE) and LTE-Advanced (LTE-A) networks, radio resource management (RRM) research for such networks has, in recent times, been intensively pursued.*

*In this work, we primarily present a unique Radio Resource Management scheme for LTE Het-Nets that consists of Small cells and/or relays along with Macro cells. The proposed analysis has two components: (1) Received Signal Strength (RSS) based CAC policy; and (2) Dynamic Bandwidth Allocation (DBA) scheme for QoS provisioning. The novelty of this work lies in the integration of the RSS based CAC policy with the DBA scheme for improved performance in terms of different QoS parameters like New Call Blocking Probability (NCBP), Handoff Call Dropping Probability (HCDP), and Bandwidth Utilization (BU). A Continuous Time Markov Chain based mathematical model is also developed for the realistic analysis of those QoS parameters. The Joint CAC and DBA scheme (JCAC-DBA) in two-tier LTE BWA Het-Nets significantly improves NCBP, HCDP, BU, and overall capacity of the network under different combinations of macro/small cells for different classes of multimedia services.*

*The tremendous growth of contemporary wireless technologies fuelled by the penetration of smartphones has escalated the demand for increased coverage and capacity in cellular networks. Network densification has appeared as a promising network deployment technique that leverages spatial reuse to enhance coverage and throughput. By densification, it is seen as the deployment of more number of eNodeBs per unit area (or volume), while ensuring a nearly uniform distribution of users among all eNodeBs. As Network densification has appeared to be one of the key deployment architectures toward achieving the target goals of Long Term Evolution (LTE) and beyond, the evolution from hexagonal cellular architecture to densely deployed small cells has certainly increased complexity by several folds. So, the need of choosing the appropriate mathematical model has emerged as one of the significant research areas for accurate network planning and dense deployment of small cells. The spatial Point process (SPP) has emerged as a mathematically tractable technique to imitate these types of complex deployment scenarios. This work also aims to provide a reasonable performance analysis of three established SPPs, namely, Binomial Point process (BPP), Homogeneous Poisson Point Process (HPPP), Non-Homogeneous Poisson Point Process (NHPPP) in terms of QoS induced performance parameters like coverage and rate.*

*The evolution of wireless technologies has invariably contributed to the explosion in the number of subscribers as they continue to provide essential services*

through various multimedia applications. As a by-product, tele traffic density, i.e., the number of subscribers per 100 users in any particular region has increased by leaps and bounds and will certainly continue to increase in the future. The rapid growth in tele traffic density has enforced the modern wireless network to evolve in the direction of optimal deployment of HetNet which is speculated to play a key role in designing deployment strategies for modern wireless communication standards. In this work, a suitable model based on a nonhomogeneous Poisson point process (NHPPP) is designed for the heterogeneous wireless network (HetNet) consisting of two-tiers eNodeBs (Macro and Small Cell), where each of the tiers is differentiated in terms of transmitting power, eNodeB density, and supported data rate. Subsequently, analytical expressions are derived for coverage probability (CP) and average rate (AR) to assess the performance of the HetNet. The contribution of the work further lies in integrating the K-means clustering algorithm with NHPPP to find the optimal locations of the small cell eNodeBs for extended coverage and rate improvement. The proposed model is investigated under differently dense scenarios like urban and suburban areas in India. It establishes the requisite of an optimal number and placement of small cells along with the traditional infrastructure to maximize the performance in terms of CP and AR. Finally, the proposed integrated model is compared with the traditional homogeneous Poisson point process (HPPP) and NHPPP for coverage and rate analysis. It is observed that the k-means clustering algorithm in integration with NHPPP overshadows both HPPP and NHPPP in terms of coverage and rate under both urban and suburban deployment scenarios.

Although LTE's spectral efficiency does exceed that of previous 3GPP standards, the increase is much less than widely believed, on the order of a factor of 2 versus HSPA according to a variety of industry and 3GPP documents. When technology advanced from the 2G GSM to the 3G Universal Mobile Telecommunication System (UMTS), higher network speed and faster download speed allowed real-time video calls. LTE and the subsequent LTE-A offered enhanced network capacity and reduced delay in application-server access, making triple-play traffic (data, voice, and video) access possible wirelessly, anytime anywhere. 4G truly constitutes mobile broadband. Although 3G was the first mobile broadband standard, it was originally designed for voice with some multimedia and data consideration, whereas 2G was intended as the first digital mobile voice communication standard for

improved coverage. The data rate has improved from 64 kbps in 2G to 2 Mbps in 3G and 50–100 Mbps in 4G. 5G is expected to enhance not only the data transfer speed of mobile networks but also the scalability, connectivity, and energy efficiency of the network. It is assumed that by 2020, 50 billion devices will be connected to the global IP network, which would appear to present a challenge. To address this challenge, there has been growing interest in cellular systems for the so-called millimetre wave (mmW) bands, between 30 and 300 GHz, where the available bandwidths are much wider than today's cellular networks. The available spectrum at these higher frequencies can be easily 200 times greater than all cellular allocations today that are largely constrained to the prime RF real estate under 3 GHz. However, the development of cellular networks in the mmW bands faces significant technical obstacles, and the feasibility of mmW cellular communication requires in depth analysis propagation pathloss models are used to help engineers design, deploy, and compare candidate wireless technologies. Due to the importance of mmWave channel modelling and the novelty of using frequencies above 6 GHz for mobile communications, many researchers around the world during the whole last decade have embarked on sharing knowledge and producing channel models for operating frequencies ranging between 0.5–100 GHz. Finally 3GPP come up with channel model definitions for frequencies ranging between 0.5–100 GHz in Release 17. Therefore, we compared the performance of 5G systems using these various channel models of literatures and 3GPP channel model as well. Nevertheless, our methodology can be extended to other models. The purpose of this work is to not create channel models, rather to construct a real world 5G HetNet scenarios with important considerations as urban teledensity and try to determine the best suited model and selection of operating frequencies as well.

Massive boost in data traffic demand and inconsistent user's behaviour have necessitated modern cellular networks to evolve toward multitier heterogeneous architectural framework consisting of macro and small cells to accommodate ever-increasing user's density. Literature survey reveals that the deployment of additional small cells can encounter the booming coverage, capacity, and QoS constraints by maintaining the overall operational cost of the network. However, most of the works are mainly confined to two-tier network having one tier of macro eNBs and another tier of small cell eNBs. However, in reality, in this era of massive real estate



development in major cities, small cells deployed in urban areas need further categorization into outdoor small cells served by urban micro (UMi) eNBs and indoor small cells served by indoor hotspots (InH). 3GPP too in their TR 38.901 version 16.1.0 Release 16 document has published separate channel models for frequencies from 0.5 to 100 GHz for Urban Macro (UMa) and two different small cell deployment scenarios i.e. UMa and InH based on both line of sight (LoS) and non-line of sight (nLoS) propagation scenarios. Hence, in this work, finally a three-tier UDHN model consisting one tier of MeNBs and two-tiers of SeNBs is proposed for the coverage and rate analysis in designing deployment architecture in Indian urban scenarios. Comparative results among several cases having different combination of 5G frequency bands are analyzed which advocates that the proposed three-tier UDHN serves as an effective solution to guarantee QoS in terms of improved coverage and rate.

Ultra-dense Heterogeneous Network (UDHetNet) consisting of densely deployed small cells eNodeB (SeNB) underlaying traditional macro cell eNodeB (MeNB) are the emerging network architectures for increase user handling capacity, higher throughput, extended coverage. However, ultra-dense deployment of small cells is expected to elicit a possible escalation of network energy consumption which not only stirs up the operating expenditure (OPEX) of the mobile operators but also trivially increases the carbon footprint contributed by mobile communication industry on global climate. To this end, this work first identifies the deployment strategies for small cells that embarks sustainable green communication (SGC) one of the challenging problems in 5G wireless networks and beyond. Further to this, we present the SGC techniques used in wireless HetNets and discuss their individual importance for a sustainable green future. Based on the detailed literature survey, we find Strategic Sleeping Policy (SSP) and Energy Harvesting (EH) Techniques as most promising solution. Hence, in this work, we present Strategic Sleeping Policy (SSP) of the SeNBs based on M/M/1 queuing theory and investigate its impact in reducing the power consumption of the proposed HetNet based on performance metrics like Energy Efficiency (EE) and Area Energy Consumption Ratio (AECR). Further, we also introduce a novel Sleep Cycle Modulated Energy Harvesting (SCMEH) Technique, for SeNBs to ensure proper utilization of energy resources. An analytical model based on Continuous Time Markov Chain (CTMC) is also developed to evaluate the Energy

*Utilization (EU) of the proposed SCMEH methodology. The comprehensive performance analysis reveals that the SCMEH enabled SeNBs under HetNet can not only guarantee QoS requirements under concurrent time varying urban tele-traffic condition but also ensure Sustainable Green Communication (SGC) by radically controlling the estimated power consumption on hourly basis throughout a day.*

# Table of Contents

List of Publications.....	i
Statement of originality.....	vi
Certificate from supervisor.....	viii
Acknowledgement.....	xii
Abstract.....	xiv
Table of Content.....	xx
List of Figures.....	xxiv
List of Tables.....	xxx
List of Abbreviations and Acronyms.....	xxxii
<b>Chapter 1 Introduction.....</b>	<b>1</b>
1.1 Overview of the research problem.....	1
1.2 Motivation.....	22
1.3 Contributions embodied in this thesis.....	23
1.4 Thesis organization.....	27
<b>Chapter 2 Background study.....</b>	<b>31</b>
2.1 Introduction.....	31
2.2 Radio Resource Management Techniques in BWA Networks.....	32
2.3 Deployment of Small Cells: Introduction to Heterogeneous Networks (HetNet).....	37
2.4 The fundamental limit of network densification.....	40
2.5 Sustainable Green Communication Techniques in HetNet.....	44
2.6 Chapter Summary.....	47
<b>Chapter 3 A Joint Call Admission Control and Dynamic Bandwidth Allocation Techniques for Capacity and QoS analysis in LTE based BWA HetNet.....</b>	<b>49</b>
3.1 Abstract.....	49
3.2 Introduction.....	50
3.3 System Model.....	53
3.3.1 Class Based QoS Framework.....	53
3.3.2 Scenario Description.....	54
3.3.3 Bandwidth Allocation.....	59
3.3.4 RSS Calculation.....	59
3.4 Joint CAC and DBA scheme: The Proposed Algorithm	61

3.4.1	RSS based JCACDBA scheme.....	61
3.4.2	SINR based JCACDBA scheme.....	66
3.5	CTMC based analytical model.....	68
3.6	QoS metrics for performance evaluation.....	71
3.7	Performance Evaluation.....	74
3.8	Chapter summary.....	86
<b>Chapter 4</b>	<b>Designing SPP based deployment models for k-tier 5G HetNet: pathloss, coverage and rate analysis.....</b>	<b>89</b>
4.1	Abstract.....	90
4.2	Introduction.....	90
4.3	SPP based stochastic modeling of k-tier HetNet.....	95
4.3.1	Binomial Point Process (BPP).....	95
4.3.2	Poisson Point Process (PPP).....	95
4.3.2.1	Homogeneous PPP.....	96
4.3.2.2	Non Homogeneous PPP.....	96
4.4	Tired Deployment of HetNet.....	99
4.4.1	One-Tier.....	99
4.4.2	Two-Tier.....	100
4.4.3	Three-Tier.....	102
4.5	Location optimization of SeNBs via k-means clustering algorithm.....	104
4.6	Pathloss model.....	106
4.6.1	4G Pathloss model-3GPP Rel. 9.....	107
4.6.2	CI/ABG pathloss model leading to 5G.....	108
4.6.3	5G pathloss model – 3GPP Rel. 16.....	109
4.7	Performance Metrics.....	110
4.7.1	SINR expression.....	110
4.7.2	Coverage Probability.....	111
4.7.3	Average Rate.....	111
4.8	Performance Evaluation.....	111
4.8.1	One-Tier.....	111
4.8.2	Two-Tier.....	115
4.8.3	Three-Tier.....	122
4.9	Chapter summary.....	126

<b>Chapter 5</b>	<b>Finding Optimal Small Cell Densities in Ultra Dense k- tier HetNet for Improved Area Spectral Efficiency.....</b>	<b>129</b>
5.1	Abstract.....	129
5.2	Introduction.....	130
5.3	System Model.....	134
5.3.1	Modeling Hourly User Arrival in Urban Scenario.....	134
5.3.2	Modeling a two-tier HetNet using clustered NHPPP.....	135
5.4	Determining the regime of optimal SeNB Density.....	137
5.5	Pathloss models (3GPP TR 38.901 version 16.1.0 Release 16).....	138
5.6	Distribution of SINR at random user locations.....	139
5.7	Designing QoS Metric: Area Spectral Efficiency.....	140
5.8	Performance Evaluation.....	141
5.9	Chapter summary.....	145
<b>Chapter 6</b>	<b>Developing Sustainable Green Communication Techniques for real time urban teletraffic for Heterogeneous Cellular Network: Extensive Performance Evaluation.....</b>	<b>147</b>
6.1	Abstract.....	147
6.2	Introduction.....	148
6.3	System Model.....	151
6.3.1	User arrival modelled by PAP.....	151
6.3.2	Three-Tier UDHN.....	151
6.4	Sustainable Green Communication (SGC) Techniques	156
6.4.1	Power consumption scenario of network elements of three-tier UDHN.....	157
6.4.2	Introduction to Strategic Sleeping Policy.....	158
6.4.3	Energy Harvesting Methodologies.....	159
6.4.4	Analytical Model for Performance evaluation..	162
6.4.5	Performance metrics for SGC.....	163
6.5	Performance evaluation.....	164
6.6	Chapter Summary.....	171
<b>Chapter 7</b>	<b>Conclusion and Future Scope.....</b>	<b>173</b>
7.1	Conclusion.....	173
7.2	Future Scope.....	176

<b>Bibliography</b> .....	179
<b>Appendices</b> .....	196

# List of Figures

1.1	Evolutions of Wireless Standards.....	2
1.2	Convergence of Wireless Technologies.....	5
1.3	5G use cases.....	7
1.4	5G key capabilities.....	9
1.5	Estimated user count across different technologies.....	9
1.6	Growth of Internet user (a) Global scenario (in Billions) (b) Indian Scenario (in Millions).....	10
1.7	Radio Network Planning Process.....	12
1.8	The heterogeneous network: a combination multi-tier radio access nodes.....	13
1.9	Coverage v/s capacity plot for different types of deployment environment.....	14
1.10	A typical three tier HetNet consisting one tier of MeNB and Two tiers of SeNBs.....	15
1.11	UN sustainable development goals (SDG) framework.....	20
3.1	LTE QoS Framework.....	28
3.2	Single MeNB based traditional network scenario.....	55
3.3	One MeNB and two SeNB based HetNet scenario.....	56
3.4	Multi-hop Relay Assisted HetNet Scenario.....	57
3.5	One MeNB and Three SeNB based HetNet Scenario.....	57
3.6	One MeNB and four SeNB based HetNet scenario.....	58
3.7	Flow chart of CAC policy considering single MeNB in isolation.....	62
3.8	Flow chart of CAC policy for Multihop Relay assisted Two Tier HetNet.....	63
3.9	Flow chart of Joint CAC and SBA policy for Two Tier HetNet.....	65
3.10	Flow chart of Joint CAC and DBA policy for Two Tier HetNet.....	65
3.11	Flow chart of SINR based Joint CAC and DBA policy for Two Tier HetNet.....	68
3.12	Generalized State Transition Diagram of the CTMC Model.....	69
3.13	3D State Transition Diagram of the CTMC Model.....	70
3.14	Analytical results of the comparison between JCAC-SBA for One MeNB and one MeNB with two SeNBs. (a) NCBP (b) HCDP (c) BU.....	75
3.15	Analytical results of the comparison between JCAC-SBA and JCAC-DBA	

	for one MeNB with two SeNB. (a) NCBP (b) HCDP (c) BU.....	77
3.16	Analytical results of the comparison between one MeNB with two ReNB and one MeNB with two SeNB a. NCBP b. HCDP c. BU....	78
3.17	Analytical results of the comparison between JCAC DBA for One MeNB with Two SeNB and one MeNB with Three SeNBs (a) NCBP (b) HCDP (c) BU.....	80
3.18	Analytical results of the comparison between JCAC DBA for One MeNB with Three SeNB and one MeNB with Four SeNBs. (a)NCBP (b) HCDP (c) BU.....	81
3.19	System capacity in terms of no. of users admitted with varying scenario conditions.....	82
3.20	Comparison among different scenario based on BU.....	83
3.21	Analytical results of the comparison between CAC in One MeNB and JCAC-DBA in one MeNB with three SeNB. (a) NCBP (b) HCDP (c) BU.....	84
3.22	Comparative results between One MeNB v/s One MeNB with Three SeNBs for SINR based JCAC-DBA (a)NCBP (b)HCDP (c)COP (d)BU.....	85
4.1	Thinning of a SPP.....	97
4.2	Comparisons between HPPP and NHPPP in terms of density of data points by varying mean of PPP.....	99
4.3	Projection for UE growth along with eNB density deployed by different SPPs in Indian context upto 2019.....	100
4.4	Generalized year wise deployment scenario of typical DenSNet in a geographical region of 6.25 Sq. km. Black Crosses Blue dots denote the eNBs and UEs respectively.....	100
4.5	A typical two-tier Het-Net consisting MeNB and SeNBs.....	101
4.6	Coverage regions of a Het-Net in a 2500 sq. m geographical area based on 2D NHPPP (a) Urban Scenario (UE density ~153 %) (b) Sub-urban scenario (UE density ~90 %).....	102
4.7	A typical three tier UDHN consisting one tier of MeNB and two tiers of SeNBs.....	103
4.8	Coverage areas of a three-tier UDHN in a 7000 sq. m terrain based on SCHPPP: Indian urban Scenario (UE density ~143.38 %). ....	103
4.9	Coverage regions in a 2500 sq.m. Geographical area based on Clustered NHPPP Het-Net. a. Urban (UE density 153% approx.) b. Suburban (90% approx.).....	106
4.10	Distance definition as per 3GPP TR 38.901.....	110
4.11	Year wise Coverage Probability analysis for a. HPPP b. NHPPP c. BPP.....	112
4.12	Year wise Average Rate analysis for a. HPPP b. NHPPP c. BPP.....	113



4.13	Performance Analysis of different SPPs in terms of CP for the year a. 2011 b. 2015 c. 2019.....	113
4.14	Performance Analysis of different SPPs in terms of CP for the year a. 2011 b. 2015 c. 2019.....	114
4.15	a. Coverage Probability and b. Average rate comparisons by varying MeNB to SeNB ratio in Indian Sub Urban scenario.....	116
4.16	a. Coverage Probability and b. Average rate comparison by varying MeNB to SeNB ratio in Indian Urban scenario.....	117
4.17	a. Coverage Probability and b. Average rate comparison between HPPP, NHPPP, Clustered NHPPP in Indian Sub Urban scenario.....	118
4.18	a. Coverage Probability and b. Average rate comparison between HPPP, NHPPP, and Clustered NHPPP in Indian Urban scenario.....	118
4.19	a. Coverage Probability and b. Average rate comparison between HPPP of [57] and proposed K-means Clustered NHPPP in Indian Urban scenario.....	119
4.20	a. Coverage Probability and b. Average rate comparison between HPPP of [57] and proposed K-means Clustered NHPPP in Indian Sub Urban scenario.....	119
4.21	Comparison between 5G and other pathloss models (a) CP and (b) Rate.....	122
4.22	Case 1: Performance comparison between different deployment Model a. CP b. AR.....	124
4.23	Case 2: Performance comparison between different deployment Model a. CP b. AR.....	124
4.24	Case 3: Performance comparison between different deployment Model a. CP b. AR.....	125
4.25	Comparison between different case studies considering three tier scenario.....	125
5.1	Growth of Internet users in India (in million).....	130
5.2	A Two-Tier HetNet.....	132
5.3	Enhancement of key capabilities from IMT-Advanced to IMT-2020	132
5.4	Hourly Arrival of UEs in the region of Kolkata.....	135
5.5	Generalized Graphical representation of UDHetNet in a 2500 m <sup>2</sup> Urban Region modelled by NHPPP.....	137
5.6	Generalized Graphical representation of Clustered (K means) HetNet in a 2500 m <sup>2</sup> urban region modeled by Clustered NHPPP.....	137
5.7	Distance definition as per 3GPP TR 38.901.....	139
5.8	Hourly VRC (/CH) values with respect to number of Clusters.....	141
5.9	Hourly Optimal Cluster Density.....	141

5.10	Estimated hourly modeling of a Indian Urban Scenario (Kolkata) as Two-Tier Het-Nets.....	142
5.11	Comparative analysis of hourly ASE of HetNet under Indian Urban Scenario (City of Kolkata).....	143
5.12	Mean ASE: MeNB vs HetNet.....	145
5.13	PI in ASE UDHetNet over MeNB.....	145
6.1	User Arrival Modeled by PAP.....	151
6.2	A typical three-tier UDHN.....	152
6.3	Distribution of UMa eNBs by HPPP.....	152
6.4	Distribution of two-tier HetNet by clustered NHPPP.....	153
6.5	Schematic concept of the formation of clusters in MCP.....	154
6.6	Distribution of three-tier UDHN by MCP.....	155
6.7	Estimated hourly modeling of a Indian Urban Scenario (Kolkata) as Three-tier UDHN modeled by HPPP, NHSCPPP and MCP in a 7000 sq. m geographical area with UE density ~143.38 % considering ratio of MeNB to SeNB density as 1:8.....	155
6.8	Time slot allocation of Serving Small cell eNBs.....	160
6.9	The protocol of energy harvesting for one SeNB.....	160
6.10	Generalized State Transition Diagram of the CTMC Model for EH analysis.....	163
6.11	Comparative EE analysis (hour-wise).....	165
6.12	Performance Improvement w.r.t EE: Het-Net than MeNB in %.....	165
6.13	Performance Improvement w.r.t EE: Two-tier Het-Net-SSP v/s Two-tier Het-Net (w/o SSP) in %.....	165
6.14	Performance Improvement w.r.t EE: two-tier HetNet-SSP v/s three-tier UDHN w.r.t EE in %.....	165
6.15	Performance Improvement w.r.t EE: three-tier UDHN-SSP v/s two-tier HetNet-SSP w.r.t EE in %.....	165
6.16	Comparative AECR analysis (hour-wise).....	167
6.17	Performance Improvement w.r.t AECR: Het-Net than MeNB in %....	167
6.18	Performance Improvement w.r.t EE: two-tier Het-Net-SSP v/stwo-tier Het-Net (w/o SSP) in %.....	167
6.19	Performance Improvement w.r.t EE: two-tier HetNet-SSP v/s three-tier UDHN in %.....	167
6.20	Performance Improvement w.r.t EE: three-tier UDHN-SSP v/s two-tier HetNet-SSP in %.....	168
6.21	Hourly Mean EU of Traditional MeNB.....	169
6.22	Two hourly EU variation in Traditional MeNB.....	169

6.23	Hourly Mean EU of three-tier UDHN with deterministic energy allocation (DEA).....	169
6.24	Two hourly EU variation in three-tier UDHN with DEA .....	169
6.25	Hourly Mean EU of three-tier UDHN with SCM-EH .....	169
6.26	Two hourly EU variation in three-tier UDHN with SCM-EH .....	169
6.27	Comparative analysis of Mean EU: MeNB v/s UDHN-DEA vs UDHN-SCM-EH.....	170
6.28	Performance Improvement (in %) of three-tier UDHN with DEA over MeNB w.r.t Mean EU.....	170
6.29	Performance Improvement (in %) of three-tier UDHN with SCM-EH over three-tier UDHN with DEA w.r.t Mean EU.....	170
6.30	Performance Improvement (in %) of three-tier UDHN with SCM-EH over MeNB in w.r.t Mean EU.....	170



# List of Tables

3.1	Applications, types of traffic and QoS Parameters of LTE.....	54
3.2 a	Conditions for NCBP, HCDP in the network.....	72
3.2 b	Conditions for COP in the network.....	73
3.3	System parameters for numerical analysis of JCAC-DBA Algorithm	74
3.4	Performance Improvement of JCAC-SBA in One MeNB with two SeNBs compared to CAC in one MeNB (in %).....	76
3.5	Performance Improvement of JCAC-DBA over JCAC-SBA in One MeNB with two SeNBs (in %).....	76
3.6	Performance Improvement One MeNB with two SeNBs over One MeNB (in %) with Two ReNBs w.r.t. JCAC-DBA (in %).....	79
3.7	Performance Improvement implementing JCAC- DBA Algorithm in one MeNB with three SeNBs over One MeNB with two SeNBs (in %).....	79
3.8	Performance Degradation of one MeNB with three SeNBs compared to One MeNB with Four SeNBs for DBA Algorithm (in %).....	82
3.9	Performance improvement implementing JCAC-DBA in one MeNB with three SeNBs over CAC in One MeNB (in %).....	83
3.10	Performance % improvement in SINRCAC in Het-BWA-Nets.....	86
4.1	Coefficients in the ABG and CI model.....	109
4.2	Pathloss model for different scenarios: Uma, UMi.....	109
4.3	Scenario considerations and simulation parameters for CP and AR analysis of different SPPs.....	112
4.4	Year-wise % Improvement of CP and AR of different SPPs.....	115
4.5	Performance improvement in terms of CP and AR among HPPP, NHPPP, and Clustered NHPPP in percentage.....	119
4.6	Performance improvement of proposed Clustered NHPPP compared to basic HPPP of [57] in terms of CP and AR.....	121
4.7	Scenario considerations and Simulation parameters for pathloss evaluation.....	121
4.8	Comparison of 5G pathloss model with the rest.....	122
4.9	Scenario considerations and Simulation parameter for three-tier UDHN performance evaluation.....	123
4.10	Performance improvements of Coverage and Rate for three-tier Scenario.....	126
5.1	3GPP TR 38.901 Pathloss model for different scenarios.....	138

6.1	Load dependencies of different types of eNB.....	158
-----	--	-----

# List of Abbreviations and Acronyms

Abbreviations	Descriptions
1G	First-generation mobile technology
1xEVDO	1xEvolution-Data Optimized
2G	Second-generation mobile technology
3G	Third-generation mobile technology
3GPP	Third-generation partnership project
4G	Fourth-generation mobile technology
5G	Fifth-generation mobile technology
ABG	Alpha-Beta-Gamma
ADSL	Asymmetric Digital Subscriber Line
AECR	Area Energy Consumption Ratio
AMPS	Advanced Mobile Phone System
AP	Access Point
AR	average rate
ASE	Area Spectral Efficiency
BE	Best effort
BPP	Binomial point process
Bps	Bits per second
BSs	base stations
BU	Bandwidth Utilization
BWA	Broadband wireless access network
CAC	Call admission control
CAGR	compounded annual growth rate
CBP	Call Blocking Probability
CDF	cumulative distribution function
CDMA	Code Division Multiple Access
CDMA 2000	Code Division Multiple Access 2000
CH	Calinski and Harabasz
CI	close –in
CP	coverage probability

Abbreviations	Descriptions
CSG	Closed Subscriber Group
CTMC	Continuous Time Markov Chain
DBA	Dynamic bandwidth allocation
EDGE	Enhanced Data Rate For GSM Evolution
EE	energy efficiency
EH	Energy Harvesting
e-mail	<i>Electronic mail</i>
eMBB	Enhanced Mobile Broadband
eNB	eNodeB
EPC	Evolved packet core
EU	Energy Utilization
FDMA	Frequency Division Multiple Access
FPC	Fractional Power Control
FSB	Femto-sharing bandwidth
FTP	File Transfer protocol
FUE	Femto User Equipment
Gbps	Giga bits per second
GBR	Guaranteed bit rate
GHG	greenhouse gas
GSM	Global System for Mobile Communications
HCDP	Hand off Call Dropping Probability
HeNB	Home eNB
HetNet	Heterogeneous network
HPPP	Homogeneous Poisson Point Process
HSDPA	High-Speed Downlink Packet Access
HSUPA	High-Speed Uplink Packet Access
ICT	Information and communication technologies
IEEE	Institute of Electrical and Electronics Engineers
IMT-2020	International Mobile Telecommunications 2020
IMT-A	International Mobile Telecommunications Advanced
InH	Indoor Hotspots
IoT	Internet of Things



Abbreviations	Descriptions
IS 95	Interim Standard 95
ITU-R	ITU Radiocommunication Sector
JCAC-DBA	Joint CAC and DBA
LOS	line of sight
LTE	Long Term Evolution
LTE A	Long Term Evolution Advanced
Mbps	Mega bit per second
MCP	Matérn cluster process
MDB	Macro-dedicated bandwidth
MeNB	Macro Cell eNB
MHz	Mega hertz
MIMO	multiple-input and multiple-output
mMTC	Massive Machine-Type Communications
ms	Milliseconds
MUE	Macro user equipment
NCBP	New Call Blocking Probability
NHPPP	Non-Homogeneous Poisson Point Process
nLOS	non-line of sight
non-GBR	Non-guaranteed bit rate
nrtPS	Non-Real-Time Polling Service
NSP	network service providers
OFDM	orthogonal frequency division multiplexing
OFDMA	orthogonal frequency division multiple access
OPEX	Operating Expenses
PDN-GW	Packet data network-gateway
PCP	Poisson Cluster process
PPP	Poisson point process
QCI	QoS class identifier
QoS	Quality of Service
RAN	Radio Access Network
RAT	Radio Access Technology
ReNB	Relay eNB

Abbreviations	Descriptions
RF	Radio Frequency
RRM	Radio Resource Management
rtPS	Real-Time Polling Service
SCHPPP	spatially clustered homogeneous poisson point process
SCs	small cells
SCMEH	Sleep Cycle Modulated Energy harvesting
SeNB	Small Cell eNB
SGC	sustainable green communication
SINR	Signal-to-Interference-plus-Noise Ratio
SPP	spatial point process
SSP	strategic sleeping policies
SWIPT	Simultaneous Wireless Information and Power Transfer
TACS	Total Access Communication System
TCP	Thomas Cluster Process
TDMA	Time Division Multiple Access
UDHetNet	Ultra Dense HetNets
UE	User's Equipments
UGS	Unsolicited Grant Service
UHD	Ultra-High Definition
UMa	Urban Macro cell
UMi-SC	Urban Micro cell
UMTS	Universal mobile telecommunication system
UN SDG	United Nations sustainable development goals
URLLC	Ultra-Reliable and Low-Latency Communications
VoIP	Voice over Internet protocol
VRC	variance ratio criterion
WCDMA	Wireless Code Division Multiple Access
WiMAX	Worldwide Interoperability for Microwave Access
WP5D	Working Party 5D
WPT	Wireless Power Transfer
WRC-19	2019 World Radio-communication Conference

# Chapter 1: Introduction

---

## **Outline of this chapter**

- 1.1 Overview of the Research problem
- 1.2 Motivation
- 1.3 Contributions embodied in this thesis
- 1.4 Thesis organization

## 1.1 Overview of the Research problem

Mobile wireless technology has gradually become an inseparable companion in day-to-day human life. Be it voice, video, or text, the method of communication has been revolutionized by the boon of mobile internet. The continuing growth of wireless technology has not only facilitated to improve the quality of life but also raised the demand for a better quality of service, which enables our modern living. The various conveniences the modern world avails of today are some or the other way facilitated by mobile internet. Any random mobile user is now connected to the rest of the world through some means of communication medium, which carries a reasonable amount of data/information back and forth. In fact, the accessibility of mobile internet services is nowadays considered to be a very basic amenity for modernized society [1].

During the first decade of the 21<sup>st</sup> century, billions of cellular users have adopted the Global System for Mobile (GSM) cellular standard primarily for voice communication along with some amateur internet-based applications. The onset of the mobile internet and packet-switched data networks has steered an escalating demand for ubiquitous data access over mobile wireless networks. This has enabled a rapid advancement of wireless technology from traditional voice communication to internet-based multimedia applications. In the process, the subsequent generations of wireless standards have also evolved to sustain the high-data-rate wireless ecosystem, which essentially has given birth to the third, fourth, and fifth generations of wireless standards, abbreviated as 3G, 4G, and 5G respectively. Underneath, we have illustrated some salient features of different wireless standards associated with each

generation of wireless evolution [2]. The evolution of mobile wireless standards is illustrated in Fig. 1.1.

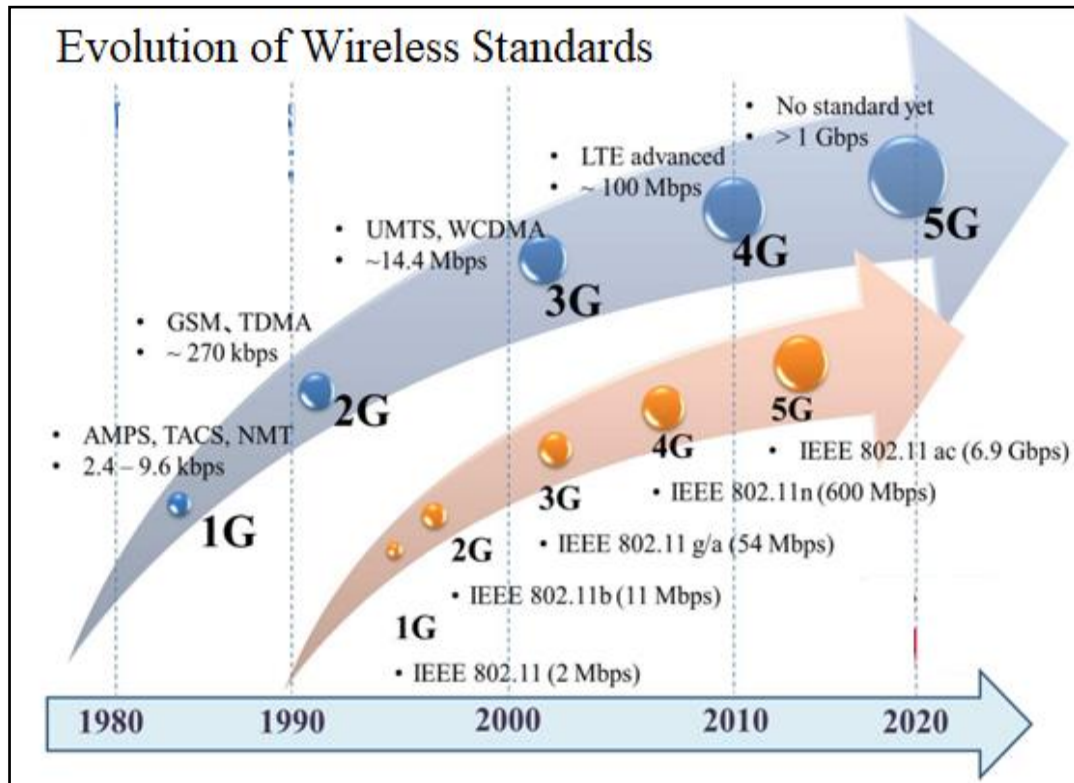


Figure 1.1 Evolutions of Wireless Standards [1-3]

The family of 2G wireless standards started to evolve around the early 1990s which brought some significant improvement over naïve 1G standards which supported only analog voice [3]. The main 2G standard, GSM, was initially proposed with the aim to provide improved access to communication mediums across the globe. While GSM [4] uses a combination of Frequency Division Multiple Access (FDMA) and Time Division Multiple Access (TDMA), IS-95 [3-6] is based on code division for multiple access (CDMA). They are primarily used for voice communication rates of around 10 kbps. However, the later add-on standards of General Packet Radio Service (GPRS) [7] that provides packet-switched core network and enhanced data for GSM evolution (EDGE) [8] uses advanced modulation and channel coding techniques. It was proposed with an idea of increasing the data rates over cellular networks to provide low-speed data access such as the Internet, e-mail, etc, to users with mobile devices [3, 8]. As discussed above, the data rates supported by such nascent data access standards were in the range of 100 kbps [8]. The increasing

demand for higher data rates over mobile devices led to the development of the 3G cellular standards described below [3].

The third generation, or 3G wireless standard or IMT 2000 [9], was proposed around the year 2000 and primarily based on CDMA technology that was designed to provide higher speed, high data rate, and better QoS [10]. 3G used a circuit-switched network for voice calls and packet switched network for data services. 3G standards are also labelled as wideband technologies as they use bandwidth in excess of 5 MHz [9, 10]. It also enabled the global roaming of subscribers for the first time. The 3G standard of wideband code division for multiple access (WCDMA) is also termed as the Universal Mobile Telecommunications System (UMTS) [11]. Another derivative of 3G is the CDMA 2000 standard, initially deployed in North America, Japan, and some other countries [12]. Both technologies are capable of providing data rates of around 300 kbps [13]. The increasing demand for higher data rates led to the evolution of High-Speed Downlink Packet Access (HSDPA) [14] and High-Speed Uplink Packet Access (HSUPA) [14]. These upgraded versions of 3G standards enabling data rates in the range of 5–30 Mbps [15] are able to provide services similar to those available on the Digital Subscriber Line (DSL) and Asymmetric Digital Subscriber Line (ADSL) available on the wired network infrastructure [14-15]. Further, the CDMA 2000 suite was also extended to embrace the 1x Evolution Data Optimized (1xEVDO) standard and its further revisions titled as rev. A and rev. B to boost the data rates as close as 30 Mbps [16]. Thus, the 3G family of cellular services built upon the above set of standards can provide data rates in excess of 10 Mbps, making it possible to transmit data demanding multimedia and video information through mobile devices [9-16]. However, the data rates are still expected to increase even further by several manifolds in 4G cellular networks [17].

The onset of 4G wireless standards is primarily based on the ground-breaking fresh technology named Orthogonal Frequency Division Multiplexing (OFDM) along with the multiple access technology termed as Orthogonal Frequency Division for Multiple Access (OFDMA) [17]. It was the era of 4G when the world gets familiar with another breakthrough technology termed Multiple-Input Multiple-Output (MIMO) [17, 18], which basically refers to employing multiple antennas at the transmitter and receiver in such systems. These flabbergasting advancements aided 4G wireless systems to achieve data rates in excess of 100 Mbps [19]. With the evolution of 4G

technology, the increased demand for heterogeneous services such as real-time video streaming, video conferencing, Voice over IP, online gaming, web browsing has led to the popularity of Broadband Wireless Access (BWA) technology [20], namely, Worldwide Interoperability for Microwave Access (WiMAX) [21-22], 3rd Generation Partnership Project (3GPP) Long Term Evolution (LTE) and LTE Advanced (LTE A) [23-25]. LTE and LTE A are the standards introduced by the 3GPP [23-25] standardization body while WiMAX is under the purview of the WiMAX forum [20]. The 4G wireless standards were designed to fulfil the requirements of IMT Advanced (IMT-A) [26] such as providing multimedia services with high data rates up to 50 Mbps [27] and wide coverage area, as well as all-IP with security and Quality of service (QoS) support [28].

The broad classifications of WiMAX are based on mobility. Initially, two versions of WiMAX were released, namely, Fixed WiMAX or 802.16d and Mobile WiMAX or 802.16e released in 2004 and 2006 respectively. These so-called 4th generation wireless technologies can provide the platform and facilitate many sophisticated multimedia applications simultaneously. For example, four different types of services are defined in the 802.16d-WiMAX standard, which include UGS (Unsolicited Grant service), rtPS (Real-time Polling Service), and nrtPS (Non-real-time Polling Service) and BE (Best Effort) [29-31]. These services come under different QoS classes directly depending upon the nature of the service. The UGS is designed to support real-time service flow with a fixed bit rate that generates fixed-size data periodically, such as T1/E1, and VoIP [29-31]. The rtPS is designed to generate variable-size data, such as video streaming services whereas the nrtPS deals with File Transfer Protocol (FTP) in a similar fashion [29-31]. Considering the variety and complexity of modern day's communication systems, the level of QoS flows in terms of different services is determined by a bearer. A bearer is a series of packet flows established between the packet data network gateway (PDN-GW) and the user equipment (UE). A bearer is assigned a unique value referred to as a QoS class identifier (QCI). The QCI determines the specific class of the bearer [28].

On the other hand, 3GPP LTE, an evolution of HSPA, quietly took the center stage among the other 4G technology in the mid-2000s. The 4G LTE technology was primarily developed for packet-data support and unlike the 3G where HSPA was just a mere “add-on” to offer high-performance packet data service on top of the existing

technology [23]. Mobile broadband multimedia services were the key focus, with hard requirements on higher data rates, truncated latency, and improved capacity. A completely fresh core network architecture was also developed, known as Enhanced Packet Core (EPC) [24, 32] that eventually replaced the architecture used by GSM and WCDMA/HSPA. The first version of LTE was a part of 3GPP release 8 specifications and commercially deployed in late 2009, followed by a rapid and worldwide deployment of LTE networks [32]. Unlike previous generations for which there have been numerous competing technologies, LTE had been accepted worldwide as a single technology (see Fig. 1.2).

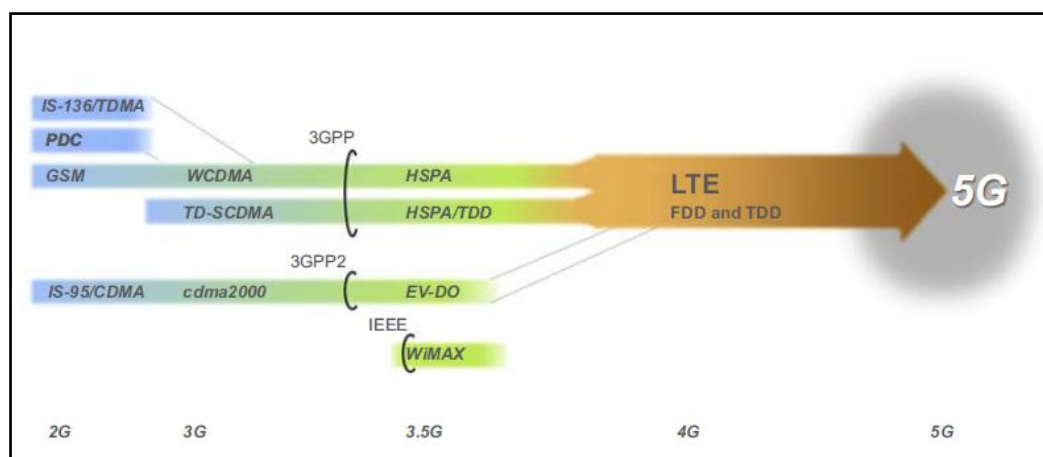


Figure 1.2 Convergences of Wireless Technologies [32]

Ever since its commercial inception in 2009, LTE has progressed significantly in terms of data rates, capacity, spectrum management and deployment strategies, and application width [32]. From macro-based deployments with peak data rates of 300 Mbps in 20 MHz of spectrum, the evolution of LTE in release 13 can provide several-Gbit/s peak data rates through developments in terms of antenna technologies, multisite synchronization, utilization of fragmented as well as unlicensed spectrum and network densifications just to mention a few areas [32, 33]. The evolution of LTE has also significantly broadened the use cases beyond mobile broadband by, for example, the introduction of massive machine-type communication and direct device-to-device communication.

3GPP LTE-A which was also appeared to be a significant improvement over its IEEE counterpart IEEE 802.16e i.e. mobile WiMAX (which used to operate with 40 MHz bandwidth at their disposal) drastically improves capacity coverage and ensured improved QoS using ultra-wide bandwidth of 100 MHz. In addition, LTE -A also

supports better mobility compared to mobile WiMAX. The QoS framework in LTE networks slightly differs from that of WiMAX [28]. There are mainly two types of bearers in LTE, namely guaranteed bit rate (GBR) and Non- Guaranteed bit rate (non-GBR) [28]. Similar to WiMAX different classes of services in LTE have different QoS requirements and thereby possess different QCI values [28]. Deployed in 2009 [23-25] LTE is leading over WiMAX [21-22] which is deployed and adopted in 2004 from different aspects like data rate, coverage, latency, spectrum efficiency, mobility, and QoS [28].

In the early 2010s, although, 3GPP LTE is still in the midst of adolescence, the industry was by now well on the move toward the next generation of mobile communication. In 2012, ITU-R WP5D set the platform for the succeeding generation of IMT systems, named IMT-2020 [34]. It has been a progress of the previous versions of IMT beyond the year 2020 and, in practice, commonly denoted as “5G,” the fifth generation of mobile standards [35]. The framework and objective for IMT-2020 is delineated in ITU-R Recommendation M.2083 [34, 35], often referred to as the “Vision” recommendation [36].

The current trends for IMT along with its future role have led to a set of use cases predicted for both human-centric and machine-centric communication, namely, Enhanced Mobile Broadband (eMBB), Ultra-Reliable and Low-Latency Communications (URLLC), and Massive Machine-Type Communications (mMTC) [34- 37]. These service verticals have extended the capabilities for IMT-2020. A first-hand feature envisioned for IMT-2020 is that it would be able to operate in potentially new frequency bands above 6GHz and beyond, including mm-wave bands [38]. At WRC-19, several new bands identified for IMT emerged as an outcome of agenda item 1.13 [39]. Three documents published late in 2017 further define the performance and characteristics of IMT-2020 and that are applied in the evaluation phase:

- **Technical requirements:** Report ITU-R M.2410 [34] outlines 13 minimum requirements related to the technical performance of the IMT-2020 radio interface(s).
- **Evaluation guideline:** Report ITU-R M.2412 [35] delineates the comprehensive method to evaluate the stringent requirements, including test environments, evaluation configurations, and channel models.



- **Submission template:** Report ITU-R M.2411 [40] delimits a meticulous template for submitting the aspiring technology for evaluation. It also specifies the evaluation benchmarks and prerequisites on service, spectrum and technical performance, based on the two aforementioned ITU-R reports M.2410 and M.2412.

With a series of innovative use cases being one key motive for 5G, ITU-R has demarcated three broad usage scenarios from the IMT Vision recommendation [41].

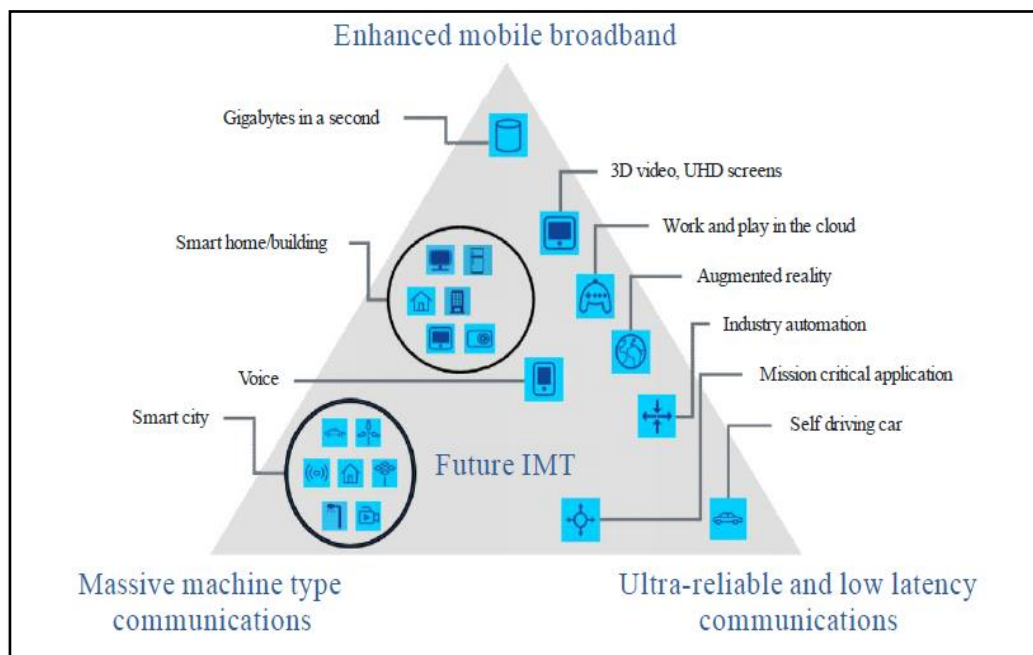


Figure 1.3 5G use cases [41]

- **Enhanced Mobile Broadband (eMBB)** corresponds to a more or less straightforward advancement of the mobile broadband services of previous technologies, supporting even higher data rates and superior user experience, for example, 3D video, UHD (Ultra-High Definition) screens, augmented reality, etc [41, 48].
- **Massive Machine-Type Communications (mMTC)** corresponds to services surrounded by a massive number of devices, for example, remote sensors, actuators, and monitoring of various equipments. Key demands for such services comprise very low device cost and energy consumption, permitting to very long device battery life. Typically, each device devours and spawns' moderate amount of data, i.e., support for eMBB is of less importance. Broad applications of this category are smart grid, smart home/building, smart cities, etc [41, 48].

- **Ultra-Reliable and Low-Latency Communications (URLLC)** type-of-services have been foreseen to prompt very low latency and extremely high reliability. Examples hereof are mission critical applications, remote surgery, traffic safety, automatic control, and factory automation [41, 48].

A broad classification of capabilities, usage scenarios, and applications for IMT-2020 was anticipated in the IMT 2020 Vision Document [41]. To aid various use cases and scenarios, the capabilities of IMT-2020, described in the following paragraphs, contained diverse significance and applicability. In addition, the limitations on network energy consumption and spectrum usage were considered. The following eight parameters are considered as the key capabilities of IMT-2020 [41]:

- **Peak data rate:** Peak data rate is defined as the maximum achievable data rate under ideal conditions per user in Gbps.
- **User experienced data rate:** It is defined as data rate that is achievable ubiquitously across the coverage area in Mbps or Gbps.
- **Latency:** The time dispersed between a source sends a packet to when the destination receives it (in ms).
- **Mobility:** It is defined as Maximum speed at which a defined QoS and seamless transfer of data/information between radio nodes which may belong to different layers and/or radio access technologies (multi-layer/-RAT) can be achieved (in km/h).
- **Connection density:** Total number of connected and/or accessible devices per unit area (per  $\text{km}^2$ ) is familiar as connection density.
- **Energy efficiency:** Energy efficiency refers to the quantity of information bits transmitted to/ received from users, per unit of energy consumption of the radio access network (RAN) (in bit/Joule) or vice versa.
- **Spectrum efficiency:** Average data throughput per unit of spectrum resource and per cell (Bps/Hz).
- **Area traffic capacity:** Total traffic throughput served per geographic area (in  $\text{Mbps/m}^2$ ).

IMT-2020 should be able to provide these capabilities without undue burden on energy consumption, network equipment cost and deployment cost to make future IMT sustainable and affordable. The key capabilities of IMT-2020 are shown in Fig. 1.4, compared with those of IMT-Advanced [41].

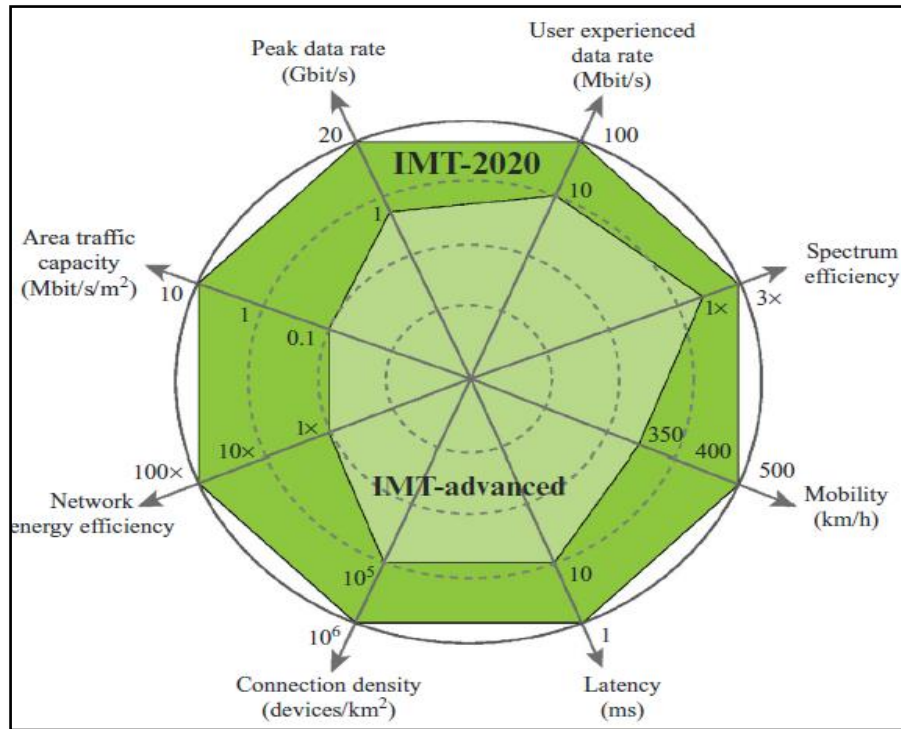


Figure 1.4 5G key capabilities [41]

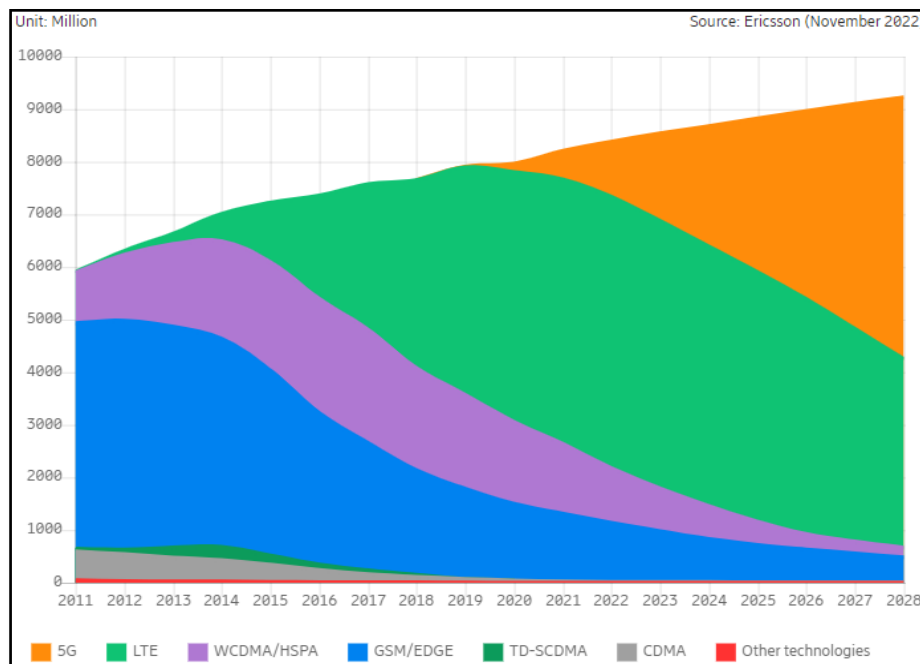


Figure 1.5 Estimated user count across different technologies [42]

With the unprecedented growth of Information and communication technologies (ICT) across generations of mobile technologies and the abundance of mobile devices like tablets, smartphones, and Internet of Things (IoT) devices facilitating multiple applications like smart sensing the indoor environment, live video streaming, conferencing, web browsing and image/video transfer spawn humongous amount of data traffic all around the world [42, 43]. According to a report published by Erricson [42], by the end of 2028, there will be 4.4 billion 5G subscriptions across the globe (refer to Fig. 1.5), accounting for 48 % of all mobile subscriptions. 5G will eventually turn out to be the principal mobile access technology by subscriptions in 2027. The 4G technology is estimated to reach 5.2 billion by the end of 2022 and then will decay to 3.6 billion by the end of 2028 as subscribers will continue to migrate into 5G. 3G subscriptions have declined by 41 million, while GSM/EDGE-only subscriptions dropped by 44 million during the Q3 of 2022 [42].

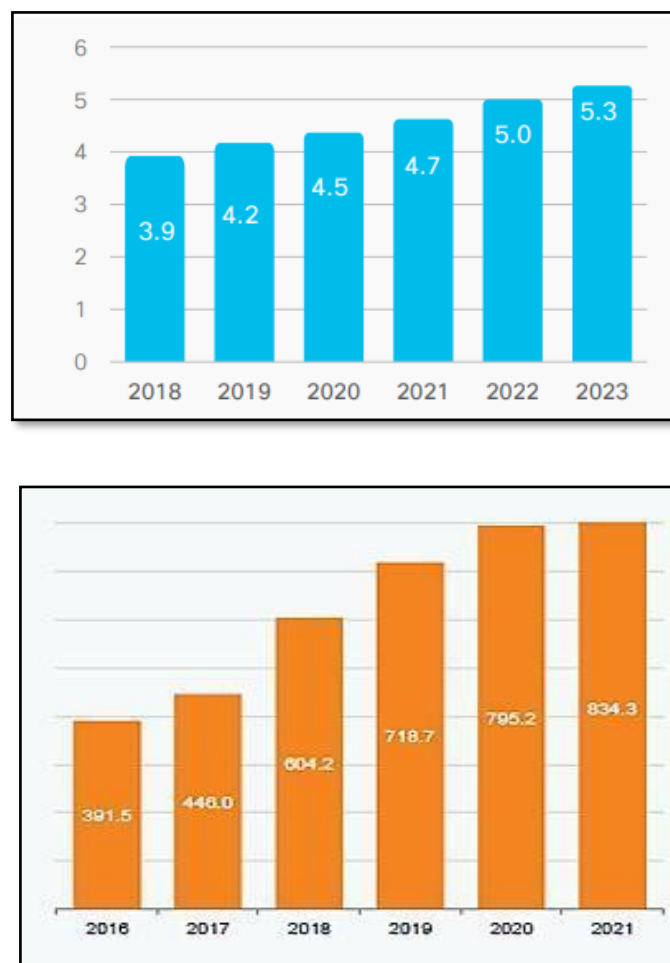


Figure 1.6 Growth of Internet user (a) Global scenario (in Billions) 2 (b) Indian Scenario (in Millions) [44]

According to another report published by CISCO [44], almost two-thirds of the global population that means 5.3 billion total users (i.e. 66% of the global population) will possess internet access by 2023 as shown in Fig. 1.6 (a) [44]. The report also claims that there will be 3.6 networked devices per capita by 2023 making the total number of networked devices climb up to 29.3 billion [44]. India being the second-largest telecommunication market has the second-highest number of internet users in the world. The population of internet users in the country has increased at a 13.38% of compounded annual growth rate (CAGR) from 391.5 million in 2016 to 834.3 million in 2021 (as shown in Fig. 1.6 (b)) [45]. The extent of internet users in the country is anticipated to stretch up even more to 900 million by 2025. India is projected to have 330 million 5G users by 2026 [45].

Ever since the initial phases of GSM development, radio network planning has sustained as one of the key areas to meet the ever-increasing demand from network operators and mobile users with issues related to better capacity and coverage [46]. Hence, Radio Network planning is the most important part of the whole network design owing to its proximity to mobile users. The prime focus of radio network planning is to provide a cost-effective solution for the radio network in terms of coverage, capacity, and quality [47]. The network planning method and design principles vary from region to region depending upon the dominating factor, which could be capacity, coverage, or resource [47].

The course of radio network planning begins with the collection of the input parameters such as frequency of operation, propagation models, capacity, coverage, and network quality [46, 47]. These inputs are then used to make the theoretical basis for resource management, coverage, and capacity plans. The radio resource management technique is the combination of (1) Resource Monitoring (2) Decision Making (3) Decision Enforcement. The coverage definition includes defining the coverage areas, service probability like call blocking, call dropping or outage, and related signal strength [46]. The capacity definition would include the subscriber and traffic distribution pattern in a particular geographical region, accessibility of the frequency spectrums, and frequency planning methods. The radio planner also needs information on the radio access system and the antenna system performance associated with it [47]. Fig 1.7 depicts the gradual building blocks of the Radio Network Planning Process.

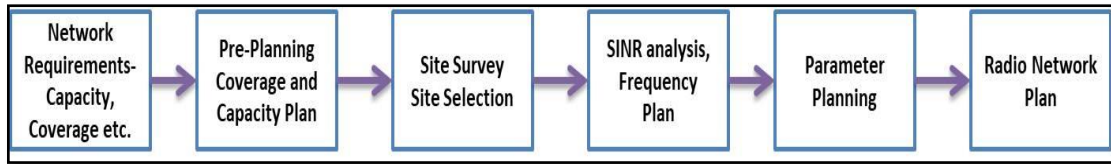


Figure 1.7 Radio Network Planning Process

In radio network planning, the land area is divided into three major classes: urban, suburban, and rural [47]. The division of these areas is based on human-made structures and natural terrains. The cells (sites) that are constructed in these areas can be classified as outdoor cells and indoor cells. Outdoor cells can be further sub-classified as macro-cellular and micro-cellular [47].

- **Macro Cell:** When the base station antennas are placed above the average rooftop level, the cell is called a macro-cell. As the antenna height is more than the average rooftop level, the area covered is wide. A macro-cell range may vary from a couple of kilometres to 35 km. The area covered depends upon the type of terrain and the propagation conditions. Hence, this concept is generally used for suburban or rural environments [49, 53].
- **Micro Cell:** When the base station antennas are placed below the average roof level, then the cell is a micro-cell. As the antenna height is less than the average rooftop level, the area covered by these kinds of cells is small making them micro-cells or small-cells. This kind of concept is applied to urban and suburban areas as the range of such cells is from a few hundred meters to a couple of kilometres [50, 53].
- **Pico Cell:** These are usually utilized for indoor coverage, i.e. coverage area is very small. They are defined as the same layer as micro-cells. They are operator-deployed cells, with lower transmission powers – typically an order of magnitude smaller – relative to macrocell eNodeBs. Typically installed in wireless hotspot areas (for example, malls) they provide access to all users [52, 53].
- **Femto Cell:** Femto cells that also called Home eNodeBs (HeNBs). They are low powered cells installed (typically indoors) by the end-consumer. HeNB access is classified either as a closed, hybrid, or as open access type. A closed-access HeNB maintains a Closed Subscriber Group (CSG) white list where

access is limited only to subscribed users (i.e. to UEs that are members of the CSG). Hybrid access HeNBs allow limited access to non-subscribed UEs but provide a differentiated higher quality of service to CSG users. Open access HeNBs provide undifferentiated access to all UEs. In Rel-10, the X2 interface is used between open-access HeNBs and between closed/hybrid access HeNBs with identical CSG IDs and between closed/hybrid HeNBs and open-access HeNBs [51].

- **Relay Nodes:** They are operator deployed and are primarily used to improve coverage in new areas (e.g. events, exhibitions, etc.). Unlike HeNBs and picocells that connect to the macrocell over X2 backhaul, relay nodes backhaul their traffic through a wireless link to a Donor eNodeB. Inband relays use the same frequency of operation over their backhaul link as the access (relay UE) links. Outband relays, on the other hand, use different spectrums over the backhaul and access links [51].

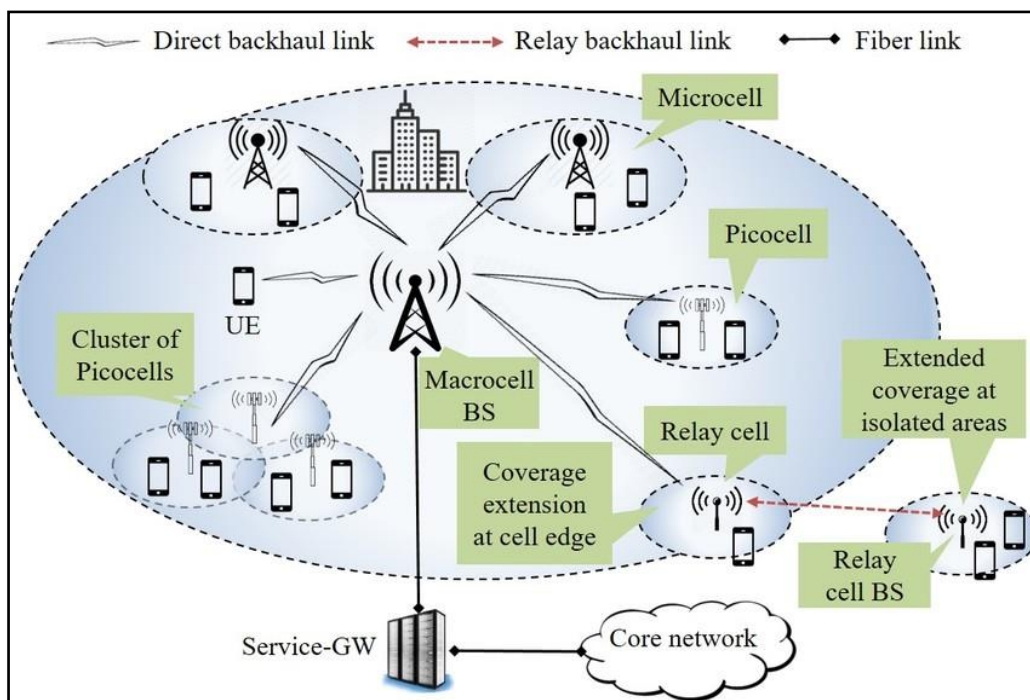


Figure 1.8 The heterogeneous network: a combination of macrocell and small-cell base stations to extend network coverage and capacity [53].

In Fig. 1.8, in a heterogeneous wireless cellular network, a large number of small cells (SCs) such as micro, pico, and relay base stations (BSs) are deployed with macrocells to improve spatial reuse [53] via cell splitting, because these small-cell BSs can operate on the same wireless channel (a certain spectrum band) as the macro-

cellular network [53]. These cell types often differ in terms of coverage regions and capacity as shown in Fig. 1.9.

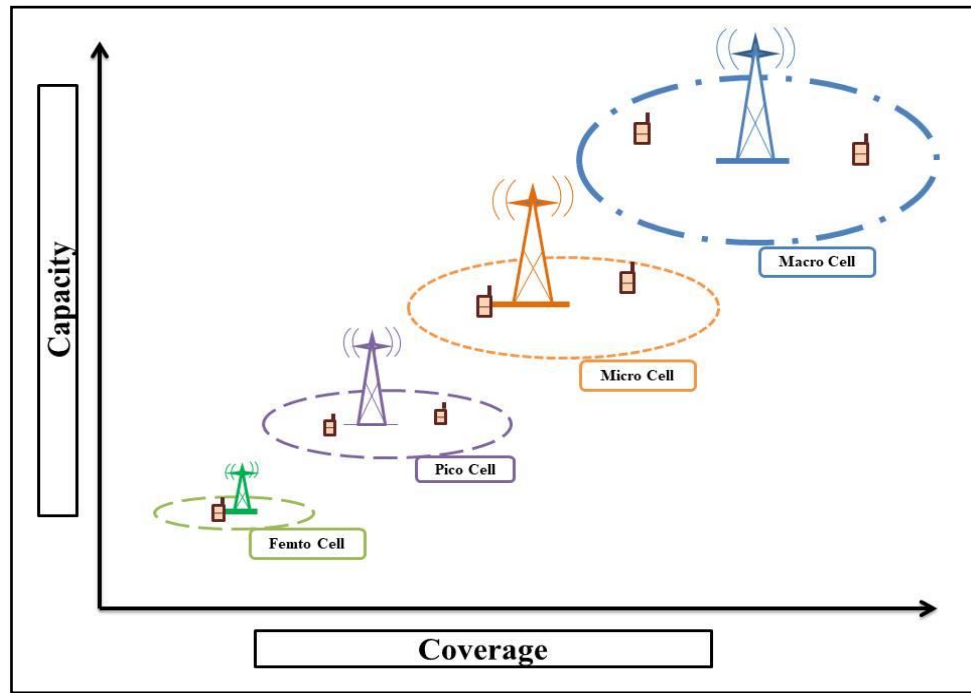


Figure 1.9 Coverage v/s capacity comparisons among different types of deployment environment [53].

The coverage of a network is estimated by the area covered by the serving base stations. The distance traveled by the transmitted signal is dependent upon the radio propagation characteristics of certain terrain [46]. Radio propagation characteristics differ from terrain to terrain and should be studied carefully, before estimating both coverage and capacity [46]. Propagation path-loss models [46] play a key role in the Radio Network Planning Process. It specifies vital network parameters such as transmission power, operating frequency, antenna heights, and so on. Numerous models have been proposed so far for cellular wireless systems operating in different environments (indoor, outdoor, urban, suburban, and rural). Certain models were estimated in a statistical manner based on field measurements whereas others were developed analytically [54, 55]. For example, the long-distance prediction models are primarily intended for macrocell networks, whereas, the prediction models are generally used for microcell systems [3, 55]. When the cell size is quite small (in the range of 10 to 100 m), deterministic models based on ray tracing methods are used. Propagation path loss models are not only used to decide the requisite number of cell sites to provide coverage for the network but also to determine where the cell sites



should be placed to achieve optimally fair coverage throughout the network [3,47,54, 55]. Various path loss models exist in the literature, like the log-distance path loss model [3, 54, 55], Okumara-Hata Model [3, 54, 55], and Cost-232 model [3, 54, 55], etc, and their further modifications. These basic models after comprehensive examination eventually converge to the respective standards.

With the evolution of wireless technologies, user behavior and their dependency on multimedia applications have drastically progressed over a period of last three decades. Therefore, the number of subscribers drastically steered up to avail of different multimedia services through their personified mobile devices [33]. This avalanche of the number of users with limited resources gradually started to become another major threat to contemporary mobile technology. In addition, the major cities of any developing country were being extended day by day to accommodate the need for ever-increasing population densities. As a result, the sub-urban regions around any major city demanded better coverage to ensure seamless multimedia activities with guaranteed QoS [28]. Considering these scenarios, it was quite evident that the traditional network architectures with hefty tower-mounted antennas were no longer capable enough to ensure guaranteed QoS [33].

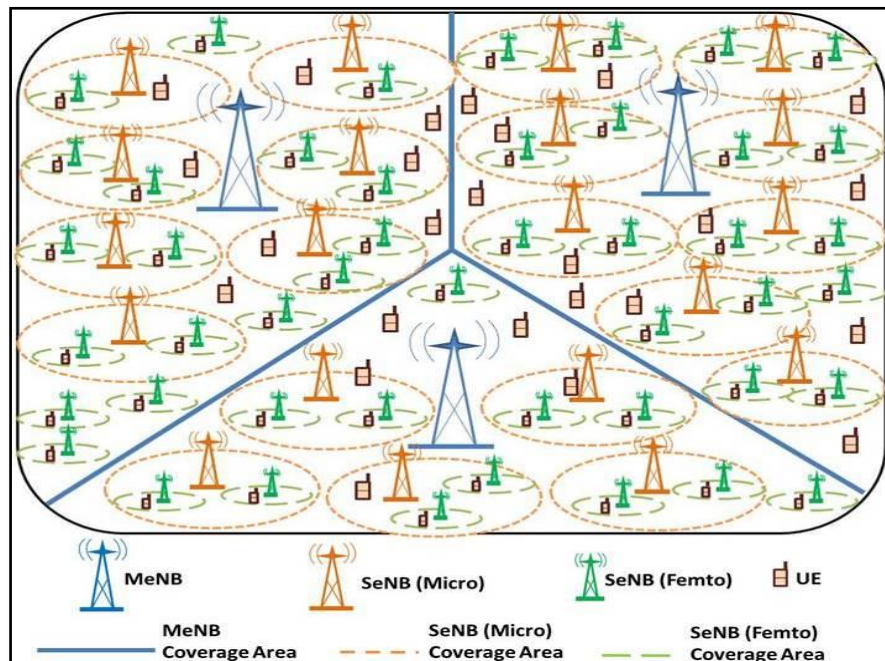


Figure 1.10 A typical **three-tier HetNet** consisting **one tier** of MeNB and **two-tiers** of SeNBs.

Besides, the Network densification of traditional Macro eNodeBs (MeNB) has potentially reached its theoretical limit [43, 56] to manage the enormous amount of

data demand with guaranteed QoS. This has opened a new frontier before the network service providers (NSP) by compelling them to bring a paradigm shift in their network deployment strategies from prudently deployed hefty tower-mounted MeNBs to irregularly distributed heterogeneous arrangements that often additionally comprise smaller micro/pico cells [57, 58, 59]. These small cells which are served by SeNBs by means of the same, different, or partially different channels with the MeNBs, which are termed co-channel, dedicated, or partially shared channel deployments, often differ in terms of operational power, transmit power, coverage regions, user admission capability, persistent spectral efficiency, path loss models and their spatial distribution [59, 60]. Due to the co-deployment of various types of low-power SeNBs with the conventional MeNBs, the resulting network architecture is often termed as a heterogeneous network (HetNet) 13. Fig. 1.10 shows one such type of hypothetical illustration of  $k$ -tier HetNet [57].

Dense deployments of HetNet [61], seek to take network densification to another level, where extreme spatial reuse is implemented. The deployments of HetNets are mostly unplanned, so a spatial network organizing mechanism requires to be developed. A representation of the locations of the eNBs in such a deployment scenario is called “spatial point process (SPP),” [62]. In reality, NSPs devote a lot of time and resources to identify the optimum locations for their eNB sites, considering factors like traffic arrival rate and/or distribution, terrain features, and user behavior, etc. However, from NSP’s point of view, the exact point pattern of eNBs is not only unknown but also very likely unknowable [62]. Hence, from the point of view of NSP, at a given time instant, the locations of the eNBs in the network can be considered to be *random* [57, 62]. Note that, it is not meant that the network operator deploys the eNBs randomly in the sense of throwing a dart at a map to get the eNB site locations. Rather, the approach, we propose may be seen as a stochastic attempt by the NSP to estimate, say, the probability that the SINR at the user remains above a fixed threshold, which requires defining a *prior* distribution on the distances to the eNBs [62]. For a tiered HetNets, in each tier, considering the number of eNBs as *countably infinite*, their locations can be modeled as *points of a spatial pointprocess (SPP)* [62].

Quite a few SPPs [57, 63] models are gaining popularity in recent literature for their effectiveness in designing deployment models for HetNets. Spatial point

processes are random point patterns in multi-dimensional space. Spatial point processes are considered to be useful statistical tools for the analysis of observed patterns of points, where the points symbolize the locations of some object of study (e.g. trees in a forest, bird nests, disease cases, or UE/eNB distribution in a wireless network). Based on their probability distribution point processes are broadly classified into two types: Binomial point process (BPP) [63] and Poisson point process (PPP) [63]. For real-world deployment purposes, due to the stochastic nature of the distribution of the eNBs over the entire geographical area, the Poisson point process (PPP) [57, 62, 64] became a popular choice to design complex HetNets. In choosing PPP for modeling eNB locations, one should consider two basic properties [64].

- There are  $n \geq 1$  eNBs in a finite region of plane and the locations of these 'n' eNBs are i.i.d over that finite region.
- Two random variables corresponding to the number of eNBs in two disjoint region of the plane are independent.

PPP can be sub-categorized into two types, namely, Homogeneous PPP (HPPP) and Non-homogeneous PPP (NHPPP) [62]. HPPP that lies in a fixed region can be fully demonstrated by a single parameter, constant density of points  $\lambda$ . In the case of HPPP, the density does not depend upon the location of the plane whereas, in the case of NHPPP, the density is considered to be a function of the coordinates i.e.  $\lambda(x, y)$ , which is now called intensity function [62]. The HPPP model is most popularly used in most of the distinguished works [57, 64, 65, 66, 67].

Optimum selection of the locations and count of eNBs to meet certain coverage and capacity constraints can effectively control the overall cost of a cellular network. In consideration of the modern complex HetNet, coverage, and capacity planning are interrelated in terms of interference. Moreover, the ever-growing capacity demand for non-uniformly distributed users, along with heterogeneous cell scenarios makes eNB location optimization a tedious task [64]. Selecting the optimal location of eNBs involves finding several eNBs within a particular deployment site without disturbing acceptable QoS to UEs [32]. Classical deployment models are not suited enough for planning HetNet eNB locations because they are only based on signal predictions and do not consider the traffic distribution, the signal quality requirements, and growing

geographic scenarios [57, 68]. As an alternative, K-means clustering can act as a useful method to find the optimal locations the cluster centers that can be considered as the optimal locations of the eNBs [71]. K-means is one of the simplest unsupervised algorithms that solve the well-known clustering problem [72, 73]. The algorithm trails a simple way to categorize a specific data set into a certain number of clusters and optimally defines  $k$  cluster centers, one for each cluster [69, 70, 71]. The notion of a multi-eNB, multi-technology network environment produces some new challenges such as the implementation of the tiered architectural framework, placement of additional infrastructure, interference management, and energy management [57, 64, 65, 67].

The signal that is transmitted from the transmitting antenna and received by the receiving antenna covers a complex path. The signal usually gets exposed to a variety of man-made structures, passes through different types of terrains, and gets affected by the combination of propagation environments from its journey between the transmitting and the receiving antennas [54, 55]. All these factors contribute to the variation in the signal level and thereby varying the signal coverage and quality in the network [47]. In addition, the operating frequency acts as a key factor in modeling the propagation path loss models for any standard technology [47]. The ultimate quality of the coverage in the mobile network is measured in terms of location probability [46]. For that, the radio propagation conditions have to be predicted with respect to the geographical aspects and landscape of the region as accurately as possible [46]. There are two ways in which radio planners can use propagation models [47]. They can either create their own propagation models for different areas in a cellular network, or they can use the existing standard models, which are generic in nature and are used for the whole area. Several notable contributions have been made to date to model suitable propagation path loss models with respect to different technologies [47]. From time to time, 3GPP has released multiple documents mentioning standard path loss models for different types of eNBs. 3GPP TR 36.931 version 13.0.0 Release 13 which specifies Radio Frequency (RF) requirements for LTE Pico Node B includes a path loss propagation model along with additional consideration for macro and pico cellular environment separately [76].

With 5G expected to enact in entirely different frequency bands, it is necessary to develop new standards with new propagation path-loss models [77]. 5G mmWave

wireless spectrum is theoretically ten times greater than today's 4G LTE 20 MHz cellular channels [78]. Since the wavelengths shrivel by an order of magnitude at 5G mmWave when compared to today's 4G microwave frequencies, diffraction, and wall penetration will suffer larger attenuation, thus uplifting the significance of line of sight (LoS) propagation, reflection, and scattering [78]. Precise propagation models are essential for the design of new mmWave air interfaces. Many thorough studies and measurements have been performed to design new path loss models for 5G systems [79]. Measurements have been taken in these works in both indoor and outdoor urban/suburban environments. Eventually, the technical report published by 3GPP TR 38.901 version 16.1.0 Release 16 has comprehensively standardized channel models for frequencies from 0.5 to 100 GHz under different deployment scenarios based on both LoS and non-line of sight (nLoS) propagation scenarios for urban macro, urban micro, and indoor environments [80].

Wireless tele traffic has been snowballing at a rate of over 50% per year per subscriber, and this tendency is estimated to speed up, over the next decade with the persistent use of video and the growth of the IoT [79]. To address this issue, the wireless industry around the globe is steadily deploying 5G of cellular technology. In 5G systems, an innovative way to handle the wireless traffic explosion is the deployment of a large number of small cells giving rise to HetNets [81]. However, it is anticipated that the deployment of additional infrastructure to handle increased data demand will increase the daily power consumption of any such HetNet. Evidently, the network energy consumption will also bear an additional price tag for mobile service providers [82, 83, 84]. According to [85], energy price has been projected to be about 10%–15% of the total network Operating Expenses (OPEX) in mature markets which can further amount to 50% of the OPEX in developing markets [86, 87]. India is the fastest-growing telecommunication market in the world and one of the key contributors to the CAGR of internet users in Asia Pacific [44, 45]. Consequently, most of the urban areas in India create immense opportunities to design deployment scenarios for sustainable green HetNet architectures for seamless penetration of 5G technology which has started to commercially roll out in the final quarter of 2022 [88, 89]. To date, the majority of the research in mobile network deployment had been revolved around QoS-based performance metrics like throughput, and spectral efficiency. Nevertheless, their recent trends show an increased interest among

academia and industry professionals toward sustainable green communication (SGC) [90] by maintaining its QoS performance intact.



Figure 1.11 UN sustainable development goals (UN SDG) framework [92]

United Nations in its ‘Agenda 2030’ for SDG (as shown in Fig. 1.11) has set some specific framework for future mobile technologies to contribute in a significant way to the various sectors of society including a greener future [91]. The mobile communication sector in general and more precisely the mobile communications sector have a close connection with the UN SDG framework (as shown in Fig. 1.10) [91]. Facilitating people’s lives for a better sustainable future, modern communication network often comes with increased energy consumption as evident in the recent 5G network [93]. In fact, it is speculated that the price paid for this enormous growth of energy consumption will arise even further if no energy-efficient method is deployed. Some recent surveys estimated that the contribution of global CO<sub>2</sub> emission is nearly 4% and projected to surpass the assessed figure with the further progress of 5G and beyond [91, 93]. However, ‘UN SDG 13: Climate action which targets net zero emission by 2050’ expects the mobile industry to be the first to make positive efforts in this regard. Future wireless technologies can aid to elude greenhouse gas (GHG) emissions by enabling other sectors to implement smart traffic management, building efficient energy management systems, remote working, industry automation through industrial IoT, and, smart grids, [93]. In a recent study [92], it is observed that some global key players like Vodafone, and Orange in this industry have made significant efforts to reduce their CO<sub>2</sub> emissions by up to 50% within a span of 14 years between 2006 and 2020.

Radio access sites consume approximately 80 % of a mobile network’s energy [91]. With the much-anticipated upsurge in the number of small cells in 5G HetNets,

energy efficiency (EE) has now become a crucial system design parameter that stresses upon eco-sustainability perspective [58, 59, 60, 61]. One way to reduce network power consumption is to switch off small cell base stations (BSs) or to keep them in energy-saving mode while preserving the QoS experienced by users [95, 96]. As the wireless tele-traffic is characterized by a non-uniform pattern in spatiotemporal domains, strategic sleep policies (SSP) techniques invoke significant reduction in the power consumption of the mobile networks by selectively turning transceivers of the SeNBs to the sleep mode [95]. Consequently, the base station operates in two different modes: active mode and sleep mode. In the active mode, the eNBs are absolutely on while its transceivers are turned off in the sleep mode except for the passage of a few control signals [96]. Typically, when some SeNBs are in sleep mode, the radio coverage is provided by their parent MeNB, in order to guarantee ubiquitous services over the network all the time [97]. Before 5G networks, sleep mode solutions have been used in WiMAX, and LTE standards and technologies for energy-saving purposes including [98-101]. They have been proven to be promising solutions to increase energy efficiency and enhance energy management policies.

The quest to reduce CO<sub>2</sub> emissions and to avoid frequent recharging of UEs has given rise to a new exciting energy-efficient technique dubbed energy harvesting or wireless power transfer. RF energy harvesting (EH) or Wireless Power Transfer (WPT), allows receivers to harvest energy from received RF signals [102, 103]. Due to the limited battery life of mobile devices, Simultaneous Wireless Information and Power Transfer (SWIPT) have been proposed as a solution to serve as a perpetual energy source for mobile terminals, hence improving the quality of user experience [43]. In SWIPT networks, UEs are able to scavenge energy from radio frequencies which are used to charge their inbuilt batteries. Further detail on SWIPT is presented in [104]. Nonetheless, the said method has primarily designed to make UEs energy efficient but later has been imitated to model EE techniques for SeNBs too [105].

In reality, it is difficult to provide a grid power supply to all the SeNBs in a cost-effective way. Moreover, a dense deployment of SeNBs, which is needed to meet the capacity and coverage of the next-generation wireless networks, will increase operators' electricity bills and lead to significant carbon emissions. Thus, it is crucial to exploit off-grid and green energy sources to power SeNBs, for which EH technology is a viable solution [105-107]. Compared to opportunistic energy

harvesting from renewable resources, WPT can be fully controlled via wireless communication technologies, which has been therefore regarded as a promising solution for powering the massive number of small UTs expected in 5G applications which can further enable SGC for future technologies beyond 5G [94,108].

## 1.2 Motivation

In the previous section, we have seen how wireless technologies and their operating principles have evolved over the years. We have also realized that radio network planning plays a pivotal role in the successful operation of an entire wireless network. Considering the present scenario, the profusion of mobile devices like tablets, smartphones, and IoT devices facilitating multiple applications like smart sensing the indoor environment, live video streaming, conferencing, web browsing, and image/video transfer has necessitated bringing newness in network planning and design so as to cope up with the demands of service providers as well as consumers.

Until 4G, all the major technology has been dominantly implemented in the sub 6 GHz band. Hence, available bandwidth and its proper utilization have remained to be the most discussed topic in between 2010 to 2020. Given the scarcity of resources, these technologies should be encapsulated by proper Radio Resource Management (RRM) techniques [19] to ensure an allowable level of QoS to the end users.

Looking into the elevated challenges induced by the popularity of multimedia services across various mobile technologies, it is understood that traditional macro cells are alone not capable enough to deal with the increasing capacity with extended coverage. Moreover, in the real world finding Macro cell sites is a challenging task and costly affair too. Hence, it is essential to reduce the cell-to-cell distance in the macro network to diminish path loss at each mobile user end leading to the research for network densification [20].

However, due to the large-scale deployment of SeNBs in random locations, limited transmit power, and the lack of complete coordination, the coexistence and efficient operation of small cells are very challenging. [6]. In the real world, the distribution HetNets are mostly unplanned proving them to be different from the theoretical understanding of cellular network in many aspects. Naturally, spatial modelling for these HetNets has been a debatable topic ever since the emergence of the said



terminology. Many stochastic geometric techniques like BPP, PPP, and their respective variations have been debated in recent literature. However, it is important to find out the right model considering the complexity of HetNets.

Most of the previously published works have considered HPPP in designing complex Het-Nets, i.e. each of the entities of a modern wireless network is distributed with a constant density. However, practically, it is understood that the deployment of eNBs in complex Het-Net environments should not be restricted to a constant density. Rather, possibly nonhomogeneous PPP, which uses intensity function (function of the coordinates) instead of constant density, should be considered as a more practical approach [6].

Also considering the popularity of mobile broadband users in countries like India, specific users' density corresponding to Urban and Suburban scenarios needs to be considered as a prime parameter in designing network models (the rural scenario is excluded because as of now they contribute very little in overall nations average Tele-density and can be left for further investigations).

To this extent, it is well understood that all the distinguished works discussed above made significant contributions to reduce power consumption in modern wireless network scenarios. However, the co-implementation of strategic sleeping policies for EH-enabled SeNBs inside a HetNet through scalable network planning and deployment under real-time urban traffic scenarios is certainly an aspect that can be investigated even further to attain tractable solutions for attaining SGC for future networks.

It is also perceived that the popularity of mobile internet users in countries like India, the world's 2nd largest telecommunication market [3], real-time traffic scenarios corresponding to urban terrain need to be deliberated as a key consideration in designing SGC models.

### 1.3 Contribution embodied in this thesis

The inspiration to investigate the development of wireless networks in order to contribute towards the design and deployment of efficient radio networks has led to the pursuance of the following specific contributions in this thesis:

The primary contribution of this thesis has been the *design of Joint Call Admission control and Dynamic Bandwidth Allocation algorithm* as an improved choice to manage radio resources efficiently in scanty spectrum-based scenarios. The said design has been able to achieve better QoS under a scenario where additional infrastructure (small cells) is underlaid in a tiered fashion under the footprint of traditional macro cells to extend coverage. The novelty of this work belongs to the fact that it performs the integration of an RSS based CAC policy and DBA for value-added performance in terms of standard QoS parameters like New Call Blocking Probability (NCBP), Handoff Call Dropping Probability (HCDP) and Bandwidth Utilization (BU). A Continuous Time Markov Chain (CTMC) based analytical model is also designed for the substantial investigation of the proposed RRM scheme under those QoS parameters. The Joint CAC and DBA scheme (JCAC-DBA) in two-tier LTE BWA Het-Nets significantly improves NCBP, HCDP, BU, and the overall capacity of the network under different combinations of macro/small cells for heterogeneous multimedia services. The proposed JCAC-DBA scheme improves as much as 90.88, 25.07, and 38.52% in NCBP, 88.79, 51.73, 38.08% for HCDP, and 41.66% in overall BU respectively for Class 1, Class 2, and Class 3 type of services on placement of three SeNBs. A comparative analysis has also been performed between multi-hop relay assisted and small cell based two-tier LTE networks. However, in totality, an improvement in BU of 2.03% is achieved in the case of MeNB-SeNB based Two-Tier architecture.

The popularity of these types of complex HetNet has led us to investigate even further in the direction of *designing a lucid and mathematically tractable spatial network model to imitate complex Het-Nets* that turn out to be the second contribution of this thesis. Here in this thesis, we have modeled complex HetNets by means of popular SPPs such as BPP, HPPP, and NHPPP. A detailed comparative performance analysis based on some popular QoS parameters, namely, Coverage Probability and Average Rate have also been performed considering the gradual progress of tele traffic density in Indian Urban conditions over the years. It has been realized that with the increase in tele traffic density, the performance of BPP deteriorates in comparison with HPPP in terms of both coverage probability (CP) and average rate (AR). As a result, under lower density scenario BPP outperforms HPPP by 21.77% and 5.89% in the case of CP and AR respectively but as the network

becomes denser, HPPP provides better performance compared to BPP in terms of both CP (improvement of 7.67 %) and AR (2.8 %). Further, it has also been observed that irrespective of any network density scenario NHPPP outperforms both HPPP and BPP because of proper thinning of eNBs deployed within a specific area. A max of 32% improved coverage and 9.33% improvements in AR are observed for NHPPP.

Now on as it is presumed that NHPPP can be a better choice to model complex Het-Nets, the next contribution of this work is to *model a multi-tier wireless HetNet in which additional tiers of SeNBs (where the upper tier represents urban macro (UMa) cell serviced by MeNB and lower tiers represent UMi-SC and InH serviced by SeNBs) are deployed in accordance with MeNBs taking into consideration India's Urban and Suburban tele-traffic scenarios* to see how the proposed model will perform under real-time traffic conditions. This analysis includes an important consideration of teledensity in the Indian context in terms of urban (153% teledensity) and suburban (90% teledensity) geographical scenarios as of FY 2018. The expressions for CP and AR are derived to justify the performance of the proposed scheme. In addition, this work also integrates the k-means clustering algorithm with NHPPP to find out the optimum locations to improve the performance of NHPPP to a further extent in terms of coverage and sustainable rate. The radio frequency at which MeNBs and SeNBs can be deployed under real-time urban and suburban conditions has also been realized with proper scrutiny from the simulation results. Extensive performance evaluation finds the best-fitted ratio of MeNB to SeNBs as 1:8 for the urban scenario and 1:5 for the suburban scenario, which is very much logical due to the fact that more SeNBs are required to serve a higher percentage of teledensity in the urban case. When compared with NHPPP over K-means clustered NHPPP for CP and AR, it is observed that K-means clustered NHPPP outperforms the former by providing 58.04% and 20.04% improvement in the urban scenario and 41.57%, 18.18% improvement in suburban scenario.

It is well understood from previous literature and fundamentals of wireless communication that the path loss propagation models play a pivotal role in designing deployment plans for any wireless network. Hence, at this juncture, this thesis also evaluates the *effect of different propagation Path Loss models in designing Two-tier Het-Nets for Coverage and Rate toward the development of 5G wireless standards*. Two important large scale propagation path loss models, namely, the 4G pathloss

model (3GPP TR 36.942 Release 9), the alpha-beta-gamma (ABG) model, the close-in (CI) free space reference distance model, and the 5G path loss model (3GPP TR 38.901 version 16.1.0 Release 16) for the analysis of achieved coverage and rate in designing two-tier 5G HetNet. It is witnessed that with a known teledensity (urban/sub-urban) the selections of frequencies for MeNB and SeNB become imperative to ratify the propagation path loss model for 5G HetNets for achieving the desired coverage and rate. Further, it is observed that implementation of 5G path loss model (3GPP TR 38.901 version 16.1.0 Release 16) in a three-tier UDN model provides better results under a certain scenario in which the terrestrial 3300-3670 MHz band is used on the macro tier whereas 24.25-28.50 GHz is used in small cells tiers which may direct small cells to be used as both outdoor small cells or hot-spots within 5G networks for higher data rate.

In the race for 5G deployment, one of the prime objectives of network planners is to ensure uniform QoS over any targeted geographical region. So determining *the optimal density of SeNBs* appears to be a valued task considering the *complexity of 5G ultra-dense HetNets (UDHetNet) under real-time traffic conditions*. This brings us to architect another key contribution which aims to implement a *cluster evaluation technique*, namely, *variance ratio criterion (VRC) or Calinski and Harabasz (CH) index*, so as to improve the *Area Spectral Efficiency (ASE)* of the entire region under test. Firstly, the User (UE) arrival process within a certain coverage region is modeled as a one-dimensional (1D) Poisson Arrival Process following the teledensity profile of an Indian urban scenario for a time span of 12 working hours of any random day. The analytical results advocate that deployment of SeNBs with optimal density can improve the ASE of an UDN, especially in peak hours under real-time Urban Tele traffic distribution scenarios. It is observed that VRC or CH index is an effective method to determine the optimal density of SeNBs as a subset of UDN deployment. Further, it is understood from the analytical results that having a known UE distribution scenario, the optimal deployment of SeNBs in terms of both location and density can significantly improve the QoS performance of an urban UDN over traditional MeNB-based scenario in terms of ASE, especially during peak hours with maximum traffic load.

The above effort of capacity and coverage enhancement by means of network densification creates a major impact on the overall power consumption of any

wireless environment. This paves the way for an in-depth analysis of network energy efficiency to create an ecosystem for sustainable green communication (SGC) for future networks. The subsequent contribution of this thesis is to adopt *suitable SGC techniques for two-tier wireless HetNet in which low powered EH enabled SeNBs are deployed with SSP considering India's Urban tele-traffic scenarios on an hourly basis (for the city of Kolkata)*. Primarily, we present an SSP of the SeNBs based on M/M/1 queuing theory and investigate its impact in reducing the power consumption of the proposed HetNet based on performance metrics like Energy Efficiency (EE) and Area Energy Consumption Ratio (AECR). Further, we also introduce a novel energy harvesting (EH) technique, namely, Sleep Cycle Modulated Energy Harvesting (SCMEH) for SeNBs to ensure proper utilization of energy resources. An analytical model based on CTMC is also developed to evaluate the Energy Utilization (EU) of the proposed SCMEH methodology. Simulation results and performance evaluations advocate that the SCMEH enabled SeNBs under Ultra Dense Heterogeneous Network (UDHN) can not only guarantee QoS requirements under concurrent time-varying urban teletraffic conditions but also achieves significant improvement (approximately 90% during peak hours and 10 % during non-peak hours) in the EU compared to traditional sole MeNB based network architecture, hence ensuring SGC by profoundly regulating the estimated power consumption on an hourly basis throughout a day.

## 1.4 Thesis Organization

The contributions depicted in this thesis cover several aspects of deployment model design for optimally positioned complex HetNets for better utilization of radio resources along with coverage and capacity enhancement. The organization of the thesis is as follows:-

**Chapter 3** aims to implement a unique RRM scheme for a heterogeneous LTE based BWA network (BWA HetNets) which consists of Small cells along with Macro cells. The proposed analysis has two components: (1) Received Signal Strength (RSS) based CAC policy; and (2) Dynamic Bandwidth Allocation (DBA) scheme for QoS provisioning. The novelty of this work lies in the integration of the RSS based CAC policy with DBA scheme for improved performance in terms of different QoS parameters like New Call Blocking Probability (NCBP), Hand off Call Dropping

Probability (HCDP) and Bandwidth Utilization (BU). A Continuous Time Markov Chain based mathematical model is also developed for the realistic analysis of those QoS parameters. The Joint CAC and DBA scheme (JCAC-DBA) in two-tier LTE BWA Het-Nets significantly improves NCBP, HCDP, BU, and the overall capacity of the network under different combinations of macro/small cells for heterogeneous multimedia services. Considering New Call Blocking Probability, Handoff Call Dropping Probability, and Bandwidth Utilization as QoS parameters, a comparative analysis has been performed between two leading HetNets, namely, Multi-hop relay assisted BWA network and Small eNodeB based two-tier BWA network.

**Chapter 4** aims to provide a reasonable performance analysis of three established SPPs, namely, the Binomial Point process (BPP), the Homogeneous Poisson Point Process (HPPP), and the Non-Homogeneous Poisson Point Process (NHPPP) in terms of achieved coverage and rate. This chapter also aims to provide the effect of different propagation path loss models, namely, the 4G path loss model (3GPP TR 36.942 Release 9), the alpha-beta-gamma (ABG) model, the close-in (CI) free space reference distance model, and the 5G path loss model (3GPP TR 38.901 version 16.1.0 Release 16) for the analysis of achieved coverage and rate in designing two-tier 5G heterogeneous network (HetNet). Furthermore, the path-loss models play a pivotal role in estimating downlink SINR that in turn leads to deriving the expressions for CP and AR. It is observed that with the increase in tele-density as well as eNB density the NHPPP outperforms both BPP and HPPP in providing better coverage and rate. Then a suitable model based on a nonhomogeneous Poisson point process (NHPPP) is designed for a heterogeneous wireless network (HetNet) consisting of two-tiers eNodeBs (Macro and Small Cell), where each of the tiers is differentiated in terms of transmitting power, eNodeB density, and supported data rate. Subsequently, analytical expressions are derived for coverage probability (CP) and average rate (AR) to assess the performance of the HetNet. The contribution of the paper further lies in integrating the k-means clustering algorithm with NHPPP to find the optimal locations of the small cell eNodeBs for extended coverage and rate improvement. The proposed model is investigated under differently dense scenarios like urban and suburban areas in India. It establishes the requisite of an optimal number of small cells along with the traditional infrastructure to maximize the performance in terms of CP and AR. Finally, the proposed integrated model is compared with the traditional

homogeneous Poisson point process (HPPP) and NHPPP for coverage and rate analysis. It is observed that the K-means clustering algorithm in integration with NHPPP overshadows both HPPP and NHPPP in terms of coverage and rate under both urban and suburban deployment scenarios. Finally, this chapter also aims to model a three-tier UDN model using a spatially clustered homogeneous Poisson Point Process (SCHPPP) consisting of one tier of MeNBs and two tiers of SeNBs for the coverage and rate analysis in designing deployment architecture in Indian urban scenarios. Comparative results among several cases having different combinations of 5G frequency bands are analyzed which advocates that the proposed three-tier UDN serves as an effective solution to guarantee QoS in terms of improved coverage and rate.

**In Chapter 5**, we present a method to determine the optimal density of SeNBs in a Non Homogeneous Poisson Point Process (NHPPP) distributed spatially clustered two-tier HetNet by incorporating its impact on overall ASE. Firstly, the User (UE) arrival process within a certain coverage region is modelled as a one dimensional (1D) Poisson Arrival Process following teledensity profile of Indian urban scenario for a time span to 12 working hours of any random day. The estimated teledensity of the city of Kolkata is considered here to represent the Indian Urban scenario. To estimate the requisite amount of SeNB density this chapter also utilizes the VRC cluster evaluation method for maintaining QoS demand. Considering the optimum MeNB, SeNB ratio, the comparative performance analysis has been performed between MeNB based traditional network and two-tier HetNet in terms of ASE. The Analytical results advocate that deployment of SeNBs with optimal density can improve the ASE of a two-tier HetNet, especially in peak hours under real-time Urban Tele traffic distribution scenarios.

**In Chapter 6**, primarily, we present the Strategic Sleeping Policy (SSP) of the SeNBs based on M/M/1 queuing theory and investigate its impact in reducing the power consumption of the proposed HetNet based on performance metrics like Energy Efficiency (EE) and Area Energy Consumption Ratio (AECR). Further, we also introduce the novel SCMEH policy for SeNBs to ensure proper utilization of energy resources. An analytical model based on Continuous Time Markov Chain (CTMC) is also developed to evaluate the Energy Utilization (EU) of the proposed SSP and EH methodologies. The comprehensive performance analysis reveals that the

implementation of integrated REH-SSP enabled SeNBs under UDN can not only guarantee QoS requirements under concurrent time-varying urban tele-traffic conditions but also ensure Sustainable Green Communication (SGC) by radically controlling the estimated power consumption on hourly basis throughout a day.

**Chapter 7**, primarily, summarises the key findings of the work and establishes the link between the objective and the findings of this thesis. It also briefly elaborates on the present telecommunication scenario along with the future course of wireless networks with the help of some key white papers published by renowned telecom service providers. Finally, this chapter as well as this thesis concludes with a visionary future direction to carry out further research investigations in the broad domain of designing cell-free deployment models for future networks to unleash the next generation 6G technology.



# Chapter 2: Background Study

---

## Outline of this chapter

- 2.1 Introduction
- 2.2 Radio Resource Management Techniques in BWA Network
- 2.3 Deployment of Small Cells: Introduction to HetNets
- 2.4 The fundamental limit of network densification
- 2.5 Sustainable Green Communication Techniques in HetNets
- 2.6 Chapter Summary

## 2.1 Introduction

As discussed in the previous chapter, wireless technology has witnessed radical progressions throughout the past decades, which has revolutionized the outlook of modern telecommunications. Starting from its naive beginning limited to a few hundreds of subscribers initially, wireless communication is now easily reached to a major segment of the global population. This has piloted in a paradigm shift in this new era of communication and connectivity. There is a substantial gain in data traffic flow over the Internet due to this paradigm shift in the usage of multimedia services. Parallel to the development of mobile technology, BWA networks initiated to offer higher data rates, better capacity, and improved network coverage. As the usage of smart mobile devices along with personified multimedia services have increased at a much rapid pace compared to the capacity and resources of the underlying network technology, heterogeneous network architectures with efficient radio resource management mechanisms are essential to provide satisfactory QoS to the users. The focus of this thesis includes design of efficient radio resource management techniques in heterogeneous BWA network to enact sustainable green communication ecosystem for present as well as future networks. It is a well-established fact that background literatures form the foundation of any rational research work. Hence, the subsequent sections in this chapter illustrate a reasonable amount of state of the art research work that gave us substantial motivation and insight to investigate even further.

## 2.2 Radio Resource Management Techniques in MeNB/SeNB based Heterogeneous network

All the mobile technologies beyond 3GPP LTE are envisaged to brace numerous real-time multimedia applications, which inflict stringent QoS requirements while guaranteeing a certain level of fairness and low-priority services [109]. RRM plays a key role in this regard. To cope up with the growing popularity of data-intensive multimedia applications, heterogeneous deployment of low-power nodes within macrocells has emerged as a widespread solution, thus forming a familiar buzzword known as HetNets. The low-powered nodes viz. microcells, picocells, femtocells, and relay nodes (RNs) are collectively known as small cells, e.g.,

Quite a lot of surveys and reviews [109-111] linked to the RRM for HetNets with femtocells and RNs have been documented lately. A survey of RRM techniques for relay-enhanced OFDMA-based networks is published in [110]. In addition, the authors of [109-111] presented a methodical analysis of selected RRM schemes, with a prime interest in their complexity and fairness. In [111], a number of primitive existing RRM schemes are analyzed first, followed by some more sophisticated approaches, to demonstrate the gradual progression in the field. Additionally, an all-inclusive qualitative evaluation has been carried out in [111] for a comparative analysis of existing RRM schemes in terms of bandwidth utilization, fairness, complexity, and QoS. The two major RRM techniques [109-111] in a heterogeneous LTE/LTE-A network include call admission control, and bandwidth allocation among macro cells and small cells, etc.

- Call Admission Control

CAC schemes have been designed for either the uplink or the downlink [112]. In the uplink, transmit power constraint is more serious than in the downlink since the MS is battery-operated. On the other hand, CAC in the downlink needs information feedback from MSs to the BSs for efficient bandwidth utilization [112]. CAC in the downlink creates more impact in designing better RRM schemes for bandwidth constraint networks [112]. Some breakthrough research work containing various downlink CAC policies is well documented in [113-122]. Downlink CAC schemes can be categorized based on the availability of multiple service classes. Mono-service-class-based CAC schemes have been prevalent in first and 2G wireless standards

when the voice was the prime (and sometimes the only) offered service [112]. With the tilt towards data-intensive multimedia services, mono-class CAC schemes are no longer adequate, and gradually multiple-service-class based CAC schemes became more relevant (e.g., [113, 114]), during 3GPP LTE and beyond. In [115] the authors have modelled the acceptable region of real-time Variable Bit Rate (rtVBR) services. The admissible region is determined based on the assessment of packet-dropping probability. The segregated admissible region for rtVBR services can be used to implement a focussed CAC scheme by inspecting the network state (when a new call arrives) to understand whether it is allowable or not. To regulate the packet-dropping frequency during video conference services, in [116], the authors have proposed a CAC scheme where multiple quality thresholds are set using various layers and encoding techniques for MPEG4 and H.263 services. With the arrival of a new call of said types, the effective bandwidth requirements of all existing users, including the new call are determined to ensure the highest quality level. The new call is admitted if and only if the total estimated bandwidth is less than the given system bandwidth. In [117], a comparative analysis has been performed considering a number of class-based CAC schemes for multiclass service-based wireless networks with respect to various parameters. The core contribution of this work is the innovative implementation of the probabilistic CAC scheme that is used to prioritize handoff calls. The levied probabilities are used to allocate higher priority to real-time services. Furthermore, the performance evaluation of CAC schemes is also performed also on fairness and throughput criteria. Unlike [117] a number of CAC schemes based on guard channel algorithms are proposed in [118], for multiclass services, imposing priority to real-time service class calls while ensuring assured QoS. The proposed schemes scrutinize the CAC issue in terms of ongoing calls and busy channels. Fairness among calls of different service classes is assessed and the network performance is compared owing to input load.

However, unlike [115-118], the works presented in [119-122] add more value in designing effective RRM schemes because these works [119-122] have inclusively considered the concept of HetNet. In [119], the authors have introduced a performance evaluation method for the CAC mechanism considering the heterogeneous RATs (similar to HetNet) and analyzed the call blocking probability (CBP) by varying the number of channels. In order to measure the CBP simulation

studies of the proposed analytical model have been performed. In the experiment setup, different types of traffic were considered, namely, type1, type2, and type3. It was observed that an upsurge in the number of type1 users had increased the CBP of type2 and type3 calls and vice versa. Additionally, growth in the traffic intensity of any one type of traffic will increase the system-blocking probability. In [120] a higher order Markov chain based performance model for CAC is proposed in a HetNet environment. In the proposed algorithm, the authors have considered three service classes of traffic having different QoS requirements within a HetNet environment that can effectively handle applications like voice calls, Web browsing, and file transfer applications that are with varied QoS parameters. This paper [120] presents the call-blocking probabilities for all three types of traffic both for fixed and varied traffic scenarios. In [121], the authors have introduced an innovative algorithm for collaborating CAC with load balancing in small cell based HetNets. The said method incorporates that when a fully occupied small cell encounters an incoming call, instead of rejecting the call due to occupancy, the collaborating CAC with the load-balancing algorithm requests for an immediate load balancing. The load balancing comforts the occupied cell to free up a chunk of its radio resources, which enables the small cell to accept the incoming call. Simulation results show that the proposed algorithm guarantees the required QoS for the UEs and maximizes the overall network throughput. Motivated by the idea of using service-based and load-based CAC policies in heterogeneous networks, in [122] the authors have documented an adaptive Joint CAC that integrates the effect of user-centric and network-centric CAC schemes, depending on network conditions and user requirements. It was also shown that the proposed adaptive JCAC scheme could fulfil the requirements of critically varying network conditions.

- **Bandwidth Allocation**

It is well understood from the aforementioned surveys and reviews [109-111] that in addition to CAC, effective bandwidth allocation/resource allocation schemes also play a key role in designing efficient RRM schemes for HetNets. Some notable works [123-128] are mentioned herewith having valuable contributions to the issue of bandwidth allocation/resource allocation in HetNets.

In one of the primitive works, a static femtocell-aware spectrum allocation scheme for two-tier LTE networks is deliberated in [123]. In this study, the available bandwidth is divided into two sections, namely a macro-dedicated bandwidth (MDB) and a femto-sharing bandwidth (FSB). Additionally, a femto-interference list (which refers to the list of macro UEs (MUE) as potential interferers to nearby femtocells) is maintained by the Femto eNB. The key idea is to allocate resource blocks to members of the femto-interference pool from the MDB, while other macro UEs and femto UEs (FUE) can be allocated resource blocks from MDB and femto-sharing spectra. In this fashion, cross-tier interference is minimized. Packet scheduling among UEs is executed using a proportional fair scheduler. The complexity of the RRM scheme in [123] stands rational, although some signaling overhead and computations are incurred. Nevertheless, its suitability for densely deployed HetNets remains unidentified as the concerns over co-tier interference and overall fairness are not studied. In [124], a simple semi-static hybrid spectrum allocation scheme is proposed for two-tier LTE based femtocell networks where a large chunk of bandwidth is allocated to MUEs while a small portion of it is assigned to FUEs. However, the amount of the bandwidth allocated can be adjusted using a bandwidth-splitting ratio that can be regulated by the operator. In addition, a max-min fair scheduler is used to accomplish a worthy trade-off between fairness and spectral efficiency, by adjusting the spectrum-splitting ratio to an optimal value. Even though the scheme proposed in [124] delivers space for adjustment of the spectrum-splitting ratio to the operator, it is still tough to determine the optimal spectrum-splitting ratio. To do this, a more intrinsic approach may be required, which may lead to high complexity, and yet cross-tier interference could remain undone. Even though local fairness is guaranteed by, using the max-min fair scheduler but global fairness needs to be further investigated. A unique semi-static hybrid spectrum assignment scheme is proposed in [125] for two-tier LTE femtocell networks in which two spectrum usage modes are proposed, i.e., co-channel and dedicated modes. In the co-channel mode, the same radio resources are shared by both MUEs and the FUEs, whereas, in the dedicated modes, the bandwidth is divided into two parts, one serving the MUEs and the other serving the FUEs. The semi-static hybrid spectrum arrangement scheme in [125] is lucid and effective for better interference mitigation and improved bandwidth utilization. In addition, the implementation and computational complexity are relatively low compared to [126]. Nevertheless, several aspects including fairness are

not studied in detail. In addition, the priority based QoS issue is not considered in these studies [124-125]. A priority-based bandwidth allocation method is proposed in [126] that is understandably a fair improvement over [123-125]. Contrary to fully sharing the whole bandwidth, the Femto eNBs [FeNBs] may utilize a certain chunk having a certain priority level.

The idea is first introduced in [126] to mitigate co-tier interference in the downlink of LTE-A femtocell networks. Initially, the entire bandwidth is subdivided into several equitable chunks with respect to the number of femtocells in the network. Then, each chunk is assigned to a femtocell. The assigned chunk of bandwidth is known as the priority chunk of the femtocell. This way, the femtocells are always ready to schedule resource blocks from the designated chunk, but lower priorities are given to the priority chunks of other HeNBs if there is any residual bandwidth available. However, the femtocells schedule the resource blocks only from their priority chunk if the amount of available PRBs is sufficient to support their traffic load. With the method proposed in [126], marginal network performance can be guaranteed with low complexity. However, a shortcoming may be manifested when the number of active femtocells fluctuates in each scheduling interval, thus demanding the said spectrum arrangement to be reconfigured in every scheduling interval. Hence, there is still enough room for improvement in this configuration [126], especially concerning bandwidth utilization. The works presented in [127-128] introduce a few innovative stochastic bandwidth allocation schemes. A stochastic bandwidth allocation method is introduced in [127], which assigns resource blocks to FUEs based on probabilities. In fact, the RRM scheme in [127] is quite similar to that of [126], as they both partition the channel bandwidth into chunks. However, unlike the scheme in [126], each chunk is assigned a selection probability rather than a priority level that certainly is a step forward from the previous one. The probabilistic bandwidth allocation scheme in [127] lowers complexity because the bandwidth allocation function is decentralized to each FeNB and the information about the partitioned spectrum can be known a priori. In [128], the authors present a decentralized dynamic bandwidth allocation technique based on a stochastic resource allocation approach for both uplink and downlink LTE networks with closed-access femtocells. In the said technique, the channel bandwidth is partitioned into two sets of resource blocks, in which one serves the indoor MUEs and the other serves the

outdoor MUEs. The proportion of the two sets relies upon the instantaneous respective traffic load generated by indoor MUEs. Similar to the scheme proposed in [126], the complexity of the bandwidth allocation scheme in [128] is relatively low, since the decentralized approach in [128] only requires macrocell broadcast signaling. However, the bandwidth allocation scheme proposed in [128] may be inefficient when a large-sized femtocell network is considered.

The aforementioned works have contributed some valuable insights into the development of effective RRM techniques for 3GPP LTE based HetNet. It is understood that both CAC and Bandwidth allocation techniques stand firm as leading RRM methods to guarantee desired QoS to the end user. Nonetheless, implementation of Joint CAC with Dynamic Bandwidth allocation considering multiple service class based QoS framework in LTE based multi-tier HetNet has not been investigated yet to the best of our knowledge. Performance parameters like NCBP and HCDP appear to be a standard choice but when it comes to designing an effective RRM scheme, bandwidth utilization needs to be considered along with NCBP and HCDP. Understandably, there is enough scope to investigate considering the importance of RRM in HetNets in the age of 3GPP LTE and beyond.

## 2.3 Deployment of Small Cells: Introduction to Stochastic Models for Heterogeneous Network

A. R. Mishra et. al. in [46, 47] illustrated the importance of network planning and deployment for smooth penetration of wireless technologies to the last mile. Considering the stochastic nature of modern wireless networks, an adaptive and scalable deployment model of the eNBs along with their QoS analysis has persisted as the most debatable topic for researchers over the years [68, 129, 130]. Hence, in recent literature, quite a few spatial point processes (SPP) [62, 63] are gaining popularity as stochastic models for their effectiveness in designing deployment scenarios for HetNets. From the analysis and application perspective, simplistic models are desirable as for complex systems; large numbers of parameters are involved for simulation study and analysis. Thus, designing a tractable model for complex HetNets is a tedious task that needs generic assumptions such as user distribution and base station transmit power for better tractability and applications. Some notable investigations have already been seen in recent literature as mentioned

earlier. Among them, PPP is found to be the most discussed method to design complex HetNets. In this chapter, a few of the recent important related works are discussed. An analytical model for multicellular systems is designed in the work of Wyner [131], which is termed as Wyner model. In this model, the channel gains from all interfering BSs are considered constant over the entire coverage area. However, this model does not even have a notion of outage probability since the signal-to-interference-plus-noise ratio (SINR) is fixed and deterministic. The hexagonal grid model proposed in the works of Catreux et al [132], Ganz et al [133], and Ekici and Ersoy [134] is perhaps the most popular and widely accepted model in terms of system-level simulations, but the numerical analysis is very complex. Additionally, the scalability and accuracy of the model are questionable considering the spatial complexity of modern HetNets. Andrews et al have developed a general and tractable model in their work [57] that consists of  $M$  different radio access technologies, each consisting of  $K$  different tiers of access points (APs), where each tier differs in terms of transmit power, path loss exponent, deployment density, and bandwidth. The authors in [57] have also modelled each type of AP and locations of mobile users as independent PPP models. The distribution of rate over the entire network is then derived for a tuneable weighted association strategy to optimize the traffic offloading to maximize SINR coverage. A load-aware cell association method along with a distributed algorithm for downlink HetNets is presented in the work of Ye et al [135], which results in optimizing the theoretic approach to the load-balancing problem. In addition, this work also considers cell association and resource allocation jointly. Furthermore, this approach provides an upper bound on achievable network utility, which can serve as a benchmark. However, in real systems, it is much more difficult to implement a multi-BS association than a single-BS association. Therefore, the authors formulate a logarithmic utility maximization problem for the single-BS association and show that equal resource allocation is actually optimal over a sufficiently large time window. The locations of base stations are modelled as a uniform binomial point process in the work of Afshang and Dhillon [136] and are presented through a generic analytical model to exemplify the performance of a randomly situated reference receiver (mobiles) in a finite wireless network. The rigorous categorization of the performance of an arbitrarily located reference receiver under two generic TX-selection policies where the serving node is a part of the transmitting node process is the focus of this paper. A new and more practical HetNet



model is developed in the work of Saha and Dhillon [137] for accurately capturing the non-uniform user distribution as well as the correlation between the locations of the users and BSs. In particular, the correlation between the users and BSs under user-centric capacity-driven deployment has been captured by assuming the BS locations as the parent point process. This model is flexible enough to include any kind of user distribution around any arbitrary number of BS tiers as well as user distribution that is homogeneous and independent of the BS locations. Afshang et al [138] characterize the statistics of nearest-neighbour and contact distance distributions for the Thomas cluster process (TCP), which is a special case of the Poisson cluster process. Precisely, the authors have derived the cumulative distribution function (CDF) of the distance to the nearest point of TCP from a reference point for three different cases. While the first corresponds to the contact distance distribution, the other two provide two different viewpoints for the nearest neighbour distance distribution. However, in the work of Afshang et al [138], the  $i^{\text{th}}$  tier BS is modelled using HPPP. In addition, this work considers uniformity in user distribution, which is certainly not the case in practical scenarios. Matérn cluster process (MCP), which is a special case of the Poisson cluster process (PCP) is designed by Afshang et al in [139] based on the statistical information of the nearest neighbour and distribution of their contact distance. The authors have also calculated the cumulative distribution function (CDF) of the distance to the closest point of TCP from a reference point corresponding to the nearest neighbour and their contact distance distribution. Vinay Suryaprakash et. al. designed a downlink interference limited system model in [140] where BSs accompanied by a single antenna are arranged according to HPPP in the Euclidean plane. Authors in [141] developed a method to analyse interference in HetNets using a Poisson cluster process and also provides critical evaluations of certain performance metrics (probability of coverage, etc.). The contributions can be divided into two parts. Firstly, a general expression for the interference based on transmit power, path loss, fading etc is derived. Secondly, a method to estimate the interference in an area is proposed based on the consideration that the user and base station intensities are known and that a user is located at a particular distance from the base station closest to it. A Heterogeneous Cellular Network comprising with  $K$  tiers is considered in [68] where each tier models BSs of a particular class, such as femtocells, picocells, microcells, or macrocells. However, practically, it is understood that the deployment of eNBs in complex DenSNets environments should not be restricted to a constant

density [62]. Marco Di Renzo et. al. in [142] analyzed the appropriateness of NHPPP for modeling cellular networks that exhibit spatial repulsion and clustering.

## 2.4 The fundamental limit of network densification

During the early 2010s, some notable contributions have been made in the domain of designing deployment models for multi-tier HetNets [57, 68, 143, 144]. However, these studies [57, 68, 143, 144] primarily focused on the analysis of outages, coverage probabilities, and average achievable rates. However, as the technology steadily progressed with time, the improved data rate demand in the IMT vision document [41] has dominantly made the issue of spectrum utilization/spectral efficiency as one of the key performance metrics for the analysis of scalable infrastructures [145-150]. Area spectral efficiency (ASE) [151] as a QoS metric [152] was first introduced as a worthy performance metric to measure the spectral efficiency of an entire cellular network. To date, it has remained as a prime performance metric in wireless communications systems. The ASE of a cell, with the unit bit/sec/Hz/m<sup>2</sup>, is defined as the sum of the maximum bit rates per Hz per unit area supported within a cell [36]. ASE as a performance metric has been widely used in several notable research studies [153-165]. Studies show that [153-156] deployment of HetNets creates a major impact in improving the ASE of a cellular network. The ASE performance indicator metric has been used to characterize how a limited frequency spectrum is utilized in two-tier HetNets [157-165]. Below are some notable research studies that showed us the path to take this research initiative.

In [153], the authors have extended the analytical framework for two-tier HetNet [57, 68, 143, 144] where the macrocell network is complemented by low power low-cost femtocell base stations through categorized cell edge deployment. The authors then derived the carrier-to-interference ratio (CIR) of the UEs and calculated their mean achievable capacity. The performance of two-tier HetNet has been critically evaluated by calculating the area spectral efficiency of the network. However, this work does not consider the load condition of the overall network. On the contrary, P. Chandhar et. al. in [154, 155] have investigated the performance of Macro-femto based HetNet under different network load conditions, since the interference experienced by the UE profoundly be influenced by the network load conditions at neighboring cells [154]. Hence in [154], the authors have investigated the ASE

performance of co-channel Macro Femto based HetNet whereas in [155], developed an analytical framework to study the ASE performance of OFDMA based co-channel deployed macrocell-femtocell networks considering varying network load condition in neighboring macrocells and femtocells. In [154], ASE of the network is obtained from the SINR distribution that is a combined function of radio parameters of macrocell and femtocells. Considering the combined effect of source activity, shadowing, and multi-path fading in the SINR distribution model the impact of these parameters on the ASE has been thoroughly studied [154]. In addition to these, the maximum achievable ASE gain with optimal transmit power and load configuration for multi-tier co-channel deployed macro Femto HetNet is analysed in [155]. The issue of link reliability and maximizing sum throughput is also an important factor in deciding the spectral efficiency of a complex het net. To do this, in [156] the authors have made a fair attempt to solve a more fundamental problem, namely the determination of the SIR distribution in a multiuser MIMO HetNet, and the resulting effect of the BS density on the network performance. By “performance improvement” the authors have improved link reliability through the analysis of the success probability and increased sum throughput per unit area which is characterized as the ASE. The link reliability vs. ASE trade-off deliberated in [156] is associated with the notion of improving “transmission capacity” by sanctioning additional simultaneous transmitters which eventually increased the spatial reuse efficiency, but the interference to the receivers have become higher and so the SINR and thus link reliability have diminished. The concept of Ultra-Dense HetNet (UDHetNet) which will take the network densification to a newer height is constructed by the denser deployment of SeNBs under the footprint of MeNB [157]. These UDHetNets are anticipated as a key enabler for the 5G wireless technologies [157], where a 1000-fold increase in data rates is expected with respect to current 4G systems [158]. The combined effect of Line-of-Sight (LOS) and Non-Line-of-Sight (NLOS) components in the radio propagation environment can severely affect the performance of UDHetNet. Based on a stochastic geometry model, C Gallilito et. al. in [159] showed that UDHetNet suffers from decreased coverage and the ASE raises sub-linearly as the LOS/NLOS propagation components are considered along with decreasing cell densities. However, the authors have also established that show that this degraded performance can be compensated by increasing the frequency reuse factor, which occurs when the eNBs become denser. The increase in frequency reuse phenomenon

improves the ASE vs coverage trade-off cell densification with respect to traditional frequency reuse, provided there is a degree of freedom on the density of cells [160]. The authors in [161] presented how average ASE scales in a cellular network with a very large density. The average ASE is defined using the Shannon rate, treating interference as noise. Further, the minimum operational SINR and the availability of channel state information (CSI) at the transmitters have been provided. A broad class of bounded path loss models capturing currently used and physically viable propagation models is defined by simple mathematical models. The spatial distribution of the eNBs is considered as PPP [161]. Considering a general small-scale fading model, the authors have also demonstrated different definitions of the ASE and presented some propositions, as the eNB density grows large. Considering that there is no limit on the smallest operational SINR and that the eNB can transmit at the Shannon rate – which infers that seamless instantaneous CSI is available at the eNB, the authors have proven that the average ASE converges to a constant [161]. However, minimum operational SINR without any threshold value is not practically viable to ensure maximum ASE. The issue has been addressed in [162] as the MISO model having multiple transmit antennas and a single receiving antenna and prove that the average SINR as the ratio of no of transmitting antenna and spatial density of eNBs and the average ASE scales to Shannon bound average throughput normalized by eNB density. For the MIMO case, the authors prove that the scaling technique of the conditional SINR and ASE are the same as the MISO case, i.e. not dependent on the number of transmitting antennas. The analytical results of the work [162] suggest that deployment of multi-antenna eNBs can help to maintain the linear increase in the ASE with eNB density, while the number of antennas at the UE and the use of eNB cooperation does not matter much. In [163], the authors have presented the novel idea of optimal caching policy to maximize the success probability and ASE in a cache-enabled HetNet. Under the purview of the probabilistic caching framework, the authors have introduced stochastic geometry theory [57, 62, 63, 68] to derive the success probability and ASE. In addition, the authors have also analyzed the impact of crucial system parameters and compared the ASE performance with traditional HetNet (the Macro tier is overlaid by a tier of SeNBs). The probabilistic optimal caching policy is less tilted among helpers to maximize the success probability given the ratios of MeNB to-helper density, MeNB to-helper transmit power, UE-to-helper density, or the data rate requirement are less. Compared with traditional HetNet, the

helper density is much lower than the SeNB density to achieve the same target ASE. The helper density can be reduced by increasing cache size. With a given total cache size within an area, there exists an optimal helper node density that maximizes the ASE. Authors in [61] investigated from the viewpoint of different dense deployment strategies both outdoor and indoor from the network ASE perspectives, with high densification levels. The results obtained show that densely deployed SeNBs provide better spectrum efficiency to address the massive capacity demands in comparison to densifying the outdoor MeNBs

It is well understood from the previous discussion that the key enabling factor to increase the data rate in wireless networks over the past few decades has been network densification [59, 60, 157, 158, 160, 164, 171]. This tendency is foreseen to endure into 5G and beyond [158, 164, 171]. In [164], authors have studied the fundamental problem of optimizing the deployment density of drone small cells to achieve the maximum coverage performance by deriving an approximate and closed-form expression of the cumulative inter-cell interference which arrives from both Line-of-Sight (LoS) and Non-Line-of-Sight (NLoS) links. The network performance enhancement and arbitrary distribution of SeNBs and users in HetNets have been scrutinized in [165], where the characteristics of SINR are measured and network throughput is optimized for both the downlink and uplink by an optimal implementation of MeNBs and SeNBs. This phenomenon will certainly have an extensive impact on the entire wireless technology landscape. Hence in [166], V. M. Nguyen et. al. has developed a universal framework, which includes multi-slope path loss models and the effect of shadowing and small-scale fading distributions considering robust cell association in a Poisson field of interferers. The analysis present that there are three scaling regimes for the downlink SINR, coverage probability, and average per-user rate. It was also shown that depending on the near-field path loss and the fading distribution, the performance of the UEs in a 5G UDHetNet would monotonically increase, saturate, or decay with increasing network density. However, this work does not include the boundary conditions for network densification in terms of ASE. Hence, in [159], the authors have incorporated a sophisticated path loss model into the stochastic geometry analysis incorporating both line-of-sight (LoS) and non-line-of-sight (NLoS) transmissions to study their performance impact based on the coverage probability and ASE in HetNet. The

Analytical results are derived assuming both a general path loss model and a path loss model recommended by the 3<sup>rd</sup> Generation Partnership Project (3GPP) standards. The performance analysis demonstrates that as the density of SeNBs crosses a certain threshold, the network coverage probability will decrease, which in turn makes the ASE suffer from slow growth or even a notable decrease.

However, in reality, there is no clear method to demarcate the fundamental boundary of network densification, especially under any real-time teletraffic arrival scenario [168-170]. Arguably, it is also speculated that over-densification will no longer be able to provide exponentially increasing data rates as it can lead to a possible downfall in SINR [168-170]. Therefore, in this work, we aim to comprehend how the ASE is associated with density for real-time tele traffic arrival scenarios since the key objective of network densification is to improve ASE which is simply the sum throughput normalized by the coverage area eNB density.

## 2.5 Sustainable Green Communication Techniques in HetNets

After about a decade of in-depth research towards the improvement of QoS standards through designing innovative deployment scenarios like Het-Net, many researchers have recently shown keen interest in improving the energy efficiency of such complex future networks to achieve SGC for future technological advancements [171, 172]. From the implementation viewpoint, naive models are desirable as for composite systems large amounts of parameters are convoluted for simulation and analysis. Thus, designing a docile model for such complex and sustainably green Het-Nets is a tiresome task and requires standard assumptions such as terrain-specific hour-wise user distribution patterns and operational specifications of different categories of eNBs. Various distinguished research in this regard has already been observed in recent literature. From a deployment designing perspective, PPP in its pure or modified form aided by teledensity dependent clustering technique is found to be the most discussed method to design complex Het-Nets for Urban scenarios. As one of the key aspects of 5G, clustered Het-Net is a promising deployment model to cope with ever-increasing numbers of mobile UEs with guaranteed QoS demands. Clustered Het-Nets can enhance the Signal-to-Interference-plus-Noise Ratio (SINR) by deploying more SeNBs to bring the network nearer to UEs [90]. Unfortunately,

deployment of Het-Net comes at an additional cost. In reality, it generates a massive challenge for the wireless communication sector in terms of better management of network energy consumption [92]. Some serious efforts have been made in recent years to cope with this most critical issue of the modern era of telecommunication. A number of notable energy-saving methodologies like strategic/dynamic sleep mode policy and/or energy harvesting techniques have been found as the most promising solutions to make those complex Het-Nets energy efficient[43, 92, 172, 173, 174] to achieve SGC. In this subsection, a few of the contemporary related research works are deliberated, which encouraged us to explore even further. SGC techniques can be summarized under two broad categories.

- Strategic Sleep mode policies
- Energy Harvesting and Scheduling

Dense deployment of eNBs imposes a major impact on network power consumption as investigated by Tiankui Zhang et. al [174]. The minimum achievable data rate and throughput in terms of the traffic load in each tier are derived. The closed-form EE equation with respect to the BS deployment is also obtained. The simulation validates that EE maximization can be achieved by the optimized BS deployment. In [175], Jiaqi Lei et.al. has developed an analytical framework for estimating the average link SE, average throughput, and EE in a two-tier ultra-dense Heterogeneous Cellular Network, as well as providing guidelines for practical deployments. In [90], authors designed Het-Net based on the Poisson Point Process and derived the coverage probability to evaluate the area spectral efficiency and energy efficiency of the network in view of three Fractional Power Control (FPC) strategies. The numerical results and Monte Carlo simulation results shown in the work reveal that optimum power control can alleviate the interference by balancing out performances UEs. Authors have also investigated the effect of eNB sleeping strategies on the performance of the network when it is moderately burdened.

In [95, 176], the authors have modeled coverage probability, average achievable rate, and EE in multi-tier Het-Net with different sleep strategies for small cells cantered around the stochastic geometry-based HetNet model. The authors [95] then tried to maximize EE under random and strategic sleeping policies with restrictions on both coverage probability and wake-up times, whereas in [176,177], precisely, the impact of dynamic sleep mode policies on the power consumption and on the EE is

inspected and demonstrated that the performance improvements rest on the level of background noise. In another work [178], the authors studied the EE analysis of cellular networks through the deployment of sleeping strategies and small cells and derived the success probability and EE in homogeneous macrocell (single-tier) and heterogeneous K-tier wireless networks under different sleeping policies. In addition, the authors have also framed the energy EE maximization problems and defined the optimal operating conditions for macrocell base stations. A unique dynamic cluster-based method for maximizing the EE of wireless small cell networks is proposed by Sumudu Samarakoon et. al. in [179, 180] which allows intra-cluster synchronization among the SeNBs for improving the downlink performance by means of load balancing while fulfilling QoS demands of UEs. In [181], the clusters-based approach creates a path for the implementation of opportunistic SeNBs sleep-wake swapping method to maintain stability between delay and energy consumption. In [180], a coordination mechanism between SeNBs is proposed to minimize a cost function, which invokes the trade-offs between EE and flow level performance. GiaKhanh Tran et. al. in [182] have designed a proactive cell activation/deactivation technique jointly with user association methodologies to maximize the network's EE entrusted upon traffic model based on realistic measurement data in metropolitan Tokyo.

The urgency to reduce CO<sub>2</sub> emission and energy costs associated with it has given birth to a novel SGC technique labeled as EH and/or WPT. Works testified over the last few years on this method are mentioned herewith. In [105], Yuyi Mao et. al. has performed a complete investigation of EH in SeNB-based networks regarding the feasibility analysis of powering SeNBs with renewable energy sources like solar. The work performed some case studies and proclaimed that among potential EH sources, the blend of solar and wind energy sources could turn out to be a good candidate to empower SeNBs. In addition, the authors have also performed trade-offs between the network performance, SeNB density, and grid power consumption. Some other noted works also discuss the use of renewable sources of energy to be the right candidates for EH solutions but these sources may not be sustainable as a long-term solution [43]. In order to guarantee the QoS demands of UEs in this age of ultra-dense Het-Net environment, network elements especially low-powered SeNBs are prone to consume more power and drain their batteries even faster. Due to the limited energy sources of SeNBs, SWIPT has been projected as a milestone solution to serve as a long-lasting



energy source for SeNBs, hence improving the QoS demands. In SWIPT networks, SeNBs are able to refill their energy repositories through RF that can be used to charge their inbuilt batteries. An elaborated explanation of SWIPT is presented in [104]. In [108] a scalable deployment model of K-tier SWIPT based HetNet is formulated for its critical performance evaluation. Additionally, the EE performance evaluation of SWIPT networks is investigated in [183]. In [184] TiejunLv et. al. have exhibited that Het-Nets with EH can improve the EE only when the density of the SeNBs is high in a HetNet. However, the works cited above have little clarity on channelizing the harvested energy whether from natural sources or by SWIPT. A key challenge for EH-enabled network deployment is to maneuver a network seamlessly regardless of the stochastic nature of traffic and energy arrivals [185]. Lakshmikanth Guntupalli et.al. in [185] proposed one such on-demand energy request technique to boost the performance of an EH-enabled IoT network.

## 2.6 Chapter Summary

Based on the previous literature it is understood that the phenomenal long-term growth of mobile technologies spanning over 3 decades has been principally attained by network densification and the technological advances necessary to support such densification. By *densification*, we mean the deployment of low-power nodes (i.e., small cells, which may be employed indoors or outdoors) offers a simpler cost-effective alternative to conventional network architecture paving the way for a new terminology i.e. Het-Net.

A lot of contributions have been done in the direction of designing Het-Net for 4G networks in previous research contributions. However, there lies enough scope for designing unique RRM techniques, especially for LTE-based Het-Nets where the available spectrum and its proper utilization have been key aspects. To the best of our knowledge, the Joint CAC and DBA for LTE-based two-tier HetNet has not been discussed yet.

In addition, as the wireless ecosystem is gradually evolving from 4G to 5G, the concept of HetNet or any of its modifications such as Ultra dense HetNet is expected to create a major impact to handle the immense growth of the use of personified mobile devices in the presence of mmWave. Spatial modeling of Ultra dense HetNet by means of stochastic geometric methods is well documented in previous research

works. However, determining the optimal position and number of additional network elements through spatial clustering in view of real-time tele traffic density to achieve guaranteed QoS has not been deliberated yet.

Deployment of complex HetNets will certainly increase the overall power consumption of the network. Many notable works have been published where the authors have distinctly designed unique energy-efficient techniques such as Energy Harvesting, Strategic Sleeping policy for HetNets. But the design of SSP for EH-enabled SeNBs under HetNets i.e. integration of EH and SSP has not been done yet.

Hence in this thesis, we propose a novel RRM technique for the dense deployment of small cells inside complex HetNets for enabling guaranteed QoS to the end user. Additionally, we also put forward a novel EE technique for the pursuance of sustainable green communication in the era of 5G and beyond.

# Chapter 3: Joint CAC and DBA Technique for QoS performance evaluation in LTE based HetNet

---

## Outline of this chapter

- 3.1 Abstract
- 3.2 Introduction
- 3.3 System Model
  - 3.3.1 Class Based QoS Framework
  - 3.3.2 Scenario Descriptions
  - 3.3.3 Bandwidth Allocation
  - 3.3.4 RSS Calculation
- 3.4 Joint CAC and DBA scheme: The proposed Algorithm
  - 3.4.1 RSS Based JCACDBA scheme
  - 3.4.2 SINR Based JCACDBA scheme
- 3.5 CTMC based Analytical Model
- 3.6 QoS metrics for performance evaluation
- 3.7 Performance Evaluation
- 3.8 Chapter Summary

## 3.1 Abstract

Very recently, LTE has started to grow strongly and has reached around 600 million subscriptions, with approximately 105 million additions in Quarter 1 of 2015. Looking into the growing traffic demand with restricted resources, it is sure that the macro cell alone is not enough to meet the service quality demand with proper coverage. Moreover, deployment of Small eNodeBs (SeNB) keeping Macro eNodeB (MeNB) as backhaul is capable of fulfilling predicted future capacity and QoS demands. Eventually, it is needless to mention that heterogeneity in the architecture, protocol, and applications are some of the cohesive traits of 3GPP LTE. To ensure the estimated service quality demands Call Admission Control (CAC) that has been exhaustively pursued in recent times plays a major role in QoS provisioning in terms

of the signal quality, signal-to-interference plus noise ratio (SINR), call blocking, dropping, and outage, and resource utilization for modern days wireless communication systems. The performance of CAC techniques has a direct contribution to each user's individual performance as well as the overall network performance. The arrival of newly originated and handoff calls are accepted/denied access to the network which is incorporated by the CAC scheme based on some predefined principles, taking the current network conditions into consideration. CAC becomes an essential tool in QoS provisioning in any wireless network. CAC is already extensively studied for Worldwide Interoperability for Microwave Access (WiMAX) networks for QoS provisioning. However, the design of the CAC algorithm in LTE based wireless networks is more complex due to the unique features of 3GPP LTE such as very high data rate, heterogeneous environment, fast handoff, and effective bandwidth utilization requirements, etc. CAC in LTE based BWA networks has been getting immense attention during the last two decades due to this growing traffic demand.

### 3.2 Introduction

After the popularity of broadband over wireless especially in the era of 4G LTE, the number of wireless subscribers has been rising day by day because of the intense use of various multimedia applications through personified mobile devices. Looking into the increasing traffic demand with limited resources, it is certain that traditional macro cells are alone not capable enough to deal with the increasing capacity with acceptable coverage. However, finding Macro cell sites is a difficult task and a costly affair too. In addition, it is needful to reduce the cell-to-cell distance in the macro network to diminish path loss at each mobile user end leading to the research for network densification [186]. The most feasible solution is to deploy Small eNodeBs defined as SeNB (low-power base stations), keeping Macro eNodeB (MeNB) as backhaul, capable of fulfilling predicted future capacity and QoS demands [187, 188]. Outdoor SeNBs are required to be deployed primarily in dense urban areas, with their deployment strategies depending significantly on the level of QoS that operators need to provide to their customers at given locations [189], whereas indoor larger locations, such as malls, metro stations, and enterprises, would require a dedicated indoor small cell deployment (known as Femtocells) [51].

Small cells are used to increase capacity in the hot spots with high user demand and filled the uncovered area of Macro cells both in outdoor and indoor areas. The result is the Het-Net that combines the large macro cells with small cells providing an increased data rate per unit area. The typical output power of these SeNBs ranges from 250 mW to approximately 2W, whereas the range reduces to 100 mW or less for that of femtocell SeNB. Now-a-day multi-tiered networks are also gaining importance for QoS guarantee and improved coverage and capacity [190]. In a few use cases, an outdoor small cell [51, 190] network placed by the streets can also assist operators to provide indoor penetration through up to three interior walls in the infrastructures like shops, restaurants, and cafes near those streets. In effect, deploying small cells at the street level would be faster, cheaper, and much simpler compared to using femtocells for every indoor location [191, 192]. Such a network which consists of the combination of these macros, picos, and femtos where some may have restricted access and most of them are wirelessly connected to the back-haul is popularly known as a Heterogeneous network (Het-Net) [187-190]. Moreover, it is quite certain that heterogeneity in the architecture, protocol, and applications are some of the key features of 3GPP LTE.

However, the avalanche of the number of users has been a major challenge to handle. Given the scarcity of resources in 4G LTE, network planning and deployment should go through proper Radio Resource Management (RRM) techniques [193] for smooth penetration of heterogeneous multimedia services to the last mile. The RRM technique is a combination of (1) Resource Monitoring (2) Decision Making (3) Decision Enforcement. Call Admission Control (CAC), Bandwidth allocation (BA) are some of the powerful strategies that can ensure an allowable level of QoS to the end users.

In this chapter, different class of services is considered depending upon their QoS requirements defined by the service provider serving the node. The two-tiered architectures considered here aim to establish heterogeneity in terms of the network deployment scenario. In the upper tier, there is the traditional Macro eNodeB (MeNB) which can be treated as the backhaul whereas in the lower tier, there are a few low-powered small eNodeBs (SeNB). A Received Signal Strength (RSS) based CAC scheme is developed. The eNodeBs (eNB) from both the tier have their corresponding RSS threshold levels depending upon the parameters like cell coverage, and

transmission power. Each and every service request is admitted to the network depending on its RSS value. The RSS value is checked at each service level. As a user moves to the cell edge the RSS value deteriorates. That means one subscriber can have different RSS values while using different multimedia services at different instants of time. In addition, the novelty of this work focuses on the allocation of required bandwidth to the SeNB in a dynamic manner by a proposed algorithm termed as dynamic bandwidth allocation (DBA) algorithm and integration of DBA with RSS based CAC policy. The joint implementation of RSS based CAC and DBA policy is termed in this work as the JCAC-DBA scheme. To justify the uniqueness of the proposed scheme initially fixed amount of bandwidth is allocated to all the MeNB along with RSS based CAC policy as well as SeNBs denoted as Static Bandwidth Allocation (JCAC-SBA). Then the results of the SBA are compared with that of the DBA scheme. The proposed work also integrates RSS based CAC and DBA algorithms and implements them in some LTE heterogeneous BWA network scenarios. Considering QoS guarantee as an important issue, in this paper, a comparative analysis has been done between Multihop Relay based and Small Cell based two-tier LTE network architecture. This chapter also proposes a signal-to-interference plus noise (SINR) based JCAC and DBA scheme to ensure guaranteed QoS to the requesting connections. The admission of the connection into the network is incorporated by its SINR value and bandwidth available in the eNB at the time of admission. The novelty of the scheme is that the proposed CAC algorithm calculates SINR at each user level. It ensures that the SINR level of the requesting connection does not exceed the SINR threshold of that network on admitting one particular connection. When a new connection request approaches, the eNB calculates the  $SINR_n$  for each connection type. If the measured  $SINR_n$  is greater than or equal to the corresponding predetermined  $SINR_{th}$ , and the minimum required bandwidth is available for the requesting connection, the connection is admitted into the system. It is also shown in this work that given the capability of an eNB in the macro cell, working as backhaul, how many SeNBs can be attached and consequently how much capacity is increased for the network. At each level, allowable performance improvement is noticed. To do this, an analytical model based on Continuous Time Markov Chain (CTMC) [194] is developed which analyses the connection blocking probability, dropping probability, and bandwidth utilization at each state level using MATLAB.

### 3.3 System Model

The system model of this work comprises several sections. Initially, a QoS framework has been proposed with respect to different service flows followed by the proposal of the Het-Net architectures. The proposed system model considers three architectures under three case studies. In case study 1, one MeNB is considered in isolation. For case 2, two low power SeNBs are deployed keeping MeNB as back haul. In case 3, the number of SeNB is further increased. Furthermore, path-loss models for both MeNB and SeNB leading to the calculations of RSS are demonstrated. Finally, the DBA algorithm is proposed and described in the final section.

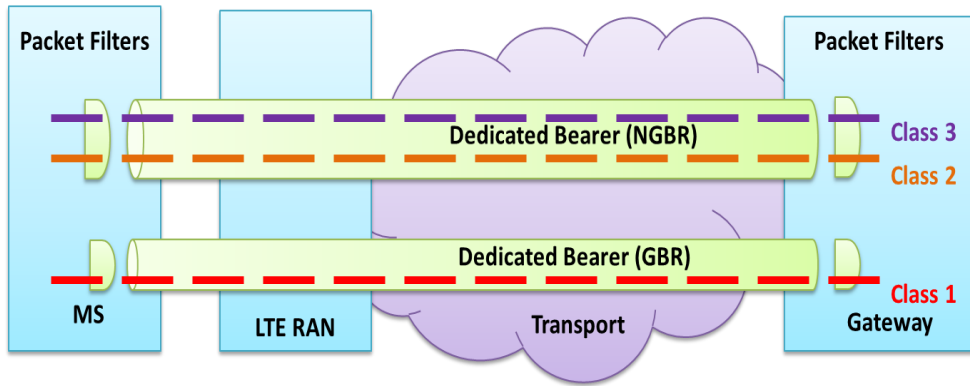


Figure 3.1 4G LTE QoS Framework [28]

#### 3.3.1 Class Based QoS framework

Multiple classes of services, namely, Conversational voice, Conversational video (live streaming), Real-time gaming, Non-conversational video (buffered stream), IMS signalling (buffered streaming) TCP-based (e.g., www, e-mail, chat, FTP, p2p sharing, progressive video, etc.), are supported simultaneously by 3GPP LTE. Different packet forwarding treatment policies (e.g. scheduling policy, rate-shaping policy) assigned to each of these services make the set of services heterogeneous. In this section, the proposed Class Based QoS framework provides differential treatment for heterogeneous traffic with different QoS requirements [195]. In the LTE evolved packet system, the QoS framework is based on bearer services. A bearer is nothing but a basic enabler for traffic separation that enables a connection flow established between the packet data network gateway (PDN-GW) and the user terminal (UE) [11]. Fig 3.1 shows an end-to-end LTE QoS framework consisting of different bearer flows. A bearer is assigned a scalar value referred to as a

QoS class identifier (QCI) [28]. The QCI determines to which class the bearer belongs. QCI refers to a set of packet forwarding treatments (e.g., scheduling weights, admission thresholds, queue management thresholds, and link layer protocol configuration) preconfigured by the operator for each network element.

Table 3.1: Applications, types of traffic and QoS Parameters of LTE				
QCI	Services	Qos Frame-work	Max. data rate (kbps)	Min. data rate (kbps)
Class1	Conversational voice/Video, real time Gaming	GBR	128	128
Class2	IMS Signalling, Live Streaming	N-GBR (Real Time)	1024	512
Class3	Buffered Streaming, TCP, E-Mail, P2P, FTP, Web Browsing.	N-GBR (Non Real Time)	1024	256

The class-based method improves the adaptability of the LTE QoS framework. LTE offers two types of bearers [28]. Fig. 3.1 illustrates the bearer based end-to-end LTE QoS framework. Table 3.1 demonstrates class based categorization for all types of traffic with respect to their QCI value, their application along with their QoS requirement and priority [28, 196]. The bearer management and control in LTE follows the network-initiated QoS control paradigm, and the network-initiated establishment, modification, and deletion of the bearers. LTE offers two types of bearers [28, 195, 196]:

- a. Guaranteed bit rate (GBR): Dedicated network resources related to a GBR value associated with the bearer are permanently allocated when a bearer becomes established or modified.
- b. Non-guaranteed bit rate (N-GBR): The non-GBR bearer has no such requirement as GBR and may experience congestion and. Hence, Variable network resources are assigned. The required resources are assigned as and when required based on the priority of the service and availability of resources. N-GBRs can be further categorized into real-time and non-real time services.

### 3.3.2 Scenario Descriptions

Being a developing country, India, most of the major cities are getting expanded day by day. There is an affinity to construct big infrastructures like University Buildings, Housing complexes in the extended regions of those cities. Naturally, the extension of those cities is getting crowded day by day. The traditional



infrastructures are no longer able to accommodate the users in the cell edges or the users may suffer from low signal strengths leading to call drop or call block in those areas. On the other hand, deployment of new MeNBs is not at all cost-effective from a service provider's point of view or in some cases, it is impossible to deploy those due to scarcity of proper place. The deployment of some low-powered SeNBs [197] and/or ReNBs [198] may increase capacity in those areas with high user demand and provide coverage in areas not covered by the macro network both outdoors and indoors. With limited computing capabilities, the ReNBs mainly focused on extending coverage area [199]. On the other hand, SeNBs not only helps in extending the coverage of MeNBs but also look up network performance and guarantee QoS by offloading from the large macro-cells. Deployment of such additional infrastructures results in a heterogeneous network (Het-Net) [53]. In the following case studies, the MeNB is represented in red colour whereas the SeNBs are represented in green colour. The light grey coloured area represents the actual coverage area of MeNB. The portions in blue colour in Case 2 and Case 3 represent the coverage area of SeNBs. It is also assumed that 'n' numbers of random call requests are generated at a maximum distance of 1500 m ( $D^{MAX}$  in Table 1) of different service classes, namely, Class 1, Class 2, and Class 3 (represented in red, yellow, and green colours in Fig. 3.2, 3.3, 3.4 and 3.5 respectively).

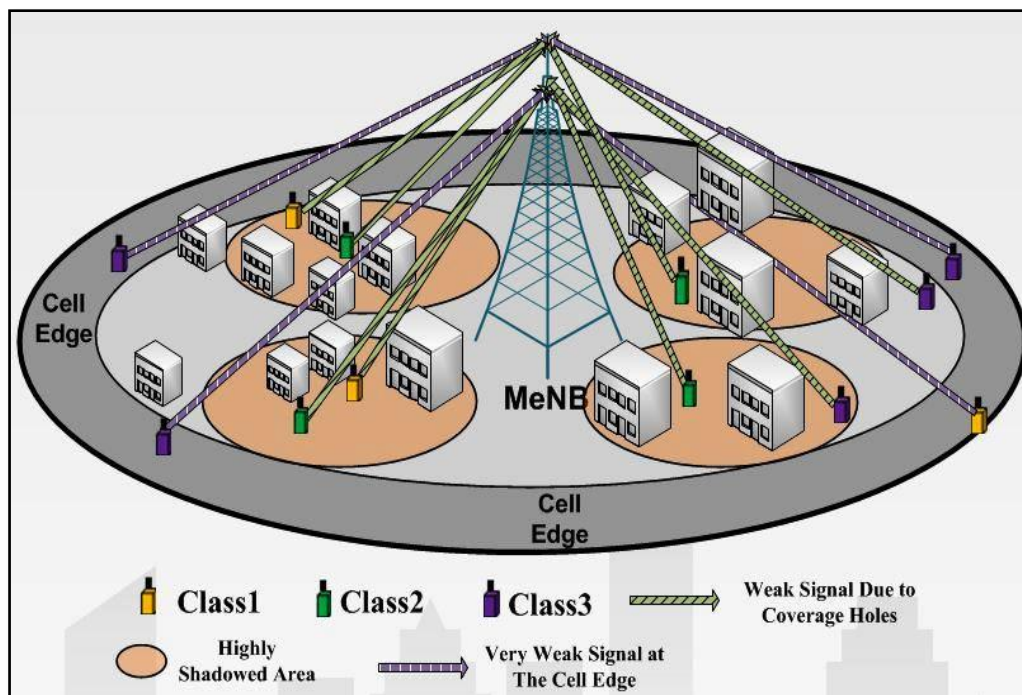


Figure 3.2 Single MeNB based traditional network

### Case 1: One MeNB

The first case considers a network scenario with only one MeNB. The typical coverage area of a MeNB is more than 1km [197]. In this work, we have emulated that the coverage area of a MeNB is 1000 meters. An amount of bandwidth that can eventually support a cumulative data rate of 10240 kbps is allocated to the MeNB to accommodate user requests with variable service rates. Fig. 3.2 demonstrates a classical network scenario having Single MeNB.

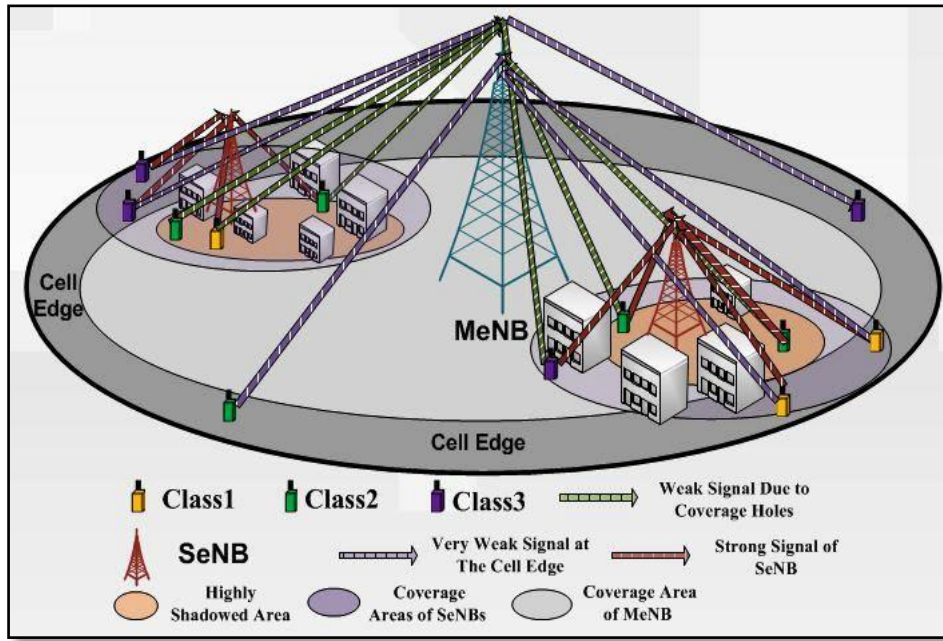


Figure 3.3 One MeNB and two SeNB based HetNet scenario

### Case 2: One Macro and Two SeNBs

In this case, two SeNBs are placed  $180^\circ$  apart near the cell edge of the macro cell, dividing the macro cell coverage into two parts and keeping the macro base station as backhaul. Typically, the coverage of a SeNB is 200 m [197]. It is assumed that the deployment of these SeNBs will maximize the overall coverage of MeNB through complimentary services with the expectation that the deployment of SeNBs can accommodate more number of users in the network. The analytical results in the forthcoming sections will justify that this type of tiered architecture can enhance the overall performance of the system to a significant level. The proposed network scenario with One MeNB and two SeNBs is depicted in Fig. 3.3.

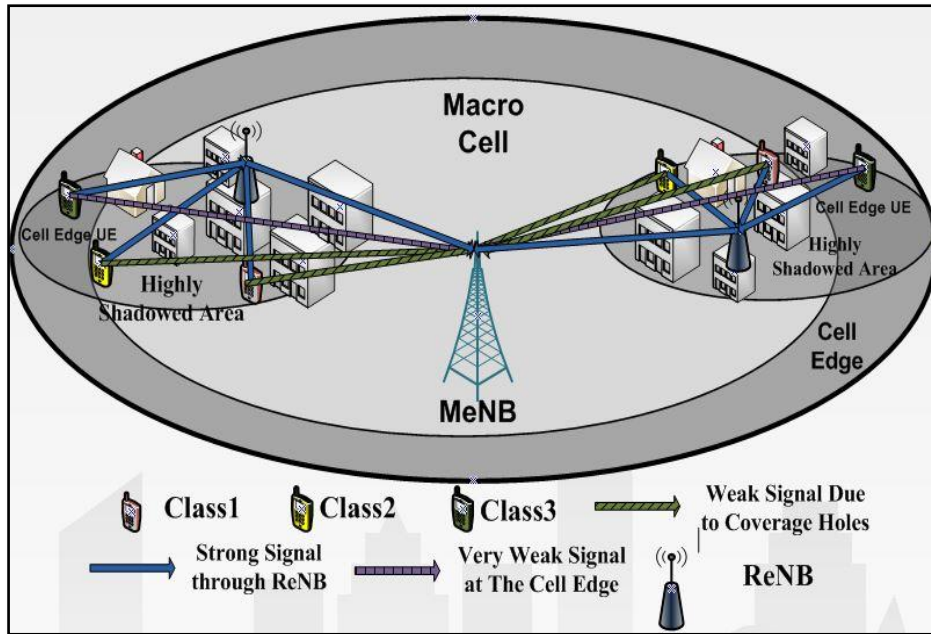


Figure 3.4 Multi-hop Relay Assisted HetNet Scenario

### Case 3: One MeNB and Two ReNBs

Multi-hop Relay Assisted BWA Network Scenario Fig. 2.4 represents a Multi-hop Relay based BWA network scenario. With the help of relay nodes, the radio link between the backhauleNodeB (denoted as MeNB) and user equipment (UE) is divided into two hops. Both links are expected to have better propagation conditions than the direct link from the eNodeB to the UE (as shown in Fig.3.4) [198].

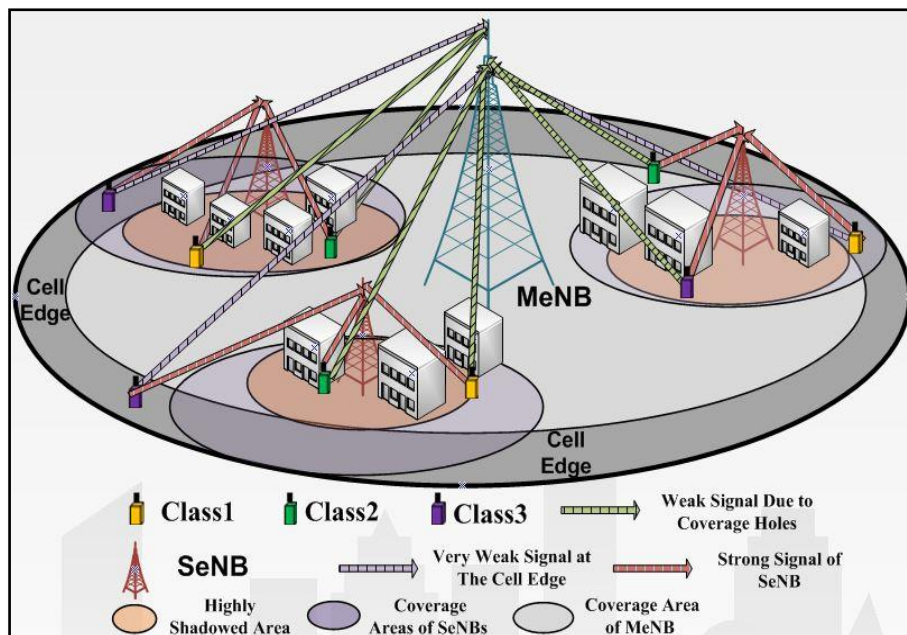


Figure 3.5 One MeNB and Three SeNB based HetNet Scenario

#### Case 4: **One MeNB and Three SeNBs**

Fig. 3.5 represents the scenario with one MeNB and three SeNBs placed in a  $120^\circ$  sectorized coverage with respect to macro cell coverage. One way to increase the capacity of a cellular network to make up for the increasing number of subscribers is to replace the omnidirectional antenna at the base station with a number of directional antennas. This method is called cell sectoring. This is a very common technique used in macro cellular systems to improve the performance against co-channel interference. In this method, each cell is subdivided into radial sectors with directional antennas. In practical terms, a number of sectorized antennas are mounted on a single microwave tower located at the center of the cell, and a subsequent number of antennas are installed to cover the full 360 degrees of the cell. The number of cells in a specific cluster is decreased in cell sectoring, and the separation between co-channels is decreased. Therefore, cell sectoring refers to the method of decreasing co-channel interference to increase the cellular system capacity by using directional antennas for each sector within a cell.

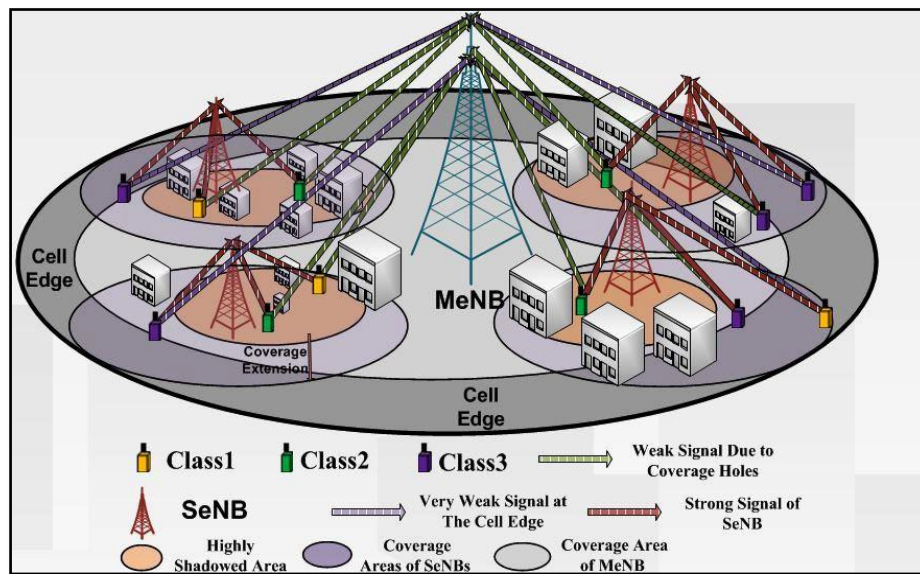


Figure 3.6 One MeNB and four SeNB based HetNet scenarios

#### Case 5: **One MeNB with four SeNBs**

The number of SeNBs is further increased to four and placed at four quadrants of macro cell edge coverage with a view to accommodate more users in the network expecting less blocking and dropping. By allocation, more numbers of new calls and handoff calls may provide a better bandwidth utilization of the overall network. Fig. 3.6 represents a two-tier LTE based BWA network having One MeNB and four



SeNBs. This case is taken into consideration to analyse optimal performance to cover a circular region under heterogeneous services in comparison to three numbers of SeNBs with  $120^\circ$  sector each.

### 3.3.2 Bandwidth Allocation

The allocation of bandwidth to the SeNBs is another major concern of our research. There are two ways to allocate bandwidth to the SeNBs.

- Static Bandwidth Allocation (SBA)

It is the process of allocation of bandwidth to the SeNBs in a proactive manner. That means the system will distribute the bandwidth to all the eNBs at the beginning of the communication process. In some cases, it may be found that an amount of bandwidth remains unused due to the random distribution and mobility of the users.

- Dynamic Bandwidth Allocation (DBA)

It is the process of allocating the bandwidth to the auxiliary eNBs in a reactive manner or on demand. That denotes the SeNBs ask for an amount of bandwidth from the MeNB only when there is a bandwidth request under that particular SeNBs.

In this proposed work, for Case 2, Case 3, and Case 4, the bandwidth allocation is made using both SBA and DBA. From the simulation results, it can be found that by implementing DBA to this sort of Two-Tier Heterogeneous BWA Network can improve the overall bandwidth utilization of the system.

### 3.3.3 RSS calculation

Our proposed work considers the arrival of any service request by means of the received signal strength of that particular mobile station that is accessing that service. The measurement of the RSS depends upon two factors. One is transmission power ( $P^{tx}$ ) another is the path loss. The requisite  $RSS^{th}$  for the requesting connection type 'i' should be determined in such a way that the wireless communication is still possible, below which communication disruption may occur. To find the  $RSS^{th}$ , the effective threshold received power of the requesting connection type is first determined.  $P_{rx}^{th}$  is defined as the threshold Transmitted power ( $P^{tx}$ ) when subtracted by the threshold path loss component ( $PL^{th}$ ). According to LTE; Evolved Universal

Terrestrial Radio Access (E-UTRA); Radio Frequency (RF) requirements for LTE Pico Node B, both MeNB and SeNB have different path-loss models for outdoor suburban scenarios [76, 200]. As path loss is a distance-dependent parameter, hence

$$PL^{th} = f(D^{coverage}) \quad (1)$$

The path loss models for MeNB, SeNB [76, 200] and ReNB [201] are shown in (2), (3), and (4) respectively.

$$PL_{MeNB}^{th}(dB) = 128.1 + 37.6 \log_{10}(D_{MeNB}^{coverage}) \quad (2)$$

$$PL_{SeNB_m}^{th}(dB) = 38 + 30 \log_{10}(D_{SeNB_m}^{coverage}) \quad (3)$$

$$PL_{ReNB_r}^{th}(dB) = 145.4 + 37.5 \log_{10}(D_{ReNB_r}^{coverage}) \quad (4)$$

Where,

$P_{rx, MeNB}^{th}$  is the threshold Path loss determined by Macro eNodeB depending upon its maximum coverage i.e.  $D_{MeNB}^{coverage}$ ;  $P_{rx, SeNB_m}^{th}$  is the threshold Path loss determined by SeNBs considering their maximum coverage as  $D_{SeNB_m}^{coverage}$ ; and  $P_{rx, ReNB_r}^{th}$  is the threshold Path loss determined by ReNBs considering their maximum coverage as  $D_{ReNB_r}^{coverage}$  such that ‘m’ is the number of SeNBs and ‘r’ is the number of ReNBs.

The resulting RSS<sup>th</sup> encountered by one mobile station with respect to MeNB,  $SeNB_m$  and  $ReNB_r$  are given by:

$$RSS_{MeNB}^{th} = P_{MeNB}^{tx} - PL_{MeNB}^{th} \quad (5)$$

$$RSS_{SeNB_m}^{th} = P_{SeNB_m}^{tx} - PL_{SeNB_m}^{th} \quad (6)$$

$$RSS_{ReNB_r}^{th} = P_{ReNB_r}^{tx} - PL_{ReNB_r}^{th} \quad (7)$$

Let the requesting connection be the  $C_i^{th}$  connection and the requesting connection’s traffic type be ‘i’. It is assumed that the connections are distributed in the network in random manner. Thus, the path loss value, which is a distance dependent parameter, varies for different connection in the network.

$$PL_{MeNB}^i(dB) = 128.1 + 37.6 \log_{10}(D_{MeNB}^i) \quad (8)$$

$$PL_{SeNB_m}^i(dB) = 38 + 30 \log_{10}(D_{SeNB_m}^i) \quad (9)$$

$$PL_{ReNB_r}^i(dB) = 145.4 + 37.5 \log_{10}(D_{ReNB_r}^i) \quad (10)$$

Where,  $0 < D_{MeNB}^i, D_{SeNB_m}^i, D_{ReNB_r}^i < D^{MAX}$ ;  $D^{MAX}$  is the maximum distance at which the connections can appear.

The received powers ( $RSS^i$ ) at core network from each connection with respect to MeNB and SeNBs are calculated as:

$$RSS_{MeNB}^i = P_{MeNB}^{tx} - 128.1 - 37.6 \log_{10}(D_{MeNB}^i) \quad (11)$$

$$RSS_{SeNB_m}^i = P_{SeNB_m}^{tx} - 38 - 30 \log_{10}(D_{SeNB_m}^i) \quad (12)$$

$$RSS_{ReNB_r}^i = P_{ReNB_r}^{tx} - 145.4 - 37.5 \log_{10}(D_{ReNB_r}^i) \quad (13)$$

### 3.4 Joint CAC and DBA Scheme: The proposed Algorithm

The proposed Quality of Service aware dynamic bandwidth allocation (DBA) scheme adjusts the admission of any service request and allocation of available resources based on the traffic behaviour and network conditions.

- RSS based JCAC and DBA scheme [203]

The traffic behaviour is characterized by the arrival rate and corresponding value of the RSS that it encounters after arrival. On the other hand, the network conditions are incorporated depending upon the remaining bandwidth. The RSS based call admission algorithms for the three cases are described in this section separately.

---

**Algorithm 3.1 RSS based CAC scheme for One MeNB in isolation.**

---

```

function = RSS_CAC_MeNB(B)
Initialize,
B=5120*(total available bandwidth*\
REMMeNB = B*(remaining bandwidth*\
    for i = 1 to maximim no of users
Initiate bandwidth request for connection 'i' ( BREQi )
Calculate RSSMeNBth, RSSMeNBi for MeNB &Check whether RSSMeNBi > RSSMeNBth
If true then check whether REMMeNB ≥ BREQi
If true then allow Connection 'i'such that REMMeNB = REMMeNB - BREQi
                                end if
                                end if
    end of for
end function

```

---

**Algorithm 3.1: CAC for network served by one MeNB**

Flow chart of the RSS Based CAC for Case Study 1 with only one MeNB is shown in Fig. 3.7. Algorithm 3.1 illustrates RSS based CAC scheme for One MeNB in isolation.

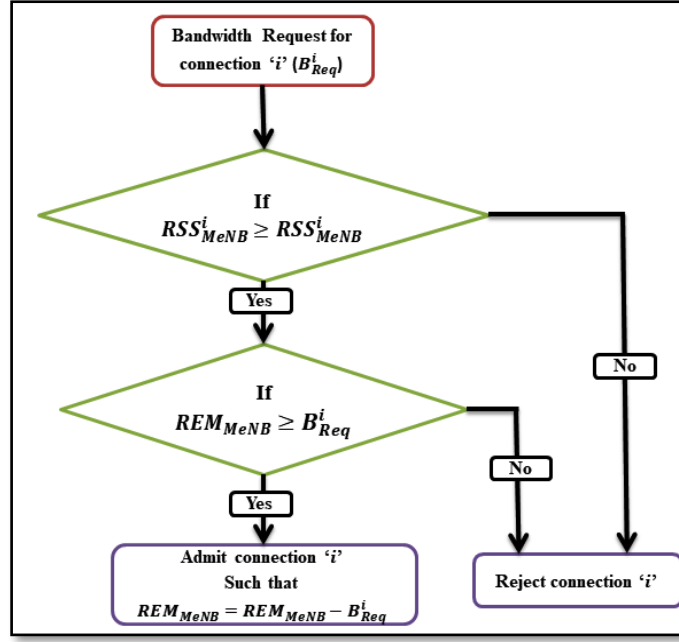


Figure 3.7 Flow chart of CAC policy considering single MeNB in isolation.

---

**Algorithm 3.2** *RSS based Call Admission Control (CAC) for One MeNB and Two ReNB.*

---

**function** = *RSS\_CAC\_oneMeNB\_two\_ReNBs* (*B*)

Initialize,

$B = 5120 * \text{total available bandwidth.}$

$REM_{MeNB} = 10240 * \text{Initially remaining bandwidth at MeNB}$

$REM_{SeNB_m} = 0 * \text{Initially remaining bandwidth at SeNB}_m$

Where,  $2 \leq m \leq 4$  No of SeNBs

**for**  $i = 1$  to maximim no of users

Initiate bandwidth request for connection 'i' ( $B^i_{REQ}$ )

Calculate  $RSS^{th}_{MeNB}$ ,  $RSS^i_{MeNB}$  & Check whether  $RSS^i_{MeNB} > RSS^{th}_{MeNB}$

**If true** then check whether  $REM_{MeNB} \geq B^i_{REQ}$  &

**If true** allow Connection 'i'

such that  $REM_{MeNB} = REM_{MeNB} - B^i_{REQ}$

**else** reject connection 'i'

**else**

**for each** relay eNB 'r'

Calculate  $RSS^{th}_{ReNB_r}$ ,  $RSS^i_{ReNB_r}$

Check whether  $RSS^i_{ReNB_r} > RSS^{th}_{ReNB_r}$

**If true** then check whether  $REM_{MeNB} \geq B^i_{REQ}$

**If true** then fetch ( $B^i_{REQ}$ ) from  $REM_{MeNB}$  and

allow Connection 'i', such that  $REM_{MeNB} = REM_{MeNB} - B^i_{REQ}$

**else** reject connection 'i'

**end if**

**end if**

**end of for**

**endif**

**end of for**

**endfunction**

---



**Algorithm 3.2: CAC policy for Multi-hop Relay based BWA HetNets [204]**

In case 3, two ReNBs have been introduced to the network along with one MeNB. Algorithm 3.2 presents CAC scheme for Multi-hop Relay based HetNets and simulation results are studied thereafter. Flow chart of the JCAC-DBA scheme for Multi-hop Relay based HetNets is shown in Fig. 3.8.

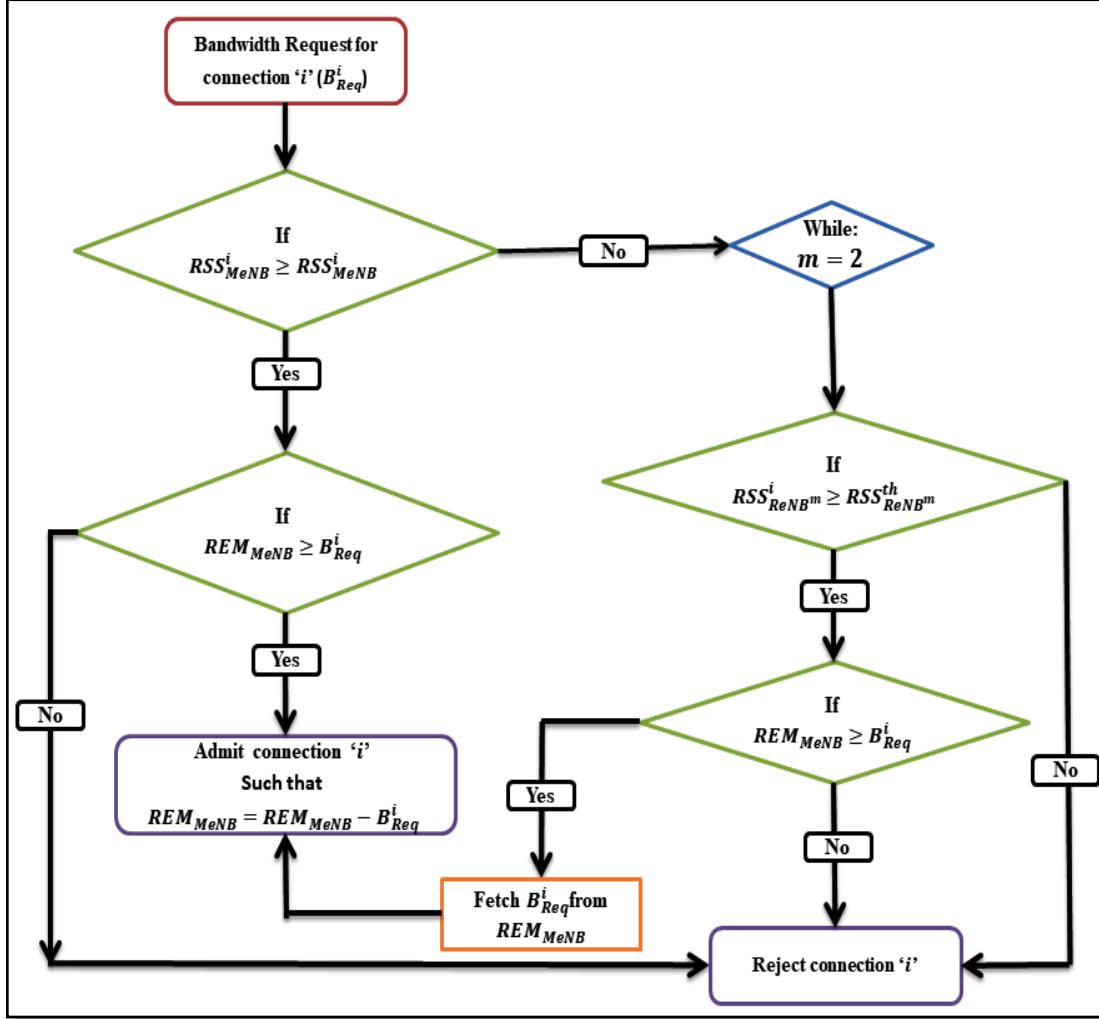


Figure 3.8 Flow chart of Joint CAC and DBA policy for Multihop Relay assisted Two-tier HetNet

**Algorithm 3.3: JCAC-SBA and JCAC-DBA for SeNB based BWA HetNets**

In case 2, case 4, and case 5, respectively two, three and four SeNBs have been introduced to the network along with one MeNB. Algorithms for both JCAC-SBA and JCAC-DBA have been developed under these cases and simulation results are studied thereafter. Flow charts of the JCAC-SBA, JCAC-DBA schemes are shown in Fig. 3.9 and Fig. 3.10 respectively. The JCAC-SBA and JCAC-DBA algorithms for BWA HetNets (case study 2, case study 4, and case study 5) are given below:

**Algorithm 3.3a: Joint CAC and Static Bandwidth Allocation for One MeNB and ‘m’ SeNBs.**

```

function
= RSS_CAC_oneMeNB_threeSeNB(B)
Initialize,
 $B = 5120 * \text{total available bandwidth.}$  *
 $REM_{MeNB} = 2560 * \text{Initially remaining bandwidth at MeNB}$  *
 $REM_{SeNB_m} = 512 * \text{Initially remaining bandwidth at SeNB}_m$  *
Where,  $2 \leq m \leq 4$  * \No of SeNBs\*
    for  $i = 1$  to maximim no of users
Initiate bandwidth request for connection ‘i’
( $B_{REQ}^i$ )
Calculate  $RSS_{MeNB}^{th}, RSS_{MeNB}^i$ 
Check whether  $RSS_{MeNB}^i > RSS_{MeNB}^{th}$ 
    If true then check whether  $REM_{MeNB} \geq B_{REQ}^i$  &
    If true allow Connection ‘i’
    such that
         $REM_{MeNB} = REM_{MeNB} - B_{REQ}^i$ 
    else
    reject connection ‘i’
    endif
    else
        for each small eNB ‘m’
Calculate  $RSS_{SeNB_m}^{th}, RSS_{SeNB_m}^i$ 
check whether  $RSS_{SeNB_m}^i > RSS_{SeNB_m}^{th}$ 
If true then check whether  $REM_{SeNB_m} \geq B_{REQ}^i$ 
If true then allow Connection ‘i’
    such that
         $REM_{SeNB_m} = REM_{SeNB_m} - B_{REQ}^i$ 
    else
    reject connection ‘i’
    endif
    endif
    end of For
endif
end of for
end function

```

**Algorithm 3.3b. Joint CAC and Dynamic Bandwidth Allocation for One MeNB and ‘m’ SeNBs..**

```

function
= RSS_CAC_oneMeNB_threeSeNBs (B)
Initialize,
 $B = 5120 * \text{total available bandwidth.}$  *
 $REM_{MeNB} = 10240 * \text{Initially remaining bandwidth at MeNB}$  *
 $REM_{SeNB_m} = 0 * \text{Initially remaining bandwidth at SeNB}_m$  *
Where,  $2 \leq m \leq 4$  * \No of SeNBs\*
    for  $i = 1$  to maximim no of users
Initiate bandwidth request for connection ‘i’
( $B_{REQ}^i$ )
    Calculate  $RSS_{MeNB}^{th}, RSS_{MeNB}^i$ 
    Check whether  $RSS_{MeNB}^i > RSS_{MeNB}^{th}$ 
    If true then check whether  $REM_{MeNB} \geq B_{REQ}^i$  &
    If true allow Connection ‘i’
    such that
         $REM_{MeNB} = REM_{MeNB} - B_{REQ}^i$ 
    else
    reject connection ‘i’
    endif
    else
        for each small eNB ‘m’
Calculate  $RSS_{SeNB_m}^{th}, RSS_{SeNB_m}^i$ 
Check whether  $RSS_{SeNB_m}^i > RSS_{SeNB_m}^{th}$ 
If true then check whether  $REM_{SeNB_m} \geq B_{REQ}^i$ 
If true then
         $REM_{SeNB_m}$  will fetch  $B_{REQ}^i$  from  $REM_{MeNB}$ 
        and allow Connection ‘i’
    such that  $REM_{MeNB} = REM_{MeNB} - B_{REQ}^i$ 
    else
    reject connection ‘i’
    end if
    end if
        end of for
    endif
    end of for
endfunction

```

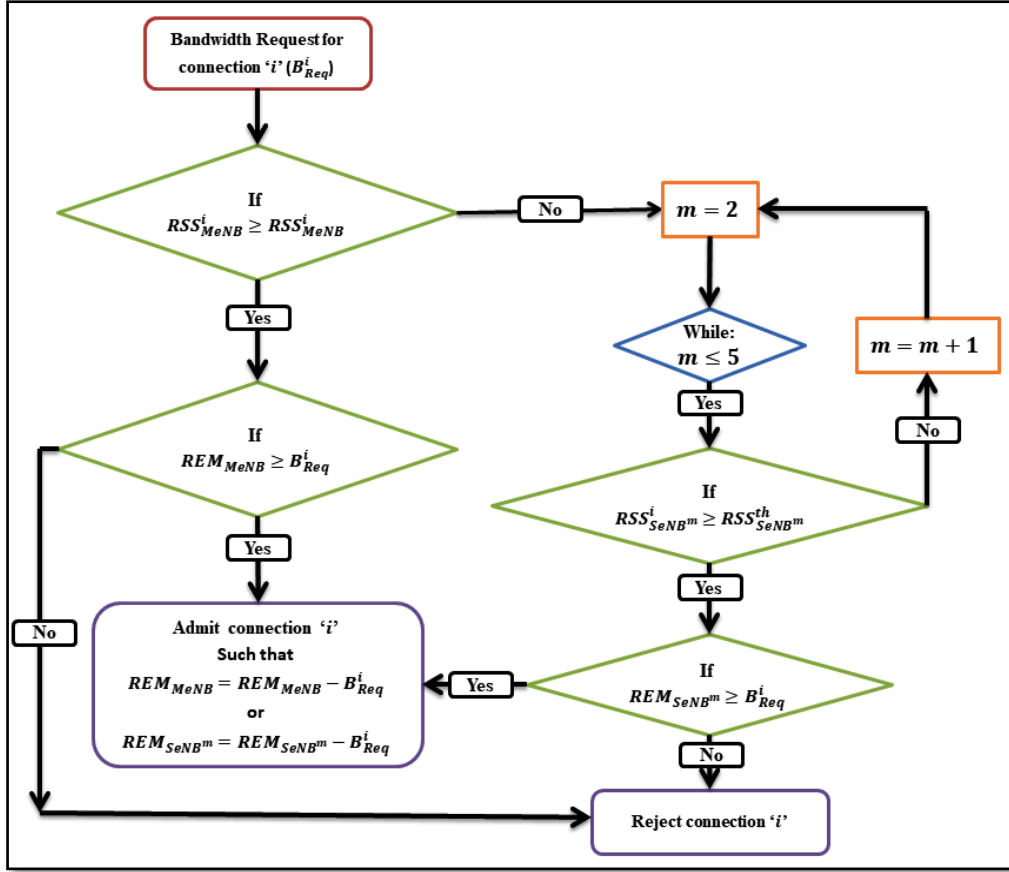


Figure 3.9 Flow chart of Joint CAC and SBA policy for Two-tier HetNet

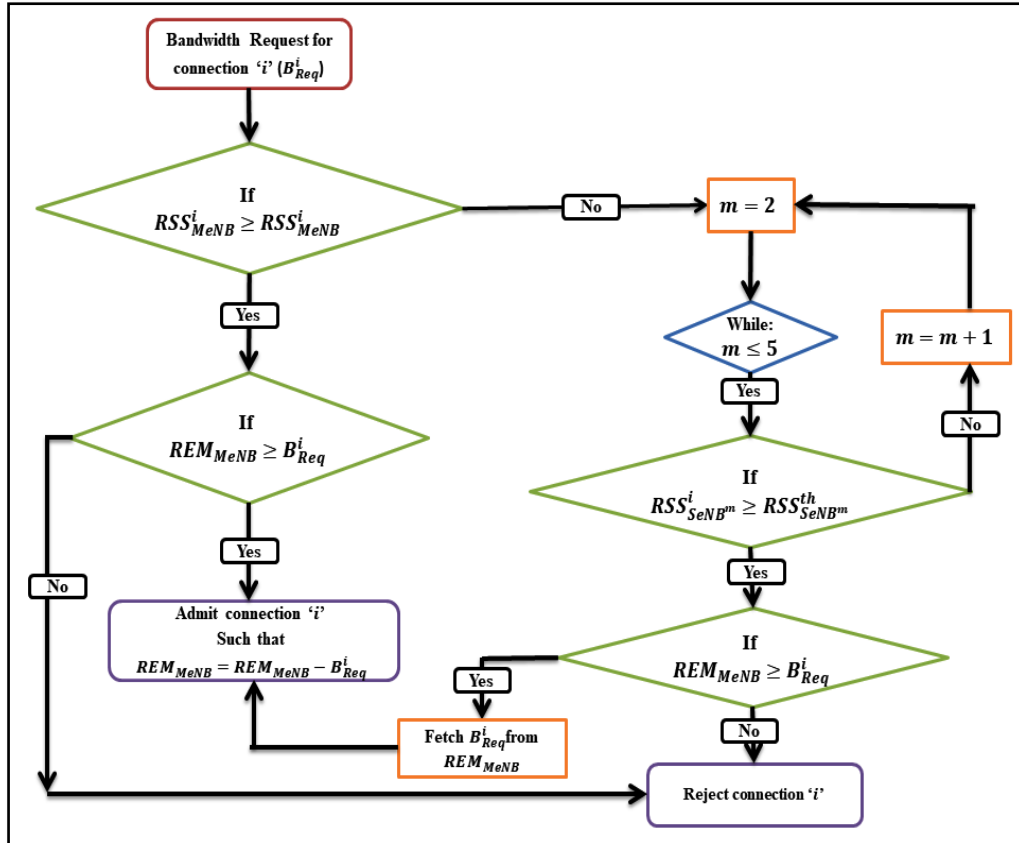


Figure 3.10 Flow chart of Joint CAC and DBA policy for Two-tier HetNet

- SINR based JCAC and DBA scheme

The SINR based JCAC and DBA scheme ensures that the SINR level of the requesting connection do not exceed the SINR threshold of that network on admitting one particular connection. When a new connection request approaches, the MeNB calculates the downlink SINR for each connection type. If the measured downlink SINR is greater than or equal to the corresponding predetermined threshold SINR, and the minimum required bandwidth is available for the requesting connection, the connection is admitted into the system.

#### 4.3.2.1 Calculation of $SINR^i$ , $SINR^{th}$

Let the requesting connection be the  $i^{th}$  connection and the requesting connection's traffic type be 'i'. The  $SINR^{th}$  for entering connection type 'i' ought to be calculated to such a degree that the interference of the wireless transmission remains below the tolerable threshold. Thus, the path loss value that is a distance dependent parameter varies for different connections in the network. The path loss models for MeNB and SeNBs are considered for this work as in [76, 200]. The measurement of  $SINR^{th}$  &  $SINR^i$  for both MeNB, and SeNBs are formulated as [205],

$$SINR_{x,y}^{th} = \frac{SNR_{x,y}^{th}}{(SNR_{x,y}^{th} \times n^{max}) + 1} \quad (14)$$

$$SINR_{x,y}^i = \frac{SNR_{x,y}^i}{\{\sum_{n=1}^k SNR_{x,y}^{(i-1) \times (i-1)}\} + 1} \quad (15)$$

Where,

$x$  = MeNB

$y$  = SeNBj,  $j = 1, 2, 3$ .

$SNR_{x,y}^{th}$  = Threshold Signal to noise ratio of MeNB, SeNBs  $\Rightarrow P_{x,y}^{th,rx} - \eta$ ;

$SNR_{x,y}^n$  = Signal to noise ratio of MeNB, SeNBs for connection type 'n'  $\Rightarrow P_{x,y}^{rx,n} - \eta$ .

$P_{x,y}^{th,rx}$  = Threshold Received Power  $\Rightarrow P_{x,y}^{tx} - PL_{x,y}^{th}$ .

$P_{x,y}^{rx,n}$  = signal power of the  $i^{th}$  connection;  $\Rightarrow P_{x,y}^{tx} - PL_{x,y}^n$ .

$P_{x,y}^{tx}$  = Transmit Power.

$PL_{x,y}^{th}$  = Threshold Path loss for MeNB, SeNBs.

$PL_{x,y}^n$  = Path loss component of the  $i^{th}$  connection.

$n^{max}$  = maximum no of connections that can be allocated  $\Rightarrow \frac{B}{MDR^n}$

$MDR^n$  = Maximum data rate (in kbps) of connection type 'i'.

$\eta$  = Uplink Noise Figure [202].

---

**Algorithm 3.4: SINR based CAC scheme for One MeNB in isolation.**

---

```

function = SINR_CAC_MeNB(B)
Initialize,
 $B = 10240 * \text{total available bandwidth}$ 
 $REM_{MeNB} = B * \text{remaining bandwidth}$ 
  for  $i = 1$  to maximim no of users
Initiate bandwidth request for connection 'i' (  $B_{REQ}^i$  )
Calculate  $SINR_{MeNB}^{th}$  for MeNB.
    Calculate  $SINR_{MeNB}^i$  for MeNB
    Check whether  $SINR_{MeNB}^i > SINR_{MeNB}^{th}$ 
  If true then check whether  $REM_{MeNB} \geq B_{REQ}^i$ 
  If true then allow Connection 'i'
    such that  $REM_{MeNB} = REM_{MeNB} - B_{REQ}^i$ 
    end if
  end if
end of for
end function

```

---

**Algorithm 3.5. SINR based Joint CAC and Dynamic Bandwidth Allocation for One MeNB and 'm' SeNBs..**

---

```

function = RSS_CAC_oneMeNB_threeSeNBs (B)
Initialize,
 $B = 10240 * \text{total available bandwidth}$ 
 $REM_{MeNB} = 10240 * \text{Initially remaining bandwidth at MeNB}$ 
 $REM_{SeNB_m} = 0 * \text{Initially remaining bandwidth at SeNB}_m$ 
Where,  $2 \leq m \leq 4 * \text{No of SeNBs}$ 
  for  $i = 1$  to maximim no of users
    Initiate bandwidth request for connection 'i' (  $B_{REQ}^i$  )
    Calculate  $SINR_{MeNB}^{th}, SINR_{MeNB}^i$ 
    Check whether  $SINR_{MeNB}^i > SINR_{MeNB}^{th}$ 
    If true then check whether  $REM_{MeNB} \geq B_{REQ}^i$  &
    If true allow Connection 'i'
      such that
         $REM_{MeNB} = REM_{MeNB} - B_{REQ}^i$ 
      else
        reject connection 'i'
      endif
    else
      for each small eNB 'm'
        Calculate  $SINR_{SeNB_m}^{th}, SINR_{SeNB_m}^i$ 
        Check whether  $SINR_{SeNB_m}^i > SINR_{SeNB_m}^{th}$ 
        If true then check whether  $REM_{SeNB_m} \geq B_{REQ}^i$ 
        If true then
           $REM_{SeNB_m}$  will fetch  $B_{REQ}^i$  from  $REM_{MeNB}$ 
          and allow Connection 'i'
          such that  $REM_{MeNB} = REM_{MeNB} - B_{REQ}^i$ 
        else
          reject connection 'i'
        end if
      end if
    end of for
  endif
end of for
endfunction

```

---

The proposed SINRCAC scheme admits any service request and allocation of available resources based on the traffic requirement profile (TRP) and current network conditions. According to the QoS requirement the SINRCAC scheme justifies itself as a prioritized algorithm. The TRP is characterized by the arrival rate and corresponding value of the SINR that it encounters after arrival. On the other hand, the network conditions are assimilated depending upon the remaining bandwidth. In this section a SINRCAC is proposed considering both scenarios respectively. Algorithm 3.4 demonstrates the SINRCAC for a traditional BWA network scenario while Algorithm 3.5 depicts the same for Het-BWA-Nets as shown in case study 4.

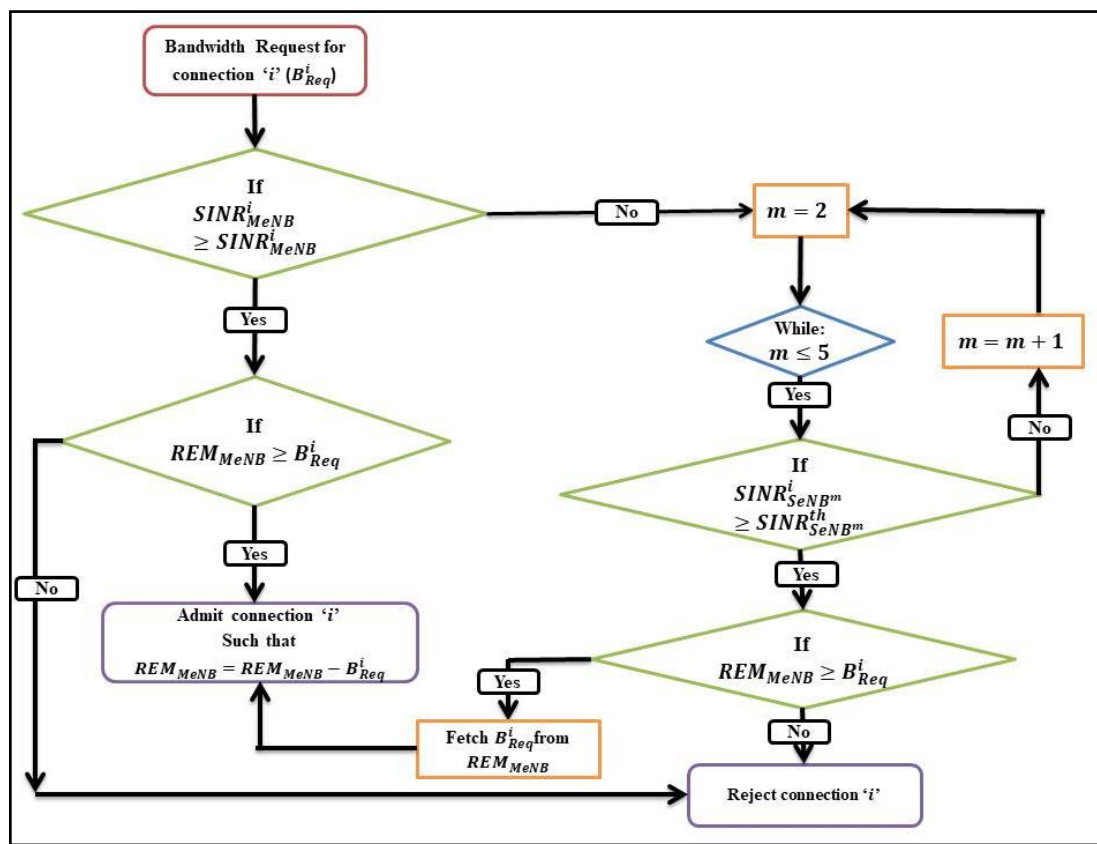


Figure 3.11 Flow charts of SINR based Joint CAC and DBA policy for Two-tier HetNet

### 3.5 CTMC based Analytical Model

In this section, a Continuous time Markov Chain [194, 203] based analytical model is developed to evaluate the performance of the QoS parameters. The Markov model is opted here because it defines the probability of being in a given state at a given point of time which the system is expected to spend in a given state, as well as the expected number of transitions between states. The BS changes its states from one to another upon the admission or rejection of a connection. It is also assumed that the BS either

admits or rejects one connection at a certain instant in time. So the next state of the BS depends only on the present state of the eNB but does not depend upon any other previous states of that eNB. This way the states of the BS form a Markov Chain and therefore the BS can analytically be modelled as shown in Fig. 3.12.

Fig. 3.12 demonstrates the generalized view of the Markov Chain. In this scenario, the states of the BS are modelled as a three dimensional Markov Chain  $(n_1, n_2, n_3)$  based on the number of connections admitted or rejected each time. State  $s = (n_1, n_2, n_3)$  represents that the BS has currently admitted ' $n_1$ ', ' $n_2$ ', and ' $n_3$ ' number of Class1, Class2, and Class3 connections respectively into the network. The BS will be in a particular States  $= (n_1, n_2, n_3)$  until a new connection of one of them i.e. Class1, Class2, Class3 is admitted into the network or an ongoing connection is terminated. The arrival process of the handoff and newly originated Class1, Class2, and Class3 connections is Poisson with rates  $\lambda_1, \lambda_2, \lambda_3$  respectively. The service time of Class1, Class2, and Class 3 is exponentially distributed with mean  $1/\mu_1, 1/\mu_2, 1/\mu_3$  respectively.

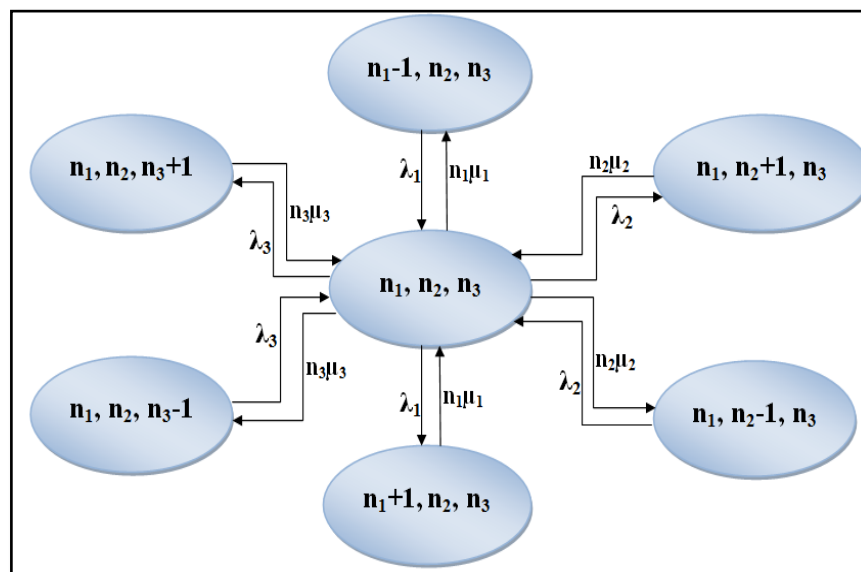


Figure 3.12 Generalized State Transition Diagram of the CTMC Model

The state space  $S$  for our proposed CAC scheme is obtained based on the following equation.

$$S = \{s = (n_1, n_2, n_3) | (n_1 \cdot B_1 + n_2 \cdot B_2 + n_3 \cdot B_3) \leq B\} \quad (16)$$

From Fig. 3.12, it is observed that every state  $s = (n_1, n_2, n_3)$  in state space ' $S$ ' is reachable from every other state i.e. each state communicates with other states in the

state space 'S'. As for example, state  $(n_1, n_2, n_3)$  communicates with state  $(n_1, n_2 + 1, n_3)$  and also communicates with state  $(n_1, n_2 - 1, n_3)$ . Hence, state  $(n_1, n_2 + 1, n_3)$  and  $(n_1, n_2 - 1, n_3)$  can also communicate to each other. In this way, each state can communicate with other state in the state space 'S'. Therefore, the state space 'S' forms a closed set and the Markov chain obtained is irreducible. Let the steady state probability of the state  $s = (n_1, n_2, n_3)$  is represented by  $\Pi_{(n_1, n_2, n_3)}$ . As the Markov chain is irreducible, thereby observing the outgoing and incoming states for a given state 's'. The state balance equation of state 's' is shown in (17).

$$\begin{aligned} & \{\lambda_1 \cdot \varphi_{(x+1,y,z)} + \lambda_2 \cdot \varphi_{(x,y+1,z)} + \lambda_3 \cdot \varphi_{(x,y,z+1)} + x\mu_1 \cdot \varphi_{(x-1,y,z)} + y\mu_2 \cdot \varphi_{(x,y-1,z)} + \\ & z\mu_3 \cdot \varphi_{(x,y,z-1)}\} \cdot \pi_{(x,y,z)} = \lambda_1 \cdot \varphi_{(x-1,y,z)} \pi_{(x-1,y,z)} + \lambda_2 \cdot \varphi_{(x,y-1,z)} \pi_{(x,y-1,z)} + \\ & \lambda_3 \cdot \varphi_{(x,y,z-1)} \pi_{(x,y,z-1)} + (x+1) \cdot \mu_1 \cdot \varphi_{(x+1,y,z)} \pi_{(x+1,y,z)} + (y+ \\ & 1) \cdot \mu_2 \cdot \varphi_{(x,y+1,z)} \pi_{(x,y+1,z)} + (z+1) \cdot \mu_3 \cdot \varphi_{(x,y,z+1)} \pi_{(x,y,z+1)} \end{aligned} \quad (17)$$

Where,  $x, y, z$  represents  $n_1, n_2, n_3$  respectively and,

$$\varphi_{(x,y,z)} = \begin{cases} 1, & (x,y,z) \in S \\ 0, & \text{Otherwise} \end{cases}$$

$\varphi_{(x,y,z)}$  represents the characteristic equation.

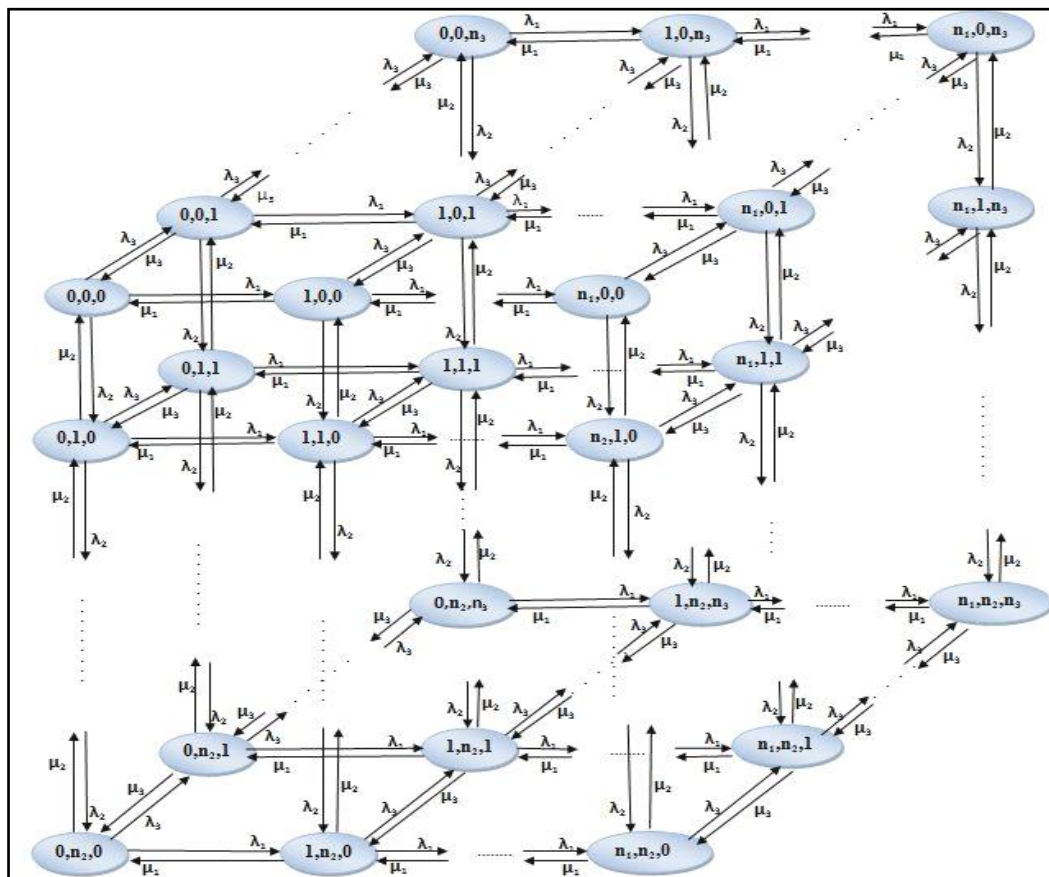


Figure 3.13 3D State Transition Diagram of the CTMC Model



By using (17), the state balance equations of each state in the state space ‘S’ are obtained. Solutions of these equations provide the steady state probabilities of all states in the state space S with the normalized condition imposed by (18).

$$\sum_{s \in S} \Pi_{(n_1, n_2, n_3)} = 1 \quad (18)$$

From the steady state probabilities, we can determine various QoS parameters of the system as given under [203]. The detailed 3D state transition diagram is shown in Fig. 3.13.

### 3.6 QoS Metrics for performance evaluation

From the steady state probabilities, we can determine various QoS parameters of the system as given under [194, 203].

#### A. New Connection Blocking Probability (NCBP)

The new connection blocking probability is the probability of rejecting a new connection request for admission into the network. Conditions for blocking a new connection request have been included in Table 3.2a.

- Estimation of NCBP for Class1, Class2, Class3 connections

While admitting a new connection, if the next state is not allowable Markov chain state in the state space ‘S’ due to the conditions as given in Table 3.2a, then the next state is considered to be a blocked state for that connection i.e. the new connection is blocked.

Let ‘S<sub>1B</sub>’, ‘S<sub>2B</sub>’, and ‘S<sub>3B</sub>’ form a state space for the states whose next state are not allowed in the Markov chain due to connection blocking.

The summation of the steady state probabilities of the states in the state space ‘S<sub>1B</sub>’, ‘S<sub>2B</sub>’ and ‘S<sub>3B</sub>’ give the NCBP of Class1, Class2, and Class3 connections respectively.

Hence,

$$NCBP_{Class1} = \sum_{s=S_{1B}} \pi_{(n_1, n_2, n_3)}(s) \quad (19)$$

$$NCBP_{Class2} = \sum_{s=S_{2B}} \pi_{(n_1, n_2, n_3)}(s) \quad (20)$$

$$NCBP_{Class3} = \sum_{s=S_{3B}} \pi_{(n_1, n_2, n_3)}(s) \quad (21)$$

### B. Handoff Connection Dropping Probability (HCDP):

The Handoff Connection Dropping Probability is the probability of rejecting a hand off connection request for admission into the network. Conditions for dropping a handoff connection request are summarized in Table 3.2a. Similar to NCBP, HCDP can also be estimated as given below, where ‘S<sub>1D</sub>’, ‘S<sub>2D</sub>’, and ‘S<sub>3D</sub>’ form a state space corresponding to Class1, Class2 and Class3 connection for the states whose next state is not allowed in the Markov chain due to connection dropping.

- Estimation of HCDP for Class1, Class2 and Class3 connections

Again, for the handoff connection if the conditions as given in Table 3.2a occur, then the handoff connection is dropped and the next state is not allowed in the Markov chain due to connection dropping. Conditions for NCBP and HCDP have been included in Table 3.2a.

Hence,

$$HCDP_{Class1} = \sum_{s=S_{1D}} \pi_{(n_1, n_2, n_3)}(s) \quad (22)$$

$$HCDP_{Class2} = \sum_{s=S_{2D}} \pi_{(n_1, n_2, n_3)}(s) \quad (23)$$

$$HCDP_{Class3} = \sum_{s=S_{3D}} \pi_{(n_1, n_2, n_3)}(s) \quad (24)$$

Table 3.2a. Conditions for NCBP, HCDP in the network			
Current state	Next state	Condition	Status
$\begin{pmatrix} n_1, \\ n_2, n_3 \end{pmatrix}$	$\begin{pmatrix} n_1 + 1, \\ n_2, n_3 \end{pmatrix}$	$((n_1 + 1)B_1 + n_2B_2^{max} + n_3.B_3^{min}) > B$	New Class 1 blocked
		$((n_1 + 1)B_1 + n_2B_2^{min} + n_3.B_3^{min}) > B$	Handoff Class 1 blocked
	$\begin{pmatrix} n_1, \\ n_2 + 1, n_3 \end{pmatrix}$	$(n_1B_1 + (n_2 + 1)B_2^{max} + n_3.B_3^{min}) > B$	New Class 2 blocked
		$(n_1B_1 + (n_2 + 1)B_2^{min} + n_3.B_3^{min}) > B$	Handoff Class 2 blocked
	$\begin{pmatrix} n_1, \\ n_2, n_3 + 1 \end{pmatrix}$	$(n_1B_1 + n_2B_2^{max} + (n_3 + 1).B_3^{min}) > B$	New Class 3 blocked
		$(n_1B_1 + n_2B_2^{min} + (n_3 + 1).B_3^{min}) > B$	Handoff Class 3 blocked

### C. Bandwidth Utilization (BU):

The Bandwidth Utilization (BU) is defined as the ratio of the total used bandwidth to the available bandwidth of the system [203]. BU of the system is encountered to

estimate whether SS lying in a bad channel state wastes precious resources. BU can be obtained as follows:

$$BU = \frac{\sum_{s \in S} (n_1 B_1 + n_2 B_2^{\max} + n_3 \cdot B_3^{\min}) \pi_{(x,y,z)}}{B} \quad (25)$$

Along with the other performance parameters mentioned above this section also considers the connection outage probability as another performance parameter to assess the performance of SINR based JCAC DBA scheme for the scenario depicted in case study 4 i.e. 1 MeNB with 3 SeNBs.

Table 3.2b. Conditions for COP in the network (only in case of SINR based JCAC DBA)			
Current state	Next state	Condition	Status
$\begin{pmatrix} n_1 \\ n_2, n_3 \end{pmatrix}$	$\begin{pmatrix} n_1 + 1 \\ n_2, n_3 \end{pmatrix}$	$SNR^{n_1} / ((n_1 + 1) \cdot SNR^i + n_2 \cdot SNR^{n_2} + n_3 \cdot SNR^{n_3}) > SINR^{th, n_1}$	Class1 Outage
	$\begin{pmatrix} n_1 \\ n_2 + 1, n_3 \end{pmatrix}$	$SNR^{n_2} / (n_1 \cdot SNR^{n_1} + (n_2 + 1) \cdot SNR^{n_2} + n_3 \cdot SNR^{n_3}) > SINR^{th, n_2}$	Class2 Outage
	$\begin{pmatrix} n_1 \\ n_2, n_3 + 1 \end{pmatrix}$	$SNR^{n_3} / (n_1 \cdot SNR^{n_1} + n_2 \cdot SNR^{n_2} + (n_3 + 1) \cdot SNR^{n_3}) > SINR^{th, n_3}$	Class3 Outage

#### D. Connection Outage Probability (COP):

The connection outage probability is the probability that the cumulative SINR of the connections in the network drops below a predetermined threshold when a new connection tries to get admitted into the network [205]. COP maintains the SINR level of the newly admissible connection as well as existing connections. Conditions for connection outages in the network are summarized in Table 3.2b. The equations to estimate COP for Class1, Class2, and Class3 connections are given as below, where, ‘S<sub>1B</sub>’, ‘S<sub>2B</sub>’, and ‘S<sub>3B</sub>’ create a state space representing Class1, Class 2, and Class 3 connections. The next states of these states are not allowed in the Markov chain due to connection dropping.

Hence,

$$COP_{Class1} = \sum_{s=S_{1B}} \pi_{(n_1, n_2, n_3)}(s) \quad (26)$$

$$COP_{Class2} = \sum_{s=S_{2B}} \pi_{(n_1, n_2, n_3)}(s) \quad (27)$$

$$COP_{Class3} = \sum_{s=S_{3B}} \pi_{(n_1, n_2, n_3)}(s) \quad (28)$$

### 3.7 Performance Evaluation

The contribution of the proposed work centres around the analysis using CTMC model of the performance of the LTE based heterogeneous BWA network for some specific scenarios. In this section, a detailed analytical assessment of the numerical results has been carried out with the input system parameters for numerical analysis given in Table-3.3. The arrival rates are assumed to be the same for all kinds of service connections classified into Class1, Class2, and Class3.

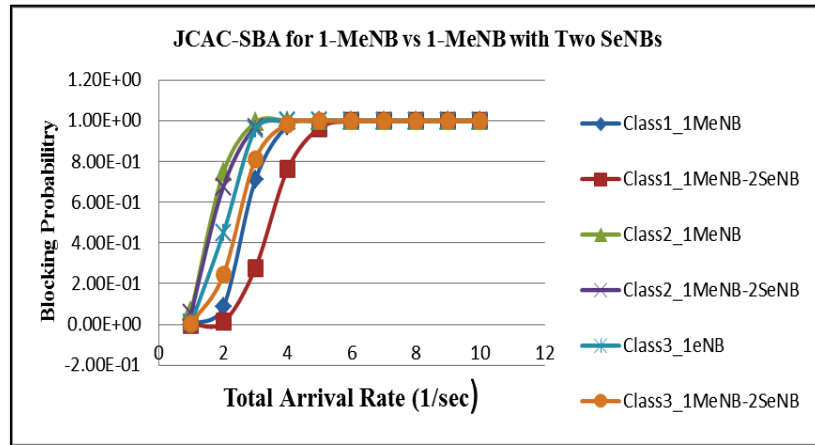
<b>Table 3.3. System parameters for numerical analysis of JCAC-DBA Algorithm</b>	
<b>Acronyms of the parameters</b>	<b>Value</b>
<b>Total Available Resource (BW) in terms of data rate</b>	10240 kbps
$P_{MeNB}^{tx}$	46 in dBm[76]
$P_{SeNB}^{tx}$	30 in dBm[76]
$P_{ReNB}^{tx}$	24 dBm [201]
<b>Cell Coverage of MeNB</b>	1000 in meters [200]
<b>Cell Coverage of SeNB</b>	200 meters [200]
<b>Cell Coverage of ReNB</b>	200 meters [200]

#### 3.7.1 RSS based JCAC and DBA scheme

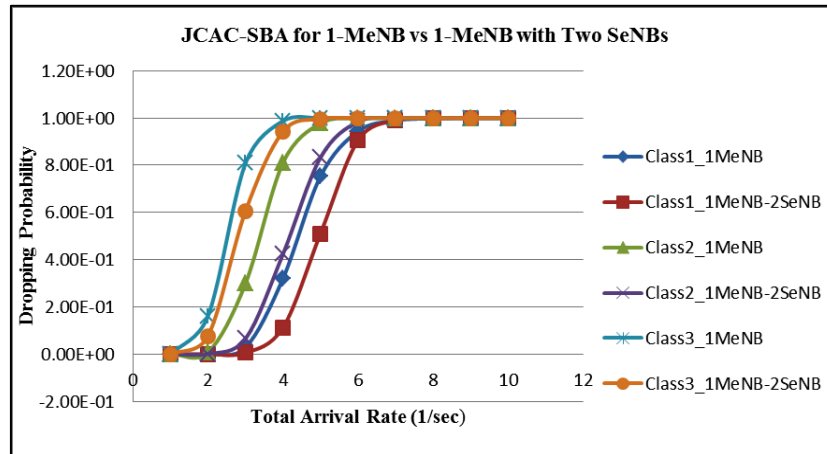
At first, the performance of the RSS based CAC algorithm is implemented with static bandwidth allocation (SBA) using CTMC model considering a single macro base station namely MeNB. Whenever there is a service request in the coverage area of this MeNB, it compares the RSS value of the service with the pre-calculated RSS threshold of the MeNB. The scenario depicted in casestudy-1 represents the traditional network.

For case study-2, two additional low power small SeNBs are deployed with the macro MeNB to improve the performances of the QoS parameters for NCBP, HCDP and BU. While in Case study 1, the whole bandwidth is dedicated only to the MeNB, for case study -2 the whole bandwidth has been distributed among one MeNB and two SeNBs in 2:1:1 ratio. From Fig. 3.14 (a), (b) and (c), it is clear that the introduction of SeNBs provides reasonable improvement in QoS parameters for NCBP, HCDP and, BU for all classes of traffic. The reason is obvious. In spite of having remaining bandwidth, sometimes-traditional infrastructures with only one MeNB at the center is unable to admit service requests due to lower RSS at the cell edges. The deployment of small cells in those areas covers the users at the cell edge. Thereby, it improves the

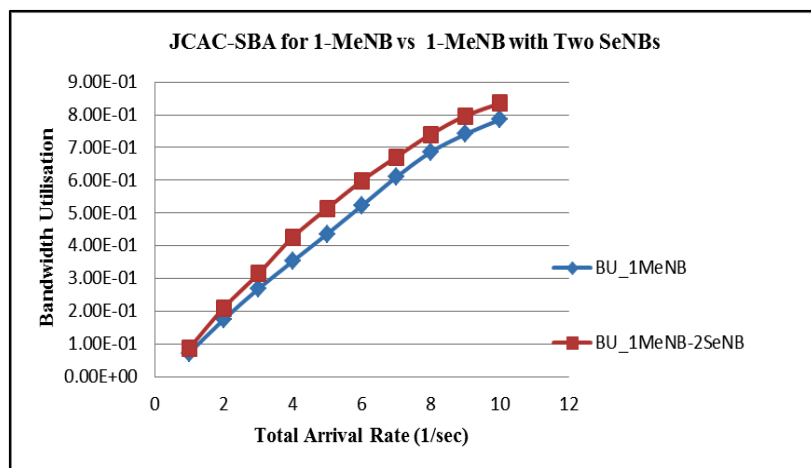
RSS of the cell edge users. As a result, less number of calls is blocked or dropped in those areas leading to better utilization of network resources. The percentage improvements of all QoS parameters are listed in Table 3.4.



a.



b.



c.

Figure 3.14 Analytical results of the comparison between JCAC-SBA for One MeNB and one MeNB with two SeNBs. (a) NCBP (b) HCDP (c) Bandwidth Utilization

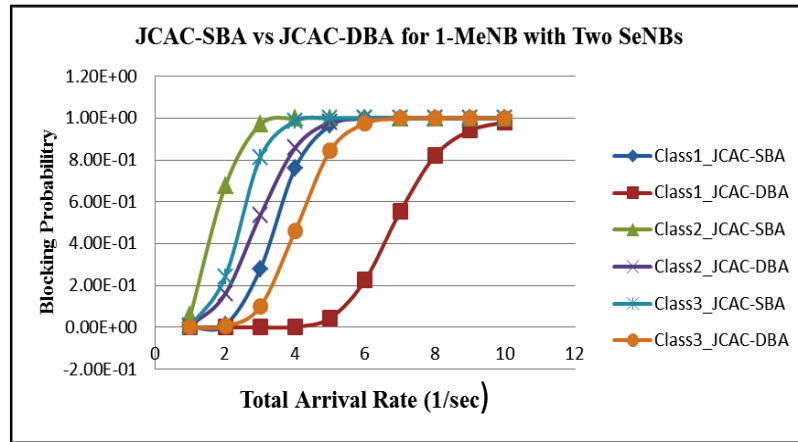
<b>Table 3.4. Performance Improvement of JCAC-SBA in One MeNB with two SeNBs compared to CAC in one MeNB (in %)</b>			
	Class 1	Class 2	Class 3
<b>NCBP</b>	26.27	2.53	9.59
<b>HCDP</b>	35.82	32.59	10.86
<b>BU</b>	14.37		

As the class-1 has the highest priority with a fixed data rate, it gets the priority call admission into the network compared to other classes, thus providing a larger improvement of all QoS parameters. While class 2 service has a lower percentage improvement in NCBP in comparison to class 3 because it has a higher maximum data rate requirement than class 3. Nevertheless, for HCDP, class 2 has a higher percentage improvement than class 3 because of ensuring higher priority admission for real time services in class 2. Above all, the overall bandwidth utilization improved significantly as 14.37% by placing small cells at the cell edge that ensures better coverage with the placement of two SeNBs.

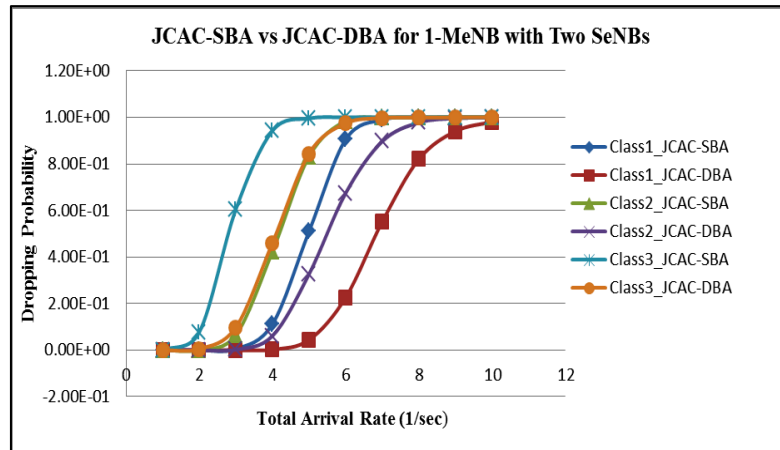
<b>Table 3.5. Performance Improvement of JCAC-DBA over JCAC-SBA in One MeNB with two SeNBs (in %)</b>			
	Class 1	Class 2	Class 3
<b>NCBP</b>	49.12	13.38	20.67
<b>HCDP</b>	35.39	21.73	16.27
<b>BU</b>	17.30		

It has been speculated that sometimes allocation of a fixed amount of bandwidth to the SeNBs may lead to underutilization of resources. Unlike Algorithm-3a, (i.e. JCAC-SBA), Algorithm-3b (i.e. JCAC-DBA) allows the joint CAC and dynamic bandwidth allocation to the SeNBs. Fig.3.15 (a),(b) and (c) demonstrate a comparative analysis between JCAC-SBA and JCAC-DBA algorithm under case 2 as summarized in Table 3.5. It is found that there exist perceptible improvements of NCBP as well as HCDP. It also enhances the overall BU of the network with two SeNBs and one MeNB. As for static bandwidth allocation with ratio 2:1:1 among MeNB, SeNB\_1, and SeNB\_2, at particular instance, there may be a situation that the entire bandwidth of SeNB\_1 is consumed by the users, while a good amount of bandwidth is remaining in SeNB\_2. In this situation, any new call or handoff call will be blocked /dropped due to unavailability of resource in SeNB\_1 resulting in underutilization of overall bandwidth. Algorithm-3b deals with this issue by implementing the dynamic JCAC-DBA algorithm, which allocates the bandwidth to

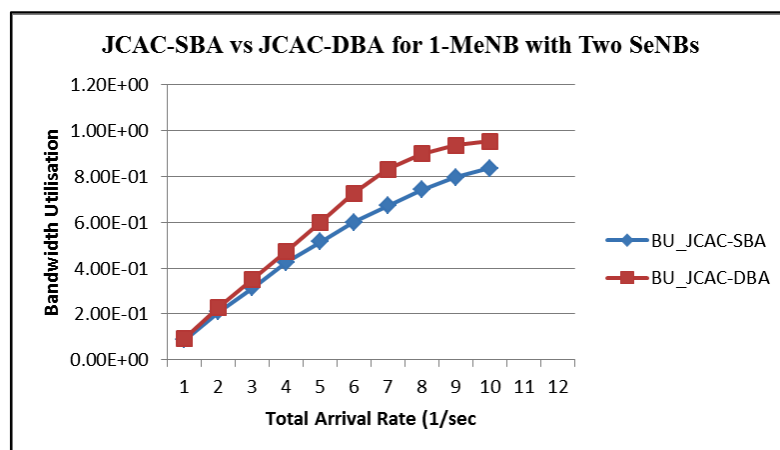
the lower tier if there is a call request under any SeNB. As a result, the probability of service requests being blocked or dropped decreases. It also maximizes the BU of the entire network.



a.

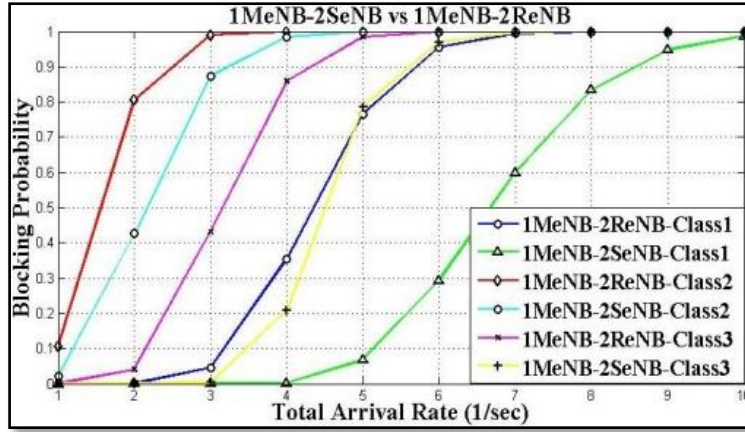


b.

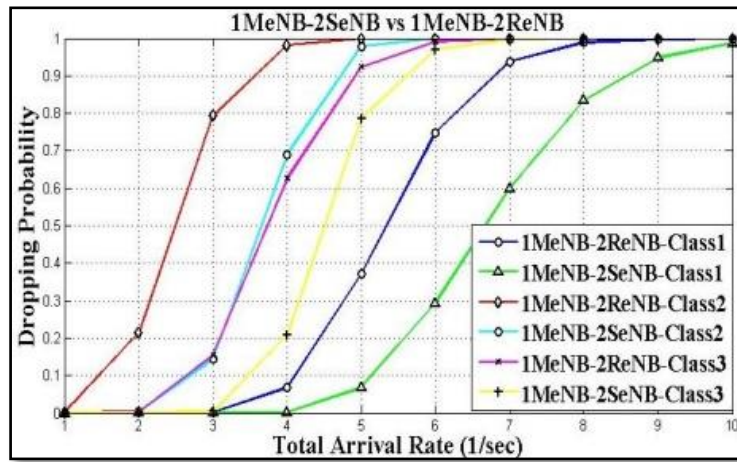


c.

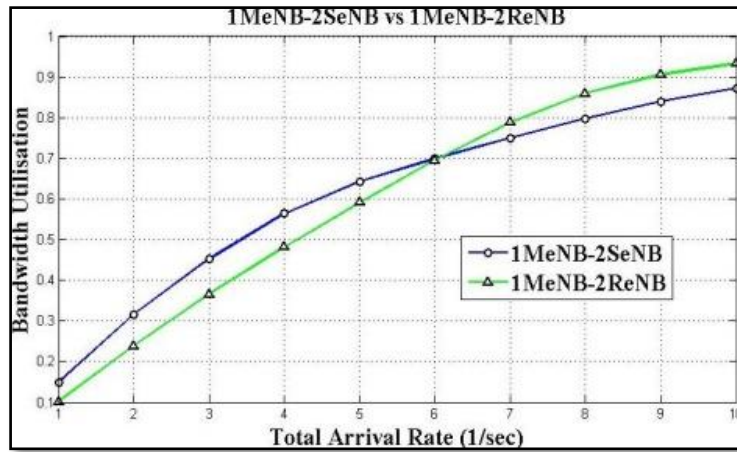
Figure 3.15 Analytical results of the comparison between JCAC-SBA and JCAC-DBA for one MeNB with two SeNB. (a) NCBP (b) HCDP (c) Bandwidth Utilization



a.



b.



c.

Figure 3.16 Analytical results of the comparison between one MeNB with two ReNB and one MeNB with two SeNB a. NCBP b. HCDP c. BU.

In the previous section, it has seen that multi-hop relays can also be an alternative for coverage and capacity enhancements in multi-tier HetNets. Fig.3.16 represents the simulation results of comparison between Multi-hop Relay based and SeNB based two-tier network architecture. In Multi-hop Relay based scenario, the users residing in



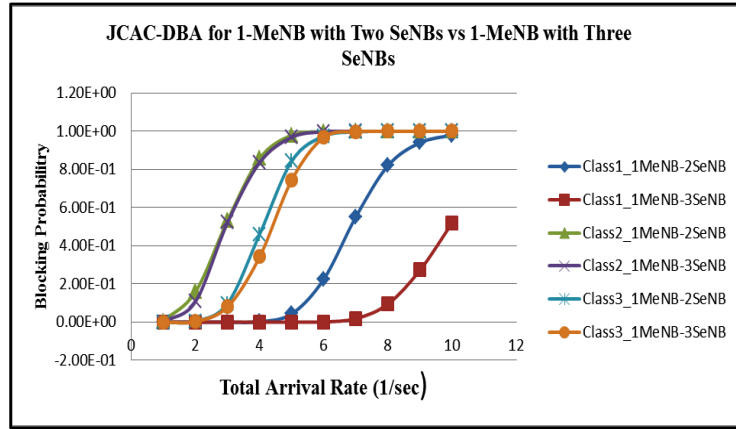
the cell edge on reception of lower RSS from MeNB are admitted to the CN through ReNB. Hence, ReNBs are placed here only to enhance the signal power. In certain cases, it may happen that a few calls get blocked due to the unavailability of the remaining bandwidth at the cell edge although the RSS profile has been improved by ReNBs. Whereas, SeNB not only enhances the RSS profile at the cell edge but also have the capability to admit service request by itself offloading the load of MeNB. Due to this reason in this work, a noticeable improvement has been found in the case of SeNB based two-tier network over the Multi-hop Relay based scenario. The performance improvements are shown in Table 3.6.

<b>Table 3.6. Performance Improvement One MeNB with two SeNBs over One MeNB (in %) with Two ReNBs w.r.t. JCAC-DBA (in %)</b>			
	Class 1 (in %)	Class 2 (in %)	Class 3 (in %)
<b>NCBP</b>	38.95	6.71	18.46
<b>HCDP</b>	26.98	14.70	10.95
<b>BU</b>	2.03		

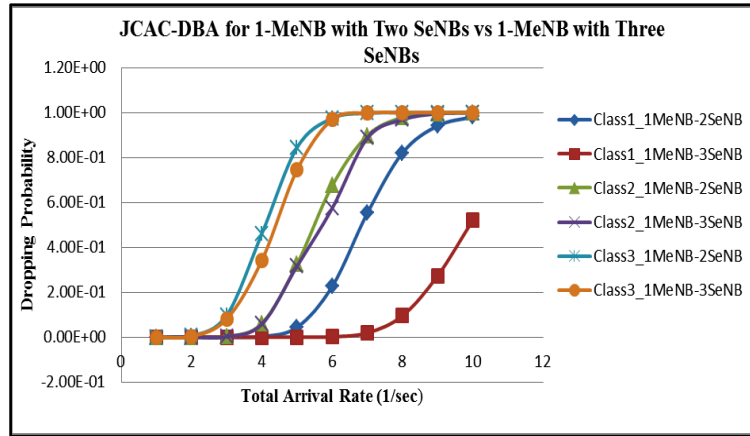
Now, while analysing Fig 3.16c., which represents the overall BU of the network, it is seen that during lower arrival rate (less than six calls per second) MeNB-SeNB based Two-tier architecture performs better whereas during higher arrival rates (more than 6 calls per second) Multi-hop Relay based architecture performs better. It should be noted that the BU of any real-time network might be treated as a useful parameter during lower arrival rates. However, in totality, an improvement in BU of 2.03% is achieved in the case of MeNB-SeNB based Two-Tier architecture.

Fig. 3.17 signifies that the addition of one more SeNBs i.e. 3-SeNBs considered for the case study-3, can improve the system performance further for Class 1, Class 2, and Class 3 traffic respectively as given in Table 3.7. In totality, this network scenario with the JCAC-DBA scheme gives a rise in the bandwidth utilization of 9.21% (Fig.3.17c), compared to the previous case with two SeNBs with JCAC-DBA because of the full judicial use of bandwidth.

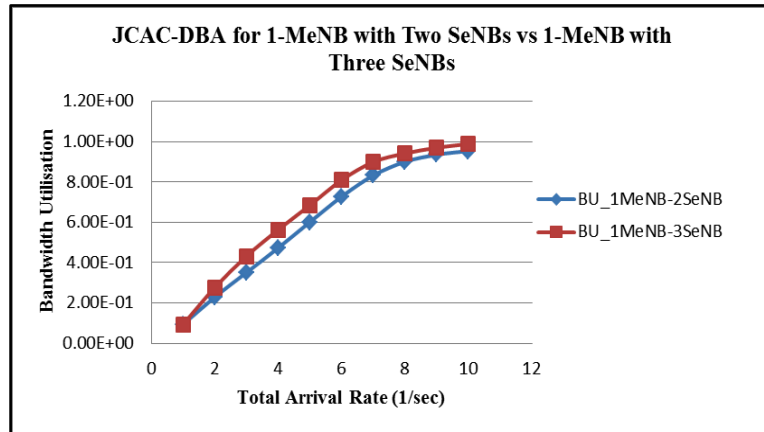
<b>Table 3.7. Performance Improvement implementing JCAC- DBA Algorithm in one MeNB with three SeNBs over One MeNB with two SeNBs (in %)</b>			
	Class 1	Class 2	Class 3
<b>NCBP</b>	76.46	1.32	3.77
<b>HCDP</b>	74.64	2.74	3.98
<b>BU</b>	9.21		



a.



b.

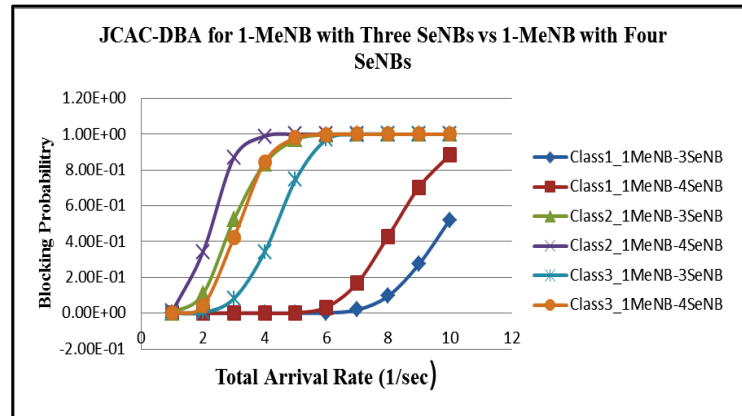


c.

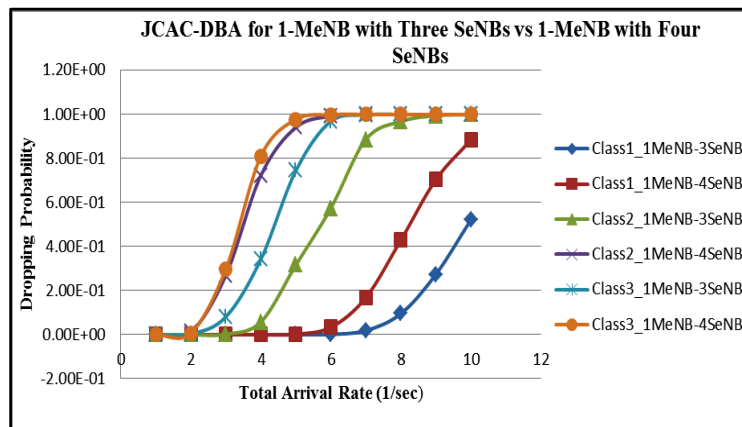
Figure 3.17 Analytical results of the comparison between JCAC DBA for One MeNB with Two SeNB and one MeNB with Three SeNBs. (a) NCBP (b) HCDP (c) BU

In case study-4, one more SeNB is increased i.e., four SeNBs along with one MeNB to see the performance in terms of QoS parameters. The objective was to observe the optimum number of SeNBs required for certain coverage with improved QoS. Strikingly it is seen from Fig.3.18 that increasing the number of small base

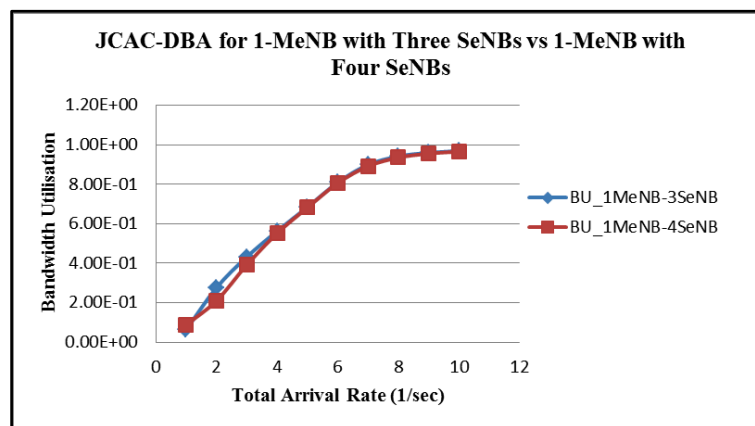
stations degradesthe QoS of the network with multiple services. It happens due to the fact that the addition of excess SeNBs may turn the network very congested leading to interference and thus RSS based CAC provides poorer network performance. Fig.3.18 represents the analytical comparison between One MeNB with Three SeNB and one MeNB with Four SeNBs from which it is very clear that performance in terms of NCBP, HCDP, and BU degrades with four SeNBs.



a.



b.



c.

Figure 3.18 Analytical results of the comparison between JCAC DBA for One MeNB with Three SeNB and one MeNB with Four SeNBs. (a) NCBP (b) HCDP (c) Bandwidth Utilization

<b>Table 3.8. Performance Degradation of one MeNB with three SeNBs compared to One MeNB with Four SeNBs for DBA Algorithm (in %)</b>			
	Class 1	Class 2	Class 3
<b>NCBP</b>	143.92	10.40	18.65
<b>HCDP</b>	141.78	44.56	15.52
<b>BU</b>	1.82		

Table 3.8 represents the percentage degradation of performance of one MeNB with three SeNBs compared to One MeNB with four SeNBs along with DBA algorithm. Considering the results in Table 3.7 & Table 3.8, it may be considered that if the system parameters are set as given in Table 3.3 implementation of JCAC-DBA scheme in one MeNB along with Three SeNBs provides optimal performance in terms of QoS parameters for NCBP, HCDP, and BU in the problem considered.

It is previously understood that SeNB based HetNet has outperformed multi-hop relay based architecture in terms of QoS metrics. Hence, considering SeNB based architecture as a feasible solution we further portray the impact of SeNB based HetNet in terms of capacity enhancement and bandwidth utilization which are two main thrust areas bandwidth limited networks as data consuming applications are getting popular day by day. Heterogeneity in architecture with proper call admission and bandwidth allocation strategy may provide the solution for better QoS management for cell edge users and the users from highly shadowed areas.

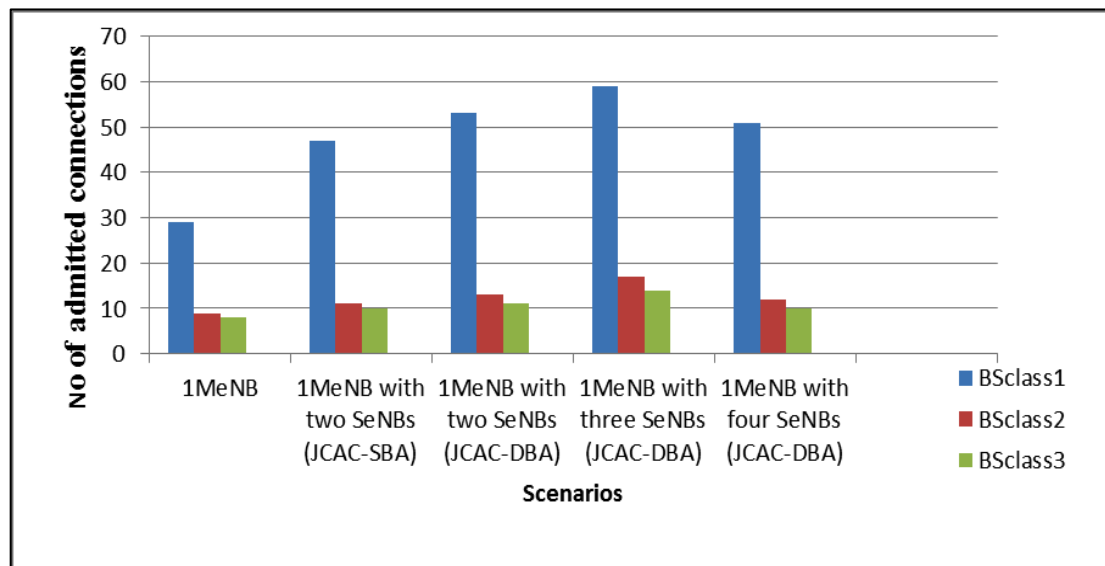


Figure 3.19 System capacity in terms of no. of users admitted with varying scenario conditions

Fig.3.19 and 3.20 it is observed how capacity and Bandwidth Utilization change when scenario conditions change from case study 1 to 4 for different service classes. Here, capacity is considered in terms of the total number of admitted connections for all types of services within a network with the given bandwidth. For a simple consideration of circular coverage, the use of 3-SeNBs with one MeNB provides the maximum capacity and maximum bandwidth utilization, which gives an insightful observation for optimizing the number of small cells placement in a heterogeneous BWA network.

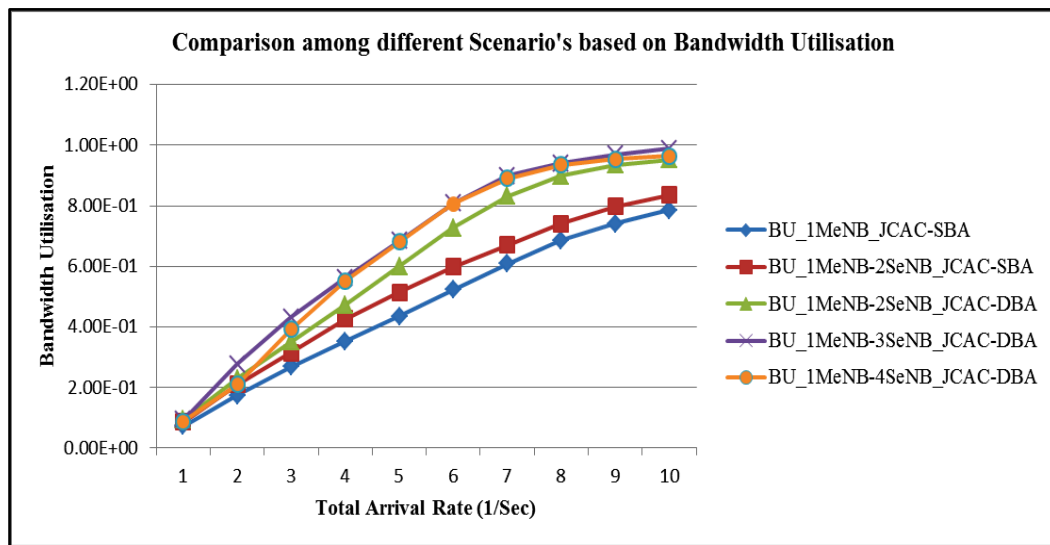
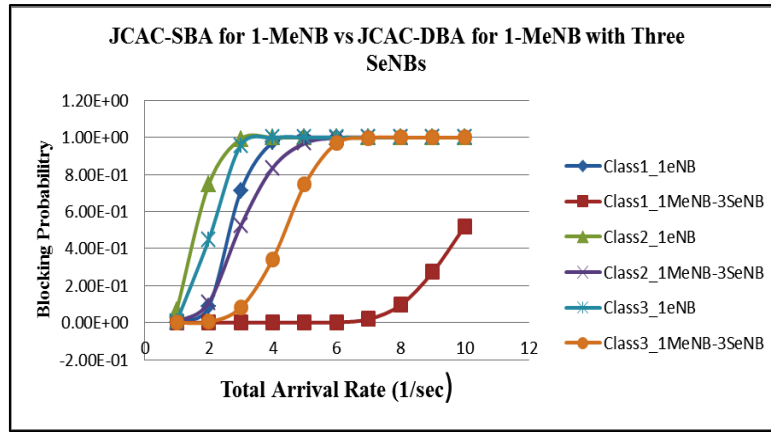


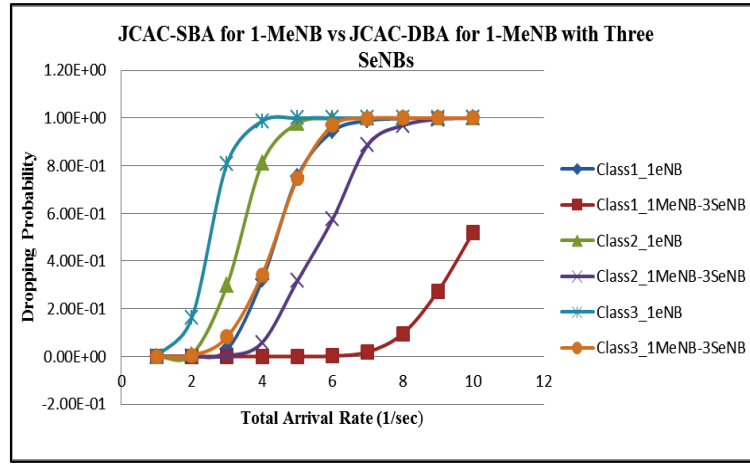
Figure3.20 Comparison among different scenario based on BU

A final performance comparison is made in Fig.3.21, for 1-MeNB v/s1-MeNB with 3- SeNBs with Joint CAC and DBA algorithm. It is seen that the overall system performance in terms of QoS compared to traditional architecture with single MeNB improves significantly as 90.88%, 25.07%, 38.52% for NCBP and 88.79 %, 51.73%, 38.08% for HCDP for class1, class2, class3 type of users respectively. Consequently, an overall 41.66 % of improvement in BU is achieved. Table 3.9 represents the percentage improvement of the performance of one MeNB with three SeNBs compared to One MeNB for Joint CAC and DBA Algorithm.

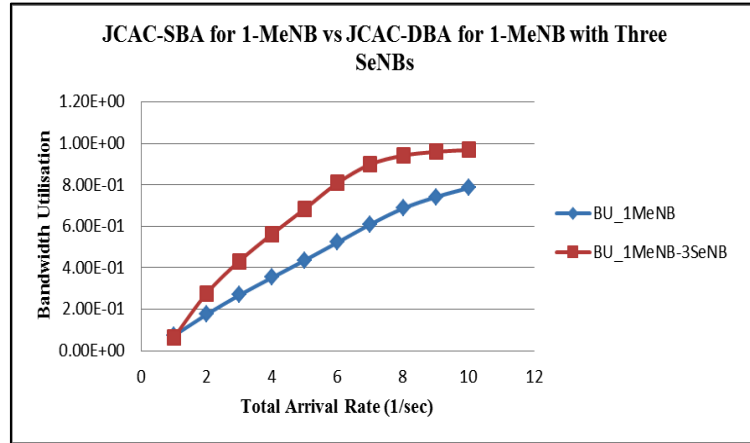
Table 3.9. Performance improvement implementing JCAC-DBA in one MeNB with three SeNBs over CAC in One MeNB (in %)			
	Class 1	Class 2	Class 3
NCBP	90.88	25.07	38.52
HCDP	88.79	51.73	38.08
BU	41.66		



a.



b.



c.

Figure 3.21 Analytical results of the comparison between CAC in One MeNB and JCAC-DBA in one MeNB with three SeNB. (a) NCBP (b) HCDP (c) BU

### 3.7.2 SINR based JCAC and DBA scheme

The significance of the SINR based JCAC and DBA scheme centres on the outage based analysis of the performance of the proposed SINRCAC in LTE based Het-BWA-Nets. To do the expressions for instantaneous SINR and SINR threshold is

derived as depicted in eq. (14) and (15). Another important aspect of the proposed SINR CAC scheme is that it considers the interference from the neighbouring connections and incorporates the measurements while designing the performance analysis in resource-constrained situation. Users are considered to be randomly distributed over the region. A comparative analysis has been done based on NCBP, HCDP and BU along with COP which it may be justified to critically analyse the proposed SINR based JCAC and DBA scheme for LTE based Het-BWA-Nets in terms of better QoS provisioning. To do this the CTMC analytical model is used as demonstrated in the previous section. A detailed analytical evaluation has been carried out from numerical results obtained by implementing SINRCAC over CTMC. Parameters for performance evaluations are listed in Table 3.3.

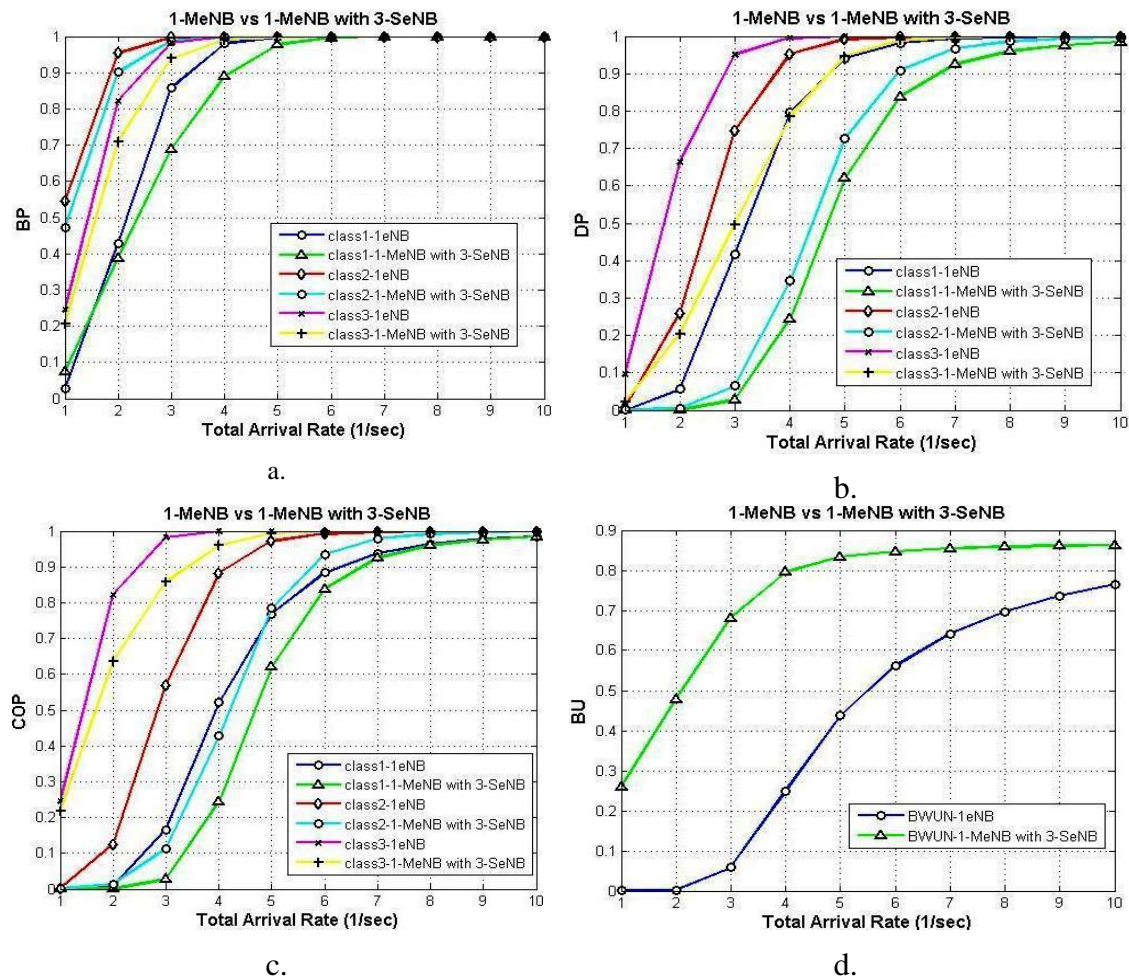


Figure 3.22. Comparative results between One MeNB v/s One MeNB with Three SeNBs for different QoS parameters a. NCBP b. HCDP c. COP d. BU.

Fig.3.22 represents a comparative graphical representation of the simulation results between One MeNB v/s One MeNB with Three SeNBs. It is considered that the bandwidth has been distributed among all the eNBs for Het-BWA-Nets. While the

traditional network, the entire bandwidth is dedicated only to the MeNB. The additional low power small SeNBs are deployed along with MeNB with the belief that it may improve performance of the QoS parameters like NCBP, HCDP, COP, and BU. From Fig. 3.22(a), (b), (c), and (d) it is clear that the introduction of SeNBs provides a reasonable improvement in QoS parameters for all class of traffics. The reason is quite obvious. In spite of having remaining bandwidth, sometimes traditional infrastructures with only one MeNB at the center (as demonstrated in case study 1), become unable to admit service requests due to lower SINR at the cell edges. Whereas, the deployment of small cells in those areas solves the problem of cell edge users by improving the received signal strength. As a result, less no of calls get blocked or dropped in those areas leading to better utilization of network resources.

<b>Table 3.10. Performance % improvement in SINRCAC in Het-BWA-Nets</b>			
	Class 1	Class 2	Class 3
<b>NCBP</b>	3.35	1.44	2.27
<b>HCDP</b>	22.36	24.62	14.54
<b>COP</b>	10.23	17.22	4.26
<b>BU</b>	76.70		

The analytical results of the experiments are shown in Fig.3.22 (a-d) for NCBP, HCDP, COP, and BU. Table 3.10 depicts their respective percentage improvements. The performance improvements in terms of NCBP for Class 1, Class 2, and Class 3 traffic are 3.35%, 1.44%, and 2.27% respectively. On the other hand, there are 22.36%, 24.62% and 14.54% of less dropping of handoff calls respectively for Class 1, Class 2, and Class 3 traffic, which is the desired one as handoff call dropping is more annoying than new call blocking. In addition, the performance improvements in terms of COP are 10.23%, 17.22%, and 4.26% respectively for Class 1, Class 2, and Class 3. Furthermore, we have 76.70% of improvement in terms of the overall bandwidth utilization of the network.

### 3.8 Chapter Summary

In this research investigation, a novel JCAC-DBA algorithm is developed for Multi-hop Relay based and MeMB-SeNB based BWA HetNets scenarios with improved QoS of subscribers accessing heterogeneous multimedia services. The proposed two-tier architecture justifies heterogeneity in terms of network scenarios and different service classes. The developed CTMC based analytical model establishes the optimal



number of three small cells (SeNBs) along with one MeNB as backhaul for achieving the highest QoS parameters for a random placement of SeNB within small cell coverage areas (200m) in a three 1200 sectored region. The proposed joint CAC and DBA scheme improves as much as 90.88%, 25.07%, 38.52% in NCBP, 88.79 %, 51.73%, 38.08% for HCDP, and 41.66% in overall BU respectively for Class 1, Class 2, and Class 3 type of services on the placement of three SeNBs in comparison to one macro SeNB. Moreover, it is observed that only increasing the number of small cells will not increase capacity and bandwidth utilization, but an optimal number of small cells are required. However, finding the optimum location of SeNBs is an NP hard problem to find the joint power efficiency and optimized number and location of small cells in a constrained resource environment, which will be our future research work. A CTMC Analytical Model is also developed for a bandwidth constrained SINR based CAC Scheme, which ensures QoS guarantee at each end user considering the interference level for each connection within the LTE BWA HetNets. The CTMC based analytical model for Het-Net is able to compute the QoS parameters like NCBP, HCDP, COP, and BU. Simulation results exhibit that applying this SINRCAC model in the LTE BWA HetNets delivers enhanced performance in terms of QoS guarantee to each end user, improving the outage probability of the overall network i.e COP decreases (4%) when SeNBs are used along with MeNB and also enhances HCDP (14%), NCBP (1.4%), and spectrum utilization (76%) of the network. Our future work is in the direction of green communication for LTE Het-Nets considering the joint location and power optimization of small nodes for overall improvement of quality of user's experience.

## ❖ Publications from this chapter

### ▪ SCI Indexed Journal

1. Arijeet Ghosh, and Iti Saha Misra, "A joint CAC and dynamic bandwidth allocation technique for capacity and QoS analysis in heterogeneous LTE based BWA network: few case studies." Wireless Personal Communications, Springer, 97(2), pp.2833-2857. **Impact Factor: 2.017.** DOI: <https://doi.org/10.1007/s11277-017-4637-x>

## ▪ **International Conferences**

1. Arijeet Ghosh, Iti Saha Misra, “A QoS based comparative analysis between relay assisted and small eNodeB based two-tier LTE network”, In International Conference on Computers and Devices for Communication, (CODEC 2015), pp. 1-5, IEEE, 2015.
2. Arijeet Ghosh, Iti Saha Misra, “An analytical model for a resource constrained QoS guaranteed SINR based CAC scheme for LTE BWA Het-Nets”, In International Conference on Advances in Computing, Communications and Informatics (ICACCI 2016),pp. 2186-2192, IEEE, 2016.

# Chapter 4: Designing SPP based Deployment models for k-tier HetNet: Pathloss, Coverage and Rate analysis

---

## Outline of the Chapter

- 4.1 Abstract
- 4.2 Introduction
- 4.3 SPP based stochastic modelling of K-tier HetNet
  - 4.3.1 BPP
  - 4.3.2 PPP
    - 4.3.2.1 HPPP
    - 4.3.2.2 NHPPP
- 4.4 Tiered Deployment of HetNets
  - 4.4.1 One tier
  - 4.4.2 Two-tier
  - 4.4.3 Three Tier
- 4.5 Location optimization of SeNBs via k-means clustering algorithm
- 4.6 Pathloss model
  - 4.6.1 4G Pathloss model-3GPP Rel. 9
  - 4.6.2 CI/ABG pathloss model leading to 5G
  - 4.6.3 5G pathloss model – 3GPP Rel. 16
- 4.7 Performance Metrics
  - 4.7.1 SINR expression
  - 4.7.2 Coverage Probability
  - 4.7.3 Average Rate
- 4.8 Performance Evaluation
  - 4.8.1 One Tier
  - 4.8.2 Two-tier
  - 4.8.3 Three Tier
- 4.9 Chapter summary

## 4.1 Abstract

As the current era of wireless architecture moves toward the evolution of 5G, there is an increasing demand for providing flexibility in the architectural framework that delivers lucrative services to address consumer Quality of Service (QoS) requirements. The future 5G HetNet environment will, therefore, be characterized as a multi-eNB, multi-technology network environment that is capable of reconfiguring its mode of operation so as to carry out a guaranteed QoS through the all-inclusive HetNet, taking into consideration huge traffic load and fluctuating user behaviours. The notion of a multi-eNB, multi-technology network environment produces some new challenges such as the implementation of the tiered architectural framework, placement of additional infrastructure, interference management, and energy management. Hence, in this work, primarily an elicited performance evaluation has been pursued considering different Spatial Point Processes. The evolution of different path loss models from 4G to 5G is studied. Finally, a novel tractable analytical model is developed by means of NHPPP to design and deploy a two-tier wireless Het-Net consisting of MeNBs and SeNBs. A supplementary mathematical analysis is also provided by deriving simple expressions for downlink SINR followed by CP and AR. Based on CP and AR, it is observed that NHPPP performs better when compared to its parent counterpart HPPP. The improvement rises even further by in the case of three-tier HetNet modelled using NHPPP integrated with the K-Means Clustering algorithm. The analysis is done for both sub-urban and urban scenario conditions by varying the UE teledensity.

## 4.2 Introduction

The exponential increase of cellular data traffic due to the popularity of mobile broadband services has enforced modern wireless network architecture to adopt a major paradigm shift in almost every part of the world. As of February 2018, teledensity, i.e., defined as the number of telephone connections for every 100 individuals, in India, has increased from 17.9% in FY07 (Financial Year 2007) to 90.89% in FY18 of which urban teledensity stood at 153.24% [205]. As a result, the new age cellular wireless network topologies have been evolving day by day to fulfil exponentially increasing demand for mobile data. Nowadays, practical deployment of cellular networks, which are organically deployed to provide high capacity, is

considered heterogeneous and irregular [206]. To handle the ever-increasing pattern of mobile data traffic, the so-called traditional single Macro eNodeB (MeNB)-based network, often built using a homogeneous radio environment, is gradually evolving into an environment supported by the dense deployment of small cells categorized as a complex heterogeneous wireless network, or HetNet [129, 207]. Heterogeneous networks (HetNets) are treated as a key ingredient of future mobile networks where operator/consumer deployed small-cells, such as femtocells, relays, and distributed antennas (DAs), to share the load, increase capacity, and extend the coverage of the existing macrocell infrastructure ranging from outdoor to indoor environments such as office buildings, homes, and underground areas [33, 207, 208].

Over the last decade due to the unprecedented popularity of 4G technologies, the massive use of smartphones and increased demand for personified broadband applications has coined a huge demand for higher data rate and improved QoS [33]. So, the Service providers in the wireless industry foresee a strong persistence of network evolution for several years to come. Hence, to encounter this upsurge in Tele-density, “network densification” which includes dense deployment of small cells can be viewed as a long-term solution under the umbrella of 5G technology [208]. Dense deployments of HetNets [208], seek to take network densification to another level, where extreme spatial reuse is implemented. Since the architecture of denser HetNets plays a key role in evaluating system performance in 4G and future cellular networks, the analysis of the networking topology is emerging as a primary task for subsequent accurate performance characterization [209]. By far, the most common assumption widely used in analytical calculations for cellular networks is that eNBs are uniformly distributed in the covered areas. Accordingly, hexagonal grids or square lattices are pervasively utilized to model the locations of eNBs. Both models, however, are generally intractable and structurally different from the real BS deployment. Therefore, much of the researchers’ focus has been shifting to more accurate eNBs’ spatial characterization, to cope with the non-uniformity of practical deployment. In that regard, Spatial Point Process (SPP) has proven to be an effective means to model BS placement [210, 211].

SPP has succeeded to provide a unified mathematical paradigm to model different types of wireless networks, characterize their operation, and understand their behaviour [63, 211]. The main strength of the analysis based on SPPs can be

attributed to its ability to capture the spatial randomness inherent in wireless networks [64]. Furthermore, SPP based models can be naturally extended to account for other factors in wireless network planning such as path loss propagation model, SINR distribution, enhance capacity, and coverage with QoS guarantee [33]. In some special cases, SPP analysis can lead to closed-form expressions of instantaneous throughput that govern the response of any wireless network [64]. These expressions enable the understanding of network operation and provide insightful design guidelines, which are often difficult to get from computationally intensive simulations.

Optimum selection of the locations and count of eNBs to meet certain coverage and capacity constraints can effectively control the overall cost of a cellular network. In consideration of the modern complex HetNet, coverage, and capacity planning are interrelated in terms of interference. Moreover, the ever-growing capacity demand for non-uniformly distributed users, along with HetNet scenarios, makes eNB location optimization a tedious task [212]. Selecting the optimal locations of eNBs involves finding several eNBs within a particular deployment site without disturbing the acceptable QoS to the user equipment (UE) [66]. Classical deployment models are not suited enough for planning HetNet eNB locations because they are only based on signal predictions and do not consider the traffic distribution, the signal quality requirements, and growing geographic scenarios [213, 214]. As an alternative, K-means clustering can act as a useful method to optimally locate the centers of the clusters, which can be considered as the optimal locations of the eNBs. The K-means [215] is one of the simplest unsupervised algorithms that solve the well-known clustering problem. The algorithm trails a simple way to categorize a specific data set into a certain number of clusters and optimally defines K cluster centers, one for each cluster.

Over the last few years, the sudden demand for more spectrum spaces has necessitated urgency for the inclusion of upcoming Fifth-Generation (5G) technology [143] as a long-term solution. 5G cellular systems are theoretically anticipated to function in the millimeter-wave (mmWave) frequency bands of 30–300 GHz. But for all real-world deployment scenarios, ambassadors at the World Radio Communication Conference 2019 (WRC-19) have acknowledged some other radio-frequency bands for International Mobile Telecommunications (IMT) 2020, which will expedite the implementation of 5G mobile networks worldwide [216, 217]. According

to[218]spectrum in the 3300-3670 MHz band has been auctioned for the first time in India. This band has surfaced as a crucial band for deploying 5G services in the country. Department of Telecommunication (DoT), Govt. of India, through its reference dated 13h September 2021 has also recommended to consider the 24.25 – 28.5 GHz band amongst the bands which were eventually auctioned in the spectrum auction last year [218]. As recently shown in [219], due to the much smaller wavelengths of these mmWave frequency bands, 5G has greater losses compared to 4G. However, in some scenarios with smaller propagation losses, these lossy mmWave bands can be made more lucrative, than today’s cellular networks [219]. With 5G expected to enact in entirely different frequency bands, it is necessary to develop new standards with new propagation path-loss models. Various extensive studies and measurements have been performed to develop new path loss models for mmWave frequency bands. Due to the massive popularity of 4G technology, Tele density (the number of mobile connections for every 100 users) is observed to evolve in increasing order over the last few years [45]. For example, teledensity in India has magnified from 17.9% in FY07 to 90.89% in FY18, of which urban teledensity of India (for the city of Kolkata) stood at ~143.38% in March 2022 [45]. Consequently, network deployment architecture and its configurations have also severely evolved over the last few years. Ultra-dense deployment of small cells underlaid by macro cells, collectively known as Ultra-Dense Heterogeneous Network (UDHN) (as shown in Fig. 9.2), have gradually become indispensable as the long-term solution for future networks [143]. Considering the rigorous use of SPPs in modeling dense deployment of small cells in previously published articles [57, 136, 142, 209, 210], it is understood that there is a requisite for comprehensive performance assessment of aforementioned SPPs with respect to the rate of change in Tele-density as well as eNB density over the year [45, 205, 211]. Having been motivated by this notion, In this work, at first, an in-depth performance analysis is pursued in this study among three major SPPs namely BPP [136], HPPP [57], and NHPPP [142] based on widely accepted performance parameters like Coverage Probability (CP) and Average Rate (AR).

Moving forward, a multitier modern complex Het-Net is modeled using NHPPP. The UEs are also distributed as independent NHPPPs. Each entity of Het-Net, namely, Macro eNodeBs (MeNB) and Small eNodeBs (SeNB) along with User Equipment

(UE) are distributed in a single two-dimensional (2D) plane. One of the major contributions of this chapter is to derive the expression for SINR with the help of transmit power and path loss only, which is quite simple and mathematically tractable, compared to the calculation of SINR in other literatures. The expression of path loss is considered from 3GPP path loss models [76-80] for Macrocell and Small cell environments for urban and suburban scenarios. Two separate expressions for CP and AR have also been derived based on the SINR at each downlink. The expression of CP and AR helps us to evaluate the proposed NHPPP model with the other SPPs. The aim is to find out the optimal numbers of SeNBs that can ensure maximum coverage and sustainable rate. To do this, the ratio of the MeNB to SeNB is varied by making the user's density constant. Another major contribution of this chapter is to optimally locate the positions of the SeNBs so as to generate the best results in terms of CP and AR. To do this, the k-means clustering algorithm has been integrated with NHPPP distributed Het-Net model. The k-means clustering algorithm segregates the UEs into multiple clusters and intends to identify the optimum centroid locations for each of the clusters so that the mean distance from each of the UE inside a cluster to its centroid should be minimized. These centroids will further serve as the optimum locations of the SeNBs. The simulation results also show that k-means based clustered NHPPP can produce prominent improvement in terms of CP and AR compared to HPPP and even NHPPP in both urban and suburban deployment scenarios.

Thereafter, a three-tier UDHN has been modeled by means of a spatially clustered homogeneous Poisson point process (SCHPPP) where the upper tier represents urban macro (UMa) cells serviced by Macro eNodeB (MeNB) and lower tiers represent UMi-SC and InH serviced by Small eNodeBs (SeNB) [220]. With transmission power ranging between 0.05W and 6W, 5G SeNBs can be further sub-categorized into micro eNBs (Mi-eNB), and femto eNBs (Fe-eNB). Mi-eNB covers small to medium open squares or street canyons with dense traffic (hotspots) such as university campuses, stadiums, large auditoriums, or train stations [220]. Mi-eNBs, typically ranging from a few hundred meters up to one kilometer, can be mounted in street fittings like lampposts or traffic signal posts due to their small form factor [220]. Fe-eNBs, typically ranging up to a few meters, are mostly intended to cover smaller areas such as private houses or indoor hotspots [220]. This research work intends to show the effect of path loss models approved by 3GPP 5G [80] for UMa, UMi-SC, and InH by



performing a comprehensive analysis for achieving improved coverage and rate in designing three-tier 5G UDN.

### 4.3 SPP based stochastic modelling of k-tier HetNet

The locations of the eNBs in real world deployment scenarios are commonly modelled as “spatial point process”. From the perspective of any random user, the locations of the eNBs in any deployment scenario at a given instant can be treated as random. Note that by ‘random’ it is not meant that the telecom service providers (TSP) deploy the eNBs in a manner like throwing a dart at a map to determine the eNB locations. Rather, the methods TSP generally applies may be realised as a Bayesian attempt by the TSP to estimate, say, the probability that the SINR at any random user location exceeds a fixed threshold, which requires defining a prior distribution of the eNBs. These distributions generally form the fundamental building blocks for designing SPP based models for dense deployment of eNBs [62].

An SPP is defined as a random point pattern in  $n$ -dimensional space ( $n \geq 1$ ) in a fixed geographical area  $A \subseteq \mathbb{R}^n$  ( $n = 2$  in this case), where the points in the plane denote the locations of some entity under investigation (in this case locations of the eNBs) [63]. In this work, three major SPPs have been taken under consideration for further performance evaluation in terms of CP and AR [221].

#### 4.3.1 BPP

In this case, the locations of eNBs have been modelled as a uniform-BPP, where these eNBs are uniformly and independently distributed in a finite region  $A$ . Representing the positions of eNBs in  $y \subseteq A$ , the probability density function of each eNB  $e_i$  is given by [63, 136]:

$$f(e_i) = \begin{cases} 1/A & \text{if } e_i \in A \\ 0 & \text{otherwise} \end{cases} \quad (29)$$

#### 4.3.2 PPP

In reality, network service providers give enormous effort and resources to identify the optimum locations of the base stations (termed as eNodeB or eNB in this literature) considering factors such as traffic load, user density, and geographical obstacles. However, from a user's point of view, it is quite tough to know the pattern

of the distribution of the eNBs. Thus, eNB distribution can be treated as random. Due to this stochastic nature of the distribution of the eNBs over the entire geographical area, the Poisson point process (PPP) [210] became a popular choice to design complex HetNets. In choosing PPP for modelling eNB locations, one should consider two basic properties [63].

- There are  $n > 1$  eNBs in a finite region of the plane and the locations of these “n” eNBs are independent and identically distributed over that finite region.
- Two random variables corresponding to the number of eNBs in two disjoint regions of the plane are independent.

The PPP can be subcategorized into two types, namely, homogeneous PPP (HPPP) and nonhomogeneous PPP (NHPPP) [63]. The HPPP that lies in a fixed region  $A \subseteq \mathbb{R}^2$  can be fully demonstrated by a single parameter, ie, the constant density of points  $\lambda$ . In case of HPPP, the density does not depend upon the location of the plane, whereas in case of NHPPP, the density is considered to be a function of the coordinates, ie,  $\lambda(x,y)$ , is now called as intensity function [63]. The HPPP model is most popularly used in most of the distinguished works [57, 62, 64].

#### 4.3.2.1 HPPP

The points (locations of the eNBs) of the process that are spatially distributed in an Euclidean plane  $A \subseteq \mathbb{R}^2$  emerge to be a Poisson Random Variable with mean  $\mu_h(A) = \phi \times A$ , given that the constant density  $\phi$  of points represents the mean number of points of the process per unit area [57, 62]. This point process is known as the Homogeneous Poisson Point Process (HPPP) because  $\phi$  is independent of the locations in the plane. The number of eNBs in any finite region  $A \subseteq \mathbb{R}^2$  denoted as  $N_h(A)$ , is a random variable with the homogeneous Poisson distribution [62],

$$\mathbb{P}[N_h(A) = \eta_h] = \frac{e^{-\mu_h(A)} \mu_h(A)^{\eta_h}}{\eta_h!}, \quad \eta_h = 1, 2, 3 \dots (30)$$

#### 4.3.2.2 NHPPP

Unlike HPPP in NHPPP, it is considered that the number of points (locations of the eNBs in this case) in the process in a Euclidian space  $A$  is considered to be a Poisson Random Variable with mean  $\mu_{nh}(A) = \iint_A \phi(x,y)$  where  $\phi(x,y)$  is understood as Intensity Function [62]. In this case, the number of eNBs in any finite

region  $A \subseteq \mathbb{R}^2$  denoted as  $N_{nh}(A)$ , is a random variable with non-homogeneous Poisson distribution [62],

$$\mathbb{P}[N_{nh}(A) = \eta_{nh}] = \frac{e^{-\mu_{nh}(A)} \cdot \mu_{nh}(A)^{\eta_{nh}}}{\eta_{nh}!}, \quad \eta_{nh} = 1, 2, 3 \dots (31)$$

This work follows the process of ‘Thinning’ for generating NHPPP which is considered as a computationally easy and comparatively proficient method as described in [63].

One tractable way to generate a new point process may be done by transforming or changing an existing point process. Fitting transformation methods include thinning, and clustering [63]. The Method to design clustered point process and make an efficient deployment model is discussed in later in this chapter..

- Generating NHPPP from HPPP: **Thinning**

Fig.4.1 demonstrates the process of thinning an HPPP, say,  $X$ , in which some of the points of  $X$  are selectively omitted. The remaining points form the thinned HPP, say,  $Y$ . The thinning procedure can be formulated by supposing that each point  $x \in X$  is labelled with an indicator random variable  $I_x$  taking the value 1 if point  $x$  is to be retained, and 0 if it is to be deleted. Then the thinned process consists of those points  $x \in X$  with  $I_x = 1$  [63]. Probabilistically, the method is to generate a HPPP on  $A$ , with intensity  $\lambda^*$ , and to thin out the points by accepting each point with probability  $\mu(A)/\lambda^*$  for  $\mu(A) = \iint_A \lambda(x, y) dx dy$ .

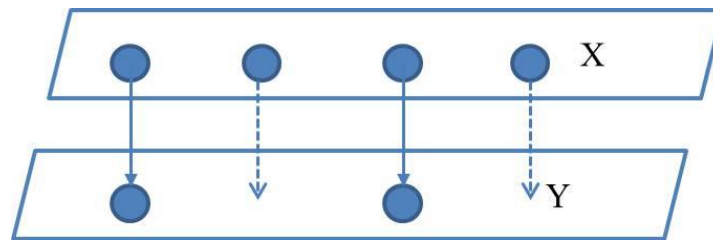


Figure 4.1 Thinning of a SPP. Points of the original process  $X$  (above) are either retained (solid lines) or deleted (dotted lines) to yield a thinned process  $Y$  (below).

A computationally simple and comparatively competent technique for generating one-dimensional NHPPP is described in [142, 222]. Thinning is a very useful method for simulating NHPPP in one dimension and two dimensions, as compared to other methods. The method uses a bounding process that is homogeneous with a rate function equal to the maximum value of the given rate function. This technique can be

easily generalized for two-dimensional cases. Theorem 1 provides the foundation for generating two-dimensional NHPPP as an alternate solution to HPPP. Here, we consider two-dimensional NHPPP because we describe each of the points (MeNBs or SeNBs or UEs or as a whole in a Het-Net Environment) in NHPPP as a two-dimensional function of their coordinates. The method can be applied to handle any rate function. The method in [222] alleviates the numerical integration of the rate function described in (25) for generating NHPPP.

**Theorem 1:** If a HPPP with rate function  $\{\lambda^*(x,y)|\lambda(x,y) \leq \lambda^*(x,y)\}$  in a rectangular plane is thinned according to  $\lambda(x,y)/\lambda^*(x,y)$  (i.e.  $(X_z, Y_z)$  is deleted independently if a uniform  $(0, 1)$  random number  $U_z$  is greater than  $\lambda(x,y)/\lambda^*(x,y)$ ), the result is a Non-Homogeneous Poisson Process with rate function  $\lambda(x,y)$ .

Proof: Refer to Appendix A

---

#### Algorithm 4.1 2D NHPPP

---

- 
- Step 1: Generate 1DHPPP with rate  $\lambda y_0$  on interval  $(0, x_0]$ , if the number of points generated is  $n$ , such that  $n=0$ , exits; there are no points in the rectangle.
- Step 2: Denote the points generated by  $X_1 < X_2 < X_3 \dots \dots \dots < X_n$
- Step 3: Generate  $Y_1, Y_2, Y_3 \dots \dots \dots Y_n$  as independent uniform distributed random numbers on  $(0, y_0]$
- Step 4: Return  $(X_1, Y_1), (X_2, Y_2), \dots \dots \dots, (X_n, Y_n)$  as the coordinates of 2D HPPP.
- Step 5: Using first four steps generate points of rate  $\lambda^*$  in the rectangle  $R^*$ . If there is no point in  $n^*$ , such that  $n^* = 0$ , exits; there are no NHPPP.
- Step 6: From the  $n^*$  points generated in 5, delete the points that are not in  $R$ , and denote the remaining points by user  $(X_1^*, Y_1^*), (X_2^*, Y_2^*), \dots \dots \dots, (X_m^*, Y_m^*)$  with  $X_1^* < X_2^* \dots \dots \dots < X_m^*$ . Set  $i=1$  and  $k=0$ .
- Step 7: Generate  $U_z$  uniformly distributed between 0 and 1. If  $U_z \leq \frac{\lambda(X_z^*, Y_z^*)}{\lambda^*}$ , set  $p=p+1, X_p = X_z^*$  and  $Y_p = Y_z^*$ .
- Step 8: Set  $i$  equal to  $i+1$ . If  $i \leq m^*$ , go to 7.
- Step 9: Return  $(X_1, Y_1), (X_2, Y_2), \dots \dots \dots, (X_n, Y_n)$  where  $n=p$ .
- 

At this point, this work investigates the relation between the mean and densities of the node entities of Het-Net. Comparing HPPP and NHPPP based on simulation results of mean–density trade off using Algorithm 1, Fig. 4.2 is plotted from which it is observed that the node density/square km tends to decrease in case of NHPPP

compared to HPPP for higher mean that implies NHPMP would provide better thinning for the ultra-dense network.

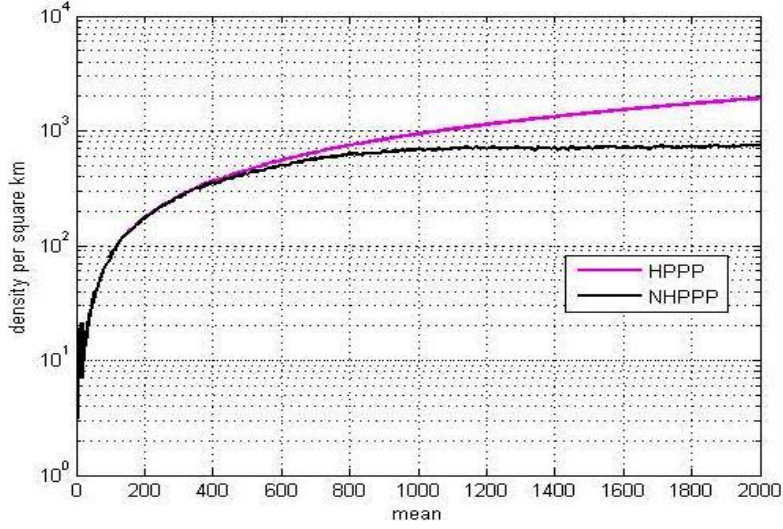


Figure 4.2 Comparisons between HPPP and NHPMP in terms of density of data points by varying mean of PPP

## 4.4 Tiered Deployment of HetNet

Before going into the detailed analysis of the proposed model it is very much essential to emulate a practical Het-Net with all its entities (MeNB, SeNB, UE) and their corresponding coverage regions.

### 4.4.1 One Tier

In the regime of technological evolution, network densification can be one of the leading candidates to encounter an upsurge in data rate demand. By definition, the maximum average achievable rate [208] of a UE in a cellular wireless system is given by (32),

$$\mathcal{R} = E[\mathbb{C} * \log_2(1 + SINR)] \quad (32)$$

Where, number of co-channel cells ( $\mathbb{C} \geq 1$ ) can be increased substantially by network densification, which involves deployment of large number of eNBs within a given geographical area. In addition, compared with the conventional cellular networks, it is obvious that Dense HetNets can significantly reduce the distance between a UE and its serving eNB leading to drop in path loss [208].

The year wise gradual growth in Tele-density (UE) is demonstrated in Fig.4.3 by Blue Coloured Bar Graph. Tele-density in India increased from 70.9 per cent in FY11 to 92.84 percent in FY19 [205]. To be able to support such demand, future networks

will need to be dense and multi layered. Subsequently, the hike in eNB density modelled by different SPP has also been demonstrated in Fig.4.3.

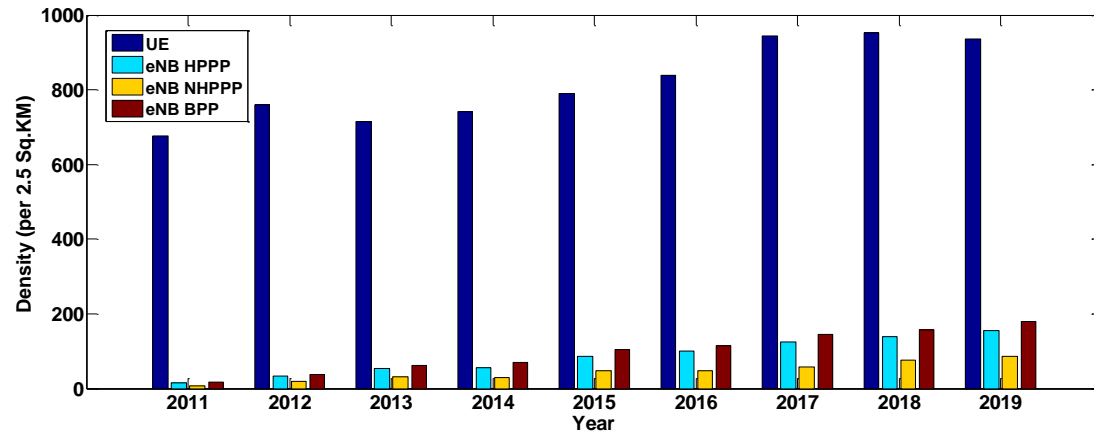


Figure 4.3 Projection for UE growth along with eNB density deployed by different SPPs in Indian context upto 2019

Fig.4.4 (generated by MATLAB Simulations) demonstrates the spatial evolution of the wireless network over the year by incorporating the upsurge in eNB (black dot markers) as well as UE (blue dot markers) Density in a geographical region of 6.25 km<sup>2</sup>. It is quite clear from Fig.4.3 that the number of eNBs and UEs has increased drastically in 2019 compared to 2011.

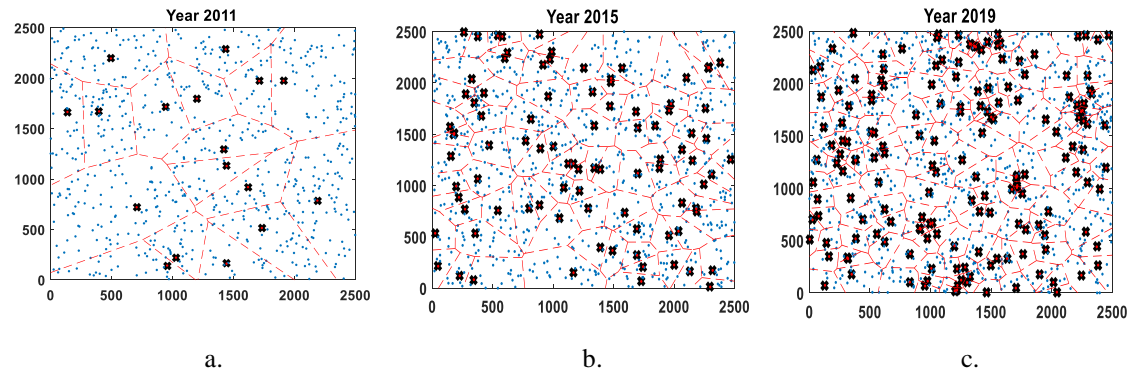


Figure 4.4 Generalized year wise deployment scenario of typical one tier network in a geographical region of 6.25 km<sup>2</sup>. Black Crosses Blue dots denote the eNBs and UEs respectively.

Over the years, spatial densification of macro cells has gradually reached its limit to further enhance the end user QoS. To cope up with the evolving pattern of wireless networks, network planning, and deployment in contemporary times gradually moved in the direction of k-tier HetNet.

#### 4.4.2 Two-tier

The concept of Het-Net is expected to encounter issues regarding the propagation losses in 5G networks by indulging the end users to get closer to the

access nodes [129, 207]. The realization of this is simply done by the co-deployment of small cells in the hotspots where massive traffic is generated under the footprint of Macro cells as shown in Fig 4.5 [207]. These small cells are the access nodes with lesser transmission power, smaller coverage and smaller user handling capacity, thus differ from the macro base station in respect of path-loss propagation [129].

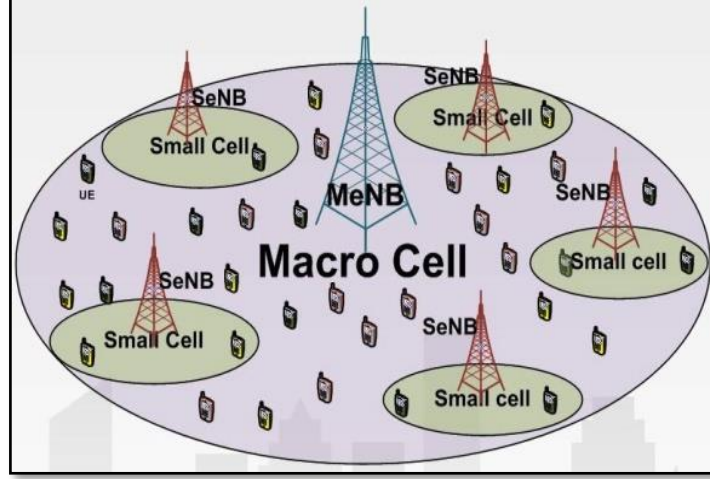


Figure 4.5 A typical Het-Net consisting MeNB and SeNBs.

In this work, a two-tier ( $k=2$ ) Heterogeneous network is modelled where each tier corresponds to each class of eNBs. These classes of eNBs differ from each other in terms of transmit power, coverage areas, user handling capacity, sustained service rate, path loss models, and their special distribution. Primarily, it is considered that the eNBs of  $k^{\text{th}}$  ( $k \in K$ ) tier are spatially distributed according to an NHPPP  $\Psi_k$  of density  $\lambda_k$  in the Euclidean plane [62]. The number of points of the process in any finite region  $A \subset \mathbb{R}^2$  denoted as  $N_k(A)$ , is a random variable with the Poisson distribution,

$$\mathbb{P}[N_k(A) = \eta] = \frac{e^{-\mu_n(A)} \cdot \mu_n(A)^\eta}{\eta!} \quad , \quad \eta = 1, 2, 3 \dots$$

With mean (rate function),

$$\mu_k(A) = \iint_A \lambda_k(x, y) dx dy \quad (33)$$

For ease of understanding the generalised form of NHPPP denoted in (33) will be hereafter used in this work. It is noteworthy that a mobile UE can only be served by  $j^{\text{th}}$  eNB of the  $k^{\text{th}}$  tier if and only if the received downlink SINR with respect to that particular eNodeBs is greater than threshold SINR,  $\gamma_k^{\text{th}}$ . The mobile UEs are also distributed in the same finite region  $A \subset \mathbb{R}^2$  as independent NHPPP  $\Psi_m$  of



density  $\lambda_m$ . Thus, each set of eNodeBs belonging to a particular tier can be uniquely represented as,

$$\Psi_k = f(P_k^{tx}, \lambda_k, \gamma_k^{th})(34)$$

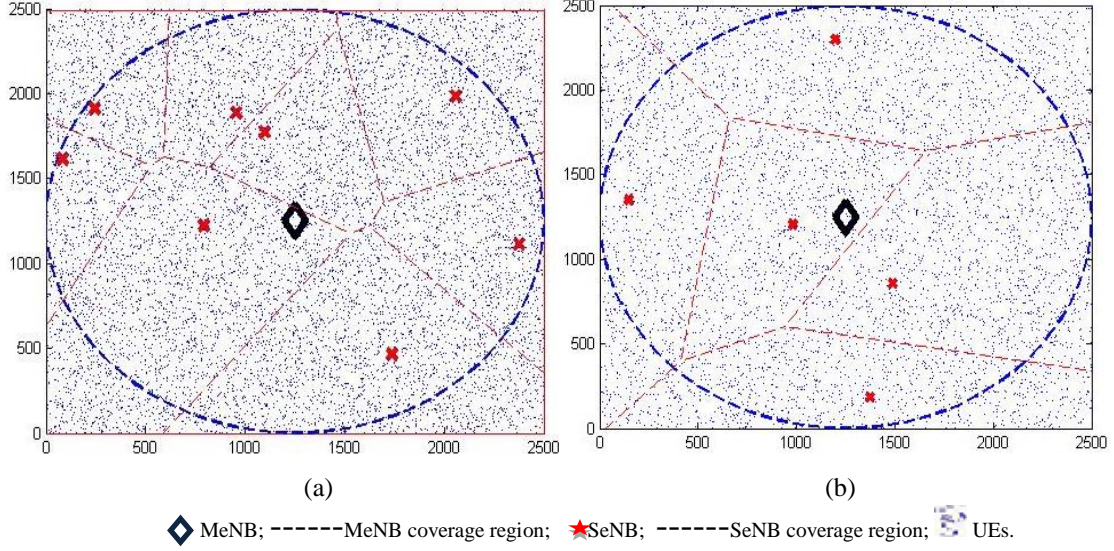


Figure 4.6 Coverage regions of a Het-Net in a 6.25 sq. km geographical area based on 2D NHPPP (a) Urban Scenario (UE density ~153 %) (b) Sub-urban scenario (UE density ~90 %);

Fig. 4.6 (a) represents an Indian urban scenario having a tele-density of 153 % whereas Fig. 4.6 (b) represents a typical Indian suburban scenario with a tele-density of 90 % approximately [205]. Primarily, one MeNB is placed deterministically in each of the center locations with transmit power  $P_1$ . In both scenarios, SeNBs are distributed using algorithm 4.1 as 2D NHPPP  $\Psi_2$  with transmit power  $P_2$  and rate  $\lambda_2$ . The UEs are also distributed as a separate 2D NHPPP  $\Psi_3$  with rate  $\lambda_3$ . As all the entities of the HetNet demonstrated in Fig.4.6, correspond the points of PPP, their densities used to vary depending upon the mean of the Poisson process.

#### 4.4.3 Three Tier

India being the 2<sup>nd</sup> largest telecommunication market has the 2<sup>nd</sup> highest number of internet users in the world. The magnitude of internet users in the country is expected to expand even more to 900 million by 2025. As a result, in India, the teledensity has magnified from 17.9% in FY07 to 90.89% in FY18, of which urban teledensity of India (for the city of Kolkata) stood at ~143.38% in March 2022 [45, 205]. This will eventually generate a huge amount of teletraffic load, especially in urban regions of the country, and necessitates the deployment of adding another tier in the network's deployment architecture and analysis for sustainable improvement in



QoS demand. In addition, the idea of UDHN is estimated to meet concerns regarding the propagation losses in 5G networks by indulging the end users to get closer to the access nodes [129, 207]. This realization is accomplished by the co-deployment of both indoor and outdoor small cells in an urban terrain where massive traffic is generated under the footprint of macro cells [207]. Urban small cells are typically of two types, namely, Urban Micro cells or UMi-SC deployed in the street canyons (SC) and Indoor Hotspots or InH [63]. These small cells are the transmit nodes with lesser transmit power, smaller coverage, and smaller user handling capacity, thus differ from the macro cell with respect to path-loss propagation [129, 80]. Fig. 4.7 depicts a hypothetical demonstration of a three-tier UDHN.

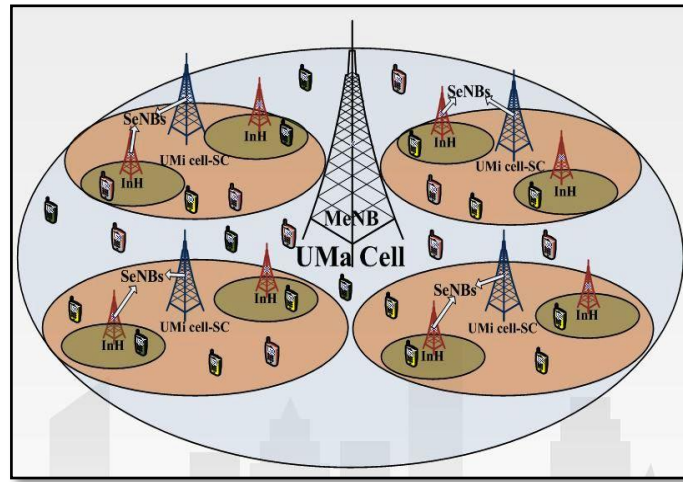


Figure 4.7 A typical three-tier UDHN consisting one tier of MeNB and two-tiers of SeNBs

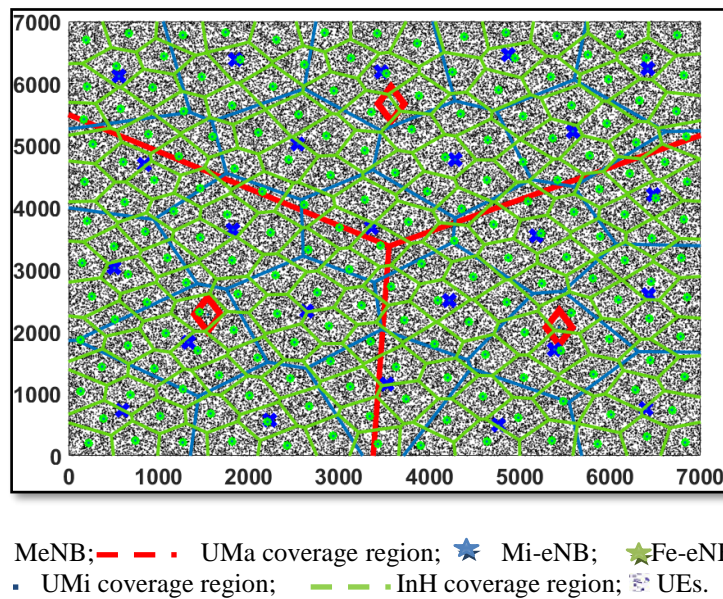


Figure 4.8 Coverage areas of a three-tier HetNet in a 7000 sq. m terrain in Indian urban Scenario (UE density ~143.38 %) [224].

In this subsection, at first, a three-tier UDN is modelled by means of NHPPP [70, 223] where individual tier represents the eNBs of a specific type, such as MeNBs, Mi-eNBs or Fe-eNBs in a two-dimensional finite region  $A \subset \mathbb{R}^2$ . The number of eNBs in the  $k$ th tier (where  $k=3$  represents MeNB, Mi-eNB, and Fe-eNB respectively) in any finite region  $A \subset \mathbb{R}^2$  symbolized as  $N_k(A)$ , is a random variable with the Poisson distribution [62, 70],

## 4.5 Location optimization of SeNBs via k-means clustering algorithm

In Fig. 4.6, the SeNBs and UEs of the two-tier HetNet are generated as disjoint sets of NHPPP. Assuming that the locations of the MeNBs are predetermined and constant, the key objective is to find out the optimum locations of SeNBs so that the SeNBs can further improve the SINR in each downlink leading to the improvement in overall CP and AR. The k-means clustering algorithm [215] is a utility tool that can partition NHPPP distributed UEs into ‘ $k$ ’ Voronoi cells or clusters. Consequently, the k-means can also determine the centroid locations of each of the clusters in iterative manner so that the mean distance between centroid location (SeNB position) and all the cluster members (UEs) should be minimized. These centroid locations can be considered as the optimal location of SeNBs. In this subsection, it is shown elaborately how implementing the k-means clustering generates a noticeable effect in the CP and AR.

### ➤ Overview of K means Clustering Algorithm:

The k-means clustering [215] is a well-known algorithm that classifies a set of data into a certain number of clusters (assume  $k$  clusters). The algorithm also defines  $k$  centroids, one for each of the clusters. The next step is to assign each point belonging to a given data set to the nearest centroid. At this point ‘ $k$ ’ new centroids are re-determined as the barycenter of the clusters caused from the preceding stage. The data under test will now be reassigned to the new centroids. This process of finding new centroids locations will be carried on until the centroid will not move anymore.

The procedure follows a simple and easy way to classify a given data set through a certain number of clusters (assume  $k$  clusters) fixed a priori.

---

**Algorithm 4.2** Finding optimum location of the SeNBs using k means Clustering

---

**Step 1.** Initial SeNB positions (as distributed by NHPPP in  $\Psi_k$ ) will be considered as the primary centroid (or primary locations of the SeNBs) for each cluster.

**Step 2.** Assign each of the UE from  $\Psi_m$  to any of the centroid (temporary positions of the SeNB). Let assume there are q clusters and  $C_q$  cluster centers.

**Step 3.** For each clusters  $q= 1.....Q$  and for each centroid recompute the positions of the centroids by taking mean of the  $\gamma_k(x,y)_i^j$  of all the UEs those are assigned to a particular SeNB or centroid.

**Step 4.** Repeat these Step 3 until convergence.

---

Finally, this algorithm aims at minimizing an objective function as shown in (35), in this case, a squared distance function. Generally, the minimization of such an objective function is pursued by iterative methods that initiates with randomly selected initial cluster configurations, and then reconfigures the cluster association in an iterative fashion to acquire an improved shape. The sum of the squared distance function has been accepted in most of the pre-existing literature, due to its computational simplicity [225-227]. The convergence criterion of such an objective function is a well-known topic and has been discussed in several notable studies [228, 229].

$$\text{Minimize } Z = \sum_{j=1}^q \sum_{i=1}^n \| \chi^i - C_j \|^2 \quad (35)$$

Where,  $\| \chi^i - C_j \|$  is a chosen distance measure between a data point  $\chi^i$  and the cluster center  $C_j$ , is an indicator of the distance of the n data points from their respective cluster centers.

Fig. 4.9 represents the demonstration of NHPPP distributed Het-Net after applying algorithm-2. While comparing clustered NHPPP in Fig 4.9 with sole NHPPP in Fig.4.7, it can be found that the SeNBs (denoted by red-cross in Fig.4.7 and Fig.4.9) are well organized with the aid of k-means algorithm and optimally distributed throughout the whole scenario. As a result, almost all the UEs can reside at a minimal distance with respect to their serving eNBs, which seems to have a positive effect on the coverage probability and the average rate experienced by the UEs.

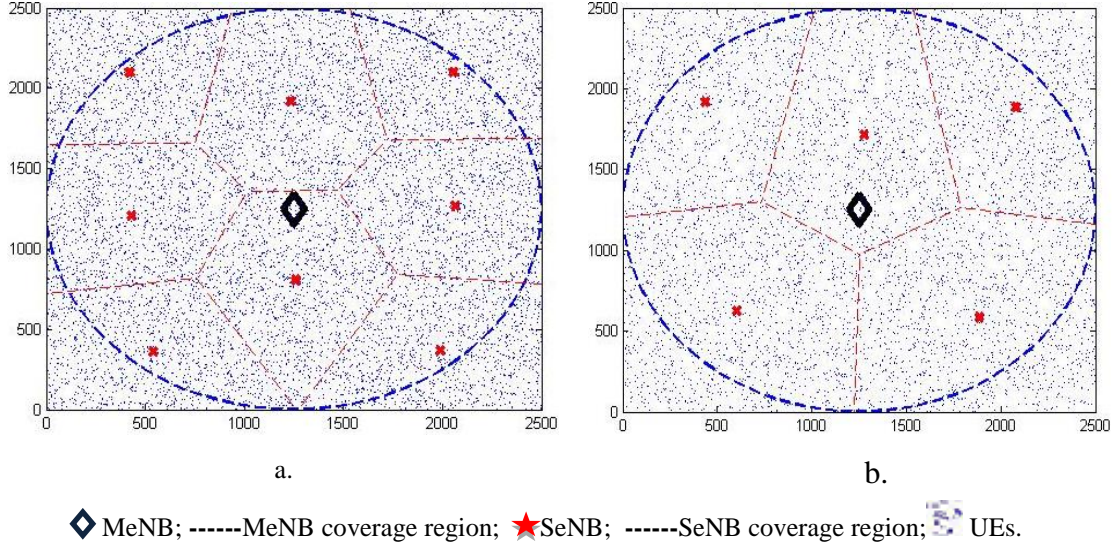


Figure 4.9 Coverage regions in a 6.25 sq.km. Geographical area based on Clustered NHPPP Het-Net. a. Urban (UE density 153% approx.) b. Suburban (90% approx.)

## 4.6 Pathloss model

Tele density which is defined as the number of telephone connections [45, 205] for every 100 individuals is seen to evolve in increasing order due to the massive popularity of 4G technology over the last few years. Naturally, before inclusion into the standard, any such propagation model needs to be verified under the current teledensity scenario based on reliable performance parameter such as coverage or achievable rate. With this motivation, this chapter aims to provide the effect of two important large-scale propagation path loss models, namely, the alpha-beta-gamma (ABG) model and the close-in (CI) free space reference distance model (as demonstrated by Rappaport et. al. in [28]) for the analysis of achieved coverage and rate in designing two-tier 5G heterogeneous network (Het-Net).

As the eNBs in 5G HetNets will be expected to operate in both 3300-3670 MHz, 24.25 – 28.5 GHz bands (in India) [218], the realization of accurate Radio propagation models are necessitated to have seamless penetration of 5G services to the last mile. 5G mmWave wireless channel bandwidths will be more than ten times greater than today's 4G Long-Term Evolution (LTE) 20 MHz cellular channels [79]. Since the wavelengths shrink by an order of magnitude at mmWave when compared to today's 4G microwave frequencies, diffraction and material penetration will incur greater attenuation, thus elevating the importance of line-of-sight (LOS) propagation, reflection, and scattering. Accurate propagation models are vital for the design of new

mmWave signalling protocols (e.g., air interfaces) [79]. Over the past few years, measurements and models for a vast array of scenarios have been presented by many companies and research groups [76-80].

#### 4.6.1 4G Pathloss model-3GPP Rel. 9

In this subsection, the distribution of SINR at any random location of a user for a given scenario is calculated analytically. To begin, we consider a random user at any random location at a distance  $d_0$  from its serving eNodeB(S-eNB) (note that the serving eNodeB is selected based on the maximum received power at any random user location). Other eNodeBs in the network will be considered as non-serving eNodeB (NS-eNB) and will be treated as interferers to that particular user. Now as SINR is dependent upon the received power at any random user location it is primarily necessary to derive the expressions for received power. There are basically two components of received power, i.e. transmit power ( $P_k^{tx}$ ) and path loss of the link. Here, in this chapter, the popular 3GPP path loss models for macrocell and smallcells are considered [76]. Macrocell and Small Cell propagation models for urban area is valid for scenarios in urban and suburban zones except for high-rise core where buildings are of nearly uniform height (3GPP TR 36.942) [76]. Considering that the base station antenna height is fixed at 15 m above the rooftop, and a carrier frequency of 2 GHz is used, the path losses for Macro and Small cell environment  $PL^{MeNB}$  and  $PL^{SeNB}$  are expressed by (36) and (37) respectively [76].

$$PL^{MeNB} = 128.1 + 37.6 \log_{10}(D_{MeNB-UE}) \quad (36)$$

$$PL^{SeNB} = 38 + 30 \log_{10}(D_{SeNB-UE}) \quad (37)$$

Where

$D_{MeNB-UE}$  is the separation between MeNB and UE in kilometres.

$D_{SeNB-UE}$  is the separation between MeNB and UE in meters.

Here, Shadow fading standard deviation is assumed to be 10 dB and 6 dB for MeNB and SeNB respectively [76].

Without loss of generality the equation of path loss will be considered for the rest of the calculations as,

$$PL_k^{4G}(x, y)_i^j = A + B \log_{10}(D_k(x, y)_i^j) \quad (38)$$

#### 4.6.2 CI/ABG pathloss model leading to 5G

The propagation models considered in this work have followed the most recent significant work of Rappaport et al. [77] covering the frequency range of 2 GHz to 73.5 GHz. The analysis is based on line of sight (LoS) and non-line of sight (nLoS) propagation environments across varied user's locations. Both the ABG and CI models are generic for all frequency models for large-scale propagation path loss [77] which is a function of distance and frequencies.

##### ▪ ABG Model

The equation for the ABG model is given by (39):

$$PL_k^{(ABG)}(f_k, d_k(x, y)_i^j)[dB] = 10\alpha_k \log_{10} \left( \frac{d_k(x, y)_i^j}{1m} \right) + \beta_k + 10\gamma_k \log_{10} \left( \frac{f_k}{1GHz} \right) + \chi_{\sigma_k}^{ABG} \quad (39)$$

Where,  $PL_k^{(ABG)}(f_k, d_k(x, y)_i^j)$  denotes the path loss in dB over frequency and distance,  $k$  is an indicator to specify the tier of eNBs,  $\alpha_k$  and  $\gamma_k$  are parameters showing distance and frequency dependency of pathloss, respectively,  $\beta_k$  is an offset value for path loss in dB,  $d_k$  is the distance between transmitter-receiver (T-R) in meters,  $f_k$  is the operating carrier frequency in GHz, and  $\chi_{\sigma_k}^{ABG}$  is the shadow fading (SF) standard deviation denoting large-scale signal variations about the mean path loss over distance. The coefficients  $\alpha_k$ ,  $\beta_k$ , and  $\gamma_k$  are obtained from measured data of [77] that minimize the SF standard deviation given in Table 4.1.

##### ▪ CI Model

The equation for CI model is given in (40)

$$PL_k^{CI}(f_k, d_k(x, y)_i^j)[dB] = FSPL_k(f_k, 1m)[dB] + 10n_k \log_{10}(d_k(x, y)_i^j) + \chi_{\sigma_k}^{CI} \quad (40)$$

Where,  $n_k$  is the path loss exponent (PLE),  $d_k$  is the T-R separation distance,  $\chi_{\sigma_k}^{CI}$  is the SF standard deviation indicating large-scale signal variations about the mean path loss over distance and  $FSPL_k(f_k, 1m)$  stands for free space path loss in dB at a T-R parting distance of 1 m at the carrier frequency  $f_k$ :

$$FSPL_k(f_k, 1m)[dB] = 20 \log_{10} \left( \frac{4\pi f_k}{c} \right) \quad (41)$$

Where,  $c$  is the speed of light. Notably the CI model integrally has an fundamental frequency dependency of path loss embedded within the 1 m free space

path loss value, and it has only one parameter  $n_k$ , PLE, to be evaluated, as opposed to three parameters in the ABG model ( $\alpha_k$ ,  $\beta_k$ , and  $\gamma_k$ ).

Table 4.1. Coefficients in the ABG and CI model [77]							
Env.	Freq. Range	Dist. Range (m)	Model	$\alpha_k$	$\beta_k$	$\gamma_k$	$\sigma_k$
nLoS	2-73.5	45-1429	ABG	3.3	17.6	2.0	9.9
			CI	2.7	-	-	10
LoS	2-60	5-88	ABG	2.6	24.0	1.6	4.0
			CI	1.9	-	-	4.7
LoS	2-73.5	5-121	ABG	2.0	31.4	2.1	2.9
			CI	2.0	-	-	2.9

### 4.6.3 5G pathloss model – 3GPP Rel. 16

The technical report published by 3GPP TR 38.901 version 16.1.0 Release 16 has comprehensively standardized channel models for frequencies from 0.5 to 100 GHz under different deployment scenarios based on both line of sight (LoS) and non-line of sight (nLoS) propagation [80].

The pathloss models for different scenarios used in this work are summarized in Table 4.2. The distance characterizations are shown in Fig. 4.10. The distribution of the shadow fading (SF) is considered to be log normal, and SF standard deviations for different deployment scenario are mentioned in Table 4.2 scenarios [80].

Table 4.2 Pathloss model for different scenarios [80]	
Scenario	Pathloss models [carrier Frequency, $f_c$ in GHz, distance, $d_{3D}$ in meters] $\sigma_{SF}$ = Shadow fading std. [db] $O2I = 5 + 4f_c$ , denotes the outdoor to indoor penetration constant of concrete wall.
Urban Macro (UMa-NLoS)	$32.4 + 20 \log_{10}(f_c) + 30 \log_{10}(d_{3D}) + O2I$ $\sigma_{SF} = 7.8$
Urban Micro –Street canyon (UMi-Sc-NLoS)	$32.4 + 20 \log_{10}(f_c) + 31.9 \log_{10}(d_{3D}) + O2I$ $\sigma_{SF} = 8.2$
Indoor Hotspot (InH)	$32.4 + 20 \log_{10}(f_c) + 17.3 \log_{10}(d_{3D})$ $\sigma_{SF} = 3$ Note that, in case of InH O2I is not applicable assuming that InH will generally operate in LoS condition.

The expression of path loss for  $i^{\text{th}}$  user will be considered for the rest of the work as,

$$PL_k^{5G}(x, y)_i^j = 32.4 + 20 \log_{10}(f_c^k) + \alpha^k \log_{10}(d_{3D}^{i \rightarrow k}(x, y)_i^j) + \beta^k \quad \text{Where,}$$

$\alpha^k$  = Coefficient of the logarithmic distance term corresponding to UMa, UMi, and InH type of deployment scenario.



$\beta^k$ = O2I penetration loss for UMa and UMi type of deployment scenario. Note that, for InH, value of this coefficient will be null.

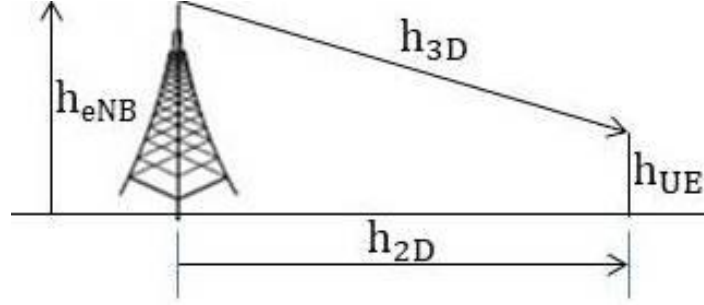


Figure 4.10. Distance definition i.e.  $d_{3D} = \sqrt{(d_{2D})^2 + (h_{eNB} - h_{UE})^2}$  [80]

## 4.7 Performance Metrics

The QoS performance metrics used in the work are Coverage probability and average rate. Both the parameters are derived from the expression of SINR.

### 4.7.1 SINR expression

Hence, the received power at a typical UE from an eNB located at  $(x, y)_n$  is given as,

$$P_k^{rx}(x, y)_i^j = P_k^{tx} - PL_k^{4G, ABG, CI, 5G}(x, y)_i^j \quad (43)$$

Simultaneously, the received SNR of the link between typical UE and an eNB located at  $(x, y)_n$  is given as,

$$SNR_k(x, y)_i^j = P_k^{rx}(x, y)_i^j - \Theta \quad (44)$$

Where,  $\Theta$  is the downlink Noise Figure [201] in dB.

The cumulative SINR can be calculated by taking the ratio of received SNR from serving eNB and that of non-serving eNBs. The received SNR at  $(x, y)_i$  from all other non-serving interfering eNBs can be given as  $\sum_{k \in K} \sum_{l=1}^{j-1} SNR_k(x, y)_i^l$ . Hence, the resulting expression for SINR at a typical UE from a eNB located at  $(x, y)_i$  is given as,

$$\gamma_k(x, y)_i^j = \frac{SNR_k(x, y)_i^j}{\{\sum_{k \in K} \sum_{l=1}^{j-1} SNR_k(x, y)_i^l\} + 1} \quad (45)$$

Here, in this work it is assumed that the UE will be served by its strongest eNB i.e. the UE will be connected to the eNB which offers best SINR. So, a random UE at  $(x, y)_i$  is in coverage if:

$$\max_{(x, y)_i \in \Psi_k} \gamma_k(x, y)_i^j > \gamma_k^{th} \quad (46)$$



### 4.7.2 Coverage Probability (CP)

The coverage probability is defined as the complimentary cumulative distribution function (CCDF) of the effective received SINR for an arbitrary randomly located mobile user when all the tiers have same target SINR threshold [57].

Theorem 2: The expression of CP which is used further for analysis is given in Theorem 1

$$P_c(P_k^{tx}, \lambda_k, \gamma_k^{th}) = \sum_{k=1}^K \lambda_k \iint_A \mathbb{P} \left( \frac{SNR_k(x,y)_i^j}{\{\sum_{l=1}^{j-1} SNR_k(x,y)_i^l\} + 1} > \gamma_n^{th} \right) (47)$$

Proof: Refer to Appendix B

### 4.7.3 Average Rate (AR)

The AR experienced by a randomly chosen mobile while in coverage is that when the Shannon bound is achieved, i.e., the AR in coverage is  $E(\log_2(1+\text{SINR})|\text{coverage})$  [57]. This expression is easily computable but need integral so it is not in closed form.

Theorem 3: The closed form expression is derived and the subsequent expression for AR is given as below:

$$\bar{\mathcal{R}} = \frac{\mathbb{P}(\Gamma\{\max(v, \gamma_k^{th})\})}{\mathbb{P}\{\Gamma(\gamma_k^{th})\}} \quad (48)$$

Proof: Refer to Appendix C

## 4.8 Performance Evaluation

The comparative performance analysis of different SPPs in terms of ensuring improved QoS provisioning has been thoroughly performed in this subsection with the ultimate goal to adapt the right choice of SPP in view of evolving wireless network scenarios. In the process, we also provide performance analysis in terms of different pathloss propagation models as the technology evolves from 4G to 5G.

### 4.8.1 One Tier

The performance of different SPPs in the light of network densification has been analysed through MATLAB simulation considering the scenarios depicted in Fig.4.3 which corresponds to network conditions in the years 2011, 2015, and 2019 respectively. The input parameters for various scenarios under simulation are provided in Table 4.3.

Table 4.3. Scenario considerations and Simulation parameters	
Parameters	Value
Scenario Area under test (A)	2.5 Square KM
Path Loss Model	$PL^{SeNB} = 38 + 30 \log_{10}(D_{SeNB-UE})$ [76]
Transmit Power ( $P_j^{tx}, P_q^{tx}$ )	30 dBm [13]

Considering the change in the density of UE as well as eNBs (as shown in Fig.4.3), at first, this work pursues a year-wise comparison in terms of change in CP and AR for HPPP, NHPPP, and BPP respectively. It is observed from Fig.4.11 and Fig.4.12 that there is a tendency of degradation in the performance of all the SPPs in terms of both coverage and rate as we proceed from the year 2011 to the year 2019 (considering that the network becomes denser as the year progresses). The reason behind that as the network becomes denser the number of eNBs in a particular geographical area increases which in turn contributes to more interference from non-serving eNBs in the denominator of the link SINR leading to the degradation in  $Y(x,y)_i^j$ . This observation clearly suggests that any change in  $Y(x,y)_i^j$  will have a direct impact on CP and AR correspondingly.

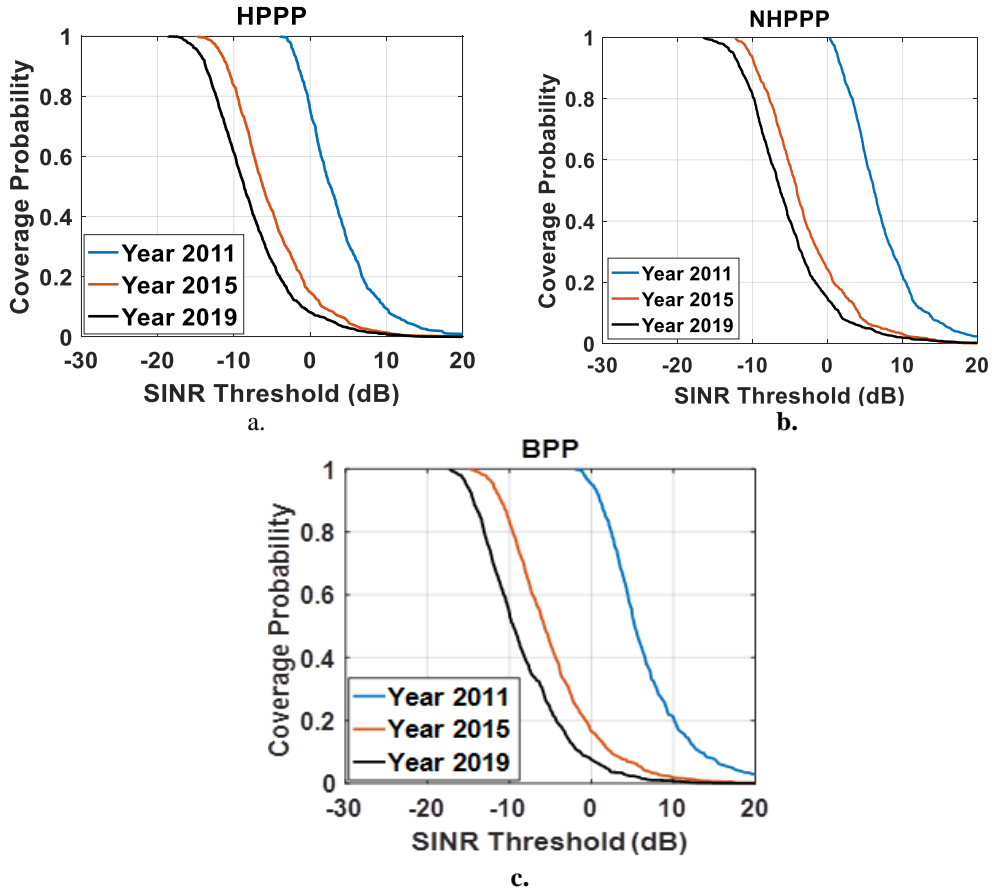


Figure 4.11 Year wise Coverage Probability analysis for a. HPPP b. NHPPP c. BPP

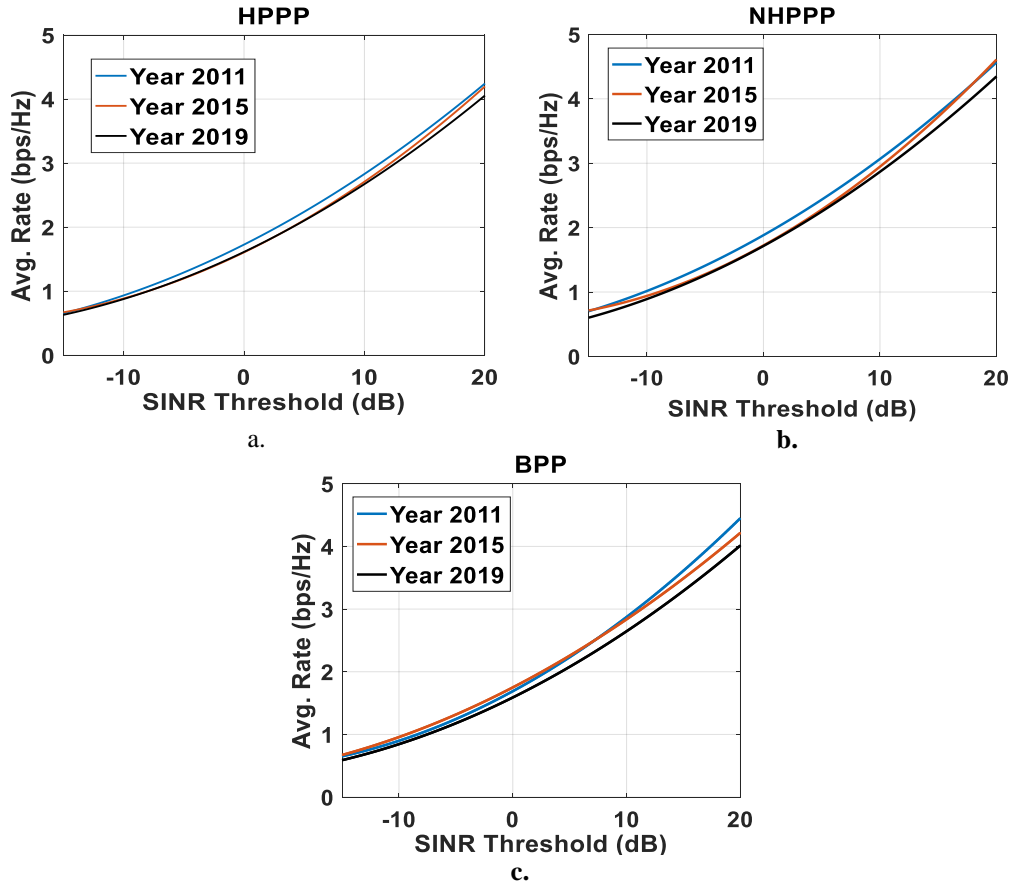


Figure 4.12 Year wise Average Rate analysis for a. HPPP b. NHPPP c. BPP

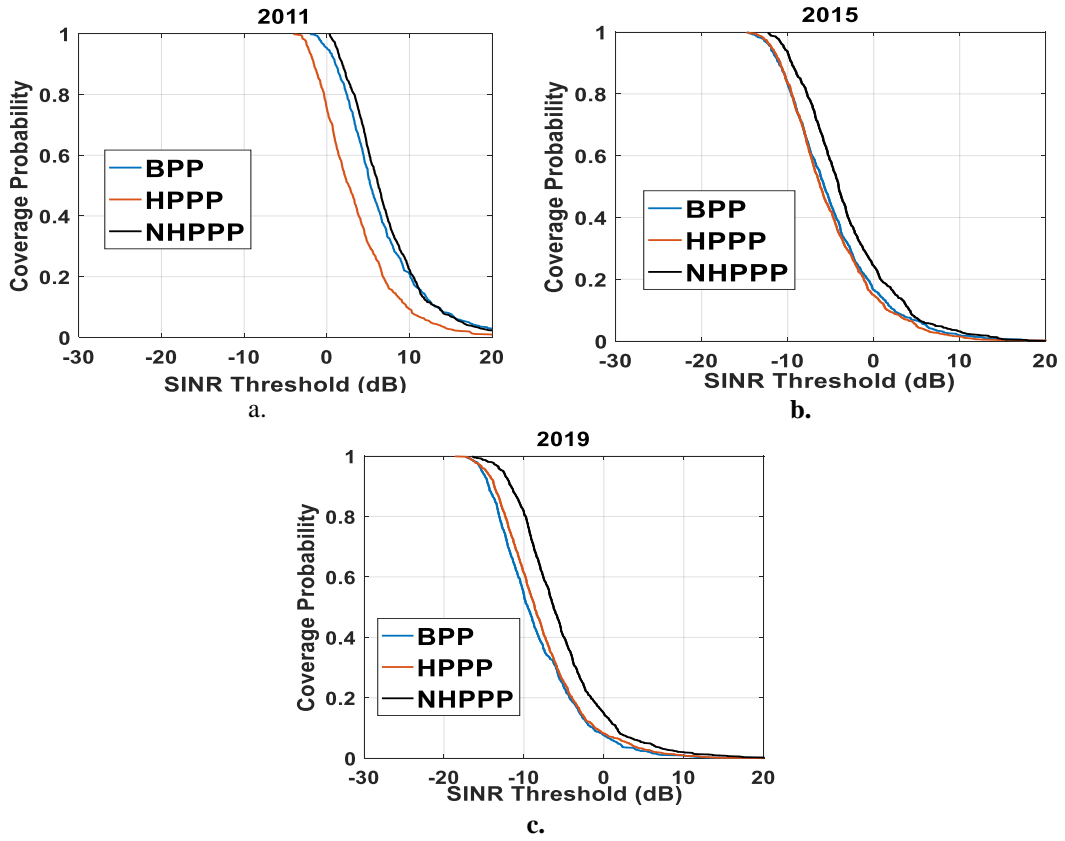


Figure 4.13 Performance Analysis of different SPPs in terms of CP for the year a. 2011 b. 2015 c. 2019

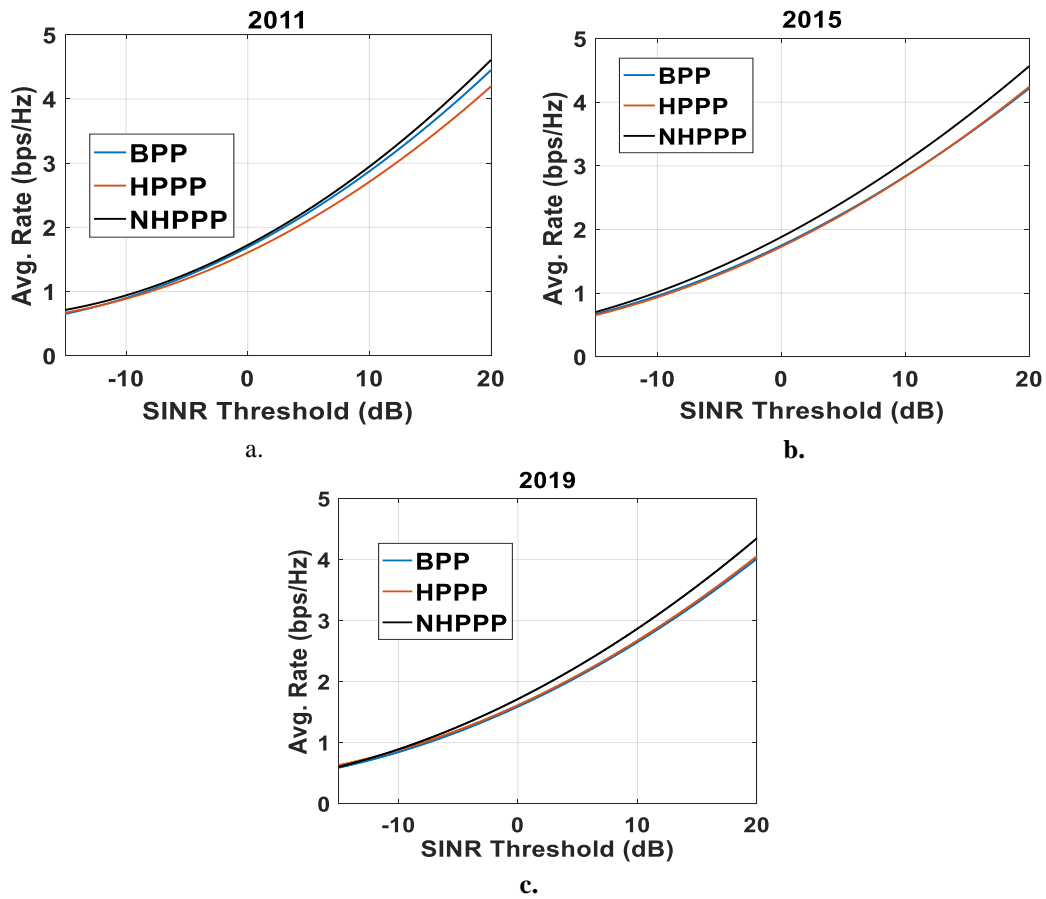


Figure 4.14 Performance Analysis of different SPPs in terms of CP for the year a. 2011 b. 2015 c. 2019

Now it is essential to check how these different SPPs perform individually making eNB density fixed from year-to-year. The comparisons shown in Fig.4.13 and Fig.4.14 justify that irrespective of any network density scenario NHPPP performs reasonably well compared to HPPP and BPP throughout the overall range of SINR threshold for both the performance parameter CP and AR because of the right thinning of eNBs deployed within a specific area. Table 4.4 is the % improvement of the NHPPP process for CP and AR over HPPP and BPPP for three different years (2011, 2015, and 2019) under different teledensity. A max of 32% CP and 9.33% AR improvements are observed for NHPPP. Notably, decreasing pattern of the performance parameters is observed from 2011 to 2019 because of the increased interfering nodes.

In addition, it has been visualized from Fig.4.13 and 4.14 that as the network density increases the performance of BPP deteriorates in comparison with HPPP in terms of both CP and AR (represented by Red and Blue Lines in Fig. 4.13 and Fig. 4.14). As a result, under the lower density scenario of 2011, BPP outperforms HPPP

by 21.77% and 5.89% in the case of CP and AR respectively (Note that the ‘-’ sign used in Table 4.4 as a logical expression to denote the degradation in performance) but as the network become denser, HPPP provides better performance compared to BPP in terms of both CP (improvement of 1.11% in 2015, 7.67 % in 2019) and AR (improvement of 0.5% in 2015, 2.8 % in 2019).

Table 4.4 Year-wise % Improvement of CP and AR for different SPPs				
		2011	2015	2019
<b>NHPPP over HPPP</b>	CP	32.90	7.04	12.40
	AR	9.33	8.35	8.18
<b>NHPPP over BPP</b>	CP	3.96	8.24	21.01
	AR	2.92	8.92	11.26
<b>HPPP over BPP</b>	CP	-21.77	1.11	7.67
	AR	-5.89	0.55	2.8

#### 4.8.2 Two-tier

The analytical results in this subsection center around the performance analysis of HPPP, NHPPP, and Clustered NHPPP models for HetNets based on two major performance parameters, namely, CP and AR. These are globally acclaimed performance parameters to analytically access the stochastic models while designing heterogeneous cellular networks. To do the comparative numerical analysis it is assumed that the MeNBs, and SeNBs transmit in fixed power  $P_1^{\text{tx}}=46$  dBm;  $P_2^{\text{tx}}=30$  dBm respectively [24]. Before going into the detailed performance analysis of the proposed model, it is also essential to find out the optimum number of SeNBs required for providing maximum performance in terms of CP and AR. So the analysis of the proposed model progress through two stages.

Firstly, this work finds the optimum number of SeNBs required, considering Indian urban and suburban density separately. Further, considering the optimum ratio of MeNB to SeNBs the comparative performance analysis of HPPP, NHPPP, and Clustered NHPPP models for Het-Nets is done.

##### A. Determining the optimum number ratio of MeNB and SeNB

Initially, the urban and suburban scenarios as depicted in Fig. 4.15, and Fig. 4.16 are considered to realize the optimum ratio of MeNB to SeNBs. The teledensities of UE are approximately considered as 153 % for urban conditions and 90 % for sub

urban conditions. Primarily, the MeNBs is placed in the center locations of both scenarios and the number of SeNBs are gradually increased starting from 3 (three).

Fig. 4.15(a) and (b) depict the comparative performance analysis based on CP and AR respectively. It is observed that the MeNB to SeNB ratio of 1:5 (i.e. 1 MeNB and 5 SeNBs) gives the best performance in terms of CP and AR (as shown By the Cyan colour plot in Fig. 4.15(a) and (b) considering Sub Urban scenarios of Fig. 4.7a and 4.9a). The reasons are as follows:

- The MeNB to SeNB ratio of 1:3, 1:4 seem to be insufficient in accommodating most of the UEs particularly those which are in the Cell Edge or in the shadowed regions.
- On the contrary, given a particular user density if the number of network component is increased further then the additional infrastructure will contribute more in the denominator of the SINR equation (refer to eq. (45)) leading to degradation of overall SINR as well as CP.

So the MeNB to SeNB ratio of 1:5 appears to be optimal in producing better SINR considering sub-urban UE density. The similar characteristic can be observed while analysing the performance in terms of AR. Here also the MeNB to SeNB ratio of 1:5 provides optimum performance as demonstrated in Fig. 4.15(b).

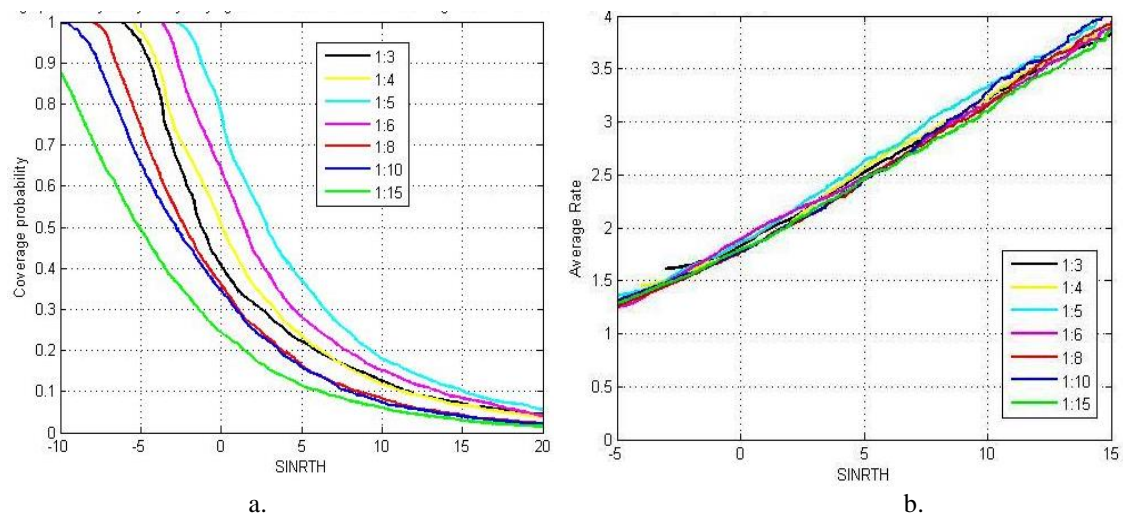


Figure 4.15. a.Coverage Probability and b. Average rate comparison by varying MeNB to SeNB ratio in Indian Sub Urban scenario

Moving to the denser urban scenario, it can be found that one may require more SeNBs to produce optimum performance in terms of coverage and rate. From Fig. 4.16 (a) and (b) it is witnessed that the MeNB to SeNBs ratio of 1:8 will produce

optimum performance with respect to both CP and AR respectively. This analysis discovers a moderately unique way to find out the requirement of an optimum number of additional infrastructures to produce improved performance in terms of CP and AR. Considering these results further analysis will be done that will justify how Clustered NHPPP should be an obvious choice in designing models for complex Het-Nets.

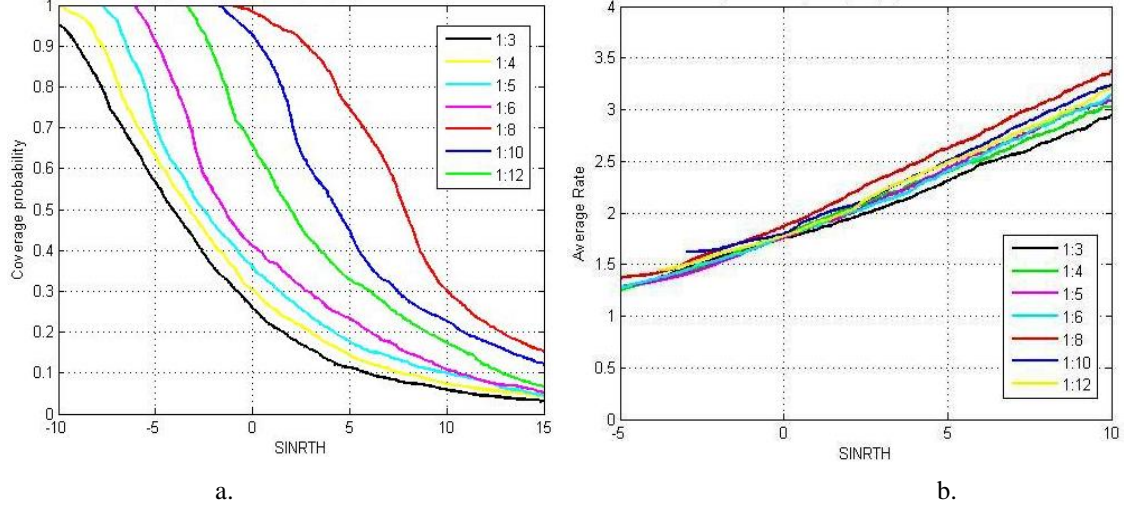


Figure 4.16. a.Coverage Probability and b. Average rate comparison by varying MeNB to SeNB ratio in Indian Urban scenario

#### A. Comparative performance analysis among HPPP, NHPPP and Clustered NHPPP in Urban and Suburban Scenarios

Considering MeNB to SeNB ratio of 1:5 for the sub-urban scenario and 1:8 for the urban scenario, the comparative performance analysis among HPPP, NHPPP and clustered NHPPP will be pursued in this subsection. Fig. 4.17(a), (b) demonstrate the performance comparisons among aforementioned algorithms based on CP and AR respectively for the suburban scenario. Moderate improvement is noticed in CP in case of NHPPP (represented by the blue line in Fig.4.17(a)) compared to HPPP (represented by red line in Fig. 4.17(a)) due to the fact that NHPPP does not accept all the points (SeNBs) those are present in HPPP by virtue of thinning (as described in subsection 4.3.2.2) and reduces the effect of interference from all other non-serving eNBs. The CP improves even further as the k-means clustering is applied to the NHPPP distributed Het-Net. By applying K-means clustering the positions of the SeNBs are optimized by minimizing the distances of each of the UEs to its respective serving eNBs. As path-loss is a function of distance and SINR is dependent on path loss, reduction of distance improves the overall SINR at any randomly chosen UE. Improvement in SINR subsequently leads to the improvement in coverage probability.



It is observed in 4.17(a) that Clustered NHPPP (represented by the green line) generates the best performance in terms of CP.

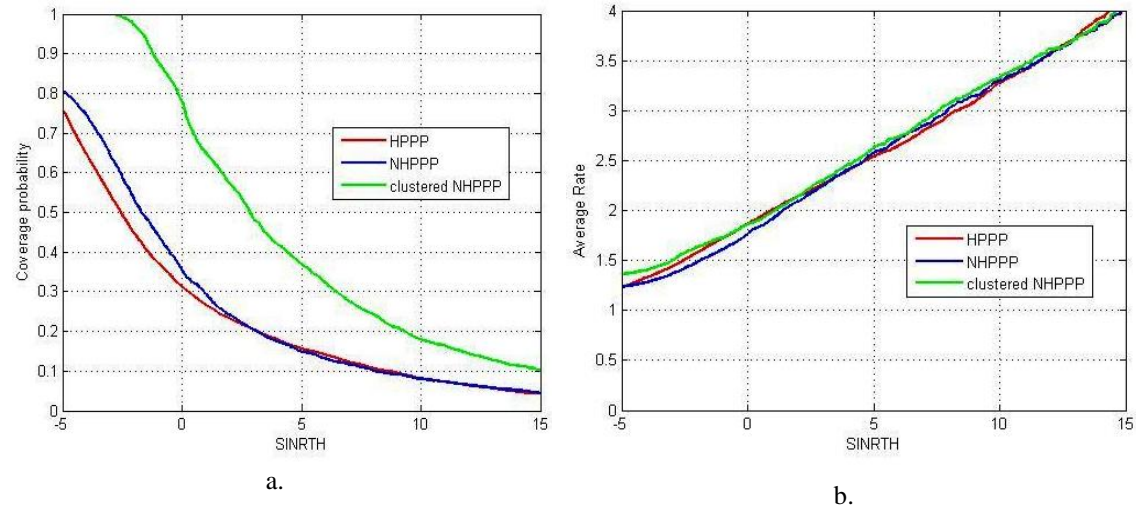


Figure 4.17. a.Coverage Probability and b. Average rate comparison between HPPP, NHPPP, Clustered NHPPP in Indian Sub Urban scenario

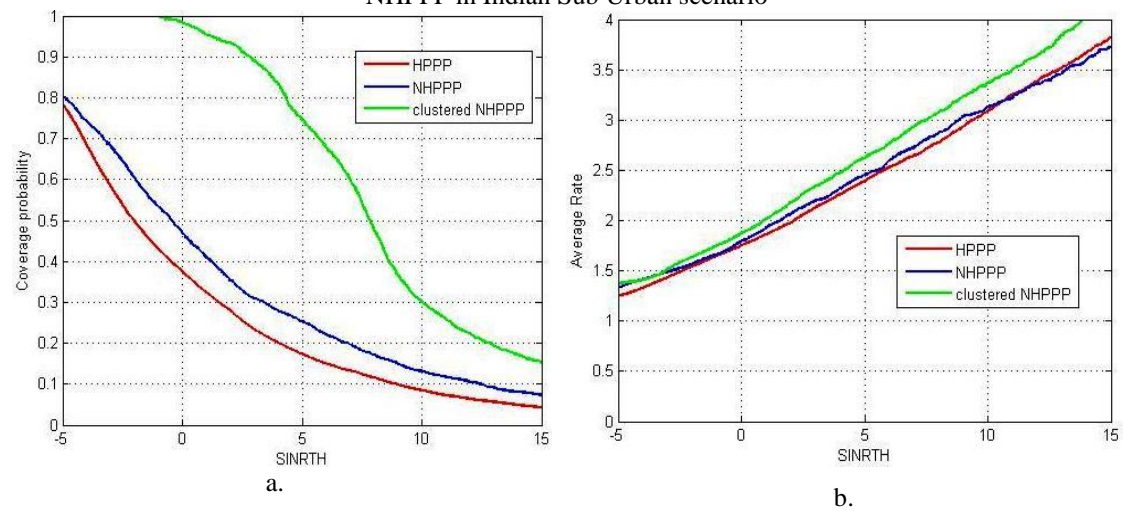


Figure 4.18. a.Coverage Probability and b. Average rate comparison between HPPP, NHPPP, Clustered NHPPP in Indian Urban scenario

Fig. 4.17(b) includes the performance analysis with respect to AR experienced by any randomly chosen UE which is in coverage. The simulation result shows that the application of k-means clustering in NHPPP distributed Het-Net generates the maximum rate experienced by any randomly selected user. In Fig 4.17(b) the green line represents the graphical demonstration of AR with respect to different values of SINRTH. Similarly, considering the urban scenario conditions, the MeNB to SeNB ratio of 1:8 is considered as optimum from the previous analysis. Fig. 4.17(a) and (b) represent the analysis of the performance of the proposed algorithm based on CP and AR under an urban scenario and it is found that as the UE density increases from



90.03% to 153% in the case of urban Scenario, NHPPP assisted by k-means clustering performs better in improving the coverage and rate (as shown by Green line in fig 4.18(a), 4.18(b)). The performance comparisons justify that the clustered NHPPP performs reasonably well throughout the overall range of SINR threshold for both the performance parameter CP and AR. The percentage improvements with respect to CP and AR are demonstrated in Table 4.5.

<b>Table 4.5. Performance improvement in terms of CP and AR among HPPP, NHPPP, and Clustered NHPPP in percentage</b>			
		Performance Improvement in NHPPP w. r. t. HPPP (%)	Performance Improvement in Clustered NHPPP w. r. t. NHPPP (%)
<b>Sub-Urban Scenario</b>	CP	4.09	41.57
	AR	0.81	18.18
<b>Urban Scenario</b>	CP	5.8	58.04
	AR	4.4	20.04

It can be observed that integration of K-means clustering with NHPPP produces better performance in terms of CP and AR considering both Urban and Suburban scenario conditions. However, the rate of improvement is much better in the case of the urban scenario. Under sub-urban scenario the NHPPP produces 4.09 % and 0.81 % performance improvement with respect to HPPP whereas under Urban scenario conditions the improvements are 5.8% and 4.4% respectively. The rate of improvements is even better as K-means is integrated with NHPPP. The clustered NHPPP delivers 41.57% improvement in CP and 18.18 % improvement in AR under Sub-Urban scenario where as the improvement increases to 58.04% and 20.04 % respectively for CP and AR under Urban Scenario. The results ensure that the proposed Clustered NHPPP performs better in handling highly dense scenarios. The key reason is that the optimum placement of SeNBs in the centroid by means of k-means minimizes the distance of each and every UE to its corresponding serving base station. Eq. (47) firmly indicates that distance is inversely proportional to CP.

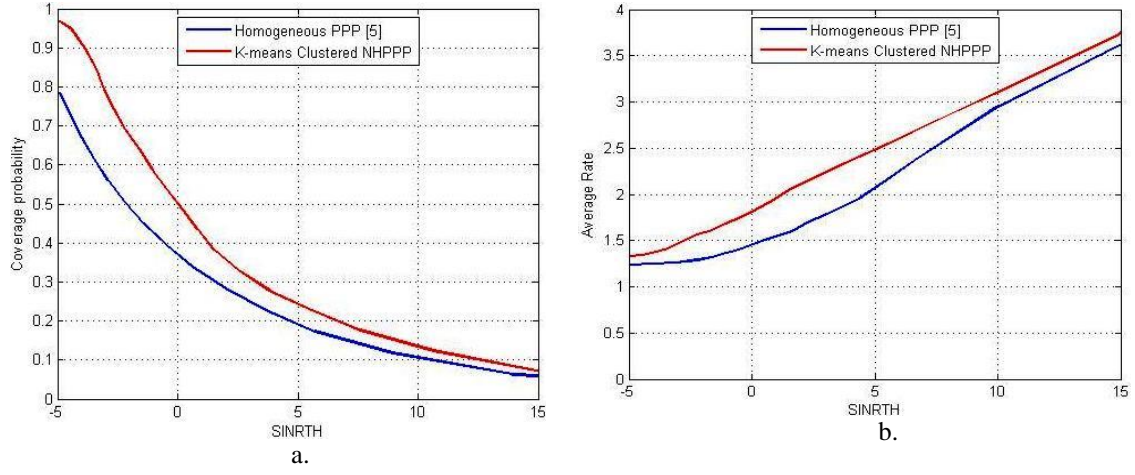


Figure 4.19 a.Coverage Probability and b. Average rate comparison between HPPP of [57] and proposed K-means Clustered NHPPP in Indian Urban scenario

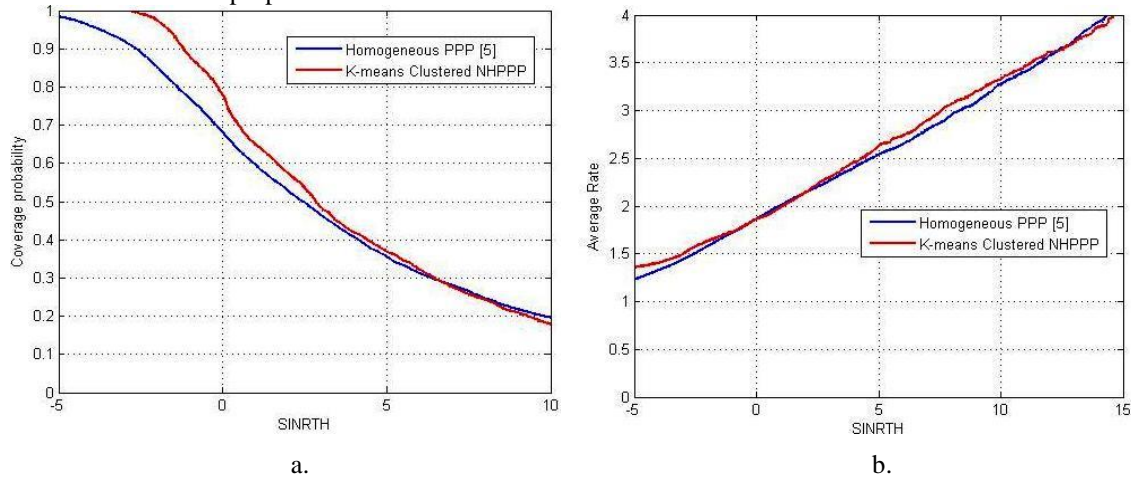


Figure 4.20 a.Coverage Probability and b. Average rate comparison between HPPP of [57] and proposed K-means Clustered NHPPP in Indian Sub Urban scenario

The proposed NHPPP assisted by K-Means Clustering is then evaluated for performance analysis with basic HPPP as included in reference [57]. The ratio of the transmit power and density of MeNBs and SeNBs are considered as  $P_1^{\text{tx}}:P_2^{\text{tx}} = 25:1$  and  $\lambda_1:\lambda_2 = 1:5$  respectively [57]. In Fig 4.19, and Fig 4.20 it is observed that the proposed clustered NHPPP performs better than the basic HPPP with respect to CP and AR under both Urban and Suburban user density because the HPPP method of reference [57] did not perform any optimum base station placement strategy which, in our sense, is quite necessary from the dense urban or sub urban scenario perspectives. Unlike ref [57], the integration of k-means clustering algorithm with NHPPP optimally deploys the SeNBs over the entire scenario which in turn improves the overall CP and AR of the overall network. The percentages of improvements are sequentially listed in Table 4.6.

Table 4.6 Performance improvement of proposed Clustered NHPPP compared to basic HPPP[57] in terms of CP and AR		
		Performance Improvement in Clustered NHPPP w. r. t. HPPP (%)
Sub-Urban Scenario	CP	12.65
	AR	8.001
Urban Scenario	CP	19.53
	AR	13.59

#### 4.8.3 Performance comparisons between different Pathloss model in Two-tier HetNet

Considering the HetNet architecture of Fig. 4.9(b) which indicates the deployment of two-tier HetNet by means of clustered NHPPP, a comparative performance analysis among 4G (3GPP TR 36.942 Release 9) [76], ABG [77], CI [77], and 5G (3GPP TR 38.901 Release 16) [80] pathloss models are performed. All simulation parameters are given in Table 4.7. It is assumed that MeNB and SeNBs operate in nLoS and LoS modes respectively.

Table 4.7 Scenario considerations and Simulation parameters for pathloss evaluation		
Ratio of density of MeNB to SeNB	$\Lambda_{\text{MeNB}} : \Lambda_{\text{SeNB}} = 1:8$	
Transmit power ( watt) ratio of MeNB and SeNB	$P_{\text{MeNB}} : P_{\text{SeNB}} = 40:1$	
Urban scenario Tele-density	153% approx. (in Indian context)	
MeNB	nLoS	
SeNB	LoS	
MeNB operating Freq.	2 GHz	
SeNB operating Freq.	4G	2 GHz
	ABG	28.50 GHz
	CI	
	5G	

The 5G pathloss models as defined in 3GPP TR 38.901 Release 16 provide the best performance considering a deployment scenario (Non-standalone) that contemplates a combination of terrestrial 4G cellular network frequency (2GHz) in the macro tier and mm-wave frequency (28.50GHz) in the small cell tier in providing better coverage and rate. This is because when mmWave frequency is used in a macro cell for long range communication, remotely positioned nLoS UE experience a very weak signal due to the lossy nature of mmWave.

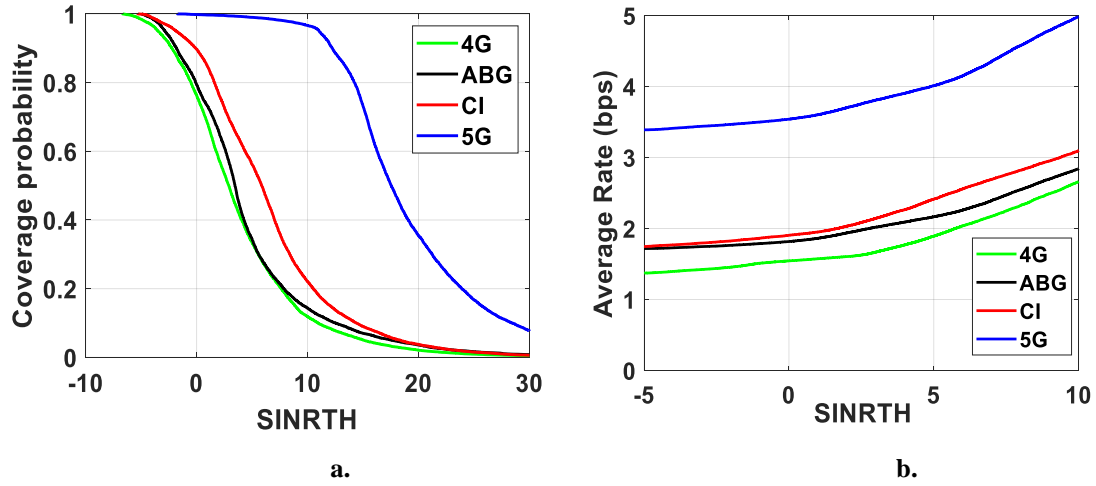


Figure 4.21. Comparison between 5G and other pathloss models (a) CP and (b) Rate

Fig.4.21(a) and (b) demonstrate the performance comparisons based on coverage and rate. The percentage improvements in coverage and rate are listed in Table-6.3. A coverage improvement of 6.15% along with 64.21% in average rate can be achieved in case of adopting the 5G pathloss model defined in 3GPP TR 38.901 Release 16 compared to the 4G pathloss model in (3GPP TR 36.942 Release 9). Both the intermediate pathloss model ABG and CI perform better than 4G pathloss model (3GPP TR 36.942 Release 9) as they use quite a higher spectrum (28.50 GHz) in small cell tiers.

Table 4.8 Comparison of 5G pathloss model with the rest		
	Performance Improvement in %	
	Coverage	AR
<b>v/s 4G</b>	6.1579	64.2150
<b>v/s ABG</b>	6.2345	78.0593
<b>v/s CI</b>	7.1360	94.2649

Performance improvements in coverage and rate are noticed for CI over ABG and 4G path loss model due to the fact that the CI model has only one path loss exponent parameter ( $n_k$ ) compared to ABG's three parameters including three exponents ( $\alpha_k$ ,  $\beta_k$ , and  $\gamma_k$ ). Eventually the ABG and CI models have contributed significantly for the development of the 5G pathloss model as documented in 3GPP TR 36.942 Release 9. The subsequent percentage improvements in terms of coverage and rate are listed in Table 4.8.

#### 4.8.4 Three Tier

The analytical results in this subsection largely revolve around the QoS based performance study among sole UMa based, UMa-UMi based two-tier, and UMa-

UMi-InH based three-tier UDHN depending on two major performance metrics, namely, CP and AR. The teletraffic density (percentage of mobile per user) and population density of an Indian urban scenario are considered as 143.38% [225] and 24760/SqKm (as of March 2022) [230].

Table 4.9 Scenario considerations and Simulation parameter for three-tier UDHN performance evaluation		
Ratio of eNB density between UMa, UMi and InH[70]	$\Lambda_{UMa} : \Lambda_{UMi} : \Lambda_{InH} = 1:8:64$	
Transmit power (Watt) [220]	UMa	40
	UMi	6.3
	InH	0.05
eNB Height (Meter) [80]	$h_{UMa}$	25
	$h_{UMa-SC}$	10
	$h_{InH}$	4
UE Height (Meter)	$h_{UE}$	1.70
Case 1	UMa	nLoS [80]
	UMi	
	InH	LoS [80]
	UMa operating Freq.	24.25-28.50 GHz [218]
	UMi operating Freq.	
	InH operating Freq.	
Case 2	UMa	nLoS
	UMi	
	InH	LoS
	UMa operating Freq.	3300-3670 MHz [218]
	UMi operating Freq.	
	InH operating Freq.	
Case 3	UMa	nLoS
	UMi	LoS
	InH	
	UMa operating Freq.	3300-3670 MHz
	UMi operating Freq.	24.25-28.50 GHz
	InH operating Freq.	

For further analysis, this work refers to the technical report published by 3GPP TR 38.901 version 16.1.0 Release 16 has comprehensively standardized channel models for frequencies from 0.5 to 100 GHz under different deployment scenarios based on both line of sight (LoS) and non-line of sight (nLoS) propagation. The predetermined parameters for simulation are indicated in Table 4.8.

Considering the UDHN architecture of Fig. 4.8, three use cases are considered in which different combinations of operating frequency are deliberated along with the path loss. In Case 1, the operating frequencies for all three different types of deployment scenarios are considered to be within the 24.25-28.50 GHz band. Due to higher loss corresponding to more travel distance with higher frequency, the received

signal from MeNB based network tend to attenuate more providing degraded coverage in an urban ultra-dense environment. However, the proposed k-tiered architecture which brings the network nearer to the end user specifically the three-tier UDHN ( $k=3$ ) tend to provide better coverage as shown in Fig. 4.22 (a) which eventually gives an improved rate as given in Fig. 4.22 (b).

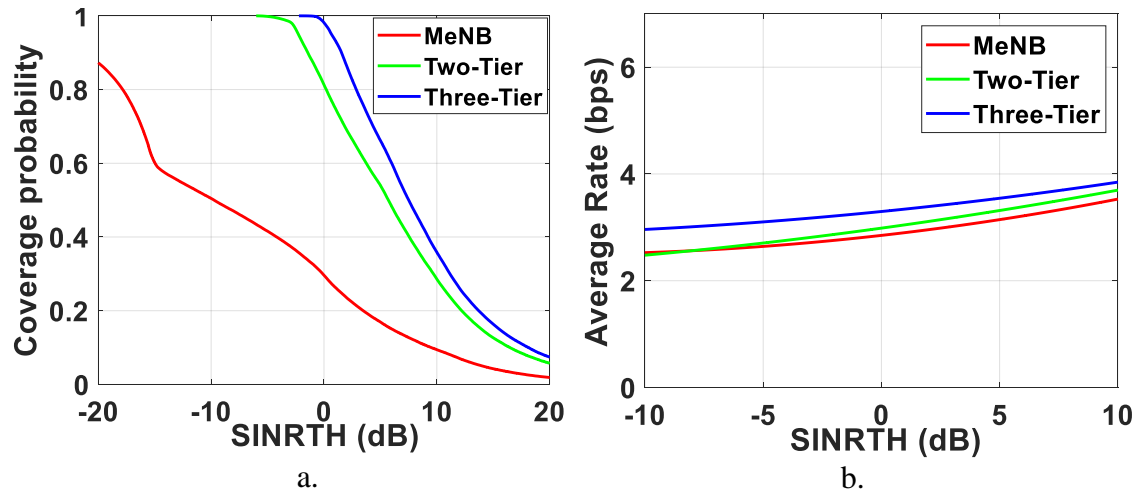


Figure 4.22 **Case 1:** Performance comparison between different deployment Model a. CP b. AR

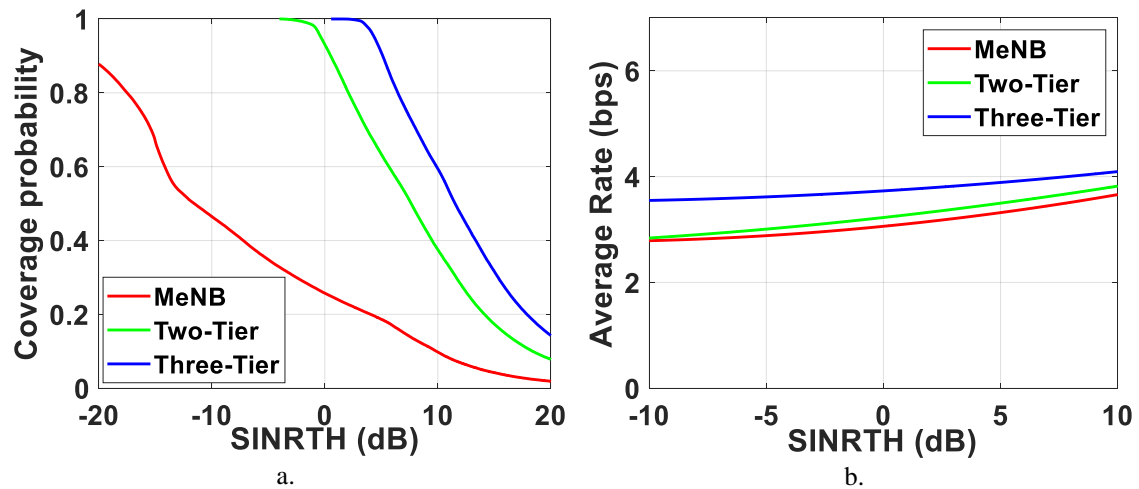


Figure 4.23 **Case 2 :** Performance comparison between different deployment Model a. CP b. AR

Case 2 considers the 3300-3600 MHz frequency band for selecting the operating frequency. Performance comparisons in terms of CP and AR are shown in Fig. 4.23(a) and Fig. 4.23(b) respectively. The trend shows that the proposed three-tier UDHN architecture provides the most improved performance in the case of both CP and AR.

Finally, in Case 3, the 3300-3670 MHz band is considered as the operating frequency for the UMa scenario and the 24.25-28.50 GHz frequency band is considered as the operating frequency in UMi and InH based scenarios. The

comparative analytical results showed in Fig. 4.24(a) and Fig. 4.24(b) show that the three-tier UDHN provides better performance in view of CP and AR respectively.

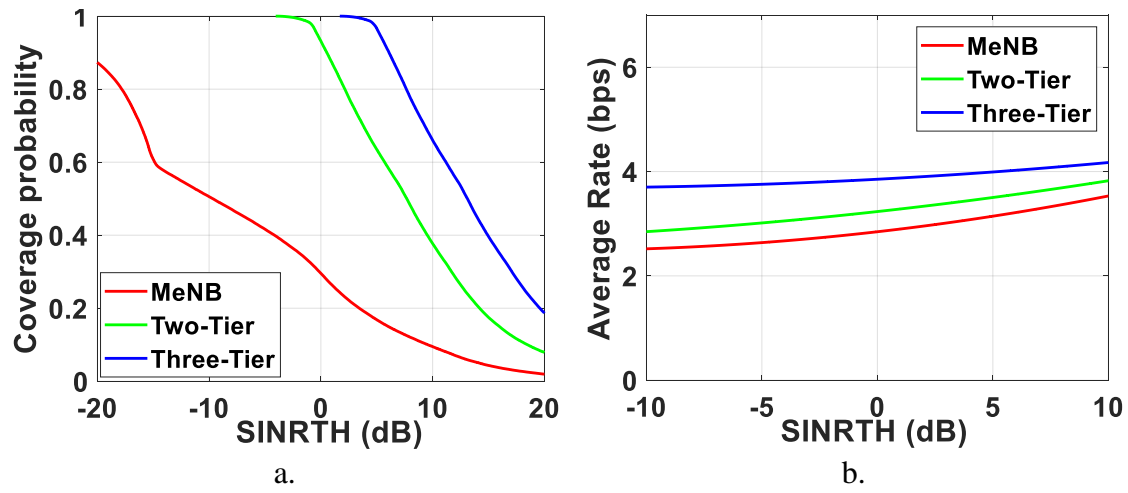


Figure 4.24 Case 3 : Performance comparison between different deployment Model a. CP b. AR

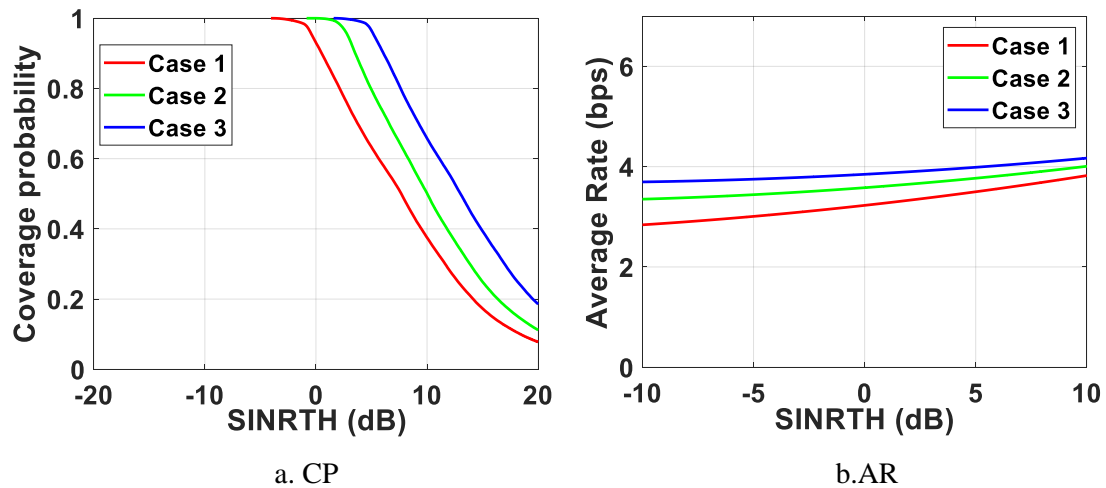


Figure 4.25 Comparison between different case studies considering three-tier scenario

It is perceived that the O2I penetration loss (as shown in Table 4.8) which adds up additional loss in the case of UMa and UMi makes the received SINR weaker for indoor users. This eventually affects negatively in terms of both coverage and rate. However, the inclusion of InH as the third tier in a three-tier UDHN which is generally deployed in indoor LoS conditions does not contain any O2I loss term in its pathloss model. Thus, the proposed three-tier UDHN brings the network nearer to the indoor end user which ends up improving the coverage as well as rate in all three cases. This brings us to a further comparative analysis among those use cases (listed in Table 4.9) considering the proposed three-tier UDHN model.

The comparative analysis in Fig. 4.25 establishes the fact that considering the proposed three-tier UHDN operating in the environment as described in Case 3 provides furthest better QoS by ensuring maximum coverage and enhanced rate because in Case 3 the use of the 3300-3670 MHz band in the UMa tier reduces the attenuation loss as link distance of some users those are being served by MeNB reduces. On the other hand, the use of the 24.25-28.50 GHz band in UMi eNBs and especially in InHs gives scope of utilizing a larger bandwidth to their users. The percentage improvements in Case 3 compared to Case 1 and Case 2 in terms of CP and AR are denoted in Table 4.9 respectively.

<b>Table 4.9 % improvements of Coverage and Rate for three-tier Scenario</b>		
	CP	AR
<b>Case 3 vs Case 1</b>	61.85	16.01
<b>Case 3 vs Case 2</b>	26.62	5.83

## 4.9 Chapter summary

SPPs are essential techniques in designing DenSNets in which eNBs are deployed independently within the network following a typical eNB density. It is understood from previous literature that with a time varying teledensity the choice of a particular SPP becomes a tricky task in view of achieving better coverage and rate. The initial observation reveals that with the increase in density of both UE and eNBs, the performances of each SPPs, namely, BPP, HPPP, and NHPPP tend to deteriorate. Therefore, a detailed performance analysis has been done for the choice of the best SPP considering increased network densification over the year. The simulation results advocate that the performance of BPP gradually deteriorate compared to HPPP with the upsurge in network density per year. Finally, it is observed that NHPPP provides better coverage as well as rate compared to all other SPPs, which makes NHPPP a better choice in designing deployment models for DenSNets.

The deployment issue for SeNBs is optimally resolved using k-means clustering algorithms. In addition, the optimum ratio of MeNB to SeNB is also determined for both sub-urban and urban scenarios. It is found that additional infrastructures are required for sustained performance in terms of coverage and rate. However, it may be seen that the percentage improvements are better under highly dense urban scenario conditions. By this observation, it can be understood that the proposed clustered NHPPP can be considered as a better choice in designing ultra-dense complex Het-



Nets. The possible extension of this work can be in the direction of incorporating network operational cost optimization as well as energy minimization. In addition, some other variants of unsupervised clustering algorithms can also be examined to encounter the location optimization problem, which will consider parameters like energy cost, and operational cost. Additionally, the introduction of sleeping modes or cognitive capabilities to the SeNBs may improve the system performance in terms of energy consumption that will lead us to the notion of greener communication.

It is also observed that with a known teledensity (urban/sub-urban) the choices of frequencies for MeNB and SeNB become important aspects to consider propagation path loss for 5G Het-nets for achieving the desired coverage and rate. Further, the CI model provides better results under certain scenario considerations i.e. terrestrial 4G cellular network frequency is used on the macro tier whereas mmWave is used in the small cells tier, which may direct small cells to be used as hotspots within 5G networks for higher data rate. SCHPPP is a useful technique in designing three-tier 5G UDHN where users are independently distributed within the network coverage region according to a distinctive user density. With a known teledensity (Indian urban scenarios), it is observed that the selection of operating frequencies for UMa, UMi, and InH has turned out to be a vital aspect to ratify the right propagation path loss model for a three-tier 5G UDHN for attaining better coverage and rate.

## ❖ Publications from this chapter

### ▪ SCI Indexed Journal

1. Arijeet Ghosh, Iti Saha Misra, and Anindita Kundu, “Coverage and rate analysis in two-tier heterogeneous networks under suburban and urban scenarios.” Transactions on Emerging Telecommunications Technologies, Wiley 30(12), p.e3648. **Impact Factor: 3.310.** DOI: <https://doi.org/10.1002/ett.3648>

### ▪ International Conferences

1. Arijeet Ghosh and Iti Saha Misra., Ultra Dense Three-Tier 5G Heterogeneous Network Model for Improved Coverage and Rate. In 2022 IEEE Calcutta Conference (CALCON) (pp. 60-64). IEEE. 2022. DOI: 10.1109/CALCON56258.2022.10060694

2. Arijeet Ghosh, Iti Saha Misra, “Role of different spatial point processes on network densification towards 5G development: Coverage and Rate analysis”, In 2020 IEEE Calcutta Conference (CALCON), pp. 15-19. IEEE, 2020. DOI: 10.1109/CALCON49167.2020.9106542
3. Arijeet Ghosh, Iti Saha Misra, “Effect of propagation path loss in designing two-tier 5G Het-Nets for coverage and rate”, In 2019 URSI Asia-Pacific Radio Science Conference (AP-RASC 2019), pp. 1-2, IEEE, 2019. DOI: 10.23919/URSIAP-RASC.2019.8738431

# Chapter 5: Finding Optimal Small Cell Densities in Ultra Dense HetNet for Improved Area Spectral Efficiency

## Outline of this chapter

- 5.1 Abstract
- 5.2 Introduction
- 5.3 System Model
  - 5.2.1 Modeling Hourly User Arrival in Urban Scenario
  - 5.2.2 Modeling a two-tier HetNet using clustered NHPPP
- 5.4 Determining the regime of optimal SeNB Density
- 5.5 Pathloss models
- 5.6 Calculation of SINR
- 5.7 Designing QoS Metric: Area Spectral Efficiency
- 5.8 Performance Evaluation
- 5.9 Chapter Summary

## 5.1 Abstract

The rapid growth in tele traffic density has enforced the modern wireless network to evolve in the direction of Network capacity and coverage. Wireless capacity enhancement may be viewed under a common umbrella of “network densification.” But, the network densification of traditional Macro eNodeBs (MeNB) has potentially reached its theoretical limit to manage the enormous amount of data demand with guaranteed QoS. This has opened a new frontier before the network service providers (NSP) by compelling them to bring a paradigm shift in their network deployment strategies from prudently deployed hefty tower mounted MeNBs to irregularly distributed multi-tier HetNet that often additionally comprise of smaller micro/pico cells. As the technology slowly penetrates through 5G mobile technology, one of the focuses of network planners is to ensure fair QoS distribution over any targeted geographical terrain. Hence, estimating *the optimal density of SeNBs* seems to be an essential task considering the *complexity of 5G multi-tier HetNets (HetNet) under*

*real-time traffic conditions*. Therefore, this chapter aims to implement a *cluster evaluation technique*, namely, *variance ratio criterion (VRC) or Calinski and Harabasz (CH) index*, to improve the *Area Spectral Efficiency (ASE)* of the entire region under test.

## 5.2 Introduction

The exponential growth of traffic-intensive applications including HD video streaming, virtual reality, wearable gadgets, and many more generates an immense amount of traffic in this new age of 5G mobile communications [32, 157, 231]. Besides, the evolution of Enhanced Mobile Broadband (eMBB) has drastically increased the number of mobile internet users all over the world. According to the CISCO annual report 2018-2023, there will be 3.6 mobile gadgets per capita by 2023 making the total number of networked devices climb up to 29.3 billion [44]. The figure of internet users in India, the second-largest telecommunication market, has increased at a 13.38% of compounded annual growth rate (CAGR) from 391.5 million in 2016 to 834.3 million in 2021 [Fig. 5.1] [45]. The extent of internet users in the country is anticipated 330 million 5G users by 2026 [45]. This will lead to a faster increase in mobile traffic, especially in dense urban areas in a country like India.



Figure 5.1 Growth of Internet users in India (in million) [44]

It is well-discussed that the evolution of wireless technology is a continuous process and it will continue to grow rather at a faster pace as evolution will move beyond 5G. Below are some graphics that clearly depicts the present as well as future scenario, estimated and well-documented by Ericson, one of the World's leading multinational networking and Telecommunications Company [158]. 5G subscriptions steered from 110 million during the third quarter to around 870 million, and that

number is likely to touch 1 billion by the end of 2022. As shown in Fig 2, there will be 5 billion 5G subscriptions globally by the end of 2028, accounting for 55 % of all mobile subscriptions [158]. The growth of 5G subscriptions is faster than that of 4G following its launch in 2009, with 5G estimated to reach 1 billion subscriptions 2 years sooner than 4G. Key factors include the timely availability of devices from several vendors, with prices falling faster than for 4G [158].

After the great success of the spectrum auction, 5G is about to roll out commercially in India around the end of this year [158, 232]. In early October, service providers in India announced the launch of commercial 5G services. Initially, enhanced mobile broadband (eMBB) will be the main use case in India. Meanwhile, 4G continues to be the dominant subscription type driving connectivity growth [158]. The eMBB which appears to be one of the three major usage scenarios endorsed by ITU for 5G/IMT 2020 in their recommendation ITU-R M.2083 strictly requires very high network throughput for hotspot scenarios with ubiquitous seamless connectivity. Meanwhile, 4G continues to be the dominant subscription type driving connectivity growth [158]. 4G subscriptions are expected to peak in India in 2024 at around 930 million, and from there will decline to an estimated 570 million by the year 2028 [158]. Aggressive 5G deployments by service providers, coupled with growing affordability and availability of 5G smartphones, should see 5G subscriptions in the India region reach around 31 million by the end of 2022 and 690 million by the end of 2028 [158]. 5G will represent around 53 % of mobile subscriptions in the region at the end of 2028. Total mobile subscriptions in India are estimated to grow to 1.3 billion in 2028 [158]. This abrupt evolution of wireless outlook has invariably contributed to the explosion in the number of subscribers as they continue to provide essential services through various multimedia applications. As a by-product, tele traffic density, i.e., the number of subscribers per 100 users in any particular region, has increased by leaps and bounds and will certainly continue to increase in the future. As of July 2022, Tele-density that is defined as the number of telephone connections for every 100 individuals, in India, has increased from 17.9 percent in FY07 (Financial Year 2007) to 85.03 percent in FY22, of which urban tele-density stood at 143.66 percent [232].

To achieve the radically augmented demand on extremely high throughput, one emerging solution is to deploy a large number of dense Small cell eNBs (SeNBs) under the footprint of traditional macrocell eNBs (MeNBs), namely, Heterogeneous

networks (HetNet). HetNet has now become one of the core characteristics of 5G cellular networks [57, 58, 59]. These SeNBs which are often mounted by the operators in street-side structures like lampposts differ from MeNBs in terms of transmit power, coverage area, traffic handling capabilities, etc. Fig. 5.2 demonstrates one such type of abstract HetNet [59, 60].

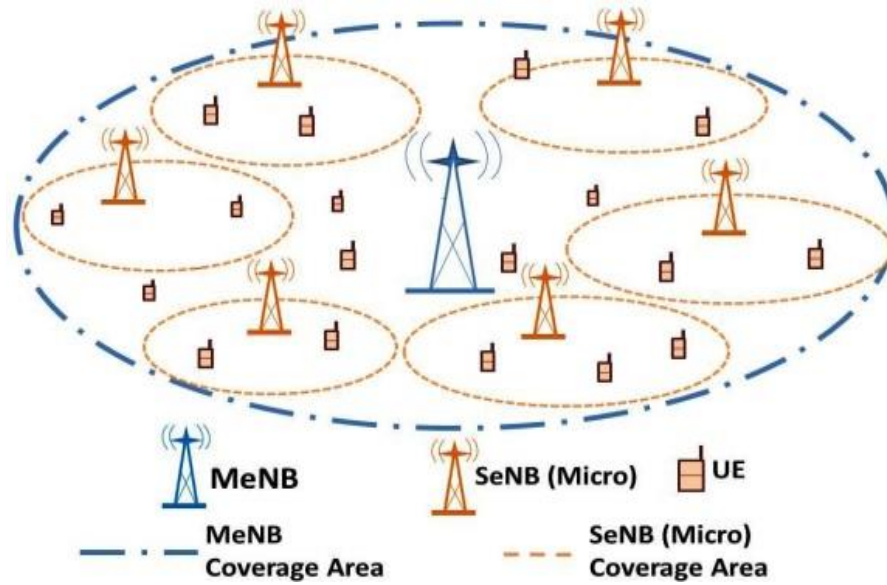


Figure 5.2. A Two-Tier HetNet

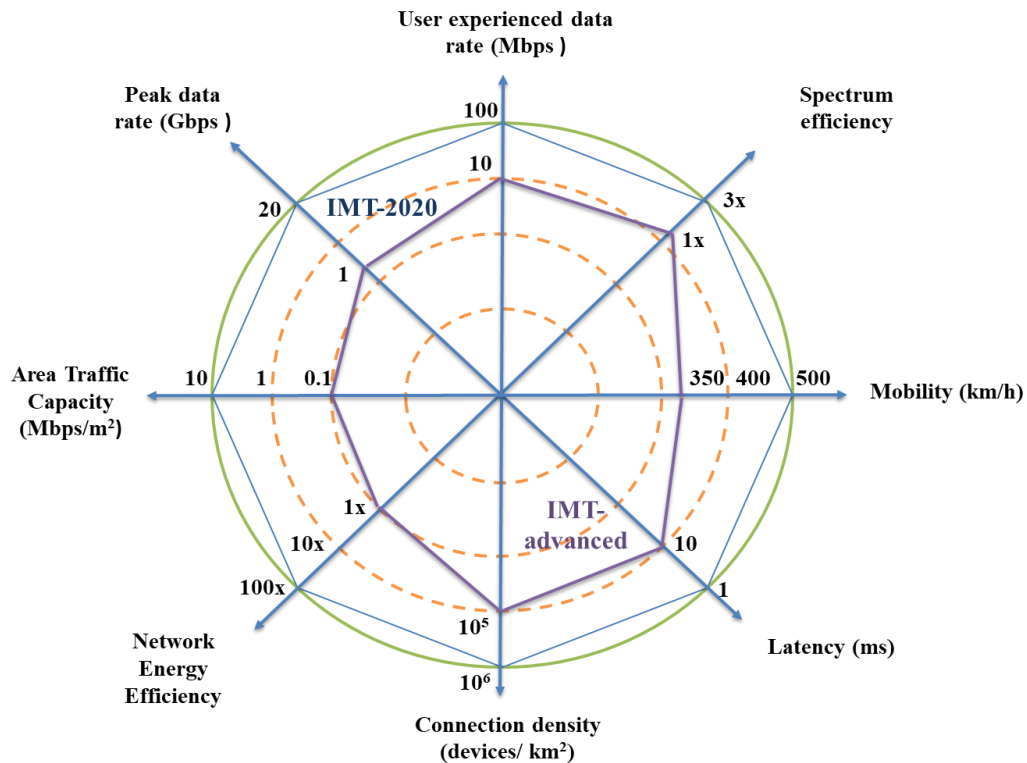


Figure 5.3 Enhancement of key capabilities from IMT-Advanced to IMT-2020 [41]

The recent developments for IMT and its expected future role have headed to diverse use cases foreseen for both human-centric and machine-centric communication, namely, Enhanced Mobile Broadband (eMBB), Ultra-Reliable and Low-Latency Communications (URLLC), and Massive Machine-Type Communications (mMTC) [34, 35, 231]. These service verticals have extended the capabilities for IMT-2020 [36]. A first-hand feature envisioned for IMT-2020 is that it would be able to operate in potentially new frequency bands above 6GHz and beyond, including mm-wave bands [36]. A broad classification of capabilities, usage scenarios, and applications for IMT-2020 was anticipated in the IMT 2020 Vision Document [41]. The eMBB which appears to be one of the three major usage scenarios endorsed by ITU for 5G/IMT 2020 in their recommendation ITU-R M.2083 strictly requires very high network throughput for hotspot scenarios with ubiquitous seamless connectivity. The key service requirements of 5G radio technology capabilities are shown in Fig. 5.3. In some typical scenarios, the area throughput requirement may reach as high as 10 Mbits/s/m<sup>2</sup> [41]. Thus, Area Traffic Capacity (ATC) or Area spectral efficiency (ASE) becomes one of the key metrics to evaluate future mobile systems, especially in highly dense urban traffic scenarios [90, 151, 153-155, 160- 162].

Deployment of HetNets can significantly improve area spectral efficiency and QoS by virtue of the reuse of spectrum across a geographic area, Cell Range Expansion, and off-loading of users [143, 157]. As long as power-law pathloss models approximated to the signal-to-interference plus noise ratio (SINR), in principle, cells can densify almost indeterminately without a minimum expense in SINR, until nearly each eNB serves a single user [143]. This allows each eNBs to bestow its resources to an ever-smaller number of users. Besides the reduced distance between the network element and the end user also can contribute to a better link SINR at every end user especially those in the cell edges [208].

Some recent research works have thoroughly scrutinized to analyze the impact of network densification on network QoS performance. It is well understood from the previous discussion that the key enabling factor to increase the data rate in wireless networks over the past few decades has been network densification [60, 157, 159, 231, 233, 167-169]. This tendency is foreseen to endure into 5G and beyond [3, 9, 33]. However, at some juncture, further densification will no longer be able to provide

improvement in data rates [167] and there is no such clear method available in the literature to demarcate the fundamental boundary of network densification, especially under any real-time teletraffic arrival scenario [167-169]. Arguably, it is also speculated that over-densification will no longer be able to provide exponentially increasing data rates as it can lead to a possible downfall in SINR [167-169]. Therefore, in this work, we aim to comprehend how the ASE is associated with density for real-time tele traffic arrival scenarios since the key objective of network densification is to improve ASE which is simply the sum throughput normalized by the coverage area eNB density. The major contributions of this paper are given below. Firstly, in subsection 2.1, the user equipment (UE) arrival process is modeled as a one dimensional (1D) Poisson Arrival Process (PAP) following the teledensity profile of the Indian urban scenario (for the city of Kolkata) within a 7 km<sup>2</sup> coverage region for a time span of 12 working hours (10 am to 9 pm) of any random day.

In this chapter, a user distribution model based on an hourly tele traffic arrival scenario is designed with Poisson Arrival Process (PAP). Subsection 7.2.1 presents the modeling of two tiers of eNB distribution based on the Non Homogeneous Poisson Point Process (NHPPP) considering HetNet. The path loss propagation model for different deployment scenarios is considered from 3GPP TR 38.901 version 16.1.0 Release 16, which is mentioned in. The distribution of cumulative SINR at any arbitrary user location is also derived. The notion of clustering (k-means) over the NHPPP based HetNet is used to optimize the location of the SeNBs. This chapter introduces the variance ratio criterion (VRC) or The Calinski-Harabasz (CH) index method to find out the optimal density of SeNBs under HetNet. The definition of the Quality of Service (QoS) performance parameters, namely, ASE, is depicted in subsection 7.2.6. Section 7.3 includes the detailed analysis of the proposed model and demonstrates the impact of SeNB density on Network ASE.

## 5.3 System Model

### 5.3.1 Modelling Hourly User Arrival in Urban Scenario

Firstly in this paper, the User Equipment (UE) arrival process within a certain coverage region is modelled as a one dimensional (1D) PAP [63] following certain assumptions.



1. The number of UEs which arrive within an interval  $(a, b]$  has expected value equivalent to the duration of the interval:

$$\mathbb{E}[N(m, n)] = \mu(n - m) \quad (49)$$

Where,  $\mu > 0$  is the rate of the UE arrival process;

2. UE arrivals in disjoint time intervals are independent i.e. if

$m_1 < n_1 < m_2 < n_2 \dots \dots \dots m_r < n_r$  then random variables  $N(m_1, n_1], \dots, N(m_r, n_r]$  are independent.

3. The probability of two or more UE arrivals in an infinitesimal time interval is given as:

$$\mathbb{P}[N(m, m + t) \geq 2] = o(t), \quad t \downarrow 0. \quad (50)$$

Based on the above considerations, it leads that the number of UEs arriving within a time interval should trail a Poisson distribution:

$$N(m, n] \sim \text{Poisson}(\mu(n - m)) \quad (51)$$

Where, Poisson ( $\delta$ ) implies the Poisson distribution with mean  $\delta = \mu(b - a)$ , is hereby defined as

$$\mathbb{P}[N = \eta] = \frac{e^{-\delta} \cdot \delta^\eta}{\eta!}, \quad \eta = 1, 2, 3, \dots \quad (52)$$

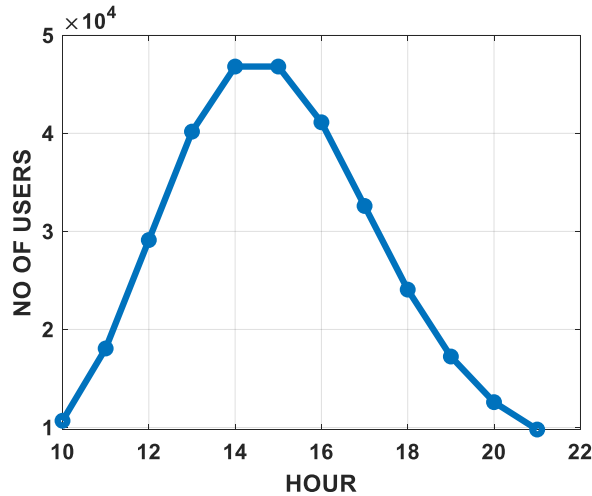


Figure 5.4 Hourly Arrival of UEs in the region of Kolkata bearing the Tele traffic of 143.66% [45], and population density of 24760/km<sup>2</sup> (as of July 2022) [230]. The sampling instants in the x axis purely indicate time stamps in a day in 24 hour format.

### 5.3.2 Modelling a Two-Tier HetNet using clustered NHPPP

Prior to estimating the optimal density of SeNBs, it is very much essential to emulate the hourly deployment of HetNets with all its entities (MeNB, SeNB, UE) and their corresponding coverage regions as each of them modeled as clustered NHPPP. In this work, a two-tier ( $K=2$ ) UDHetNet is considered where each tier relates

to different types of eNBs. These different types of eNBs contrast with each other in terms of transmit power, coverage regions, user accommodating capabilities, area spectral efficiency, path loss propagation models, and their spatial distribution. Primarily, it is assumed that the eNBs of the  $k^{\text{th}}$  ( $k \in K$ ) tier are spatially dispersed according to an NHPPP  $\Psi_k$  of density  $\lambda_k$  in Euclidean plane [62, 63]. The number of points of the process in any finite region  $A \subset \mathbb{R}^2$  denoted as  $N_k(A)$ , is a random variable with the Poisson distribution,

$$\mathbb{P}[N_k(A) = \eta] = \frac{e^{-\mu_n(A)} \cdot \mu_n(A)^\eta}{\eta!}, \quad \eta = 1, 2, 3 \dots$$

With mean (rate function)

$$\mu_k(A) = \iint_A \lambda_k(x, y) dx dy \quad (53)$$

Note that a UE can only be served by  $j^{\text{th}}$  eNB of  $k^{\text{th}}$  tier if and only if the downlink SINR with respect to that  $i^{\text{th}}$  eNB is greater than threshold SINR,  $\gamma_k^{\text{th}}$ . The UEs are also scattered in the same finite region  $\gamma_k^{\text{th}}$  as independent NHPPP  $\Psi_m$  of density  $\lambda_m$ . Thus each class of eNBs appropriated to a specific tier can be uniquely characterized as,

$$\Psi_k = f(P_k^{\text{tx}}, \lambda_k, \gamma_k^{\text{th}}) \quad (54)$$

A computationally simple and relatively proficient technique for producing 1D NHPPP is described in Chapter 4.

This work also implements k-means clustering algorithm over NHPPP to optimize the locations of SeNBs within a HetNet. The k-means clustering algorithm is an effective tool that can group NHPPP distributed UEs into ‘k’ Voronoi cells or clusters [70, 215]. Subsequently, k-Means can also optimize the centroid locations of each of the clusters in an iterative manner so that the average distance between the centroid (SeNB position) and all the cluster members (UEs) will be minimized. The centroid locations can be seen as the optimum location of SeNBs [70, 215]. The implementation of k means clustering algorithms on the top of NHPPP leads to another spatial point process termed in this research work as Clustered NHPPP.

The resulting coverage region for a HetNet generated by k-means clustered NHPPP is depicted in Fig. 5.6. This led us to switch the focus of this work to determine the optimal number of SeNBs corresponding to varying teledensity in such HetNet in the next subsection.

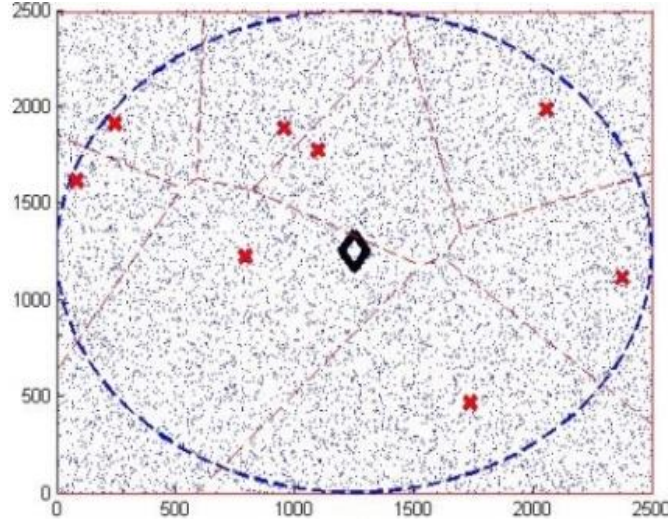


Figure 5.5 Generalised Graphical representation of UDHetNet in a 2500 m<sup>2</sup> Urban Region modelled by NHPPP

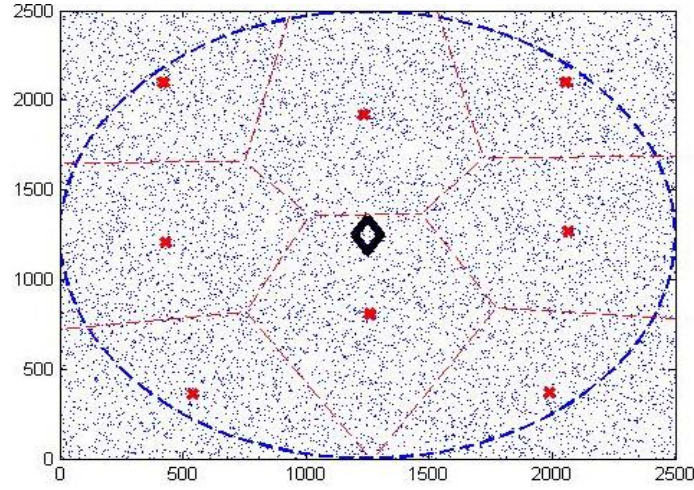


Figure 5.6 Generalized Graphical representation of Clustered (k-means) HetNet in a 2500 m<sup>2</sup> Urban region modeled by Clustered NHPPP [70]

## 5.4 Determining the regime of optimal SeNB Density

To determine the optimal number of SeNB corresponding to the optimal number of cluster we consider a cluster evaluation technique which will determine the initial value of 'k' for the K means clustering algorithm. The Variance Ratio Criterion (VRC) [234] is a popular method which can determine the optimal number of initial centroids pertaining to the density of data points (UE density  $\gamma_m$  in this work).

- Variance Ratio Criterion (VRC)

The variance ratio criterion (VRC) or The Calinski-Harabasz (CH) index is defined as,

$$\text{VRC}_k = \frac{\Pi_B}{\Pi_W} \times \frac{(\Delta-k)}{(\Delta-1)} \quad (55)$$

Where,  $\Pi_B$  is the overall between-cluster variance,  $\Pi_W$  is the overall within-cluster variance,  $k$  is the number of clusters, and  $\Delta$  is the number of observations.

The overall between-cluster variance  $\Pi_B$  is defined as

$$\Pi_B = \sum_{o=1}^k \delta_o \|\omega_o - \omega\|^2 \quad (56)$$

Where,  $k$  is the number of clusters,  $\delta_o$  is the number of observations in cluster  $o$ ,  $\omega_o$  is the centroid of cluster  $o$ ,  $\omega$  is the overall mean of the sample data, and  $\|\omega_o - \omega\|$  is the L2 norm (Euclidean distance) between the two vectors.

The overall within-cluster variance  $\Pi_W$  is defined as

$$\Pi_W = \sum_{o=1}^k \sum_{\psi \in \tau_o} \|\psi - \omega_o\|^2 \quad (57)$$

Where,  $k$  is the number of clusters,  $\psi$  is a data point,  $\tau_o$  is the  $o^{\text{th}}$  cluster,  $\omega_o$  is the centroid of cluster  $o$ , and  $\|x - m_i\|$  is the L2 norm (Euclidean distance) between the two vectors. Well-organized clusters should have a large between-cluster variance ( $\Pi_B$ ) and a small within-cluster variance ( $\Pi_W$ ).

## 5.5 Pathloss Models

The technical report issued by 3GPP TR 38.901 version 16.1.0 Release 16 has broadly standardized pathloss models for frequencies from 0.5 to 100 GHz under diverse deployment scenarios [80]. The pathloss propagation models for various scenarios considered in this work are abridged in Table 5.1. The definition of distance is demonstrated in Fig. 5.7. The shadow fading (SF) for different deployment aspects are considered to be log-normal (given in Table 5.1).

Tabl 5.1. Pathloss model for different scenarios [80]	
Scenario	Pathloss Propagation models [Center Frequency, $f_c$ (FR1), in GHz, distance, $d_{3D}$ in meters] $\sigma_{SF}$ = Shadow fading std. [db]
Urban Macro Cell nLoS served by MeNB	$32.4 + 20 \log_{10}(f_c) + 30 \log_{10}(d_{3D})$ $\sigma_{SF} = 7.8$
Urban Micro Cell nLoS served by SeNB	$32.4 + 20 \log_{10}(f_c) + 31.9 \log_{10}(d_{3D})$ $\sigma_{SF} = 8.2$

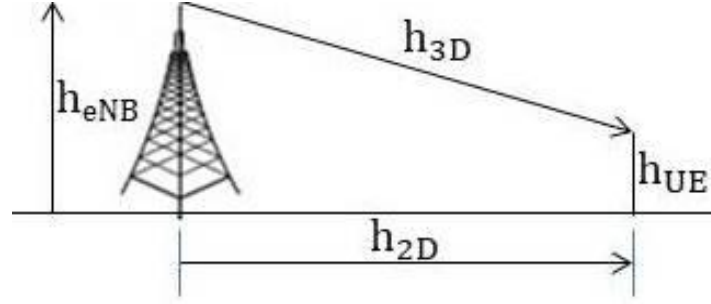


Fig 5.7. Distance definition i.e.  $d_{3D} = \sqrt{(d_{2D})^2 + (h_{eNB} - h_{UE})^2}$  [19]

## 5.6 Distribution of SINR at random user location

In this subsection, the main focus is engaged to calculate downlink SINR at any random location for a given scenario. To start with, it is considered that a random user is located at a distance  $\Delta_0$  from the serving eNodeB (S-eNB) from which it receives maximum power. All other eNBs belong to that network will be orchestrated as non-serving eNodeB (NS-eNB) and will eventually treated as source of interference to that particular user. Now to derive the expression of SINR, it must be noted that it primarily depends upon two parameters i.e. transmit power ( $P_k^{tx}$ ) and path loss of the link. Here, in this work the 3GPP path loss models for Macro Cell and Small cells are considered [80]. Macro cell and Small Cell propagation models for urban area is valid for scenarios in urban zones except the high rise core where buildings are of nearly uniform height (3GPP TR 36.942) [80]. Assuming that the eNB antenna height is fixed at 15 m above the rooftop, and a carrier frequency of 2 GHz is considered, the path losses for MeNB and SeNB environment and are articulated by (58) [80].

Without the loss of generality the amount of path loss measured at any arbitrary  $i^{th}$  user for  $n \in N$  (where,  $N$  is the total no of users) located at  $(x, y)$  from any of its serving  $j^{th}$  eNB of  $k^{th}$  tier is considered as

$$PL_k(x, y)_i^j = 32.4 + 20 \log_{10}(f_c^{j \in k}) + B^{j \in k} \log_{10}(d_{3D, n}^{j \in k}) \quad (58)$$

Where,

$B^{j \in k}$  = pathloss exponent of the logarithmic distance term corresponding to MeNB, SeNB type of network infrastructure.

The resultant received power at any arbitrary  $i^{th}$  user from  $j^{th}$  eNB of  $k^{th}$  tier is given as

$$P_k^{rx}(x, y)_i^j = P_k^{tx} - PL_k(x, y)_i^j \quad (59)$$

Simultaneously, the downlink SNR of the link between a typical  $j^{th}$  eNB and  $i^{th}$  UE located at  $(x, y)_i^j$  is given as,

$$SNR_k(x, y)_i^j = P_k^{rx}(x, y)_i^j - \theta \quad (60)$$

Where,  $\theta$  is the downlink Noise Figure [201] in dB.

Hence, the cumulative SINR at any arbitrary  $n^{th}$  user from  $i^{th}$  eNB of  $k^{th}$  tier can be calculated as,

$$\gamma_k(x, y)_i^j = \frac{SNR_k(x, y)_i^j}{\left\{ \sum_{k \in K} \sum_{l=1}^{j-1} SNR_k(x, y)_i^l \right\} + 1} \quad (61)$$

Note that, UE will be served by its strongest eNB i.e. the UE will be connected to the eNB which offers best SINR. So, a random  $i^{th}$  UE located at  $(x, y)_i$  served by any  $j^{th}$  eNB belonging to  $\Psi_k$  is considered to be in coverage if:

$$\max_{(x, y)_i \in \Psi_k} \gamma_k(x, y)_i^j > \gamma_k^{th} \quad (62)$$

## 5.7 Designing QoS performance parameters

The QoS parameter in this work, namely, Area Spectral efficiency is derived aiming to analyse the performance of proposed Het-Net modelled by NHSCPPP in the midst of hourly varying nature of customer arrival as demonstrated in Fig.5.5.

- Area Spectral Efficiency (ASE)

The performance metric we consider for QoS assessment is the ASE [159], which represents the estimated instantaneous throughput for all users when the Shannon bound is achieved. Given our system model, we define the conditional ASE[160] as

$$\Phi_A(A) \triangleq \frac{T_p}{A \cdot \Omega_{Av}} = \frac{\mathcal{R} \cdot \Omega_{utl} \cdot (M+S)}{A \cdot \Omega_{Av}} \quad (63)$$

Where,

$T_p$  = Throughput of the entire network

$A$  = Total area under coverage

$\Omega_{Av}$  = Total Available Bandwidth

$\Omega_{utl}$  = Total Utilised Bandwidth

$\mathcal{R}$  = Constrained Spectral Efficiency

$M$  = No of MeNB

$S$  = No of SeNB

The  $\Phi_A(A)$  can be written as a function of the eNB density and of the Instantaneous Constrained Spectral Efficiency [159] as follows

$$\Phi_A \triangleq \lim_{A \rightarrow \infty} \Phi_A(A) = \frac{\mathcal{R} \cdot \Omega_{utl} \cdot (M+S)}{A \cdot \Omega_{Av}} \xrightarrow{p} \frac{\mathcal{R} \cdot \Omega_{utl} \cdot (\lambda_M + \lambda_S)}{\Omega_{Av}} \xrightarrow{q} \frac{\mathcal{R} \cdot (\lambda_k + \lambda_k)}{\Omega_{fr}} \quad (64)$$

Where, the equality operation (p) is obtained by replacing  $\lim_{A \rightarrow \infty} \frac{(M+S)}{A}$  by  $(\lambda_M + \lambda_S)$  such that  $\lambda_M, \lambda_S \in \lambda_K$  are the density of the MeNBs and SeNBs respectively within the coverage region  $A \subset \mathbb{R}^2$  while equality operation (q) follows its trail from the definition of frequency reuse factor  $\Omega_{fr} = \frac{\Omega_{Av}}{\Omega_{utl}}$ . The Constrained Spectral Efficiency ( $\mathcal{R}$ ) in following can be computed similarly as the calculation of average rate Section 4 of Chapter 4.

$$\mathbb{E}[f(\lambda_m, \gamma_k^{th})] = \lambda_m \cdot \mathbb{E} \left[ \left\{ \log_2 \left( 1 + \max_{(x,y)_i^j \in \Psi_k} (\gamma_k(x,y)_i^j) \right) \mid \bigcup_{k \in K, (x,y)_i^j \in \Psi_k} \gamma_k(x,y)_i^j > \gamma_k^{th} \right\} \right] \quad (65)$$

## 5.8 Performance Evaluation

The analytical results in this work primarily center on finding an optimal solution to SeNB locations and density considering variable teletraffic scenario (considering the hourly teledensity profile of the Kolkata, India as shown in Fig. 5.4.).

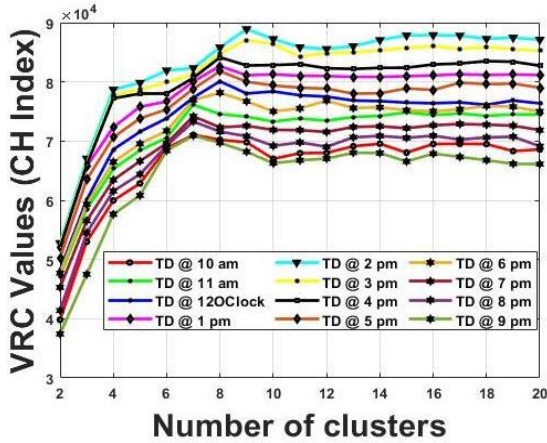


Figure 5.8 Hourly VRC (/CH) values with respect to number of Clusters

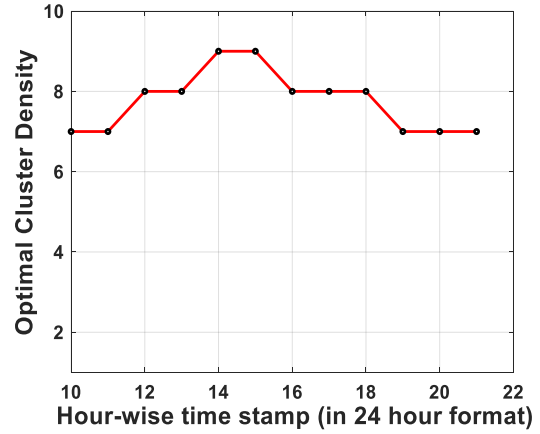


Figure 5.9 Hourly Optimal Cluster Density

K means clustering followed by VRC cluster evaluation technique clearly ratify that as the density of UE varies, the optimal number of cluster also changes. The exit condition implies here is that larger  $VRC_k$  ratio (CH Index) results in better the data partition. To determine the optimal number of clusters, maximize  $VRC_k$  with respect to



k. The optimal number of clusters corresponds to the solution with the highest CH index value (or  $SeNB_{opt} = \max_K VRC_k$ ).

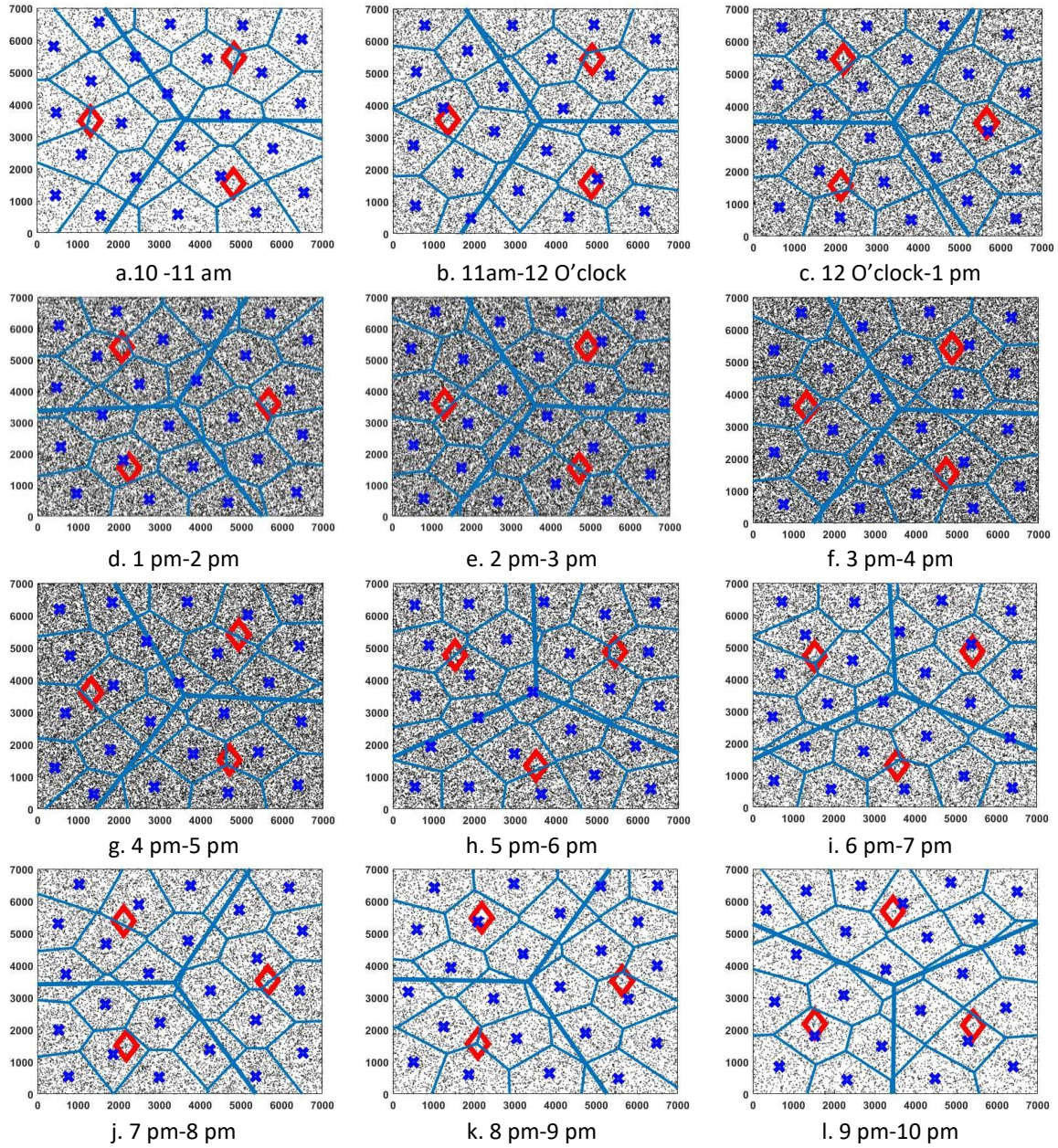


Figure 5.10. Estimated hourly modelling of a Indian Urban Scenario (Kolkata) as Two-Tier Het-Nets (MeNB, SeNB, UE) modelled by NHSCPPP in a 7000 sq. m geographical area with UE density ~143.38 % considering ratio of MeNB to SeNB density as 1:8

MeNB; MeNB coverage region; SeNB; SeNB coverage region; UEs.

Results shown in Fig. 5.8 clearly demonstrate that the VRC/CH Index value indicates respective highest values corresponding to different hours in a day which encounters different UE load into the network. The peak hours (around 2 pm to 3 pm) which handle maximum number UEs (as shown in Fig. 5.4) in a random day requires



most number of clusters i.e. 9 clusters (i.e. 9 SeNBs as depicted in Fig. 5.9) to accommodate all the UEs of a aforementioned region.

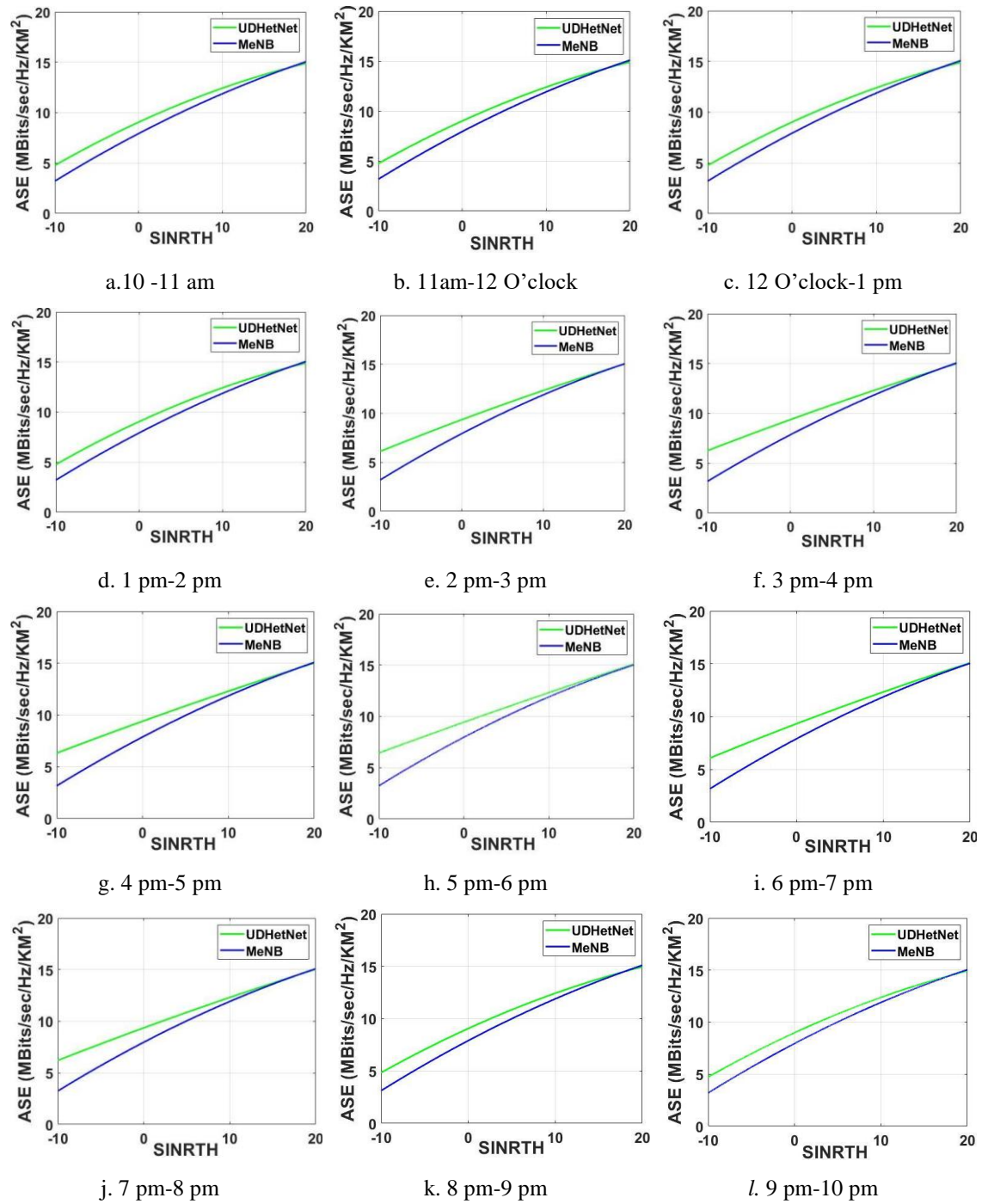


Figure 5.11 Comparative analysis of hourly ASE of HetNet under Indian Urban Scenario (Kolkata)

The non-peak hours (around 10 am to 11 am in the morning and 7 pm to 9 pm in the evening) naturally need less number of clusters (7 clusters as shown in Fig 5.9) owing to less UE load into the system. However, it is well understood that the main motto of implementing HetNet is to improve the overall ASE. So, the next part of this

analysis focuses upon hour wise comparative ASE analysis between traditional MeNB based networks, and two tier HetNet considering time varying tele-density (per Sq. Km) and the respective optimal number of SeNBs (per sq. Km) of the Indian Urban scenario.

Further, this section aims to model the customer arrival process in a typical Indian Urban condition (considering the population and subsequent teledensity for the city of Kolkata) as an One dimensional PAP within a total time span of 12 hours (typically busy office hours from 10 am in the morning to 9 pm in the late evening) with a step size of one hour each. Fig. 5.10 shows the hourly estimation of the customer arrival process of the city of Kolkata, a test case for an Indian urban scenario for a total duration of 12 hours within a coverage region (mostly office area) of 7 sq. km through MATLAB simulation. The corresponding hour wise optimal density of SeNBs ( $\text{SeNB}_{\text{opt}}$ ) is traced from Fig 5.9. Prior to modelling and in-depth ASE analysis of the above teletraffic scenario, it is very much essential to emulate the hourly deployment of Het-Nets with all its entities (MeNB, SeNB, UE) and their corresponding coverage regions as each of them modelled as clustered NHPPP. Fig 5.10(a)-5.10(l) depicts the same where the hourly customer arrival is considered as demonstrated in Fig 5.10. It is observed that between 1 pm to 4 pm a typical urban scenario encounters the maximum inflow of customers (as shown in Fig.5.10 (d)-5.10(f)).

Considering hourly optimal SeNB density in an UDHetNet deployed to serve Indian Urban traffic arrival Scenario (as depicted in Fig. 5.4), this work further investigates that an UDHetNet is better equipped to deliver improved ASE throughout a day. Fig. 5.11 exhibits a comparative performance analysis between HetNet and MeNB based urban scenarios using the expression as presented in (61) through MATLAB simulations. It is visibly witnessed that under variable user distribution scenarios over a certain region, two-tier HetNet is able to provide better ASE, thus may guarantee better QoS within span of 12 hours. Fig. 5.12 justifies the remark which shows comparative analysis of the hour wise Mean-ASE between UDHetNet and traditional MeNB based deployment respectively. The percentage improvements are demonstrated in Fig.5.13. Notably, it is also realized from the above observations that the percentage improvement leads to over 10% from 2 pm to 5 pm between which peak hours lies. This validates the fact that optimal deployment of SeNBs inside a

HetNet can provide significant improvement in the overall ASE of the Network even in the presence of peak tele traffic in dense urban scenarios.

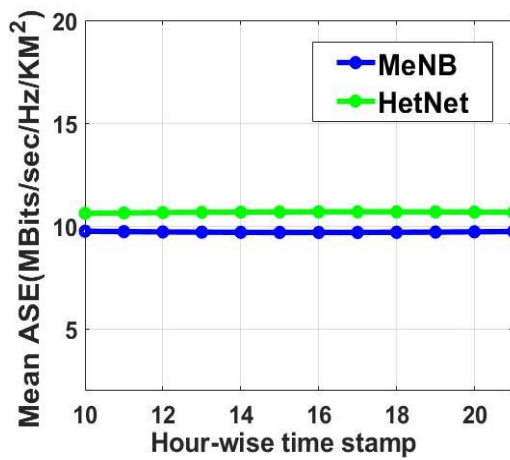


Figure 5.12 Mean ASE: MeNB v/s Two-tier HetNet

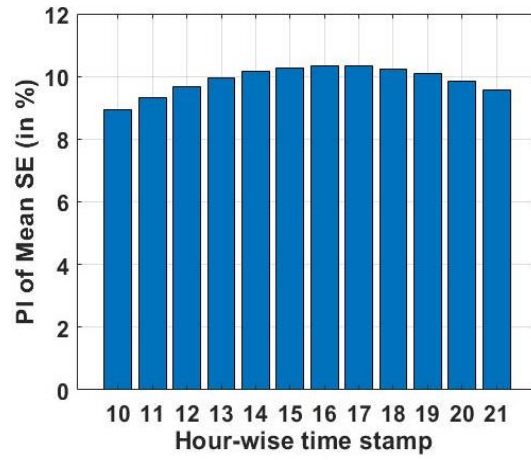


Figure 5.13 Performance Improvement (PI) in ASE Two-tier HetNet over MeNB

## 5.9 Chapter Summary

In this chapter, at first, the HetNet deployment model is developed using NHSCPPP to encounter real time hourly tele traffic Poisson arrival scenario considering the teledensity of 143.6% in Kolkata city. An additional mathematical analysis is also presented by developing simple expressions for downlink SINR, which essentially culminate in deriving the subsequent expression of SE full term. It is observed that deployment of Het-Net clearly outnumbers traditional sole MeNB based network arrangements by spawning approximately 11% performance improvement in SE in peak hours. However, improved SE and the dense deployment of Small cell eNodeBs (SeNBs) predictably because a likely growth in the energy consumption of the overall network. The K-Means clustering is a robust algorithm that classifies a set of NHPPP distributed UEs to a certain number of clusters having a centroid in each. These optimally placed centroids correspond to the location of SeNBs inside a HetNet. Additionally, VRC or CH index is an effective method to determine the optimal density of SeNBs as a subset of HetNet deployment. Further, it is understood from the analytical results that having a known UE distribution scenario, the optimal deployment of SeNBs in terms of both location and density can significantly improve the QoS performance of an urban HetNet over traditional MeNB based scenario in terms of ASE especially during peak hours with maximum traffic load.

## ❖ Publications from this chapter

### ▪ International Conferences

1. **Arijeet Ghosh** and Iti Saha Misra, “A Method of Dynamic Small Cell Deployment in 5G Two-Tier HetNet for Improved Area Spectral Efficiency.” published in 2023 IEEE 8th International Conference on Computers and Devices for Communication, CODEC-2023, on 20<sup>th</sup> March, 2024. **DOI:** [10.1109/CODEC60112.2023.10466153](https://doi.org/10.1109/CODEC60112.2023.10466153)

# **Chapter 6: Developing Sustainable Green Communication Techniques for real time urban teletraffic for Heterogeneous Cellular Network: Extensive Performance Evaluation**

---

## **Outline of this chapter**

- 6.1 Abstract
- 6.2 Introduction
- 6.3 System Model
  - 6.3.1 User arrival modelled by Poisson Arrival Process
  - 6.3.2 Three-Tier Ultra Dense HetNet
- 6.4 Sustainable Green Communication (SGC) Techniques
  - 6.4.1 Power consumption scenario of network elements of HetNet
  - 6.4.2 Introduction to Strategic Sleeping Policy
  - 6.4.3 Energy Harvesting Methodologies
  - 6.4.4 Analytical Model for Performance evaluation
  - 6.4.5 Performance metrics for SGC
- 6.5 Performance Evaluation
- 6.6 Chapter Summary

## **6.1 Abstract**

The demand to avail higher data rates over various mobile platforms has been increasing with the evolution of mobile technology over the past few years. This necessitates the service providers to deploy multi-tier Heterogeneous Networks (HetNet) consisting of densely deployed small cells eNodeB (SeNB) underlying traditional macro cell eNodeB (MeNB). Dense deployment of multitier HetNet or ultra-dense HetNet (UDHN) is the emerging network architecture having improved user handling capacity, higher throughput, and extended coverage. However, ultra-

dense deployment of multi-tier small cells will possibly increase the overall network power consumption which not only shoot up the operating expenditure (OPEX) of the mobile service providers but also consistently intensify the carbon footprint contributed by the telecommunication industry on global climate. Hence in this chapter, we present some efficient Sustainable Green Communications (SGC) techniques for multi-tier HetNets and discuss their impact to avail a sustainable green future. Derived from the comprehensive background survey, we find Strategic Sleeping Policy (SSP) and Energy Harvesting (EH) as two of the most promising solution. Therefore, in this work, primarily, we present the Strategic Sleeping Policy (SSP) of the SeNBs based on M/M/1 queuing theory and investigate its impact in reducing the power consumption of the proposed three-tier UDHN which consists of one tier of Macro eNodeB (MeNB) and two tiers of SeNBs based on performance metrics like Energy Efficiency (EE) and Area Energy Consumption Ratio (AECR). Further, we also introduce a novel Sleep Cycle Modulated Energy Harvesting (SCM-EH) Technique for SeNBs to ensure proper utilization of energy resources. An analytical model based on Continuous Time Markov Chain (CTMC) is also developed to evaluate the Energy Utilization (EU) of the proposed SCMEH method. The comprehensive performance analysis reveals that the implementation of integrated SCMEH enabled SeNBs under HetNet can not only guarantee QoS requirements under concurrent time-varying urban tele-traffic conditions but also ensure Sustainable Green Communication (SGC) by radically controlling the estimated power consumption per hour basis throughout a day.

## 6.2 Introduction

Current trends anticipate that 5G mobile networks will be composed of ultra-dense deployments of heterogeneous Base Stations (BSs) [235], where BSs using different transmission powers coexist to provide the 1000x network capacity increase that is required by 2020. Accordingly, the traditional macro cell layer will be complemented or replaced with multiple overlapping tiers of smaller cells, which extend the system capacity, thanks to higher spatial reuse and to better spectral efficiency. Despite such benefits, researchers have already identified new issues raised by an ultra-dense scenario, such as user association and mobility management, interference management and mitigation, macro cell offloading, and energy saving [231]. Also, 5G

subscribers will be equipped with a large and diverse set of devices and BSs may need to support high-rate mobile equipment (such as smartphones and laptops) [143] as well as a huge number of low-rate devices (such as environmental or wearable sensors) [236], as envisaged by the IoT paradigm. This makes new generation networks challenging to operate, control and monitor. Moreover, such systems are also very demanding in terms of energy consumption from the power grid, due to their high capacity requirements. As a tractable tool for modelling and analysing cellular networks, most of the prior research based on the PPP focused on the standard success (coverage) probability as the performance metric [57, 68, 237]. The coverage probability is the spatial value averaging over the Signal to Interference plus Noise Ratio and the point process. Recently, the Poisson Point Process (PPP) has been widely accepted as the most tractable model to mimic the modern HetNet.

In the previous chapter, we focus on designing  $k$ -tier ultra-dense HetNet (UDHN) architecture using clustered NHPPP. The idea of UDHN is estimated to meet concerns regarding ever-increasing QoS demand generated by modern age multimedia services in 5G networks. Tiered deployment of UDHN not only improves the spectral efficiency but also improves the coverage by bringing the end users nearer to the access nodes [129, 207]. Each entity of a  $k$ -tier HetNet ( $k=3$ , in this case), namely, one tier of Macro eNodeBs (MeNB) and two tiers of SeNBs along with UEs are scattered in a particular two-dimensional NHPPP [221-223]. In urban terrain, the SeNBs are typically deployed where massive data traffic is generated under the footprint of macro cells and/or in the extensions of major cities [207]. Urban SeNBs are classically of two types, namely, Urban Microcell or UMi-SC deployed in the street canyons (SC) and Indoor Hotspots or InH [80]. These small cells are the transmit nodes with lesser transmit power, smaller coverage and smaller user handling capacity, thus differ from the macro cell with respect to path-loss propagation [80, 129].

The modern era blessed with 5G technology is indeed unwrapped new opportunities for individuals as well as organizations. However, the massive use of data-intensive multimedia applications enabled by multi-tier UDHN is also consuming more energy due to the deployment of additional infrastructure. The services enabled by 5G technology come at the expense of a tremendous challenge for the telecommunication sector in terms of both carried data and energy consumption.

In a report of 2013, the Digital Power Group [238] highlighted that the Compound Annual Growth Rate of energy consumption by telecommunication infrastructure was of around 10%. In fact, it is forecasted that 51% of the electricity consumption and 23% of the carbon footprint by human activity will be due to future wireless networks [239]. Hence, any further development in wireless technology and in its infrastructure has definitely to cope with their energy sustainability towards a greener future. Significant reduction in energy consumption through the more flexible design of telecommunication networks entails the need for more sophisticated network planning equipped with energy efficient infrastructure. Considering the aforementioned aspect, the third generation partnership project (3GPP) stakeholders have already called for a 90% reduction in the energy consumption of 3GPP NR compared to 3GPP long term evolution (LTE) [56]. However, whether these gains can be realised or not in practical networks will not only depend on what the new specification can do and/or the energy performance of a single site, but also on how the actual network is deployed and operated as a whole [56].

Hence in this chapter, some significant efforts have been made to reduce the power consumption of the proposed  $k$ -tier UDHN ( $k=3$ ) deployment model. At first, we start with modelling the three-tier UDHN using different SPPs. The distribution of MeNBs is modelled by HPPP. The upper SeNB tier, i.e. UMi SCs are distributed using clustered NHPPP. The novelty of this chapter lies in the fact that the distribution of InH i.e. the third tier of SeNBs is modelled as a particular category of Poisson Cluster Process i.e. Matérn cluster point process (MCP) considering the InHs as cell-free distributed antenna system. Additionally, the power consumption scenario of each network element has been modelled. Then a novel Strategic Sleeping Policy is proposed based on M/M/1 queuing theory for both UMi-SCs and InHs. In addition, this chapter also introduces a novel Sleep Cycle Modulated Energy Harvesting (SCMEH) policy for UMi-SCs and InHs. Further, an analytical model based on Continuous Time Markov Chain (CTMC) is developed for designing metrics for further performance evaluation. The performance of the proposed Het-Net model under the urban traffic arrival scenario is then evaluated based on SGC metrics like Energy Efficiency (EE), Area Energy Conservation Ratio (AECR), and Energy Utilization (EU) in subsection. Simulation results in section 6.5 critically evaluate the performance of proposed SCMEH policy under three tier 5G UDHN under time



varying urban teletraffic conditions to ensure substantial reduction in the power consumption per hour basis throughout a day.

## 6.3 System Model

### 6.3.1 User arrival modeled by Poisson Arrival Process (PAP)

Firstly, the User arrival process within a certain coverage region is considered. From the previous chapter, which is modelled as a one dimensional (1D) PAP [63] considering hourly user arrival scenario of the region of Kolkata bearing the Tele traffic density (percentage of mobile per user) of 143.60 % [240], and population density of 24760 per Square K.M. (as of August 2022) [230].

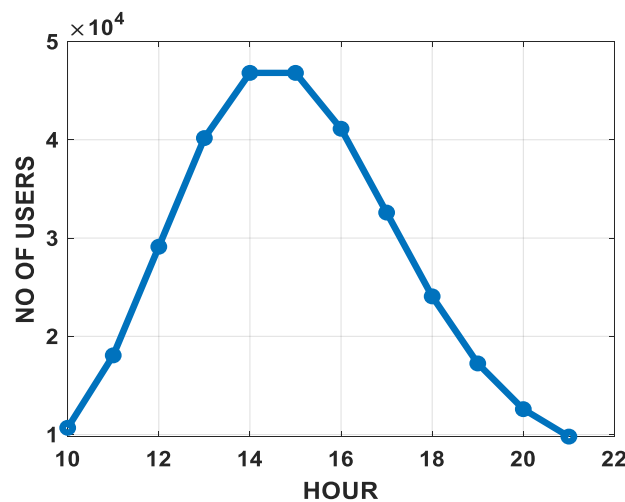


Figure 6.1 shows the hourly estimation of customer arrival process of the city of Kolkata, a test case for Indian urban scenario for a total duration of 12 hours within coverage region (mostly office area) of 7 sq. km through MATLAB simulation.

### 6.3.2 Three-Tier UDHN

The huge amount of teletraffic loads especially in urban regions of the country and necessitates the deployment of adding another tier in the networks deployment architecture and analysis for sustainable improvement in QoS demand. In addition, the idea of UDHN is estimated to meet concerns regarding the propagation losses in 5G networks by indulging the end users to get closer to the access nodes [129, 207].

This realization is accomplished by the co-deployment of both indoor and outdoor small cells in an urban terrain where massive traffic is generated under the footprint of macrocells [207]. Urban small cells are typically of two types, namely, Urban Microcell or UMi-SC deployed in the street canyons (SC) and Indoor Hotspots or InH

[80]. Fig. 4.7 depicts a hypothetical demonstration of a three-tier UDHN. The modelling of three-tier network is sectioned into two segments. Primarily, a two-tier HetNet consisting of UMa underlaid with UMi-SC is modelled using NHPPP followed by optimizing the location of UMi-SCs using K means Clustering. After that, the third tier of access nodes i.e. InH are distributed as a Matérn cluster point process [139] is a type of cluster point process, meaning that its randomly located points tend to form random clusters. Fig 6.2 depicts a hypothetical three-tier UDHN.

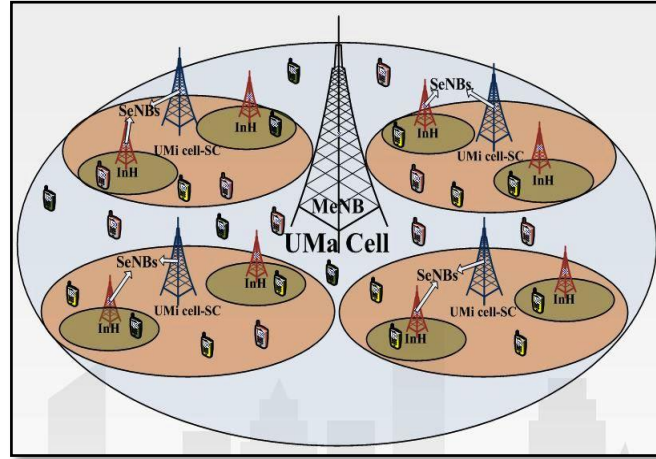


Figure 6.2 A typical three-tier UDHN

In this subsection, at first, a three-tier UDHN is considered where individual tier represents the eNBs of a specific type, such as MeNBs, Mi-eNBs in a two-dimensional finite region  $A \subset \mathbb{R}^2$ .

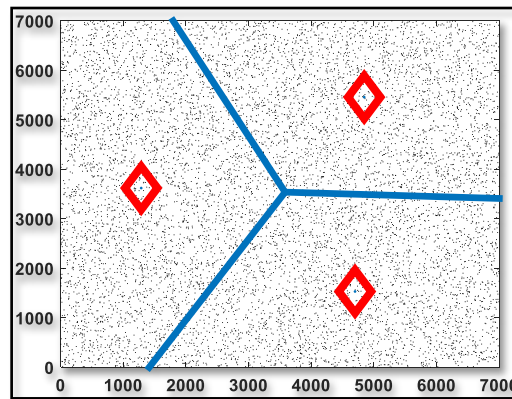


Figure 6.3 Distribution of UMa BY HPPP;  $\blacklozenge$  UMa; — UMa coverage area

- Distribution of UMa BY HPPP

MeNBs are spatially distributed as independent HPPP (as shown in Fig 6.3),  $\Psi_{UMa}$  of density,  $\lambda_{UMa}$ . The number of MeNBs in any finite region  $A \subset \mathbb{R}^2$  denoted as  $N_{UMa}(A)$ , is a random variable with the Poisson distribution [57],

$$\mathbb{P}[N_{UMa}(A) = \eta_{UMa}] = \frac{e^{[-\mu_{UMa}(A)]} \cdot \mu_{UMa}(A)^\eta}{\eta_{UMa}!}, \quad \eta_{UMa} = 1, 2, 3 \dots$$

With mean (rate function)

$$\mu_{UMa}(A) = \lambda_{UMa} \times A \quad (66)$$

- Distribution of UMi

UMi usually deployed in the street canyons are spatially distributed as independent NHPPP,  $\Psi_{UMi}$  of density,  $\lambda_{UMi}$ . The points of the NHPPP associated with each UMi eNBs in the 2<sup>nd</sup> tier in any finite region  $A \subset \mathbb{R}^2$  are symbolized as  $N_{UMi}(A)$ , is a random variable with the Poisson distribution [57],

$$\mathbb{P}[N_{UMi}(A) = \eta_{UMi}] = \frac{e^{[-\mu_{UMi}(A)]} \cdot \mu_{UMi}(A)^\eta}{\eta_{UMi}!}, \quad \eta_{UMi} = 1, 2, 3 \dots$$

With mean (intensity function)

$$\mu_{UMi}(A) = \iint_A \lambda(x, y) dx dy \quad (67)$$

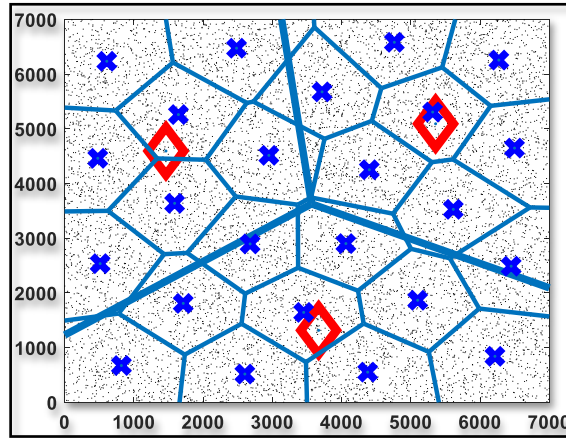


Figure 6.4 Distribution of two-tier HetNet by clustered NHPPP  UMa;  UMa coverage area  UMi-SC;  UMi-SC coverage area

Note that the UEs are also spatially distributed as independent HPPP,  $\Psi_{UE}$  of density,  $\lambda_{UE}$ . Considering each UE that belongs to  $\Psi_{UE}$  as the data points and the positions each UMi in  $\Psi_{UMi}$  as initial positions of the cluster centres, this work implements the k-means clustering algorithm on the top of NHPPP  $\Psi_{UMi}$  to form two-tier HetNet using clustered NHPPP. The details of the process have already been elaborated in subsection 4.4 of the 4<sup>th</sup> chapter. The resulting two-tier HetNet is depicted in Fig 6.4.

- Distribution of InH

The distribution of InH in the hotspot region in an urban environment can be collectively perceived as a cell free distributed antenna system (DAS) [241] around each UMi eNBs belonging to  $\Psi_{UMi}$ . They are also considered as point process  $\Psi_{InH}$  in the same finite region  $A \subset \mathbb{R}^2$  and are distributed as MCPP [139] a special case of Poisson Cluster Process (PCP) because they trace a correlation with elements of  $\Psi_{UMi}$ . For generating a Poisson cluster process consider each  $j_{UMi}^{th} \in \Psi_{UMi}$  is associated with some random but finite set of points  $Z_{j_{UMi}^{th}}$  which are denoted as the offsprings of each parent  $j_{UMi}^{th} \in \Psi_{UMi}$  as depicted in Fig 6.5. The superposition of all such clusters of daughter points yields the cluster point process  $\Psi_{InH} = \bigcup_{j_{UMi}^{th} \in \Psi_{UMi}} Z_{j_{UMi}^{th}}$ . Notably in our work, the parent process  $\Psi_{UMi}$  is a uniformly distributed PPP in the finite region  $A \subset \mathbb{R}^2$  and each cluster  $Z_{j_{UMi}^{th}}$  consists of a random number of points  $z_{InH} \in Z_{j_{UMi}^{th}}$ , where  $z_{InH} \sim \text{Poisson}(\mu_{UMi}(A))$ , is independently and uniformly distributed in the disk  $\Phi(j_{UMi}^{th} \in \Psi_{UMi}, r_{j_{UMi}^{th}})$  of radius  $r_{j_{UMi}^{th}}$  centered on  $j_{UMi}^{th} \in \Psi_{UMi}$ .

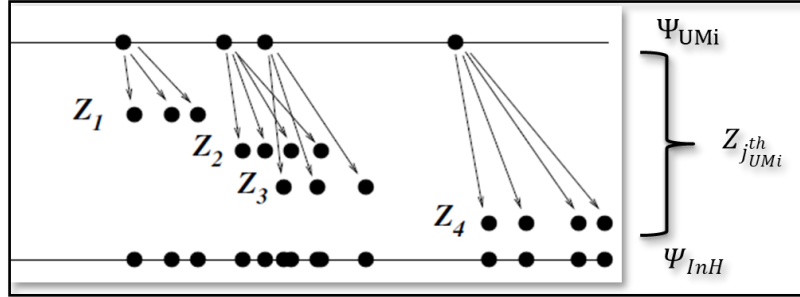


Figure 6.5. Schematic concept of the formation of clusters in MCPP.

Thus the locations of the first tier UMa follow HPPP,  $\Psi_{UMa}$  with rate  $\mu_{UMa}(A)$ , locations of the second tier UMi follow K means clustered NHPPP,  $\Psi_{UMi}$  with intensity,  $\mu_{UMi}(A) = \iint_A \lambda(x, y) dx dy$ , and the locations of the third tier InHs ( $\Psi_{InH}$ ) follows MCPP with density  $\mu_{UMi}(A) \times \overline{\lambda_{InH}}$  whose parent point process is  $\Psi_{UMi}$ . The demonstration of three-tier UDHN is depicted in Fig 6.6. For notational simplicity, we denote  $k \in \{UMa, UMi, InH\}$  as the index of the tier with which a typical user is associated.



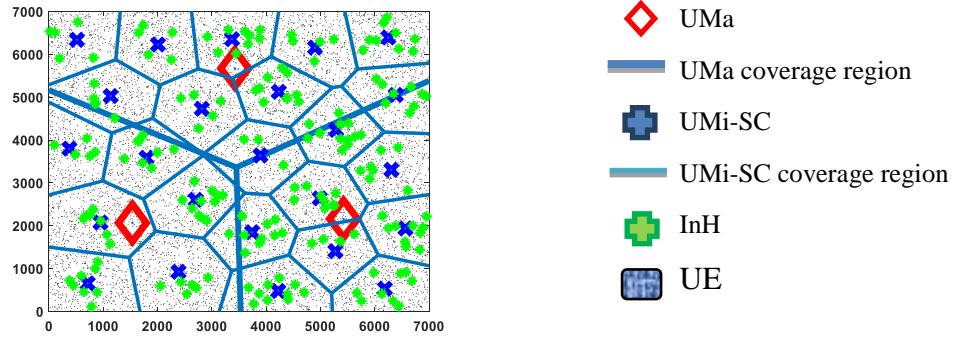


Figure 6.6 Distribution of three-tier UDHN [241]

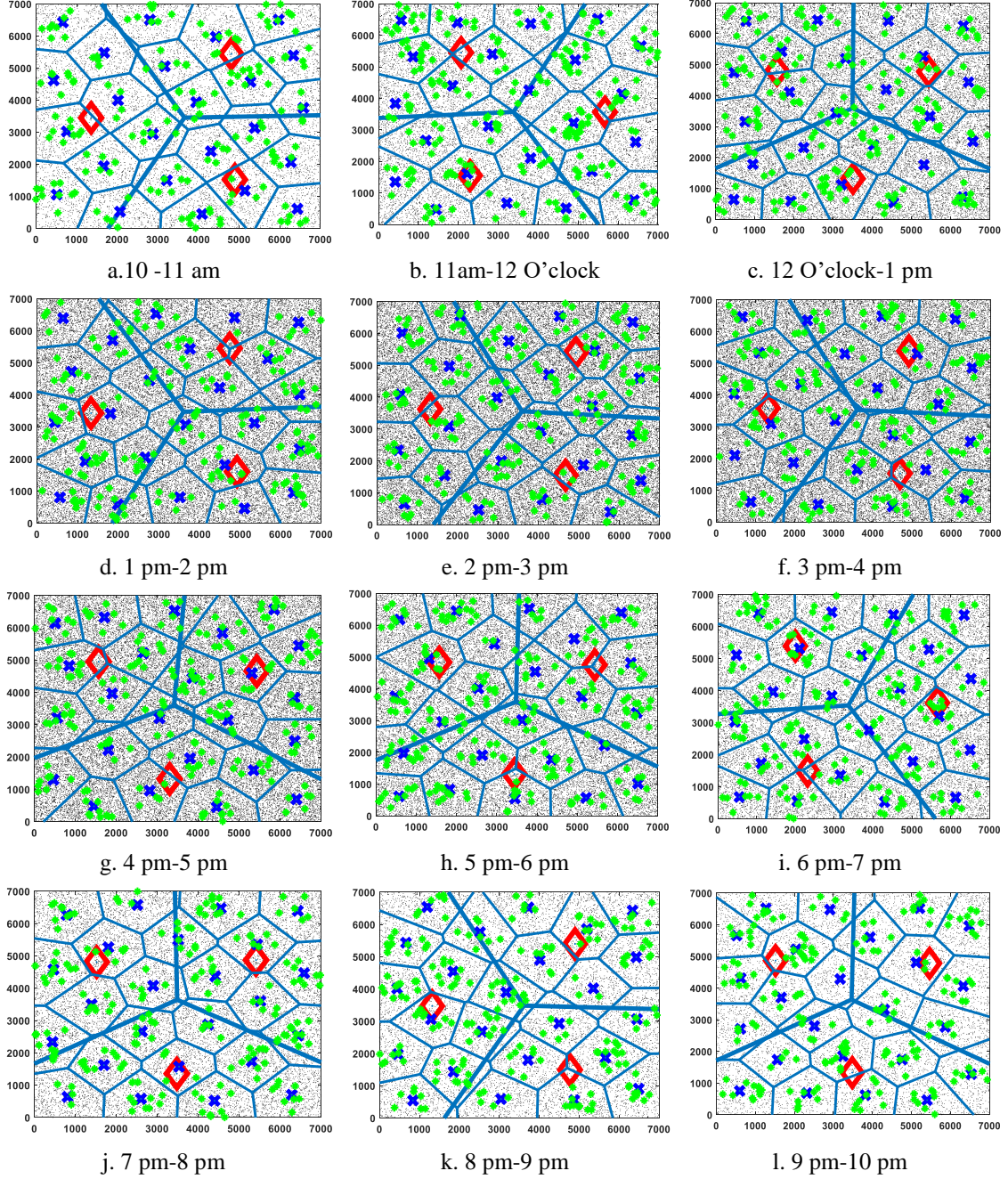


Figure 6.7. Estimated hourly modelling of a Indian Urban Scenario (Kolkata) as Three-tier UDHN modelled by HPPP, NHSCPPP and MCP in a 7000 sq. m geographical area with UE density ~143.38 % considering ratio of MeNB to SeNB density as 1:8

The actual hourly scenarios of two-tier UDHN are portrayed in Fig. 6.7. The main focus of the previous chapter is to find out the optimal density of SeNBs within a two-tier HetNet in the presence of real time hourly user arrival scenario and finally analyse the proposed model in terms of ASE. However, In this chapter, we not only extended the modelling of the network to generate a three-tier UDHN but also present a detailed Energy Efficiency analysis of the said model to evaluate its sustainability in terms of greener communication.

## 6.4 Sustainable Green Communication (SGC) Techniques

In the preceding chapters, urban HetNets (the precursor of UDHN) in general, have been planned aiming to optimize coverage, capacity, spectral efficiency or throughput. Clearly, it is not necessarily expected to deal with anything about energy efficiency. In addition, traditional deployment strategies were mostly intended to withstand peak load and extreme conditions. Thus, at times they encounter redundancy or provide extra capacity, which makes the system underutilized during non-peak hours at the cost of energy drainage. This opens up a new opportunity for investigating possible energy saving techniques, which makes SGC an interesting and technically challenging research field. Therefore, a new deployment paradigm is immediately desirable so that current set-ups will uphold the same level of QoS while decreasing the aggregate energy consumption in the future [235].

Prior to designing SGC techniques for the depicted k-tier UDHN model (Fig 6.7), it is essential to have some prerequisite formulations that will eventually help us to design necessary SGC techniques.

The equation of pathloss models for UMa, UMi-SCs, and InHs (refer to Table 4.2 in Chapter 4) followed by the formulation of SINR traces its root from the previous chapter (Chapter 4). The cumulative SINR at any arbitrary  $i$ th user from  $j^{\text{th}}$  eNB of  $k^{\text{th}}$  tier can be calculated as,

$$\gamma_k(x, y)_i^j = \frac{SNR_k(x, y)_i^j}{\{\sum_{k < K} \sum_{l=1}^{j-1} SNR_k(x, y)_i^l\} + 1} \quad (68)$$

Note that, UE will be served by its strongest access node i.e. the UE will be connected to the eNB that offers best SINR. So, a random  $i$ th UE located at  $(x, y)_i$  served by any  $j$ th eNB belonging to  $\Psi_k$  is considered to be in coverage if:

$$\max_{(x,y)_i \in \Psi_k} \gamma_k(x,y)_i^j > \gamma_k^{th} \quad (69)$$

The Constrained Spectral Efficiency ( $\mathcal{R}$ ) or the estimated network throughput ( $T_p$ ) in following can be formulated as

$$\mathbb{E}[f(\lambda_m, \gamma_k^{th})] = \lambda_m \cdot \mathbb{E} \left[ \left\{ \log_2 \left( 1 + \max_{(x,y)_i^j \in \Psi_k} (\gamma_k(x,y)_i^j) \right) \middle| \bigcup_{k \in K, (x,y)_i^j \in \Psi_k} \gamma_k(x,y)_i^j > \gamma_k^{th} \right\} \right] \quad (70)$$

#### 6.4.1 Power consumption Model of HetNet

Before exploring the methods to make the urban Het-nets energy efficient, we design power consumption models considering all network components. 5G base stations popularly mentioned as eNodeB (eNB) can be classified into two main groups, depending on transmission power and coverage range.

- Urban Macro (UMa): with a transmission power of about 40W for devices with a channel bandwidth of 20 MHz and 80W for LTE-A devices with channel bandwidth of 40 MHz [220]. MeNBs typically range up to a few kilometers.
- Urban Micro (UMi): with transmission power ranging between 0.05W and 6W, SeNBs can be further categorized into UMa-SCs and InHs. UMa-SCs target small to medium zones typically spanning from a few hundred meters up to one kilometer with opaque traffic (hotspots) such as shopping malls, office places, stadiums, or train stations, whereas InHs typically ranging within a few meters are designed to serve smaller areas such as private homes or indoor spaces. UMa-SCs in general can be mounted lampposts or traffic lights for outdoor scenarios because of their small form factor [220].

The power usage at full system load of the different types of eNBs can range from about 6W for anUMi to 1 kW for anUMa [14]. Typically, this power consumption is exhibited as the sum of a static value and a dynamic and load-dependent value [220]:

$$P_c^j = \begin{cases} N_{TRX}^j (P_0^j + \alpha^j P_{out}^j) & 0 < P_{out}^j < P_{max}^j \\ N_{TRX}^j \cdot P_{sleep}^j & P_{out}^j = 0 \end{cases} \quad (71)$$

Where  $j=1, 2$  represents the MeNBs or SeNBs respectively

$N_{TRX}^j$  = number of transmit/receive channels

$P_0^j$  = eNB power consumption at zero Radio Frequency (RF) output power

$\alpha^j$  = slope of the load dependent power consumption curve

$P_{out}^j$  = load-dependent part of the RF output power

$P_{max}^j$  = value of  $P_{out}^j$  at maximum load

$P_{sleep}^j$  = eNB power consumption at no load

Table-6.1 specifies the load dependencies of the different eNB types. The power consumed by an UMa eNB rises more steeply with the increasing traffic load than that of a UMi eNB due to the more powerful power amplifier that UMa eNBs use to cover widespread zones, whereas SeNBs need an amplifier designed for much lower coverage and, as a result, reside lower in energy consumption. Remarkably,  $P_0^j$  represents a significant part of the total energy consumed by any eNB and, due to this reason, in this work, the use of sleep modes have been scrutinized in front of varying traffic arrival scenario throughout the whole day.

<b>Table-6.1. Load dependencies of different types of eNBs [220]</b>				
eNB Type ( $j=1,2,3$ for $j \in k$ )	$P_0^j$ (in Watt)	$P_{max}^j$ (in Watt)	$\alpha^j$	$P_{sleep}^j$ (in Watt)
<b>UMa eNB (<math>j=1</math>)</b>	130	40	4.7	75
<b>UMieNB (<math>j=2</math>)</b>	56	6.3	2.6	39
<b>InH (<math>j=3</math>)</b>	4.8	0.05	8.0	2.9

## 6.4.2 Introduction to Strategic Sleeping Policy

Based on the power consumption model, we adopt power saving modes for UMi-SCs and InHs. Let us consider the UMi-SCs (outdoor small cells) and InHs as a subset of SeNB. We consider two modes of operation. During ‘Always on’ mode, the SeNB is in full operation and consuming maximum power. On the other hand, during sleep mode when the SeNB is in the idle state having no or minimal traffic, only the power supply, backend connection, and generic CPU core will be on. Instead of randomly selecting these sleeping periods this work presents a planned sleeping strategy based on M/M/1 Queuing theory [242] to reduce the unnecessary energy drainage during no traffic hours.

- Strategic Sleeping policy (SSP) for SeNBs:

Consider any eNB from UMi-SCs or any InH as a single server system in which UEs arrive following a Poisson process with rate  $\lambda$  so that the inter-arrival times are i.i.d exponential random variable with mean  $1/\lambda$ . Assume that the service times are i.i.d exponential random variable with mean  $1/\mu$  and inter-arrival times and service times are independent of each other [242].



Let  $N_s(t)$  be the number of customers that are being served at time  $t$  and let  $\tau$  denote the service time. Now if we designate the set of servers to be the system then the Little's formula becomes [242]

$$E[N_s(t)] = \lambda(t)E[\tau] \quad (72)$$

Where,  $E[N_s(t)]$ =Estimated number Busy server in the system.

For a single server system  $N_s(t)$  can only be 0 or 1, so  $E[N_s(t)]$  represents the proportion of the time that the server is busy [242]. If  $p_0 = P[N_s(t) = 0]$  denotes the steady state probability that the system is empty then we can write  $1 - p_0 = \rho = E[N_s(t)] = \lambda(t)E[\tau]$ , i.e, the proportion of the time that the server is busy or in other words proportion of the time a SeNB is in the active state [242]. Consequently,  $(1 - \rho)$  gives the proportion of the time one SeNB is in the idle state [242]. Note that Arrival rate  $= \lambda(t) < \mu(t)$ = Service rate, i.e.,  $\rho < 1$ . Applying SSP, (71) for SeNBs can be rewritten as

$$P_c^{j=2,3} = \begin{cases} T_{TRX}^{j=2,3} \cdot \rho^{j=2,3} \cdot (P_0^{j=2,3} + \alpha^{j=2,3} P_{out}^{j=2,3}) & 0 < P_{out}^{j=2,3} < P_{max}^{j=2,3} \\ T_{TRX}^{j=2,3} \cdot (1 - \rho^{j=2,3}) \cdot P_{sleep}^{j=2,3} & P_{out}^{j=2,3} = 0 \end{cases} \quad (73)$$

Eventually the total power consumption ( $P_{tot}^j$ ) can be derived as,

$$P_{tot}^j = T_{TRX}^{j=1} \cdot \rho^{j=1} \cdot (P_0^{j=1} + \alpha^{j=1} P_{out}^{j=1}) + T_{TRX}^{j=2,3} \cdot \rho^{j=2,3} \cdot (P_0^{j=2,3} + \alpha^{j=2,3} P_{out}^{j=2,3}) + T_{TRX}^{j=2,3} \cdot (1 - \rho^{j=2,3}) \cdot P_{sleep}^{j=2,3} \quad (74)$$

Where,  $T_{TRX}^{j=2,3}$  = total operational period for UMi-SCs or InHs

#### 6.4.3 Energy Harvesting Methodologies

Energy harvesting models play key roles in improving energy efficiency of modern day wireless networks [183, 184]. In this work, we mainly focus on designing a novel energy harvesting model for UMi-Sc and InH, namely, SCMEH that enables user admission into the network.

In the SCM-EH model, the necessary energy required to endure data transmission is harvested during the time when any UMi-Sc or InH is in sleep mode such that the harvesting mechanism doesn't affect data transmission cycle. The SCM-EH model of the three-tier UDN will be analysed in this section. The working period of the any eNB from two small cell tiers is assumed as  $T_{TRX}^{j=2,3}$ . The working period is divided into two parts, which are energy harvesting ( $T_{EH}$ ), information transmission reception

( $T_{INF}$ ). Considering the eNB as a single server system, it is well elaborate in the previous section that  $\rho$  is the proportion of the time that the server is busy or in other words, proportion of the time a SeNB is in the active state [242]. Consequently,  $(1 - \rho)$  gives the proportion of the time one SeNB is in the idle state [242]. Hence, the proportion of the energy harvesting time in whole period is  $(1 - \rho)$ . During the period of energy harvesting, the serving UMi-SC eNB or InH harvest energy from the electromagnetic wave transmitted by UMa eNB. The generalised notion of the time slot allocation is demonstrated in Fig.6.8.

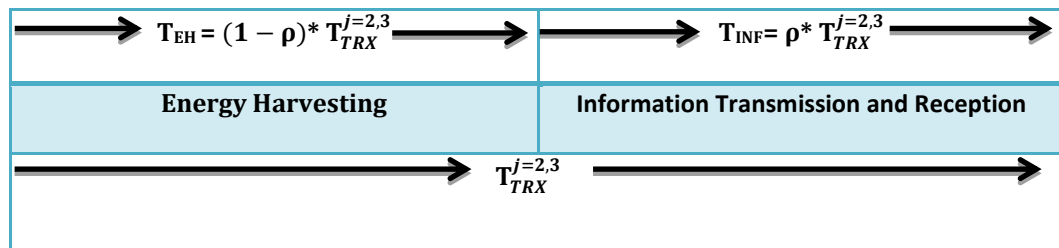


Figure. 6.8 Time slot allocation of Serving Small cell eNBs.

The energy harvested by the serving node in the energy harvesting time can be expressed as follows:

$$E_{EH}^{j=2,3} = P_k^{rx}(x, y)^{j=2,3} \times (1 - \rho) * T_{TRX}^{j=2,3} \quad (75)$$

Fig.6.9 represents protocol of energy harvesting for one serving eNB of two consecutive time slots. The entire operation period is subdivided into  $n$  numbers of time-frames. Here each time-frame consists of seven time slots. The distribution of  $T_{EH}$  and  $T_{INF}$  within a time slot is not deterministic rather they depend upon the value of  $(1 - \rho)$  and  $\rho$  respectively with in a frame. The serving eNB chooses the time slot for energy harvesting when it is in idle mode and transmits information in the other time slots when it is in active mode.

Frame 1							Frame 2						
$T_{EH}$	$T_{INF}$	$T_{INF}$	$T_{EH}$	$T_{INF}$	$T_{INF}$	$T_{INF}$	$T_{EH}$	$T_{EH}$	$T_{INF}$	$T_{INF}$	$T_{INF}$	$T_{EH}$	$T_{INF}$

Figure. 6.9 The protocol of energy harvesting for one SeNB

The time complexity of the proposed SCMEH algorithms can be realised by estimating the loops of the algorithm. However, in our research, the time complexity is calculated for best and worst case scenario. The best case time complexity of our proposed SCMEH algorithm will be  $O(N_{UE}(A) \times 1) = O(N_{UE}(A))$ , considering the

best case scenario where all the UEs are accommodated in one urban macro base station. Note that The number of UEs in any finite region  $A \subset \mathbb{R}^2$  denoted as  $N_{UE}(A)$ , is a random variable with the Poisson distribution [6],

$$\mathbb{P}[N_{UE}(A) = \eta_{UE}] = \frac{e^{[-\mu_{UE}(A)]} \cdot \mu_{UE}(A)^\eta}{\eta_{UMa}!}, \quad \eta_{UE} = 1, 2, 3 \dots$$

$$\text{With mean (rate function) } \mu_{UE}(A) = \lambda_{UE} \times A \quad (76)$$

However, the worst-case time complexity of our proposed SCMEH algorithm will be  $O(N_{UE}(A) \times N_{UMa}(A) \times N_{UMi}(A) \times N_{InH}(A))$  where  $N_{UMa}(A)$ ,  $N_{UMi}(A)$ ,  $N_{InH}(A)$  are the random variables representing the numbers of Urban Macros, Urban Micros and Indoor Hotspots respectively in any finite region  $A \subset \mathbb{R}^2$ .

---

**Algorithm 2 Connection Allocation through SCMEH Technique for SeNBs**

---

**function** = *SCMEH*( $E_{tot}$ )

Initialize,

$M$  = No of UMa eNBs

$S_{UMi-SC}$  = No of UMi-SC eNBs

$S_{InH}$  = No of InHs

$E_{tot}$  = total available Energy

\*\Allocation of Energy Blocks to UMa eNB and SeNBs.\*\

$AVL\_EN_{\Phi_{j=1}} = (\frac{E_{tot}}{2})/M$  \*Initially Available energy at UMa eNBs \*\

$AVL\_EN\_int_{\Phi_{j=2}} = (P_c^{j=2} | T_{TRX}^{j=2} = 1 \text{ hour})$  \*Initially Available energy at UMi-SC eNBs \*\

$AVL\_EN\_int_{\Phi_{j=3}} = (P_c^{j=3} | T_{TRX}^{j=3} = 1 \text{ hour})$  \*Initially Available energy at InHs \*\

$AVL\_EN_{\Phi_{j=2}} = (AVL\_EN\_int_{\Phi_{j=2}} + E_{EH}^{j=2})$  \*Actual energy at UMi-SC eNBs after EH \*\

$AVL\_EN_{\Phi_{j=3}} = (AVL\_EN\_int_{\Phi_{j=3}} + E_{EH}^{j=3})$  \*Actual Available energy at InHs after EH \*\

Where,  $1 \leq m \leq M$  \*No of UMa eNBs \*\

Where,  $1 \leq s_{\Phi_{j=2}} \leq S_{UMi-SC}$  \*No of UMi-SC eNBs \*\

Where,  $1 \leq s_{\Phi_{j=3}} \leq S_{InH}$  \*No of InHs \*\

**for**  $i = 1$  to maximim no of users

**for each** MeNB 'm'

Initiate energy request for connection 'i' ( $E_{REQ}^i$ )

Calculate  $SINR_{\Phi_{j=1}}^{th}$ ,  $SINR_{\Phi_{j=1}}^{im}$  & Check whether  $SINR_{\Phi_{j=1}}^{um} > SINR_{\Phi_{j=1}}^{th}$

If **true** then check whether  $AVL\_EN_{\Phi_{j=1}} \geq E_{REQ}^i$  & allow Connection 'i'

---

---

```

such that  $AVL\_EN_{\Phi_{j=1}} = AVL\_EN_{\Phi_{j=1}} - E_{REQ}^i$ 

else

  for each UMi-SC eNBs ' $s_{\Phi_{j=2}}$ '

    Calculate  $SINR_{\Phi_{j=2}}^{th}, SINR_{\Phi_{j=2}}^{is}$  & Check whether  $SINR_{\Phi_{j=2}}^{is} > SINR_{\Phi_{j=2}}^{th}$ 

    If true then check whether  $AVL\_EN_{\Phi_{j=2}} \geq E_{REQ}^i$  & allow Connection 'i'

    such that  $AVL\_EN_{\Phi_{j=2}} = AVL\_EN_{\Phi_{j=2}} - E_{REQ}^i$ 

  else

    for each InHs ' $s_{\Phi_{j=3}}$ '

      Calculate  $SINR_{\Phi_{j=3}}^{th}, SINR_{\Phi_{j=3}}^i$  & Check whether  $SINR_{\Phi_{j=3}}^i > SINR_{\Phi_{j=3}}^{th}$ 

      If true then check whether  $AVL\_EN_{\Phi_{j=3}} \geq E_{REQ}^i$  & allow Connection 'i'

      such that  $AVL\_EN_{\Phi_{j=3}} = AVL\_EN_{\Phi_{j=3}} - E_{REQ}^i$ 

    else

      reject connection 'i'

    endif

  end of for

endif

end of for

end if

end of for

end of for

end function

```

---

#### 6.4.4 Analytical Model for Performance Evaluation

In this section, a CTMC [202] based analytical model is developed to evaluate the readiness of the performance metrics. The Markov model is chosen here as it establishes the probability of being in a given state at a given point of time, as well as the expected number of transitions between states upon the admission or rejection of a connection 'i'. Note that an eNB either admits or rejects one connection at a certain instant in time.

Fig. 6.10 reveals the general notion of the Markov Chain. In this work, the states of each eNB are modelled as a separate one dimensional Markov Chain. State  $s = (u_i)$  represents that the BS has currently admitted  $u_i$  number of connections under one per

eNB. The BS will be in a particular State  $s = (u_i)$  until a new connection is admitted into the network or an ongoing connection is terminated. The arrival process of newly originated connection is considered to be Poisson with rates  $\lambda_i$  and the service time of the same is exponentially distributed with mean  $1/\mu_i$  respectively.

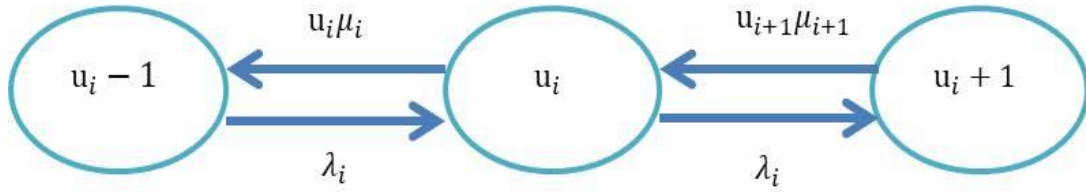


Figure 6.10 Generalized State Transition Diagram of the Markov chain Model for EH analysis

The state space  $S$  for our proposed connection allocation scheme powered by proactive/reactive EH is obtained based on the following equation.

$$S = \{s = (u_i) | (u_i, E_i \leq E)\} \quad (77)$$

From Fig. 6.10, it is observed that every state  $s = (u_i)$  in state space ‘ $S$ ’ is accessible from every other state i.e. each state communicates with other states in the state space ‘ $S$ ’. Therefore, the state space ‘ $S$ ’ forms a bounded set and the Markov chain obtained is irreducible. Let the steady state probability of the state  $s = (u_i)$  is represented by  $\Pi_{(u_i)}$ . The state balance equation of state ‘ $s$ ’ is given as,

$$\begin{aligned} \{\lambda_i \cdot \varphi_{(u_i+1)} + u_i \mu_i \cdot \varphi_{(u_i-1)}\} \cdot \pi_{(u_i)} &= \lambda_i \cdot \varphi_{(u_i-1)} \pi_{(u_i-1)} + (u_i + 1) \cdot \mu_i \cdot \varphi_{(u_i+1)} \pi_{(u_i+1)} \\ \text{Where, } \varphi_{(u_i)} &= \begin{cases} 1, & (u_i) \in S \\ 0, & \text{Otherwise} \end{cases} \end{aligned} \quad (78)$$

Here,  $\varphi_{(u_i)}$  represents the characteristic equation. By using (78), the state balance equations of each state in the state space ‘ $S$ ’ are obtained. Solutions of these equations provide the steady state probabilities of all states in the state space  $S$  with the normalized condition imposed by (79).

$$\sum_{s \in S} \Pi_{(u_i)} = 1 \quad (79)$$

#### 6.4.5 Performance metrics for SGC

With a motive to analyse the effectiveness of Het-nets deployment and their respective energy saving methodologies to achieve SGC, different performance metrics are used in this work. Energy consumption metrics can be broadly written off

into two categories [43]: Absolute metrics and Comparative metrics. Energy efficiency, Energy Consumption ratio are some of the familiar absolute metrics in many of the literature.

- Energy Efficiency (EE) (in bps/kilo-watt): EE aims to put a figure on energy savings at the macrocell area in an heterogeneous network as well as small cells as the 2nd tier and is given as [43, 159].

$$EE = \frac{\text{Network Throughput}}{\text{Network Power Consumption}} = \frac{\mathcal{R}}{P_{tot}^j} (\text{Mbits/Joule}) \quad (80)$$

- Area Energy Consumption Ratio (AECR) (in kilo-watt/bps/km<sup>2</sup>): AECR is defined as the ratio of the network consumption to the system throughput calculated per square km coverage area ( $\Pi$ ) [85]. The metric  $\mathcal{R}$  and  $P_{tot}^j$  is derived from eq. (70) and (74) respectively.

$$AECR = \frac{\text{Total Power Consumption}}{\text{Average Rate} * \text{Coverage Area}} = \frac{P_{tot}^j}{\mathcal{R} * \Pi} (\text{KWH.MBPS}^{-1}.\text{KM}^{-2}) \quad (81)$$

Beside these absolute metrics, this work also introduces one important relative metrics for comparative performance analysis.

- Energy Utilization (EU): The EU is defined as the ratio of total Energy consumed for successful connection admission to the total available energy of the system [183]. EU can be obtained as follows:

$$EU = \frac{\sum_{s \in S} (u_i \cdot E_i) \pi(u_i)}{E_{tot}} \quad (82)$$

## 6.5 Performance Evaluation

The analytical results direct that lower energy requirement of SeNBs in a three-tier UDHN reduces the energy consumption. However, the proposed SCMEH methodology proposed in this work provided a sustainable solution to reduce energy consumption even further while maintaining its QoS specifications intact. In the second part of this section, we have emphasized upon critically analysing the performance of SCMEH based SGC solutions based on some absolute and comparative performance metrics as well. Further investigation also shows that modulating EH interval in sync with the sleep cycles of SeNBs (both UMi-SCs, and InHs) produces the best outcome with an aim to accomplish SGC.

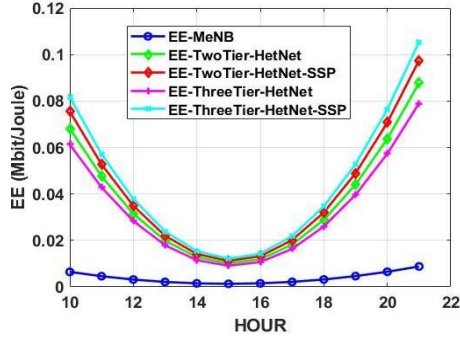


Figure 6.11. Comparative EE analysis (hour-wise)

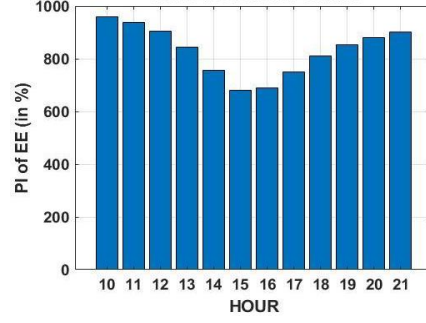


Figure 6.12. Performance Improvement w.r.t EE: Het-Net v/s MeNB in %

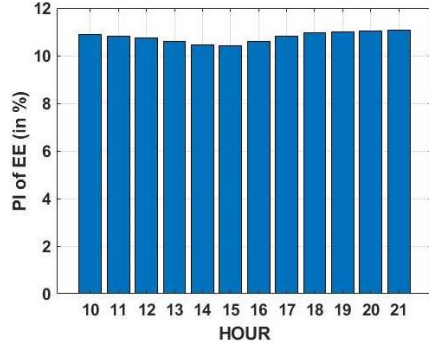


Figure 6.13. Performance Improvement w.r.t EE: Two-tier Het-Net-SSP v/s Two-tier Het-Net (w/o SSP) in %

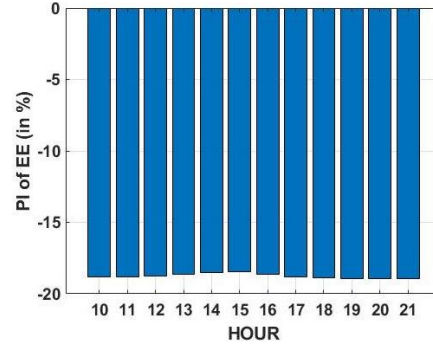


Figure 6.14 Performance Improvement w.r.t EE: two-tier HetNet-SSP v/s three-tier UDHN w.r.t EE in %

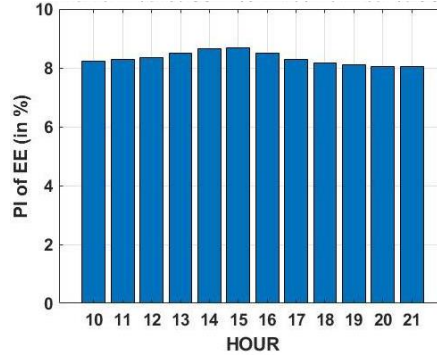


Figure 6.15 Performance Improvement w.r.t EE: three-tier UDHN-SSP v/s two-tier HetNet-SSP w.r.t EE in %

- Hour-wise comparative performance analysis of proposed SSP to achieve sustainable green communication Technique under Indian Urban context:

In this subsection, we primarily focus upon hour-wise comparative performance analysis between traditional MeNB based scenario, two-tier Het-Net (Fig. 5.11 of Chapter 5) and three-tier UDHN considering urban scenario (as shown in Fig 6.7) in terms of aforementioned absolute SGC metrics. Further, the numerical results also examine the impact of employing the proposed SSP on the top of two-tier HetNet and three-tier UDHN. The x-axis level in Fig (6.11- 6.20, 21, 23, 25, 27, 28, 29, 30) which ranges from 10 to 21 is adopted to represent the time stamp on a particular day at

which users arrive into the network in accordance with PAP based user arrival model depicted in Fig. 6.1

- Comparative performance analysis with respect to EE (in Mbps/Joule):

Numerical results shown in Fig. 6.11-6.15 leads us to the fact that the introduction of two-tiers of SeNBs (UMa-SCs and InHs as additional network element) consumes much less power compared to traditional larger MeNBs by the virtue of less load dependencies (as shown in Table 6.1). This makes them a better choice to make the network energy efficient as well. Hour-wise performance improvements based on EE metric between traditional MeNB (denoted by blue line plot in Fig 6.11) and two-tier HetNet (in %) (denoted by green line plot in Fig. 6.11) implicates that during peak hours near about 900% improvement in EE is achieved. However, during non-peak hours (viz. 21 pm) the percentage improvement reduces near 700% (see Fig.6.12). The proposed SSP of SeNBs in two-tier HetNet deployment addresses this issue and improves the EE largely during non-peak hours under lower traffic conditions as shown by red line plot in Fig. 6.11. The maximum percentage improvement of Het-Net with SSP than Het-Net without SSP reaches up to approximately 11% during 10 am in the morning and 21 pm in the evening as shown in Fig 6.13.

The addition of the third tier of SeNBs i.e. InHs distributed as MCP around each UMi-SC eNBs improves the Spectral Efficiency of the overall network as they bring the network nearer to the user. In addition, implementation of 5G FR2 i.e. (24.5-28.6) GHz as operating frequency in InHs paves the way for higher throughput as InH are debarred from the grasp of wall penetration loss (refer to table 4.2) by creating LoS links between the end user and itself. The detailed analysis regarding this issue has been duly included in subsection 4.8.4 of chapter 4.

However, the inclusion of another tier of eNBs i.e. InHs inevitably increases the overall power consumption leading to a subsequent reduction in the EE performance of the three-tier UDHN as shown by the magenta colour line plot in Fig 6.11. It is observed from Fig 6.14 that implementation of three-tier UDHN leads to 19% reduction in EE performance peak hours and an 18% reduction in non-peak hours as compared with two-tier HetNet with SSP due to continuous signalling overheads as the InHs are considered to be deployed as the so-called cell free coordinated multipoint distributed antenna system. Hence proper SSP need to be incorporated in



the InH tier also to achieve the best performance in terms of EE. It is observed from Fig 6.11 that implementation of SSP in both the small cell tiers i.e. in UMi-SCs and in InHs leads to the most improved EE performance as depicted by Fig 6.15. A maximum of 8% performance has been observed in three-tier UDHN with SSP during peak hours when compared to two-tier HetNet with SSP.

- Comparative performance analysis with respect to AECR (in KWH/Mbps/KM<sup>2</sup>):

AECR being an inclusive SGC metric containing all three factors viz. bit rate, Energy consumed and total coverage area provides a holistic impression about an emerging SGC solution. As the previous metric Fig. 6.16-6.20 envisages that the three UDHN with SSP will provide better AECR than the sole MeNB based traditional network. It is perceived that the low power requirement of SeNBs contributes significantly in improving the AECR.

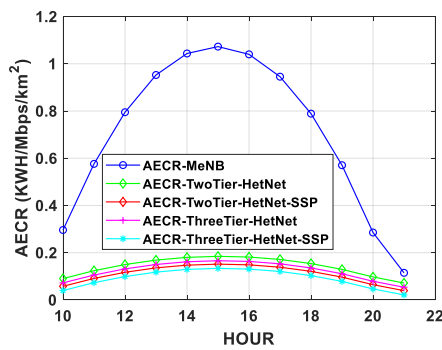


Figure 6.16. Comparative AECR analysis (hour-wise)

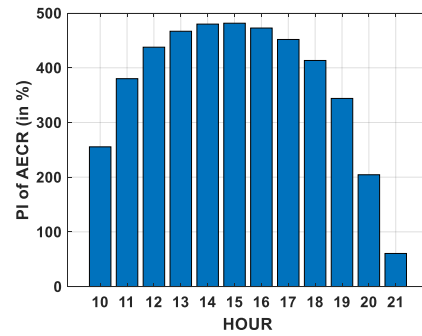


Figure 6.17. Performance Improvement w.r.t AECR: Het-Net v/s MeNB in %

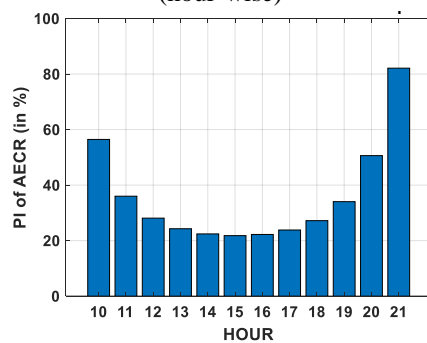


Figure 6.18. Performance Improvement w.r.t EE: two-tier Het-Net-SSP v/stwo-tier Het-Net (w/o SSP) in %

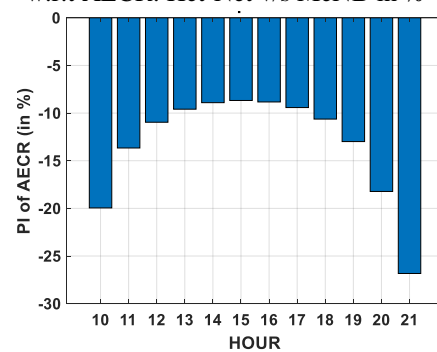


Figure 6.19 Performance Improvement w.r.t EE: two-tier HetNet-SSP v/s three-tier UDHN in %

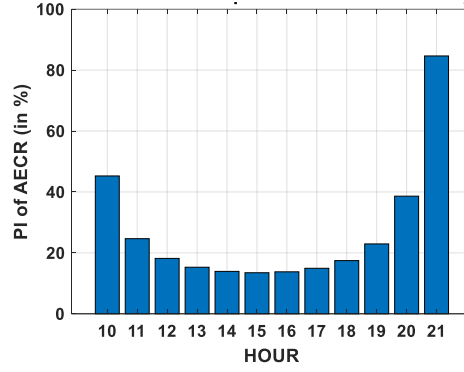


Figure 6.20 Performance Improvement w.r.t EE: three-tier UDHN-SSP v/stwo-tier HetNet-SSP in %

Fig. 6.17 displays that during peak hours (at 2 pm) the AECR performance (in %) of two-tier HetNet rallies up to 600% and during non-peak hours (at 21 pm) lower down to 200 %. However, the percentage comparisons between two-tier HetNet with SSP and without SSP (as shown in Fig. 6.18) foresee that the proposed SSP enabled SeNBs within HetNet improves the AECR with a better success rate reaching up to approximately another 90%, especially during non-peak hours (at 21 hours). However, the AECR performance of a three-tier UDHN degrades than that of a two-tier HetNet due to cumulative signalling overhead in a coordinated multipoint deployment pattern of InHs as shown in Fig 6.19. Nevertheless, the implementation of SSP in three-tier UDHN is able to attain more than 80% (depicted in Fig. 6.20) improvement in AECR with its closest competitor i.e. two-tier HetNet with SSP.

The numerical results and their subsequent performance analysis in the aforementioned paragraphs clearly implicate that deployment of three-tier UDHN will definitely emerge as a better choice than traditional MeNB based deployment and two-tier HetNet in encountering abundant urban traffic by not only ensuring guaranteed QoS (in terms of SE) but also leading with an adequate margin in accomplishing SGC (in terms of EE and AECR). Further, it is also observed that implementation of SSP on small cell tiers makes the UDHN more competent explicitly during non-peak hours making the network resources utilized in a wiser manner which leads us to a stage where analysing the utilization of the proposed three-tier UDHN in terms of relative SGC metric (i.e. Energy Utilisation) have become inevitable. Additionally, we will also show that implementation of the proposed SCM-EH technique in accordance with SSP in three-tier UDHN will improve the Energy Utilisation (EU) of the network even further.

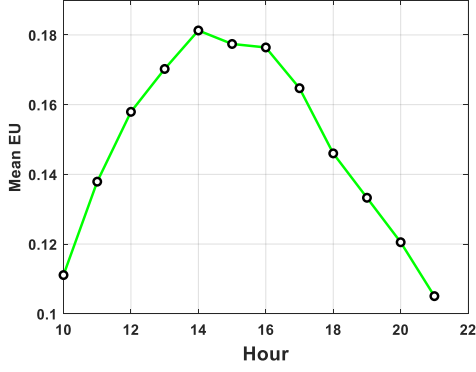


Figure 6.21. Hourly Mean EU of Traditional MeNB

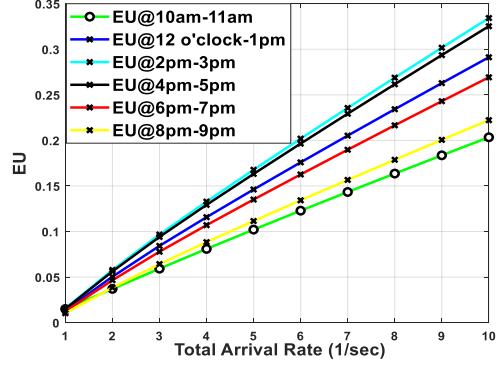


Figure 6.22. Two hourly EU variation in Traditional MeNB

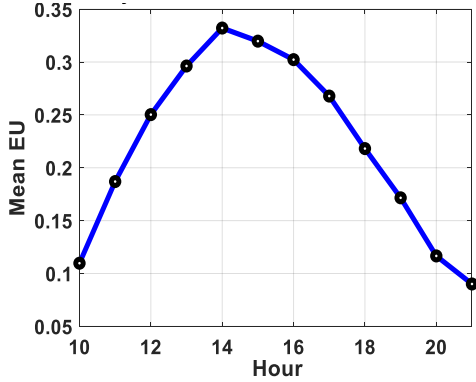


Figure 6.23. Hourly Mean EU of three-tier UDHN with deterministic energy allocation (DEA)

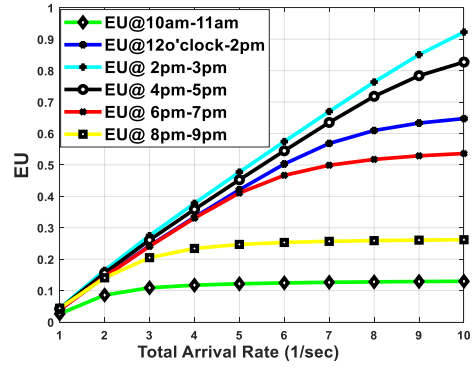


Figure 6.24. Two hourly EU variation in three-tier UDHN with DEA

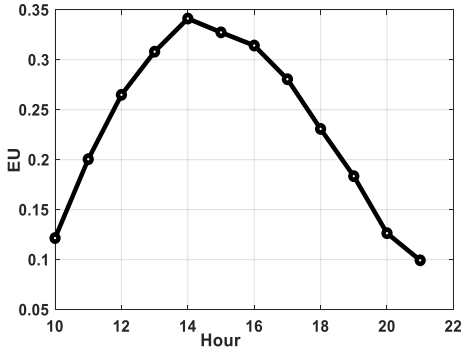


Figure 6.25. Hourly Mean EU of three-tier UDHN with SCM-EH

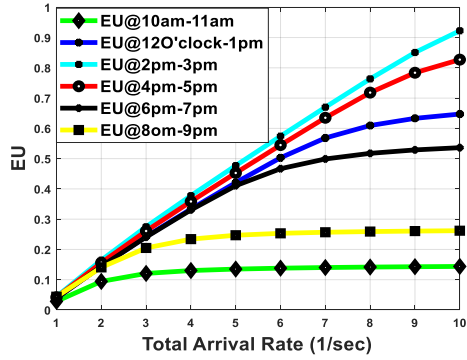


Figure 6.26. Two hourly EU variation in three-tier UDHN with SCM-EH

- Hour-wise comparative performance analysis of SCMEH techniques in three-tier UDHN under Indian Urban context:

Here in this subsection, we demonstrate the numerical performance of three-tier UDHN under the umbrella of proposed EH technique i.e. SCMEH policy, in which the required energy is harvested by serving SeNBs (UMi-SC, and/or InH) during sleep cycle of the respective serving nodes. Numerical analysis of traditional MeNB based networks and three-tier UDHN with energy allocation in a predetermined fashion has been done to realize the comparative performance analysis.

Fig 6.22, Fig 6.24, and Fig 6.26 show the hourly EU of Sole MeNB based network, three-tier UDHN with deterministic energy allocation (DEA) to the two tiers of SeNBs, and three-tier UDHN with proposed SCM-EH policy i.e. integrated SSP and EH respectively. In those figures, the EU plots are demonstrated based on two hours apart to avoid congestion in the visualization. However, Fig.6.21, Fig.6.23, and Fig.6.25 that contain the hourly mean EU for Sole MeNB based network, three-tier UDHN with DEA to the two tiers of SeNBs, and three-tier UDHN with proposed SCMEH policy respectively, establishes the fact that during peak hours (around 2 pm) all the scenarios sustain with better EU and lagging behind during non-peak hours (around 10 am of 9 pm).

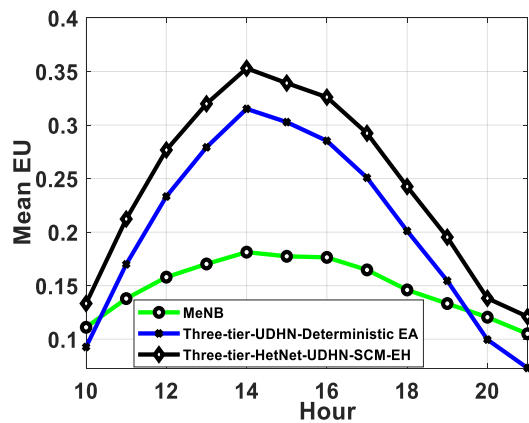


Figure 6.27. Comparative analysis of Mean EU: MeNB v/s UDHN-DEA vs UDHN-SCM-EH

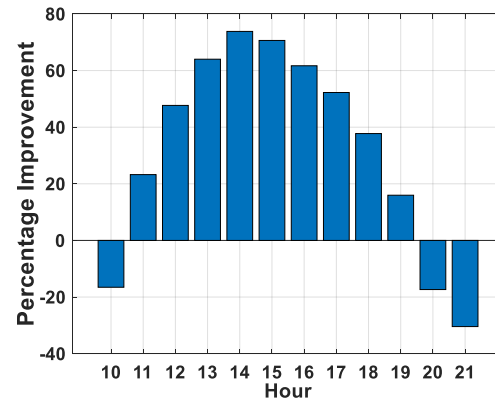


Figure 6.28. Performance Improvement (in %) of three-tier UDHN with DEA over MeNB w.r.t Mean EU

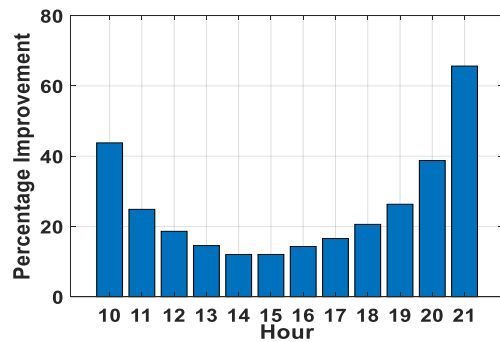


Figure 6.29. Performance Improvement (in %) of three-tier UDHN with SCM-EH over three-tier UDHN with DEA w.r.t Mean EU

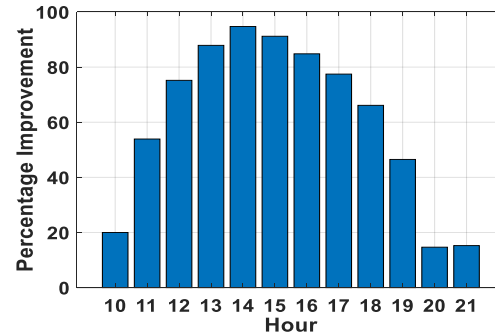


Figure 6.30. Performance Improvement (in %) of three-tier UDHN with SCM-EH over MeNB in w.r.t Mean EU

However, the comparative analysis (as shown in Fig. 6.27) among the above scenarios reveals some interesting observations. Fig. 6.28 which presents the percentage improvement of mean EU between sole MeNB based scenario and three-tier UDHN with DEA exhibits that three-tier UDHN with DEA in which the estimated required energy is allocated to the SeNBs well before initiation of user admission in a

predetermined fashion performs fairly well providing a maximum improvement of 73.82% in terms of Mean EU during peak hours (around 2 pm) but falls behind up to approximately 30.43% during non-peak hours (around 9 pm) due to less amount of inward traffic in those time intervals keeping the serving nodes in ‘ON’ or active mode for entire interval of communication. Having realized the significant concern, we propose the EH modulated by the sleeping strategies of the serving SeNBs scheme within the purview of the three-tier UDHN with acts in sync with the strategic sleeping modes of the serving nodes and harvests energy from the RF broadcast signal from UMa eNBs only during the sleeping interval. The process of SCM-EH is demonstrated in subsection 6.4.3.

Percentage improvements shown in Fig. 6.29 clearly validate that three-tier UDHN implemented with SCMEH stands superior in utilizing energy ensuring approximately 12.02% improvements in peak hours (around 2 pm) and 65.65% in non-peak hours (around 9 pm) than three-tier UDHN with deterministic energy allocation (DEA). The integration of SSP with EH addresses this issue and thereby brings novelty in ensuring an improved EU with an aim to meet the criteria for SGC. Finally, Fig. 6.30 visibly validates that the three-tier UDHN driven by SCM-EH policy in small cell tiers ensures superior EU than traditional MeNB based network throughout the entire time interval irrespective of the variability of peak (94.72% improvement in Mean EU) or non-peak hours (20% improvement in Mean EU).

## 6.6 Chapter Summary

This chapter analyses the performance of aforementioned network arrangements in terms of achieving SGC full term based on performance metrics viz. EE and AECR and EU. Simulation results validate that deployment of low powered SeNBs produces significant improvements in both the SGC metrics, especially in the peak hours. However, during non-peak hours due to less or no traffic condition, the proposed deployment scenarios often end up underutilizing available energy resources. To improve the performance even during non-peak hours, implementation of SCMEH in small cell tiers (i.e. UMi-SCs and InHs) of three-tier UDHN and their integrated execution in the later stage are proposed. Simulation results and performance evaluations shown in section 6.5 advocate that the implementation of SCMEH enabled SeNBs (both UMi-SCs and InHs) under three-tier UDHN can not only

guarantee QoS requirements under concurrent time varying urban teletraffic condition but also achieves significant improvement EE metrics as well as EU (approximately 94% during peak hours and 20% during non-peak hours) compared to traditional sole MeNB based network architecture, hence ensuring SGC by profoundly regulating the estimated power consumption per hour basis throughout a day.

### ❖ Publications from this chapter

- **SCI Indexed Journal**

1. Arijeet Ghosh, and Iti Saha Misra, “Enabling Sustainable Green Communication in Three-tier 5G Ultra Dense HetNet with Sleep Cycle Modulated Energy Harvesting” accepted in Wireless Network, Springer on 3<sup>rd</sup> May, 2024.

- **IEEE International Conference**

1. Arijeet Ghosh and Iti Saha Misra, “A Novel Sleep Cycle Modulated Energy Harvesting policy for Three Tier 5G Ultra Dense HetNet.” published in 2023 IEEE 8th International Conference on Computers and Devices for Communication, CODEC-2023, on 20th March, 2024. DOI: 10.1109/CODEC60112.2023.10465752

# Chapter 7: Conclusion & Future Scope

---

## Outline of this Chapter

7.1 Conclusion

7.2 Future Scope

## 7.1 Conclusion

Wireless technologies have experienced a great course of evolution from the first generation (1G) to the present fifth generation (5G) of wireless standards due to the increase in mobile devices with personified multimedia services such as voice over Internet protocol (VoIP), video streaming, internet surfing, and online gaming, etc. and subsequent user mobility support. The nature of these applications has stringent QoS requirements constraints. Until 4G, all the major technology operated in the sub 6 GHz band, and hence proper utilisation of available bandwidth remained as the most discussed topic between 2010 to 2020. To support various integrated communication services, radio resource management (RRM) such as Call Admission Control (CAC), and Dynamic Bandwidth Allocation (BA) techniques have become key methods to provide the desired Quality of Service (QoS) in such resource-constrained wireless networks or to increase utilization. CAC algorithms are employed to ensure that the admittance of a new call into a resource-constrained network does not violate the service level agreements guaranteed by the network to ongoing calls. CAC algorithms are essential to provide different priorities among service classes supported, achieve low call blocking probability (CBP), and increase network utilization.

The primary solution to the aforementioned issue proposed in *Chapter 3* of this thesis attempts to create a network providing guaranteed QoS for different classes of multimedia applications. The *Joint CAC and DBA (JCAC-DBA) algorithm* proposed in this work turns out to be an improved RRM technique that can handle radio resources efficiently in limited spectrum based scenarios. The said policy has been able to achieve better QoS under a scenario where tiered small cells are deployed under the footprint of a traditional macro cell to extend coverage with an ultimate aim to design HetNet. The newness in this work belongs to the fact that it integrates an RSS based CAC policy and DBA for better performance in terms of standard QoS parameters like New Call Blocking Probability (NCBP), Hand off Call Dropping

Probability (HCDP), and Bandwidth Utilization (BU). A Continuous Time Markov Chain based analytical model is also deliberated for the in-depth analysis of the proposed RRM scheme considering those QoS parameters. The JCAC-DBA in two-tier LTE Het-Nets significantly improves NCBP, HCDP, BU, and the overall capacity of the network under different combinations of macro/ small cells for heterogeneous multimedia services. However, designing an accurate HetNet deployment model considering the tele-traffic density of certain regions has remained a major task.

To perform this in **Chapter 4**, we have designed *a mathematically tractable spatial network model based on stochastic geometry to emulate complex HetNets*. Spatial Point Processes (SPP) are very effective techniques that can imitate complex HetNets. Here in this thesis, we have modeled complex HetNets by means of popular SPPs such as Binary Point Process (BPP), Homogeneous Poisson Point Process (HPPP), and Non Homogeneous Poisson Point Process (NHPPP). A detailed comparative performance analysis based on some popular QoS parameters, namely, Coverage Probability and Average Rate have also been made considering the gradual progress of tele traffic density in Indian Urban conditions over the years. It is observed that under lower density scenarios BPP outperforms HPPP in the case of CP and AR but as the network becomes denser, HPPP provides better performance compared to BPP in terms of both CP and AR respectively. Further, it has also been witnessed that irrespective of any network density scenario NHPPP outperforms both HPPP and BPP because of the proper thinning of eNBs deployed within a specific area. However, how to deploy the small cells in a HetNet environment is a non-trivial problem. There is one potentially important consideration, i.e., to improve the signal quality to improve the QoS of end users through proper network planning. To execute this, in chapter 4, we have *modelled a two-tier wireless Het-Net considering India's Urban and Suburban tele-traffic scenarios*. The expressions for Coverage probability (CP) and Average Rate (AR) are derived to evaluate the performance of the proposed scheme. In addition, this work also incorporates the k-means clustering algorithm along with NHPPP to find out the optimum locations of SeNBs to achieve improved coverage and sustainable rate. This work also realises the radio at which MeNBs and SeNBs can be deployed under real-time urban and suburban. Extensive performance evaluation finds the best-fitted ratio of MeNB to SeNBs as 1:8 for urban scenarios and 1:5 for suburban scenarios, owing to the fact that more SeNBs are



required to serve a higher percentage of teledensity in urban scenarios. Improvement of network coverage and capacity mainly depends upon natural factors such as geographical aspect/ propagation conditions and human factors such as the landscape (urban, suburban, and rural), subscriber behaviour, etc. For that, the radio propagation conditions have to be determined properly with respect to the geographical aspects and landscape of the region as accurately as possible. To achieve this, major large scale propagation path loss models have been comparatively analysed in designing a two-tier 5G HetNet with improved coverage and rate. We have considered a two-tier Het-Net as the base model. It is observed that with a known tele-density (urban/sub-urban) the choices of frequencies for MeNB and SeNB become important aspects to consider propagation path loss for 5G Het-nets for achieving a desired coverage and rate. Further, the 5G pathloss model provides better results provided the terrestrial 4G cellular network frequency is used on the macro tier whereas mmWave is used in the small cell tiers which may direct small cells to be used as hot-spots within 5G networks for higher data rate. To the best of our knowledge, most of the notable works in the literature have considered two-tier networks for the design and analysis of deployment models for ultra-dense HetNets (UDHN). However, this chapter also explicitly aims to model a three-tier UDHN model where the upper tier represents urban macro (UMa) cells serviced by Macro eNodeB (MeNB) and lower tiers represent UMi-SC and InH serviced by Small eNodeBs (SeNB) using spatially clustered homogeneous Poisson Point Process (SCHPPP) for the coverage and rate analysis in designing deployment architecture in Indian urban scenarios. Simulation results among several case studies having different combinations of 5G frequency bands are analysed. It is observed that the three-tier UDHN model provides better performance when the 3300-3670 MHz band is used on the macro tier whereas 24.25-28.50 GHz is used in small cells tiers which may direct small cells to be used as both outdoor small cells or hot-spots within 5G networks for higher data rate.

So far it is understood that in this modern era of mobile technologies ‘network densification’ stands out to be a primitive factor to enhance network QoS performance. However, in the process, sometimes over-densification or unplanned deployment may bring additional expenses or underutilization of resources under certain conditions. Hence, the determination of the optimal number of Small cells in accordance with time-varying teledensity is needed to be synced. As a feasible

solution to this, in **Chapter 5**, we present a method to determine the optimal density of SeNBs in a NHPPP distributed spatially clustered two-tier HetNet by incorporating its impact on overall ASE. Analytical results advocate that deployment of SeNBs with optimal density can improve the ASE of a two-tier HetNet, especially in peak hours under real-time Urban Tele traffic distribution scenarios.

It is quite obvious that the inclusion of additional infrastructures along with ever-increasing data-intensive applications have dominantly increased the overall network power consumption in real-time scenarios. Several efforts have been made so far to make the future network energy efficient. However, in **Chapter 6** of this thesis, we have presented a Strategic Sleeping Policy (SSP) of EH-enabled SeNBs based on M/M/1 queuing theory and investigated its impact in reducing the power consumption of the proposed HetNet based on performance metrics like Energy Efficiency (EE) and Area Energy Consumption Ratio (AECR). A novel Sleep cycle modulated Energy Harvesing (SCMEH) technique is introduced for SeNBs to ensure proper utilization of energy resources. An analytical model based on Continuous Time Markov Chain (CTMC) has been developed to evaluate the Energy Utilization (EU) of the proposed SCMEH technique. The comprehensive performance analysis reveals that the implementation of SCMEH enabled SeNBs under Ultra Dense HetNet can not only guarantee QoS requirements under concurrent time-varying urban tele-traffic conditions but also ensure Sustainable Green Communication (SGC) by radically controlling the estimated power consumption on hourly basis throughout a day.

## 7.2 Future Scope

We have started this thesis with an overview of the evolution of modern wireless technologies and discussed that how technology have evolved over the decades and eventually become a key ingredient of modern human life. It is well discussed that the evolution of wireless technology is a continuous process and it will continue to grow rather at faster pace as evolution will move beyond 5G. By the end of 2028, there will be 5 billion 5G subscriptions globally, accounting for 55 % of all mobile subscriptions [158]. The growth of 5G subscription is faster than that of 4G following its launch in 2009, with 5G estimated to reach 1 billion subscriptions 2 years sooner than 4G. Key factors include the timely availability of devices from several vendors, with prices falling faster than for 4G [158].

This phenomenal long-term growth – spanning over 3 decades – has been primarily supported by network densification and the several other associated technological advances necessary to support such densification. Although an increase in the amount of spectrum and the spectral efficiency have also played a role in Cooper’s Law, these two mechanisms combined have historically been a fairly small fraction of the total growth [61]. Therefore, further improvements in data rate as required by many future use cases will certainly require significant increase network densification [41]. But what if network densification stopped delivering significant throughput gains? Like all exponential trends, “Cooper’s Law” must eventually hit a plateau [41]. In forthcoming days, wireless technologies will be nearly as ubiquitous as chips, connecting not only people and their personal devices, but a great many other devices including automobiles and billions of other devices that traditionally have not had wireless connectivity. So, when will Cooper’s Law hit plateau as we push towards further densification of network? Or in other words, how close are we to reach the fundamental limits of densification, where further densification no longer allows (significant) further spectrum reuse and the accompanying throughput gains [41]?

These questions carry enough significance and hence to answer all these questions, firstly, it should be noticed that current wireless networks are some or the other way traces its root back to traditional cellular networks, which means that each UE connects to one AP, namely the one that provides the strongest signal [241]. It is well established fact that the Received Signal Strength (RSS) rapidly decays with the propagation distance. So, the UEs that happen to be close to an AP (i.e., in the cell center) will experience a higher signal-to-noise ratio (SNR) than those that are close to the edge between two cells [241]. Moreover, UEs at the cell edge are also affected by interference from neighbouring APs, thus the SINR can be substantially lower than the SNR at these locations. Hence, at a given time instance, the majority of active UEs are at the cell edges and their performance will determine how the customers perceive the service quality of the network as a whole [241]. Current wireless networks can attain high data rates in the cell centres, but the large variations within each cell make the QoS unreliable. Even if the rates are sufficiently high at, say, 80% of the locations in a cell, this is not fair enough when we are creating a society where wireless access is supposed to be ubiquitous [241]. When different multimedia applications viz.

online payments, navigation, video entertainment, and control of autonomous vehicles are all relying on wireless connectivity, we must provide a steady data service quality.

So, the primary goal for future mobile networks should not be limited to increase the peak rates, but the rates that can be guaranteed to the majority of the locations in the geographical coverage area. The cellular network architecture was not designed for high-rate data services but for low-rate voice services, thus it is time to look beyond the cellular paradigm and make a user centric network design that can reach the performance requirements of the future. So as a future scope of this thesis, the user centric cell-free network architecture [241], can be designed to handle the expected avalanche of massive user densification and to reach the aforementioned goal of future networks with uniformly high data rates everywhere [241, 244-246]. A cell-free network consists of multiple geographically distributed APs that are jointly serving the UEs within a geographical area. Each AP is connected via a fronthaul to a central processing unit (CPU), which is responsible for the AP cooperation [244]. There can be multiple CPUs all connected via fronthaul links, which can be wired or wireless.

Since each UE in a conventional cellular network would only be affected by interference from its own cell and a set of neighboring cells, it is only the corresponding cluster of APs that needs to cooperate to alleviate inter-cell interference for this UE. So far most of the efforts have been made network-centric clustering which is conceptually similar to having a conventional cellular network (as shown in Fig. 7.6) where each cell contains a set of distributed antennas that are controlled by a single AP. As an alternative, in user-centric clustering where each UE selects a set of preferred APs [241, 244, 247].

# Bibliography

---

- [1] S.S.Das. Evolution of air interface towards 5G. CRC Press; 2022 Sep 1.
- [2] A. K.Jagannatham. Principles of modern wireless communication systems. McGraw-Hill Education; 2015.
- [3] I. S.Misra. Wireless communications and networks: 3G and beyond. McGraw Hill Education (India) Pvt Ltd; 2013.
- [4] R.Bekkers, B.Verspagen, J.Smits,“Intellectual property rights and standardization: the case of GSM.” Telecommunications policy,vol. 26, no. (3-4), pp.171-88, Apr2002.
- [5] F. Hillebrand,“The creation of standards for global mobile communication: GSM and UMTS standardization from 1982 to 2000.” IEEE Wireless Communications,vol. 20, no. 5, pp.24-33Oct 2013.
- [6] G.Gu, G. Peng “The survey of GSM wireless communication system. In 2010 International Conference on Computer and Information Application”vol. 3, pp. 121-124, IEEE, Dec 2010.
- [7] B.Ghribi, L. Logrippo,“Understanding GPRS: the GSM packet radio service.” Computer Networks, vol. 34, no. 5, pp.763-779, Nov 2000.
- [8] A Furuskar, S Mazur, F Muller, H. Olofsson,“EDGE: Enhanced data rates for GSM and TDMA/136 evolution.” IEEE personal communications, vol. 6, no. 3, pp.56-66, Jun 1999.
- [9] T.Ojanpera, R. Prasad,“An overview of air interface multiple access for IMT-2000/UMTS.” IEEE communications Magazine, vol. 36, no. 9, pp.82-66, Sep 1998.
- [10] P.Chaudhury, W.Mohr, S. Onoe,“The 3GPP proposal for IMT-2000.” IEEE Communications magazine, vol. 37, no.12, pp.72-81, Dec 1999.
- [11] E.Dahlman, B.Gudmundson, M.Nilsson, A. Skold,“UMTS/IMT-2000 based on wideband CDMA.” IEEE Communications magazine,vol. 36, no. 9, pp.70-80, Sep 1998.
- [12] V.K.Garg,“IS-95 CDMA and CDMA2000: Cellular/PCS systems implementation.” Pearson Education; Dec 1999.
- [13] D. N.Knisely, S.Kumar, S.Laha, S. Nanda,“Evolution of wireless data services: IS-95 to cdma2000.” IEEE Communications Magazine,vol. 36, no.10, pp.140-149, Oct 1998.
- [14] H.Holma, A. Toskala, “HSDPA/HSUPA for UMTS.”John Wiley & Sons, pp.29-30, Jun 2006.
- [15] M.Assaad, D. Zeghlache,“On the capacity of HSDPA.” InIEEE Global Telecommunications Conference (IEEE GLOBECOM'03),vol. 1, pp. 60-64, Dec2003.
- [16] R.Attar, D.Ghosh, C.Lott, M.Fan, P.Black, R.Rezaifar, P.Agashe,“Evolution of cdma2000 cellular networks: multicarrier EV-DO.” IEEE Communications Magazine, vol.44, no. 3, pp.46-53, Mar 2006.
- [17] E.Dahlman, S.Parkvall, J. Skold,“4G: LTE/LTE-advanced for mobile broadband.” Academic press; Oct 2013.
- [18] J.Lee, J. K.Han, J. Zhang,“MIMO technologies in 3GPP LTE and LTE-advanced.” EURASIP Journal on wireless communications and networking, pp. 1-10, Dec 2009.

- [19] R.Schoenen, W.Zirwas, B. H.Walke,“Capacity and coverage analysis of a 3GPP-LTE multihop deployment scenario.” In 2008 IEEE International Conference on Communications Workshops (IEEEICC Workshops-2008), pp. 31-36, May 19, 2008.
- [20] E. Hossain,“IEEE802. 16/WiMAX-based broadband wireless networks: Protocol engineering, applications, and services.” In 5<sup>th</sup>Annual Conference on Communication Networks and Services Research (IEEE CNSR'07), pp. 3-4, May 14, 2007.
- [21] J. G.Andrews, A.Ghosh, R. Muhamed, “Fundamentals of WiMAX: understanding broadband wireless networking.” Pearson Education; Feb 27, 2007.
- [22] C.Eklund, R. B.Marks, K. L.Stanwood, S. Wang,“IEEE standard 802.16: a technical overview of the WirelessMAN/sup TM/air interface for broadband wireless access.” IEEE communications magazine, vol. 40, no. 6, pp.98-107,Jun 2002.
- [23] A.Ghosh, R.Ratasuk, B.Mondal, N.Mangalvedhe, T. Thomas,“LTE-advanced: next-generation wireless broadband technology.” IEEE wireless communications, vol 17, no. 3, pp.10-22, Jun 2010.
- [24] B. A.Bjerke,“LTE-advanced and the evolution of LTE deployments.” IEEE Wireless Communications. vol. 18, no. 5, pp.4-5, Oct 2011.
- [25] H.Lee, S.Vahid, K. Moessner,“A survey of radio resource management for spectrum aggregation in LTE-advanced.” IEEE Communications Surveys & Tutorials, vol. 16, no.2, pp.745-760,Nov 2013.
- [26] A. Freedman,“International Mobile Telecommunications-Advanced Tutorial Highlights.” In2009 IEEE International Conference on Microwaves, Communications, Antennas and Electronics Systems, pp. 1-2,Nov 9, 2009.
- [27] A.Akan, Ç. Edemen,“Path to 4G wireless networks.” In2010 IEEE 21st International Symposium on Personal, Indoor and Mobile Radio Communications Workshops, pp.405-407),Sep 26, 2010.
- [28] M.Alasti, B.Neekzad, J.Hui, R.Vannithamby,“Quality of service in WiMAX and LTE networks [Topics in Wireless Communications].” IEEE Communications Magazine, vol. 48, no.5, pp.104-111, May 2010.
- [29] P.Chowdhury, I. S.Misra, S. K.Sanyal. An integrated call admission control and uplink packet scheduling mechanism for QoS evaluation of IEEE 802.16 BWA networks. Canadian Journal on Multimedia and Wireless Networks. Vol. 1, no.3, pp.14-30, Apr2010.
- [30] C.Cicconetti, L.Lenzini, E.Mingozi, C.Eklund,“Quality of service support in IEEE 802.16 networks.” IEEE network, vol. 20, no. 2, pp.50-55, Mar 2006.
- [31] J Sun, Y Yao, H Zhu,“Quality of service scheduling for 802.16 broadband wireless access systems.” In2006 IEEE 63rd Vehicular Technology Conference, vol. 3, pp. 1221-1225,May 7, 2006.
- [32] E.Dahlman, S.Parkvall, J. Skold 4G, “LTE-advanced Pro and the Road to 5G.” Academic Press; Jul 2016.
- [33] S. P.Yeh, S.Talwar, G.Wu, N.Himayat, K. Johnsson,“Capacity and coverage enhancement in heterogeneous networks.” IEEE Wireless Communications, vol. 18, no.3, pp.32-38, Jun 2011.

- [34] Series M. Minimum requirements related to technical performance for IMT-2020 radio interface (s). Report. 2017:2410-0.
- [35] Series M. Guidelines for evaluation of radio interface technologies for IMT-2020. Report ITU. 2017 Oct:2412-0.
- [36] M.Fuentes, J. L.Carcel, C.Dietrich, L.Yu, E.Garro, V.Pauli, F. I.Lazarakis, O.Grøndalen, O.Bulakci, J.Yu, W. Mohr,“5G new radio evaluation against IMT-2020 key performance indicators.” *IEEE Access*,vol. 8, pp.110880-110896, Jun 2020.
- [37] M. J.Marcus, “5G and IMT for 2020 and beyond” [Spectrum Policy and Regulatory Issues], *IEEE Wireless Communications*, vol. 22, no. 4, pp.2-3,Aug 2015.
- [38] E.Dahlman, S.Parkvall, J. Skold,“5G NR: The next generation wireless access technology.” Academic Press,Sep 2020.
- [39] M. J.Marcus,“ITU WRC-19 spectrum policy results.” *IEEE Wireless Communications*, vol. 26, no. 6, pp.4-5, Dec 2019.
- [40] Series M. Guidelines for evaluation of radio interface technologies for IMT-2020. Report ITU. 2017 Oct:2411-0.
- [41] Series M. IMT Vision–Framework and overall objectives of the future development of IMT for 2020 and beyond. Recommendation ITU. 2015 Sep;2083:0.
- [42] Ericsson,“Ericsson Mobility Report June 2022”, Jun 2022.
- [43] O.Alamu, A.Gbenga-Ilori, M.Adelabu, A.Imoize, O.Ladipo,“Energy efficiency techniques in ultra-dense wireless heterogeneous networks: An overview and outlook.” *Engineering Science and Technology, an International Journal*,vol. 23, no. 6, pp.1308-1326, Dec 2020.
- [44] Cisco U. Cisco annual internet report (2018–2023) white paper. Cisco: San Jose, CA, USA. Mar 2020.
- [45] India Brand Equity Foundation. (2021). Telecommunication Industry Report 2022.
- [46] A. R.Mishra, “Advanced cellular network planning and optimisation: 2G/2.5G/3G... evolution to 4G.” John Wiley & Sons, Jan 2007.
- [47] A. R.Mishra,“Fundamentals of Network Planning and Optimisation 2G/3G/4G: Evolution to 5G.” John Wiley & Sons, Jul 2018.
- [48] J.Navarro-Ortiz, P.Romero-Diaz, S.Sendra, P.Ameigeiras, J. J.Ramos-Munoz, J. M.Lopez-Soler,“A survey on 5G usage scenarios and traffic models.” *IEEE Communications Surveys & Tutorials*,vol. 22, no.2, pp.905-929, Feb 2020.
- [49] L.Lindbom, R.Love, S.Krishnamurthy, C.Yao, N.Miki, V.Chandrasekhar,“Enhanced inter-cell interference coordination for heterogeneous networks in LTE-Advanced: A survey. arXiv preprint arXiv, pp.1112.1344, Dec 2011.
- [50] H.Huang, S.Guo, W.Liang, K.Li, B.Ye, W.Zhuang,“Near-optimal routing protection for in-band software-defined heterogeneous networks.” *IEEE Journal on Selected Areas in Communications*,vol.34, no.11, pp.2918-2934, Oct 2016.
- [51] A Barbieri, A Damjanovic, T Ji, J Montojo, Y Wei, D Malladi, O Song, G Horn,“LTE femtocells: System design and performance analysis.” *IEEE Journal on Selected Areas in Communications*, vol. 30, no. 3, pp.586-594,Mar 2012.

- [52] H.Holma, A.Toskala, J.Reunanen, "LTE small cell optimization: 3GPP evolution to Release 13" John Wiley & Sons, Jan 2016.
- [53] T Nakamura, S Nagata, A Benjebbour, Y Kishiyama, T Hai, S Xiaodong, Y Ning, L Nan, "Trends in small cell enhancements in LTE advanced." IEEE Communications Magazine, vol. 51, no. 2, pp.98-105, Feb 2013.
- [54] V. Garg, "Wireless communications & networking." Elsevier; Jul 2010.
- [55] T. S.Rappaport, "Wireless communications: principles and practice." New Jersey: prentice hall PTR, Jan 1996.
- [56] I. P.Chochliouros, M. A.Kourtis, A. S.Spiliopoulou, P.Lazaridis, Z.Zaharis, C.Zarakovitis, A.Kourtis, "Energy efficiency concerns and trends in future 5G network infrastructures." Energies, vol. 14, no. 17, pp5392, Aug 2021.
- [57] H. S.Dhillon, R. K.Ganti, F.Baccelli, J. G.Andrews, "Modeling and analysis of K-tier downlink heterogeneous cellular networks." IEEE Journal on Selected Areas in Communications, vol. 30, no. 3, pp.550-560, Mar 2012.
- [58] L.Saker, G.Micallef, S. E.Elayoubi, H. O. Scheck, "Impact of picocells on the capacity and energy efficiency of mobile networks." Annals of telecommunications-Annales des telecommunications, vol. 67, no.3, pp.133-146, Apr 2012.
- [59] S.Sidiq, J. A.Sheikh, F.Mustafa, B. A.Malik, "A new method of hybrid optimization of small cell range development and density for energy efficient ultra-dense networks." Transactions on Emerging Telecommunications Technologies, vol. 33, no. 7, e4476, Jul 2022.
- [60] C.Yang, J.Li, M.Guizani, "Cooperation for spectral and energy efficiency in ultra-dense small cell networks." IEEE wireless communications, vol. 23, no.1, pp.64-71, Mar 2016.
- [61] S. F.Yunas, M.Valkama, J.Niemelä, "Spectral and energy efficiency of ultra-dense networks under different deployment strategies." IEEE Communications Magazine, vol. 53, no. 1, pp.90-100, Jan 2015.
- [62] S. Mukherjee, "Analytical modeling of heterogeneous cellular networks." Cambridge University Press; Jan 2014.
- [63] A.Baddeley, I.Bárány, R.Schneider, "Spatial Point Process and Their Applications, Stochastic Geometry" lectures given at the CIME Summer School held in Martina Franca, Italy, September 13–18, 2004 and Berlin, Heidelberg, Springer Berlin Heidelberg, 2007.
- [64] H.ElSawy, A.Sultan-Salem, M. S.Alouini, M. Z.Win, "Modeling and analysis of cellular networks using stochastic geometry: A tutorial." IEEE Communications Surveys & Tutorials, vol. 19, no.1, pp.167-203, Nov 2016.
- [65] H.Zhang, H.Liu, J.Cheng, V. C.Leung, "Downlink energy efficiency of power allocation and wireless backhaul bandwidth allocation in heterogeneous small cell networks." IEEE transactions on communications, vol. 66, no. 4, pp.1705-1716, Oct 2017.
- [66] I. K.Valavanis, G.Athanasiadou, D.Zarbouti, G. V.Tsoulos, "Base-station location optimization for LTE systems with genetic algorithms." In 20th European Wireless Conference, pp.1-6, VDE, May 14 2014.



- [67] P.González-Brevis, J.Gondzio, Y.Fan, H. V.Poor, J.Thompson, I.Krikidis, P. J.Chung,“Base station location optimization for minimal energy consumption in wireless networks.” In2011 IEEE 73rd vehicular technology conference (IEEE VTC Spring 2011), pp. 1-5,May 2011.
- [68] J. G.Andrews, F.Baccelli, R. K.Ganti,“A tractable approach to coverage and rate in cellular networks.” IEEE Transactions on communications,vol. 59, no. 11, pp.3122-3134, Oct 2011.
- [69] Y.Yu, S.Murphy, L.Murphy,“A clustering approach to planning base station and relay station locations in IEEE 802.16j multi-hop relay networks.” In2008 IEEE International Conference on Communications 2008 May 19 (pp. 2586-2591). IEEE.
- [70] A.Ghosh, I.Saha Misra, A.Kundu,“Coverage and rate analysis in two-tier heterogeneous networks under suburban and urban scenarios.” Transactions on Emerging Telecommunications Technologies, vol.30, no. 12, e3648, Dec 2019.
- [71] J.Lyu, Y.Zeng, R.Zhang, T. J.Lim,“Placement optimization of UAV-mounted mobile base stations.” IEEE Communications Letters, vol. 21, no.3, pp.604-607, Nov 2016.
- [72] Y Liu, W Li, Y Li,“Network traffic classification using k-means clustering.” In 2<sup>nd</sup> International multi-symposiums on computer and computational sciences (IEEE IMSCCS 2007), pp.360-365,Aug 2007.
- [73] J. A.Hartigan, M. A.Wong,“Algorithm AS 136: A k-means clustering algorithm.” Journal of the royal statistical society, Series c (applied statistics),vol. 28, no.1, 100-108, Jan 1979.
- [74] Y. A. Ahmad, W. A.Hassan, T. A.Rahman,“Studying different propagation models for LTE-A system.” In2012 International Conference on Computer and Communication Engineering (IEEE ICCCE 2012), pp. 848-853, Jul 2012.
- [75] L Klozar, J. Prokopec,“Propagation path loss models for mobile communication.” InProceedings of 21st International Conference Radioelektronika 2011, pp. 1-4, Apr 2011.
- [76] 3GPP TR 36.931 version 13.0.0 Release 13LTE; Evolved Universal Terrestrial Radio Access (E-UTRA); Radio Frequency (RF) requirements for LTE Pico Node B
- [77] S Sun, T. S.Rappaport, S.Rangan, T. A.Thomas, A.Ghosh, I. Z.Kovacs, I.Rodriguez, O.Koymen, A.Partyka, J.Jarvelainen,“Propagation path loss models for 5G urban micro-and macro-cellular scenarios.” In2016 IEEE 83rd Vehicular Technology Conference (IEEE VTC Spring), pp. 1-6, May 2016.
- [78] S.Rangan, T. S.Rappaport, E.Erkip. Millimeter-wave cellular wireless networks: Potentials and challenges. Proceedings of the IEEE,vol. 102, no.3, pp.366-385, Feb 2014.
- [79] T. S.Rappaport, Y.Xing, G. R.MacCartney, A. F.Molisch, E.Mellios, J.Zhang,“Overview of millimeter wave communications for fifth-generation (5G) wireless networks—With a focus on propagation models.” IEEE Transactions on antennas and propagation. Vol. 65, no.12, pp.6213-6230,Aug 2017.
- [80] 5G; Study on channel model for frequencies from 0.5 to 100 GHz (3GPP TR 38.901 version 16.1.0 Release 16)
- [81] M.Agiwal, A.Roy, N.Saxena,“Next generation 5G wireless networks: A comprehensive survey.” IEEE Communications Surveys & Tutorials, vol.18, no. 3, pp.1617-1655, Feb 2016.

- [82] R. Q.Hu, Y.Qian. An energy efficient and spectrum efficient wireless heterogeneous network framework for 5G systems, *IEEE Communications Magazine*, vol. 52, no. 5, pp.94-101, May 2014.
- [83] H.Munir, S. A.Hassan, H.Pervaiz, Q.Ni, L.Musavian, "Energy efficient resource allocation in 5G hybrid heterogeneous networks: A game theoretic approach." In 2016 IEEE 84th vehicular technology conference (IEEE VTC-Fall), pp. 1-5, Sep 2016.
- [84] H.Pervaiz, L.Musavian, Q.Ni, Z.Ding, "Energy and spectrum efficient transmission techniques under QoS constraints toward green heterogeneous networks." *IEEE Access*, vol. 3, pp.1655-1671, Sep 2015.
- [85] F.Salahdine, J.Opadere, Q.Liu, T.Han, N.Zhang, S. Wu, "A survey on sleep mode techniques for ultra-dense networks in 5G and beyond." *Computer Networks*, vol. 201, p.108567, Dec 2021.
- [86] A.Srivastava, M. S.Gupta, G.Kaur, "Energy efficient transmission trends towards future green cognitive radio networks (5G): Progress, taxonomy and open challenges." *Journal of Network and Computer Applications*, vol. 168, p.102760, Oct 2020.
- [87] M. H.Alsharif, R.Nordin, N. F.Abdullah, A. H. Kelechi, "How to make key 5G wireless technologies environmental friendly: A review." *Transactions on Emerging Telecommunications Technologies*, vol.29, no. 1, e3254, Jan 2018.
- [88] [https://www.business-standard.com/article/current-affairs/pm-modi-launches-5g-services-at-india-mobile-congress-2022-in-new-delhi-122100100161\\_1.html](https://www.business-standard.com/article/current-affairs/pm-modi-launches-5g-services-at-india-mobile-congress-2022-in-new-delhi-122100100161_1.html)
- [89] <https://indianexpress.com/article/technology/opinion-technology/5-big-takeaways-from-india-mobile-congress-2022-8190567/>
- [90] Q.Liu, Z. Zhang, "The analysis of coverage probability, ASE and EE in heterogeneous ultra-dense networks with power control." *Digital Communications and Networks*, vol. 6, no. 4, pp.524-533, Nov 2020.
- [91] M Matinmikko-Blue, S Yrjölä, P Ahokangas, K Ojutkangas, E Rossi, "6G and the UN SDGs: Where is the Connection?." *Wireless Personal Communications*, vol.121, no.2, pp.1339-1360, Nov 2021.
- [92] D López-Pérez, A De Domenico, N Piovesan, G Xinli, H Bao, S Qitao, M Debbah, "A Survey on 5G Radio Access Network Energy Efficiency: Massive MIMO, Lean Carrier Design, Sleep Modes, and Machine Learning, *IEEE Communications Surveys & Tutorials*, vol. 24, no.1, 653-697, Jan 2022.
- [93] GSMA, "2020 Mobile industry impact report: sustainable development goals." Sep 2020.
- [94] Nokia. (2020). Nokia and the United Nations sustainable development goals. <https://www.nokia.com/about-us/sustainability/our-approach/nokia-and-the-united-nations-sustainable-development-goals/>
- [95] C.Liu, B.Natarajan, H. Xia, "Small cell base station sleep strategies for energy efficiency." *IEEE Transactions on Vehicular Technology*, vol.65, no.3, pp.1652-1661, Mar 2015.

- [96] H Xu, W Yu, A Hematian, D Griffith, N Golmie, "Performance evaluation of energy efficiency with sleep mode in ultra-dense networks." In 2018 International Conference on Computing, Networking and Communications (IEEE ICNC 2018), pp. 747-751, Mar 2018.
- [97] M. A. Marsan, L. Chiaraviglio, D. Ciullo, M. Meo, "On the effectiveness of single and multiple base station sleep modes in cellular networks. Computer Networks." Vol. 57, no. 17, pp. 3276-3290, Dec 2013.
- [98] D.D. Wisdom, I. Saidu, A.Y. Tambuwal, S. Isaac, M.A. Ahmad, N. Faruk, "An efficient sleep-window-based power saving scheme (ESPSS) in IEEE 802.16 e networks." In 2019 15th International Conference on Electronics, Computer and Computation, (IEEE ICECCO, 2019), pp. 1-6.
- [99] I. Saidu, H. Musa, M.A. Lawal, I.L. Kane, "Hyper-Erlang battery-life energy scheme in IEEE 802.16 e networks." Covenant Journal of Informatics and Communication Technology, vol. 5, no. 2, Dec 2017.
- [100] A.P. Azad, S. Alouf, E. Altman, V. Borkar, G.S. Paschos, "Optimal control of sleep periods for wireless terminals." IEEE Journal on Selected Areas of Communication, vol. 29, no. 8, pp. 1605-1617, Aug 2011.
- [101] K. Lee, Y. Mun, "Improved power saving mechanism to increase unavailability interval in IEEE 802.16 e networks." IEICE Transaction on Communication, vol. 95, no. 4, pp. 1414-1418, Apr 2012.
- [102] X. Lu, P. Wang, D. Niyato, D. I. Kim, Z. Han, "Wireless Networks with RF Energy Harvesting: A Contemporary Survey," *IEEE Communication Surveys & Tutorials*, vol. 17, no. 2, pp. 757-789, Nov 2014.
- [103] S. Bi, C. K. Ho, and R. Zhang, "Wireless Powered Communication: Opportunities and Challenges," *IEEE Communication Magazine*, vol. 53, no. 4, pp. 117-125, Apr 2015.
- [104] T. D. Perera, D. N. Jayakody, S. K. Sharma, S. Chatzinotas, J. Li, "Simultaneous wireless information and power transfer (SWIPT): Recent advances and future challenges." *IEEE Communications Surveys & Tutorials*, vol. 20, no. 1, pp. 264-302, Dec 2017.
- [105] Y. Mao, Y. Luo, J. Zhang, K. B. Letaief, "Energy harvesting small cell networks: feasibility, deployment, and operation." *IEEE Communications Magazine*. vol. 53, no. 6, pp. 94-101, Jun 2015.
- [106] A. Ghazanfari, H. Tabassum, E. Hossain, "Ambient RF energy harvesting in ultra-dense small cell networks: Performance and trade-offs." *IEEE Wireless Communications*, vol. 23, no. 2, pp. 38-45, May 2016.
- [107] S. Akbar, Y. Deng, A. Nallanathan, M. ElKashlan, A. H. Aghvami, "Simultaneous wireless information and power transfer in k-tier heterogeneous cellular networks." *IEEE Transactions on Wireless Communications*, vol. 15, no. 8, pp. 5804-5518, May 2016.
- [108] Z. Zheng, X. Zhang, L. X. Cai, R. Zhang, X. Shen, "Sustainable communication and networking in two-tier green cellular networks." *IEEE Wireless Communications*, vol. 21, no. 4, pp. 47-53, Aug 2014.

- [109] YL Lee, TC Chuah, J Loo, A. Vinel, "Recent advances in radio resource management for heterogeneous LTE/LTE-A networks." *IEEE Communications Surveys & Tutorials*. Vol. 16, no.4, pp.2142-2180, Jun 2014.
- [110] M. Salem, A. Adinoyi, M. Rahman, H. Yanikomeroglu, D. Falconer, Y. D. Kim, E. Kim, and Y. C. Cheong, "An overview of radio resource management in relay-enhanced OFDMA-based networks." *IEEE Communications Surveys & Tutorials*, vol. 12, no.3, pp.422-438, Apr 2010.
- [111] K. I. Pedersen, T.E., Kolding, F., Frederiksen, I.Z., Laselva, D. Kovács, and P.E., Mogensen, "An overview of downlink radio resource management for UTRAN long-term evolution." *IEEE Communications Magazine*, vol. 47, no. 7, pp.86-93, Jul 2009.
- [112] M. H. Ahmed, "Call admission control in wireless networks: A comprehensive survey." *IEEE Communication Survey Tutorials*, vol. 7, no1-4, pp.50-69, May 2005.
- [113] M. Naghshineh and A. Acampora, "QoS Provisioning in Microcellular Networks Supporting Multimedia Traffic," *Proc. 14th Annual Joint Conf. IEEE Comp. and Commun. Societies (INFOCOM'95)*, vol. 3, pp.1075-1084, Sep 1995.
- [114] B. Epstein and M. Schwartz, "Predictive QoS-based Admission Control for Multiclass Traffic in Cellular Wireless Networks," *IEEE Journal on Selected Areas of Communication*, vol. 18, no. 3, pp. 523-34, Mar. 2000.
- [115] J. Capone and I. Stavrakakis, "Determining the Call Admission Region for Real-time Heterogeneous Applications in Wireless TDMA Networks," *IEEE Trans. Net.*, vol. 12, no. 2, pp.38-47, Mar.-Apr. 1998.
- [116] P. Koutsakis, M. Paterakis, and S. Psychis, "Call Admission Control and Traffic Policing Mechanisms for the Wireless Transmission of Layered Videoconference Traffic from MPEG-4 and H.263 Video Coders," *Proc. 13th IEEE Int'l. Symp. Pers., Indoor and Mobile Radio Commun. (PIMRC'02)*, vol. 5, pp. 2155-59, Sept 2002.
- [117] G. I.Tsiropoulos, D. G.Stratogiannis, P. G.Cottis, J. D.Kanellopoulos, "Efficiency evaluation of class-based call admission control schemes for wireless communications." In 2008 IEEE International Symposium on Wireless Communication Systems, pp. 69-73, Oct 2008.
- [118] D. G.Stratogiannis, G. I.Tsiropoulos, P. G.Cottis, "Call admission control in wireless networks: Probabilistic approach and efficiency evaluation." In 2008 International Wireless Communications and Mobile Computing Conference, pp. 712-717, Aug 2008, IEEE.
- [119] R. H.Babu, P. S.Satyanarayana, "Call Admission Control for Next Generation Wireless Networks Using Higher Order Markov Model." *Computer and Information Science*, vol 3, no. 1, p.192, Feb 2010.
- [120] H. S. Ramesh Babu, P. S.Satyanarayana, "Call admission control mechanism for optimal QoS in next generation wireless networks." In 2010 International Conference on Intelligent Systems, Modelling and Simulation, pp. 350-355, Jan 2010, IEEE.
- [121] M. M.Hasan, S.Kwon, S. K.Kim, "Collaboration of Call Admission Control with Load-balancing in Small-cell Networks." In 2018 International Conference on Information and Communication Technology Convergence (IEEE ICTC), pp. 1230-1232, Oct 2018.

- [122] S Kaur, D. Selvamuthu, "Adaptive joint call admission control scheme in LTE-UMTS networks." In 2014 IEEE International Conference on Communication, Networks and Satellite (IEEE COMNETSAT), pp. 63-70, Nov 4, 2014.
- [123] Y.Wu, D.Zhang, H.Jiang, Y.Wu, "A novel spectrum arrangement scheme for femto cell deployment in LTE macro cells." In 2009 IEEE 20th International Symposium on Personal, Indoor and Mobile Radio Communications, pp. 6-11, Sep 2009.
- [124] M.C.Ertürk, I.Güvenç, S.Mukherjee, H. Arslan, "Fair and QoS-oriented resource management in heterogeneous networks." EURASIP Journal on Wireless Communications and Networking, vol.1, pp.1-14, Dec 2013.
- [125] Y Bai, L. Chen, "Hybrid spectrum arrangement and interference mitigation for coexistence between LTE macrocellular and femtocell networks." EURASIP Journal on Wireless Communications and Networking, vol. 1, pp.1-15, Dec 2013.
- [126] C.Stocchi, N.Marchetti, N. R.Prasad, "Self-optimized radio resource management techniques for LTE-A local area deployments." In 2011 2nd International Conference on Wireless Communication, Vehicular Technology, Information Theory and Aerospace & Electronic Systems Technology (IEEE Wireless VITAE), pp. 1-5, Feb 2011.
- [127] Z Zheng, J Hamalainen, Y Yang, "On uplink power control optimization and distributed resource allocation in femtocell networks." In 2011 IEEE 73rd Vehicular Technology Conference (IEEE VTC Spring), pp. 1-5, May 2011.
- [128] Z Zheng, AA Dowhuszko, J Hämäläinen, "Interference management for LTE-Advanced Het-Nets: stochastic scheduling approach in frequency domain." Transactions on Emerging Telecommunications Technologies vol.1, pp.4-17, Jan 2013.
- [129] I.Hwang, B.Song, S. S.Soliman, "A holistic view on hyper-dense heterogeneous and small cell networks." IEEE Communication Magazine, vol. 51, no. 6, pp.20-27, Jun 2013.
- [130] H. S.Dhillon, R. K.Ganti, J. G.Andrews, "A tractable framework for coverage and outage in heterogeneous cellular networks." Paper presented at: Information Theory and Applications Workshop (ITA); La Jolla, CA, 2011.
- [131] A. D.Wyner, "Shannon-theoretic approach to a Gaussian cellular multiple-access channel." IEEE Transactions on Information Theory, Vol. 40, no. 6, pp.1713-1727, Nov 1994.
- [132] S.Catreux, P. F.Driessen, L. J. Greenstein, "Simulation results for an interference-limited multiple-input multiple-output cellular system." IEEE Communications Letters, vol. 4, no.11, pp.1094-1096, Nov 2000.
- [133] A.Ganz, C. M.Krishna, D.Tang, Z. J. Haas, "On optimal design of multitier wireless cellular systems." IEEE Communications Magazine, vol. 35, no. 2, pp.88-93, Feb 1997.
- [134] E.Ekici, C. Ersoy, "Multi-tier cellular network dimensioning." Wireless Networks, vol. 7, no.4, pp.401-411, Jul 2001.
- [135] Q Ye, B Rong, Y Chen, M Al-Shalash, C Caramanis, JG Andrews, "User association for load balancing in heterogeneous cellular networks." IEEE Transactions on Wireless Communications, vol. 12, no.6, pp.2706-2716, Apr 2013.

- [136] M.Afshang, H. S.Dhillon,“Fundamentals of modeling finite wireless networks using binomial point process.” IEEE Transactions on Wireless Communications,vol. 16, no.5, pp.3355-3370, Mar 2017.
- [137] C.Saha, H. S. Dhillon,“Downlink coverage probability of K-tier HetNets with general non-uniform user distributions.” In2016 IEEE International Conference on Communications (IEEE ICC 2016), pp.1-6,May 2016.
- [138] M.Afshang, C.Saha, H. S. Dhillon,“Nearest-neighbor and contact distance distributions for Thomas cluster process.” IEEE Wireless Communications Letters. 6(1):130-133, Dec 2016.
- [139] M Afshang, C Saha, H. S. Dhillon,“Nearest-neighbor and contact distance distributions for Matérn cluster process.” IEEE Communications Letters,vol. 21, no. 12, 2686-2689, Aug 2017.
- [140] V.Suryaprakash, A. F.dos Santos, A.Fehske, G. P.Fettweis,“Energy consumption analysis of wireless networks using stochastic deployment models.” In2012 IEEE Global Communications Conference (IEEE GLOBECOM 2012), pp. 3177-3182, Dec 2012.
- [141] V.Suryaprakash, J.Møller, G.Fettweis,“On the modeling and analysis of heterogeneous radio access networks using a Poisson cluster process.” IEEE Transactions on Wireless Communications,vol. 14, no. 2, pp.1035-1047, Oct 2014.
- [142] M Di Renzo, S Wang, X Xi,“Inhomogeneous double thinning—Modeling and analysis of cellular networks by using inhomogeneous Poisson point processes” IEEE Transactions on Wireless Communications,vol. 17, no. 8, pp.5162-5182, May 2018.
- [143] J.G., Andrews, S., Buzzi, W., Choi, S.V., Hanly, A., Lozano, A.C. Soong, and J.C., Zhang, “What will 5G be?” IEEE Journal on selected areas in communications, vol. 32, no.6, pp.1065-1082, Jun 2014.
- [144] V.Chandrasekhar, M.Kountouris, J. G.Andrews,“Coverage in multi-antenna two-tier networks.” IEEE Transactions on Wireless Communications, vol. 8, no. 10, pp.5314-5327, Oct 2009.
- [145] A., Khandekar, N., Bhushan, J. Tingfang, and V., Vanghi, “LTE-advanced: Heterogeneous networks.” In 2010 European wireless conference (IEEE EW), pp. 978-982, 2010, April.
- [146] F Haider, CX Wang, H Haas, D Yuan, H Wang, X Gao, XH You, E Hepsaydir,“Spectral efficiency analysis of mobile femtocell based cellular systems.” In2011 IEEE 13th international conference on communication technology, pp. 347-351,Sep 2011.
- [147] H Zhang, S Chen, X Li, H Ji, X Du,“Interference management for heterogeneous networks with spectral efficiency improvement.” IEEE Wireless Communications,vol. 22, no.2, pp.101-107, Apr 2015.
- [148] P.Rysavy,“Challenges and considerations in defining spectrum efficiency.” Proceedings of the IEEE, vol. 102, no.3, pp.386-392,Feb 2014.
- [149] G. Basilashvili,“Study of spectral efficiency for LTE network.” American Scientific Research Journal for Engineering, Technology, and Sciences (ASRJETS), vol. 1, pp.21-32, Mar 2017.
- [150] P. P.Tayade, V. M.Rohokale,“Enhancement of spectral efficiency, coverage and channel capacity for wireless communication towards 5G.” In2015 International Conference on Pervasive Computing (IEEE ICPC 2015), pp.1-5, Jan 2015.

- [151] M. S.Alouini, A. J. Goldsmith,“Area spectral efficiency of cellular mobile radio systems.” IEEE Transactions on vehicular technology.”vol. 48, no.4, pp.1047-1066, Jul 1999.
- [152] H.El-Sayed, A.Mellouk, L.George, S. Zeadally,“Quality of service models for heterogeneous networks: overview and challenges.” Annals of telecommunications-Annales des telecommunications,vol. 63, pp.639-668,Dec 2008.
- [153] M. Z.Shakir, M. S. Alouini,“On the area spectral efficiency improvement of heterogeneous network by exploiting the integration of macro-femto cellular networks.” In2012 IEEE International Conference on Communications (IEEE ICC 2012), pp. 5695-5700, Jun 10, 2012.
- [154] P.Chandhar, S. S. Das,“Analysis of area spectral efficiency for co-channel deployed macrocell-femtocell OFDMA networks.” In2013 IEEE International Conference on Communications (IEEE ICC 2013), pp. 5010-5014, Jun 2013.
- [155] P.Chandhar, S. S. Das,“Area spectral efficiency of co-channel deployed OFDMA femtocell networks.” IEEE Transactions on Wireless Communications, vol. 13, no.7, pp.3524-3538, . May 2014.
- [156] C.Li, J.Zhang, J. G.Andrews, K. B.Letaief,“Success probability and area spectral efficiency in multiuser MIMO HetNets.” IEEE Transactions on Communications,vol. 64, no. 4, pp.1544-1556, Feb 2016.
- [157] X.Ge, S.Tu, G.Mao, C. X.Wang, T. Han,“5G ultra-dense cellular networks.” IEEE Wireless Communications,vol. 23, no.1, pp.72-89, Mar 2016.
- [158] Ericsson, “Ericsson Mobility Report”, November 2022, <https://www.ericsson.com/en/reports-and-papers/mobility-report/reports/november-2022>
- [159] C.Galiotto, N. K.Pratas, L.Doyle, N. Marchetti,“Effect of LOS/NLOS propagation on 5G ultra-dense networks.” Computer Networks,vol. 120, pp.126-140, Jun 2017.
- [160] A. AlAmmouri, J. G.Andrews, F. Baccelli,“A unified asymptotic analysis of area spectral efficiency in ultradense cellular networks.” IEEE Transactions on Information Theory,vol. 65, no. 2, pp.1236-1248, Jun 2018.
- [161] A.AlAmmouri, J. G.Andrews, F. Baccelli,“Area spectral efficiency and SINR scaling laws in multi-antenna cellular networks.” arXiv preprint arXiv:2002.04118. 2020 Feb 10.
- [162] D Liu, C. Yang,“Caching policy toward maximal success probability and area spectral efficiency of cache-enabled HetNets.” IEEE Transactions on Communications, vol. 65, no.6, pp.2699-2714, Mar 2017.
- [163] S.Chen, F.Qin, B.Hu, X. Li, and Z.Chen, “User-centric ultra-dense networks for 5G: Challenges, methodologies, and directions.” IEEE Wireless Communications, vol. 23, no.2, pp.78-85, Apr 2016.
- [164] C., Dong, J., Xie, H., Dai, Q., Wu, Z. Qin, and Z., Feng, “Optimal deployment density for maximum coverage of drone small cells.” China Communications, vol.15, no.5, pp.25-40, May 2018.
- [165] M.Mahbub, B. Barua, and R.M.Shubair, “Optimal Small/Macro-Cell Densities in 5G Heterogeneous Networks: Maximizing Small-Cell Throughput Under SIR Constraints.” In

- 2021 IEEE 12th Annual Ubiquitous Computing, Electronics & Mobile Communication Conference (IEEE UEMCON 2021) (pp. 0823-0829), Dec 2021.
- [166] V. M.Nguyen, &M. Kountouris, "Coverage and capacity scaling laws in downlink ultra-dense cellular networks." *arXiv preprint arXiv:1602.03305*, 2016.
  - [167] J. G.Andrews, X.Zhang, G. D.Durgin, A. K.Gupta,"Are we approaching the fundamental limits of wireless network densification?." IEEE Communications Magazine,vol. 54, no. 10, pp.184-190, Oct 2016.
  - [168] M.Kountouris,"Performance limits of network densification." IEEE Journal on Selected Areas in Communications,vol. 35, no. 6, pp.1294-1308, Mar 2017.
  - [169] M.Ding, D.López-Pérez, G.Mao, P.Wang, Z. Lin,"Will the area spectral efficiency monotonically grow as small cells go dense?." In2015 IEEE Global Communications Conference (IEEE GLOBECOM 2015), pp. 1-7, Dec 2015.
  - [170] Y Kim, S Lee, D. Hong,"Performance analysis of two-tier femtocell networks with outage constraints." IEEE Transactions on Wireless Communications,vol. 9, no. 9), pp.2695-2700, Jul 2010.
  - [171] M.Yao, M. M.Sohul, X.Ma, V.Marojevic, J. H.Reed,"Sustainable green networking: exploiting degrees of freedom towards energy-efficient 5G systems." Wireless Networks,vol. 25, no. 3, pp.951-960, Apr 2019.
  - [172] J.Wu, Y.Zhang, M.Zukerman, E. K. Yung,"Energy-efficient base-stations sleep-mode techniques in green cellular networks: A survey." IEEE communications surveys & tutorials,vol. 17, no. 2, pp.803-826, Feb 2015.
  - [173] S Zhang, X Cai, W Zhou, Y Wang,"Green 5G enabling technologies: an overview." IET Communications,vol. 13, no.2, pp.135-143, Jan 2019.
  - [174] Zhang T, Zhao J, An L, Liu D. Energy efficiency of base station deployment in ultra dense HetNets: A stochastic geometry analysis. IEEE Wireless Communications Letters. 2016 Jan 8;5(2):184-7.
  - [175] J.Lei, H.Chen, F. Zhao,"Stochastic geometry analysis of downlink spectral and energy efficiency in ultradense heterogeneous cellular networks." Mobile Information Systems, Apr 2018.
  - [176] YS Soh, TQ Quek, M. Kountouris, "Dynamic sleep mode strategies in energy efficient cellular networks." In2013 IEEE International Conference on Communications (IEEE ICC 2013), pp. 3131-3136, Jun 2013.
  - [177] Y. S.Soh, T. Q.Quek, M.Kountouris, H.Shin,"Energy efficient heterogeneous cellular networks." IEEE Journal on selected areas in communications, vol. 31, no. 5, pp.840-850, Apr 2013.
  - [178] S Samarakoon, M Bennis, W Saad, M. Latva-Aho,"Dynamic clustering and sleep mode strategies for small cell networks." In 2014 11th International Symposium on Wireless Communications Systems (IEEE ISWCS 2014), pp. 934-938,Aug 2014.



- [179] S Samarakoon, M Bennis, W Saad, M. Latva-Aho, "Dynamic clustering and on/off strategies for wireless small cell networks." IEEE Transactions on Wireless Communications, vol. 15, no. 3, pp.2164-2178, Nov 2015.
- [180] S.Samarakoon, M.Bennis, W.Saad, M. Latva-Aho, "Opportunistic sleep mode strategies in wireless small cell networks." In 2014 IEEE International Conference on Communications (IEEE ICC 2014), pp. 2707-2712, Jun 2014.
- [181] G. K.Tran, H.Shimodaira, R. E.Rezagah, K.Sakaguchi, K.Araki, "Practical evaluation of on-demand smallcell ON/OFF based on traffic model for 5G cellular networks." In 2016 IEEE Wireless Communications and Networking Conference, pp. 1-7, Apr 2016.
- [182] J.Tang, A.Shojaeifard, D. K.So, K. K.Wong, N. Zhao, "Energy efficiency optimization for CoMP-SWIPT heterogeneous networks." IEEE Transactions on Communications, vol. 66, no. 12, pp.6368-6383, Aug 2018.
- [183] T Lv, H Gao, Z Shi, X. Su, "Energy efficiency of two-tier heterogeneous networks with energy harvesting." In 2017 IEEE International Conference on Communications (IEEE ICC 2017), pp. 1-6, May 2017.
- [184] L.Guntupalli, M.Gidlund, F. Y. Li, "An on-demand energy requesting scheme for wireless energy harvesting powered IoT networks." IEEE Internet of Things Journal, vol. 5, no. 4, pp.2868-2879, Jun 2018.
- [185] S.Landstrom, H.Murai, A. Simonsson, "Deployment aspects of LTE pico nodes." In 2011 IEEE International Conference on Communications Workshops (IEEE ICC), pp. 1-5, Jun 2011.
- [186] Nokia. (2015). Nokia small cells-innovative ways to expand coverage and capacity for the future. <http://resources.alcatel-lucent.com/asset/200247>.
- [187] D. R., Bian, & Q. Yan, "Small cells big opportunities: A huawei white paper." 2014. [www.huawei.com/ilink/en/download/HW\\_330984](http://www.huawei.com/ilink/en/download/HW_330984).
- [188] Nokia. Outdoor 3G/LTE small cells deployment strategy: "The race to the pole". <http://resources.alcatel-lucent.com/asset/200206>.
- [189] A.Damnjanovic, J.Montojo, Y.Wei, T.Ji, T.Luo, M.Vajapeyam, T.Yoo, O Song, D. Malladi, "A survey on 3GPP heterogeneous networks." IEEE Wireless communications, vol. 18, no. 3, pp.10-21, Jun 2011.
- [190] L Huang, Y Zhou, X Han, Y Wang, M Qian, J. Shi, "Distributed coverage optimization for small cell clusters using game theory." In 2013 IEEE Wireless Communications and Networking Conference (IEEE WCNC 2013), pp.2289-2293, Apr 2013.
- [191] M Hughes, V. M.Jovanovic, "Small cells-effective capacity relief option for heterogeneous networks." In 2012 IEEE Vehicular Technology Conference (IEEE VTC Fall), pp. 1-6, Sep 2012.
- [192] K.Piamrat, A.Ksentini, J. M.Bonnin, C.Viho, "Radio resource management in emerging heterogeneous wireless networks. Computer Communications." 34(9):1066-1076, Jun 2011.
- [193] P.Chowdhury, I. S.Misra, S. K.Sanyal, "Cross layer QoS support architecture with integrated CAC and scheduling algorithms for WiMAX BWA networks." arXiv preprint arXiv:1204.1614, Apr 2012.

- [194] H. Ekstrom, "QoS control in the 3GPP evolved packet system." IEEE Communications Magazine, vol. 47, no. 2, pp.76-83, Feb 2009.
- [195] A. H.Ali, M. Nazir, "Radio resource management with QoS guarantees for LTE-A systems: a review focused on employing the multi-objective optimization techniques." Telecommunication Systems, vol. 67, no.2, pp.349-365, Feb 2018.
- [196] Fujitsu, "High-capacity indoor wireless solutions: Picocell or femtocell?" Tech. rep., Fujitsu Network Communications Inc., (2013).
- [197] Hoymann C, Chen W, Montojo J, Golitschek A, Koutsimanis C, Shen X. Relaying operation in 3GPP LTE: challenges and solutions. IEEE Communications Magazine. 2012 Feb 9;50(2):156-62.
- [198] T Beniero, S Redana, J Hamalainen, B Raaf, "Effect of relaying on coverage in 3GPP LTE-advanced." InVTC Spring 2009-IEEE 69th Vehicular Technology Conference, pp. 1-5, 2009 Apr 26.
- [199] 3GPP TS 36.300 v. 8.11.0, "Evolved Universal Terrestrial Radio Access (E-UTRA) and Evolved Universal Terrestrial Radio Access (E-UTRAN); Overall Description; Stage 2," Jan. 2010.
- [200] 3GPP TR 36.814 V9.0.0 (2010-03); Technical Report; 3rd Generation Partnership Project; Technical Specification Group Radio Access Network; Evolved Universal Terrestrial Radio Access (E-UTRA); Further advancements for E-UTRA physical layer aspects (Release 9).
- [201] H.Holma & A.Toskala, "WCDMA for UMTS: HSPA Evolution and LTE", John Wiley & Sons, 2010.
- [202] A. Ghosh, and I. S. Misra, "A joint CAC and dynamic bandwidth allocation technique for capacity and QoS analysis in heterogeneous LTE based BWA network: few case studies." Wireless Personal Communications, Springer, 97(2), pp.2833-2857. Impact factor: 2.017.
- [203] A. Ghosh, I. S. Misra, "A QoS based comparative analysis between relay assisted and small eNodeB based two-tier LTE network", In International Conference on Computers and Devices for Communication, (CODEC 2015), pp. 1-5, IEEE, 2015.
- [204] A. Ghosh, I. S. Misra, "An analytical model for a resource constrained QoS guaranteed SINR based CAC scheme for LTE BWA Het-Nets", In International Conference on Advances in Computing, Communications and Informatics (ICACCI 2016), pp. 2186-2192, IEEE, 2016.
- [205] Telecommunication Report April 2018. Technical Report. New Delhi, India: Indian Brand Equity Foundation (IBEF); 2018.
- [206] J. G.Andrews, R. K.Ganti, M.Haenggi, N.Jindal, S.Weber, "A primer on spatial modeling and analysis in wireless networks." IEEE Communications Magazine, vol. 48, no. 11, pp.156-63, Nov 2010.
- [207] W Guo, S Wang, X Chu, J Zhang, J Chen, H. Song, "Automated small-cell deployment for heterogeneous cellular networks. IEEE Communications Magazine, vol.51, no. 5, pp.46-53, May 2013.

- [208] N.Bhushan, J.Li, D.Malladi, R.Gilmore, D.Brenner, A.Damnjanovic, R. T.Sukhavasi, C.Patel, S.Geirhofer, "Network densification: the dominant theme for wireless evolution into 5G." IEEE Communications Magazine, vol. 52, no. 2, pp.82-99, Feb 2014.
- [209] Q.Ying, Z.Zhao, Y.Zhou, R.Li, X.Zhou, H.Zhang,"Characterizing spatial patterns of base stations in cellular networks." In 2014 IEEE/CIC International Conference on Communications in China (ICCC), pp. 490-495, Oct 13, 2014.
- [210] M Haenggi, JG Andrews, F Baccelli, O Dousse, M.Franceschetti,"Stochastic geometry and random graphs for the analysis and design of wireless networks." IEEE journal on selected areas in communications, vol. 27, no.7, pp.1029-1046,Aug 2009.
- [211] M. Haenggi,"Stochastic geometry for wireless networks." Cambridge University Press,Oct 2012.
- [212] I.Howitt, S. Y. Ham,"Base station location optimization. In Gateway to 21st Century Communications Village." IEEE VTC 1999-Fall. IEEE VTS 50th Vehicular Technology Conference (Cat. No. 99CH36324) (Vol. 4, pp. 2067-2071) Sep 1999.
- [213] P Gonzalez-Brevis, J Gondzio, Y Fan, HV Poor, J Thompson, I Krikidis, PJ. Chung Base station location optimization for minimal energy consumption in wireless networks. In 2011 IEEE 73rd vehicular technology conference (IEEEVTC Spring) (pp. 1-5). May 2011.
- [214] E.Amaldi, A.Capone, F. Malucelli,"Planning UMTS base station location: Optimization models with power control and algorithms." IEEE Transactions on wireless Communications, vol. 2, no. 5, pp.939-952, Sep 2003.
- [215] S Boyd, L. Vandenberghe,"Introduction to applied linear algebra: vectors, matrices, and least squares." Chapter 4, Cambridge university press,Jun 7 2018.
- [216] G Ancans, V Bobrovs, A Ancans, D Kalibatiene,"Spectrum considerations for 5G mobile communication systems." Procedia Computer Science,vol. 104, pp.509-516.2017 Jan 1;
- [217] Final Acts, World Radio communication Conference 2019 (WRC-19), in ITU Publications, 2019.
- [218] TRAI, 'TRAI Consultation paper on 5G', Nov 2021.
- [219] AI Sulyman, AT Nassar, MK Samimi, GR MacCartney, TS Rappaport, A. Alsanie,"Radio propagation path loss models for 5G cellular networks in the 28 GHz and 38 GHz millimeter-wave bands." IEEE communications magazine,vol. 52, no. 9, pp.78-86, Sep 2014.
- [220] N. Piovesan, A. F. Gambin, M. Miozzo, M. Rossi, P. Dini, "Energy sustainable paradigms and methods for future mobile networks: A survey." Computer Communications, Elsevier, vol. 119, pp.101-117 Apr 2018.
- [221] A. Ghosh, I. S. Misra, "Role of different spatial point processes on network densification towards 5G development: Coverage and Rate analysis", In 2020 IEEE Calcutta Conference (CALCON), pp. 15-19. IEEE, 2020.
- [222] P. W.Lewis, G. S. Shedler,"Simulation of nonhomogeneous Poisson processes by thinning." Naval research logistics quarterly, vol. 26, no.3, pp.403-413, Sep 1979.

- [223] A. Ghosh and I. S. Misra, Ultra Dense Three-Tier 5G Heterogeneous Network Model for Improved Coverage and Rate. In 2022 IEEE Calcutta Conference (CALCON) (pp. 60-64). IEEE.
- [224] Monthly Telecom Scenario-Department of Telecommunication-Government of India- March 22' report.
- [225] K.Fukunaga, "Introduction to statistical pattern recognition." Elsevier, Oct 2013.
- [226] J. A. Hartigan, "Clustering algorithms", John Wiley & Sons, Inc.; Feb 1975.
- [227] M. R.Anderberg, "Cluster analysis for applications: probability and mathematical statistics: a series of monographs and textbooks." Academic press; May 10, 2014.
- [228] S. Z.Selim, M. A. Ismail, "K-means-type algorithms: A generalized convergence theorem and characterization of local optimality." IEEE Transactions on pattern analysis and machine intelligence, vol. 1, pp.81-87, Jan 1984.
- [229] L.Bottou, Y. Bengio, "Convergence properties of the k-means algorithms." Advances in neural information processing systems, vol. 7, 1994.
- [230] Population Density of Kolkata as on March 2022-kmc.gov.in/portal
- [231] M.Kamel, W. Hamouda, and A.Youssef, "Ultra-dense networks: A survey." IEEE Communications surveys & tutorials, vol. 18, no.4, pp.2522-2545, May 2016.
- [232] TELECOM REGULATORY AUTHORITY OF INDIA New Delhi, 19th July, 2022 (www.trai.gov.in) Press Release No.43/2022
- [233] S.F.Yunas, M. Valkama, and J.Niemelä, "Spectral and energy efficiency of ultra-dense networks under different deployment strategies." IEEE Communications Magazine, vol. 53, no. 1, pp.90-100, Jan 2015.
- [234] Y. Zhang, and D.Li, "Cluster analysis by variance ratio criterion and firefly algorithm." International Journal of Digital Content Technology and its Applications, vol. 7, no.3, p.689, Feb 2013.
- [235] D López-Pérez, M Ding, H Claussen, AH. Jafari, "Towards 1 Gbps/UE in cellular systems: Understanding ultra-dense small cell deployments." IEEE Communications Surveys & Tutorials. vol. 17, no.4, pp.2078-3101, Jun 2015.
- [236] J.Gubbi, R.Buyya, S.Marusic, M. Palaniswami, "Internet of Things (IoT): A vision, architectural elements, and future directions." Future generation computer systems, vol. 29, no.7, pp.1645-1660, Sep 2013.
- [237] S. Singh, X. Zhang, J.G. Andrews, "Joint rate and SINR coverage analysis for decoupled uplink-downlink biased cell associations in HetNets", IEEE Trans. Wireless Communication, vol. 14, no. 10, pp.5360–5373, May 2014.
- [238] T.F. Stocker, D. Qin, G.K. Plattner, L.V. Alexander, S.K. Allen, N.L. Bindoff, F.M. Bréon, J.A. Church, U. Cubasch, S. Emori, and P. Forster, "Technical summary. In Climate change 2013: the physical science basis. Contribution of Working Group I to the Fifth Assessment Report of the Intergovernmental Panel on Climate Change", Cambridge University Press, pp.33-115,2013.

- [239] United Nations Environment Programme, “UN Emissions Gap Report 2019,” Tech. Rep., Nov. 2019. <https://wedocs.unep.org/bitstream/handle/20.500.11822/30797/EGR2019.pdf>
- [240] DoT, Monthly Telecommunication Report February 2022. tech. rep., Department of Telecommunication, Govt. of India; 2022.
- [241] Ö. T.Demir, E.Björnson, L. Sanguinetti,“Foundations of user-centric cell-free massive MIMO.” Foundations and Trends® in Signal Processing, vol.14, no. (3-4), pp.162-472, Jan 2021.
- [242] A. Leon-Garcia,“Probability and random processes for electrical engineering.” Chapter 12. Pearson Education India; 1994.
- [243] H. A.Ammar, R.Adve, S.Shahbazpanahi, G.Boudreau, K. V. Srinivas,“User-centric cell-free massive MIMO networks: A survey of opportunities, challenges and solutions.” IEEE Communications Surveys & Tutorials, vol. 24, no.1, pp.611-652, Dec 2021.
- [244] E.Björnson, L. Sanguinetti,“Scalable cell-free massive MIMO systems.” IEEE Transactions on Communications, vol. 68, no. 7, pp.4247-4261, Apr 2020.
- [245] A.Papazafeiropoulos, P.Kourtessis, M.Di Renzo, S.Chatzinotas, J. M. Senior,“Performance analysis of cell-free massive MIMO systems: A stochastic geometry approach.” IEEE Transactions on Vehicular Technology, vol. 69, no 4, pp.3523-3537, Jan 2020.
- [246] S Chen, J Zhang, J Zhang, Björnson E, B.Ai,“A survey on user-centric cell-free massive MIMO systems.” Digital Communications and Networks,vol. 8, no. 5, pp.695-719, Dec 2021.

# Appendices

---

## Appendix A

**Theorem 1:** If a HPPP with rate function  $\{\lambda^*(x,y)|\lambda(x,y) \leq \lambda^*(x,y)\}$  in a rectangular plane is thinned according to  $\lambda(x,y)/\lambda^*(x,y)$  (i.e.  $(X_z, Y_z)$  is deleted independently if a uniform  $(0, 1)$  random number  $U_z$  is greater than  $\lambda(x,y)/\lambda^*(x,y)$ ), the result is a Non-Homogeneous Poisson Process with rate function  $\lambda(x,y)$ .

Proof:

Since  $\{N^*(x,y): x \geq 0, y \geq 0\}$  is a HPPP and the points are deleted independently it is very clear that the number of points in  $\{N(x,y): x \geq 0, y \geq 0\}$  in any set of non-overlapping intervals are mutually independent random variables. Thus, it is sufficient to show that the number of points  $N\{(a_1, b_1), (a_n, b_n)\}$  in  $\{N(x,y): x \geq 0, y \geq 0\}$  in an arbitrary spatial interval  $\{(a_1, b_1), (a_n, b_n)\}$  with  $0 < a_1 \dots \dots a_n < x_0$  and  $0 < b_1 \dots \dots b_n < y_0$  has a Poisson distribution with mean  $\Lambda(a_n, b_n) - \Lambda(a_1, b_1)$ . Observe that with  $p\{(a_1, b_1), (a_n, b_n)\} = [\Lambda(a_n, b_n) - \Lambda(a_1, b_1)]/[\Lambda^*(a_n, b_n) - \Lambda^*(a_1, b_1)]$  we have the conditional probability,

$$p\{N\{(a_1, b_1), (a_n, b_n)\} = n | N^*\{(a_1, b_1), (a_n, b_n)\} = k\} = \begin{cases} 1 & \text{if } n = k = 0 \\ [p\{(a_1, b_1), (a_n, b_n)\}]^n [1 - p\{(a_1, b_1), (a_n, b_n)\}]^{k-n} & \text{if } k \geq n \geq 0 \text{ and } k \geq 1 \\ 0 & \text{if } n \geq 1 \text{ and } k < n \end{cases}$$

(A.1)

Eq. A.1 is a consequence of a well-known result that conditioned on  $n (>0)$ , the points in the interval  $\{(a_1, b_1), (a_n, b_n)\}$ , the joint density of the  $n$  points in the process  $\{N^*(x,y): x \geq 0, y \geq 0\}$  is  $\{\lambda^*(x_1, y_1) \dots \dots \lambda^*(x_n, y_n)\}/\{\Lambda^*(a_n, b_n) - \Lambda^*(a_1, b_1)\}^n$ . The desired result is obtained in a straight forward manner from equation 3 by removing the condition.

The NHPPP with rate function  $\lambda(x,y)$  in an arbitrary but fixed region  $R$  can be generated by enclosing the region  $R$  in a rectangle and applying the thinning algorithm. The following procedure assumes that region  $R$  has been enclosed in a rectangle  $R^*$  and that  $\lambda^* = \max \{ \lambda(x,y): x, y \in R \}$  has been determined here.

## Appendix B

Theorem 2: The expression of CP which is used further for analysis is given in Theorem 1

$$P_c(P_k^{tx}, \lambda_k, \gamma_k^{th}) = \sum_{k=1}^K \lambda_k \iint_A \mathbb{P} \left( \frac{SNR_k(x, y)_i^j}{\{\sum_{l=1}^{j-1} SNR_k(x, y)_i^l\} + 1} > \gamma_n^{th} \right) (B.1)$$

Proof of Theorem2

The CP considering a two-tier HetNet can be derived as follows:

$$\begin{aligned} P_c(P_k^{tx}, \lambda_k, \gamma_{th}) &= \mathbb{P} \left( \bigcup_{k \in K, (x, y)_i^j \in \Psi_k} \gamma_k(x, y)_i^j > \gamma_k^{th} \right) \\ &= \mathbb{E} \left[ 1 \left( \bigcup_{k \in K, (x, y)_i^j \in \Psi_k} \gamma_k(x, y)_i^j > \gamma_k^{th} \right) \right] \\ &= \sum_{k=1}^K \mathbb{E} \sum_{(x, y)_i^j \in \Psi_k} 1[\gamma_k(x, y)_i^j > \gamma_k^{th}] \\ &= \sum_{k=1}^K \mathbb{E} \sum_{(x, y)_i^j \in \Psi_k} \frac{SNR_k(x, y)_i^j}{\{\sum_{l=1}^{j-1} SNR_k(x, y)_i^l\} + 1} > \gamma_n^{th}] \\ &= \sum_{k=1}^K \lambda_k \iint_A \mathbb{P} \left( \frac{SNR_k(x, y)_i^j}{\{\sum_{l=1}^{j-1} SNR_k(x, y)_i^l\} + 1} > \gamma_k^{th} \right) \end{aligned}$$

## Appendix C

Theorem 3: The closed form expression is derived and the subsequent expression for AR is given as below:

$$\bar{\mathcal{R}} = \frac{\mathbb{P}(\Gamma\{\max(v, \gamma_k^{th})\})}{\mathbb{P}\{\Gamma(\gamma_k^{th})\}} \quad (\text{C.1})$$

Proof:

The average rate achievable by a randomly chosen user can be expressed as

$$\bar{\mathcal{R}} = E \left\{ \log(1 + \max_{(x,y)_i^j \in \Psi_k} (\gamma_k(x,y)_i^j) \mid \bigcup_{k \in K, (x,y)_i^j \in \Psi_k} \gamma_k(x,y)_i^j > \gamma_k^{th} \right\}$$

Consider random variable  $\{ \max_{(x,y)_i^j \in \Psi_k} \gamma_k(x,y)_i^j \}$  by U, and

$(\bigcup_{k \in K, (x,y)_i^j \in \Psi_k} \gamma_k(x,y)_i^j > \gamma_k^{th})$  event as  $\Gamma(\gamma_{th_n})$  and rewriting equation as

$$\begin{aligned} \bar{\mathcal{R}} &= \int_0^\infty \{ \log(1+u) f_U(u | \Gamma(\gamma_k^{th})) \} du \\ &= \int_{u=0}^\infty \int_{v=0}^u \left\{ \frac{1}{1+v} f_U(u | \Gamma(\gamma_k^{th})) \right\} dv du \\ &= \int_{v=0}^\infty \int_{u=v}^\infty \{ f_U(u | \Gamma(\gamma_k^{th})) \} \frac{1}{1+v} dv = \int_{v=0}^\infty \frac{\mathbb{P}(U > v | \Gamma(\gamma_k^{th}))}{1+v} dv \end{aligned}$$

$\mathbb{P}(U > v | \Gamma(\gamma_k^{th}))$  can be seen as the conditional CDF of  $\max_{(x,y)_i^j \in \Psi_k} \gamma_k(x,y)_i^j$

which is as follows:

$$\mathbb{P} \left( \max_{(x,y)_i^j \in \Psi_k} \gamma_k(x,y)_i^j > v \mid \Gamma(\gamma_k^{th}) \right)$$

From Bayes theorem

$$\begin{aligned} \mathbb{P} \left( \max_{(x,y)_i^j \in \Psi_k} \gamma_k(x,y)_i^j > v \mid \Gamma(\gamma_k^{th}) \right) &= \frac{\mathbb{P} \left( \max_{(x,y)_i^j \in \Psi_k} \gamma_k(x,y)_i^j > v \mid \Gamma(\gamma_k^{th}) \right)}{\mathbb{P}\{\Gamma(\gamma_k^{th})\}} \\ &= \frac{\mathbb{P}(\Gamma(v), \Gamma(\gamma_k^{th}))}{\mathbb{P}\{\Gamma(\gamma_k^{th})\}} \end{aligned}$$



$$= \frac{\mathbb{P}(\Gamma\{\max(\mathbf{v}, \gamma_k^{th})\})}{\mathbb{P}\{\Gamma(\gamma_k^{th})\}}$$